eCAM Evidence-Based Complementary and Alternative Medicine

Complementary and Alternative Therapies for Inflammatory Diseases

Guest Editors: Xiang Liu, Ying-Ju Lin, and Yong Cheng

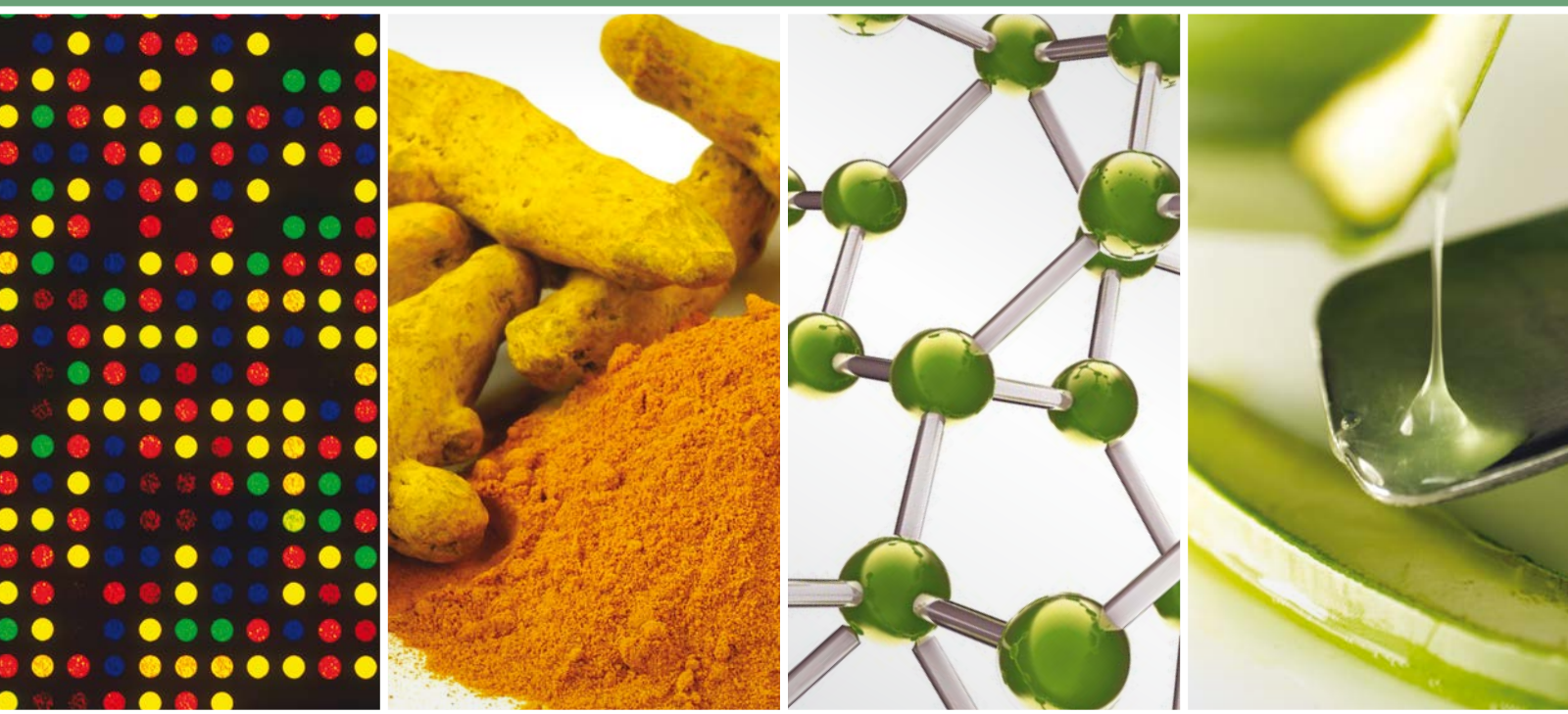

Complementary and Alternative Therapies for Inflammatory Diseases

Evidence-Based Complementary and Alternative Medicine

Complementary and Alternative Therapies for Inflammatory Diseases

Guest Editors: Xiang Liu, Ying-Ju Lin, and Yong Cheng

Editorial Board

Contents

Hindawi Publishing Corporation
Evidence-Based Complementary and Alternative Medicine
Volume 2016, Article ID 8324815, 2 pages
http://dx.doi.org/10.1155/2016/8324815

Editorial

Complementary and Alternative Therapies for Inflammatory Diseases

Xiang Liu,[1] Ying-Ju Lin,[2] and Yong Cheng[1]

[1]*National Institutes of Health, Bethesda, MD 20892, USA*
[2]*China Medical University, Taichung 40402, Taiwan*

Correspondence should be addressed to Xiang Liu; xiang.liu@nih.gov

Received 24 October 2016; Accepted 24 October 2016

Many diseases have been demonstrated to associate with acute or chronic inflammation, such as rheumatoid arthritis, Alzheimer's disease, depression, Kawasaki disease, and even cancer. However, treatment options for inflammatory diseases have been limited to anti-inflammatory medications (e.g., acetaminophen) or steroid hormones. Complementary and alternative medicines (CAMs) provide natural and effective protection for those who suffer from inflammatory diseases. This special issue is focused on the evidence-based research of CAMs for treatment of inflammatory diseases.

Inflammation occurs in response to various cellular stresses including infection, irradiation, or chemical or physical injury. One of the major responses during inflammation is the release of cytokines and/or chemokines. Y. Y. Choi et al. showed that Dangguibohyul-Tang (DBT), a herbal formula composed of *Astragalus membranaceus* (AM) and *Angelica sinensis* (AS) at a ratio of 5 : 1, helps relieve the inflammatory response through reducing IgE levels and cytokine levels. S. Park et al. showed that pomegranate peel extract (PPE) could alleviate inflammatory reactions, including production of reactive oxygen species (ROS) and expression and secretion of inflammatory cytokines.

Studies on the signaling pathways provide the anti-inflammatory mechanism of CAMs. M. Gu et al. demonstrated that genistin is cardioprotective due to its antioxidant and anti-inflammatory activities via P2X7/NF-κB pathways. T. Mao et al. showed that Qingchang Wenzhong Decoction (QCWZD) ameliorates dextran sulphate sodium- (DSS-) induced ulcerative colitis (UC) in rats by downregulating the IP10/CXCR3 axis-mediated inflammatory response. D. Wang et al. proved that Yupingfeng Pulvis (HFBP) alleviates the inflammation in the lung tissue of mice by reducing the proportion of Th17 cells and increasing the proportion of Treg cells in bronchoalveolar lavage fluid.

Using human umbilical vein endothelial cells, E. S. Choi et al. showed that Samul-Tang (Si-Wu-Tang, SMT) protects vascular endothelium from inflammation and might be used as a promising vascular protective drug. G. O. L. Carapeba et al. used animal models to evaluate the treatment effect of intra-articular hyaluronic acid in 4 dogs with osteoarthritis associated with hip dysplasia compared to traditional conservative treatment.

Hyeonggaeyeongyo-tang (HYT) is an ancient formula of oriental medicine traditionally used to treat rhinitis; however, clinical evidence has not yet been established. M. Kim et al. showed that HYT improved nasal symptoms and quality of life in patients with allergic rhinitis and nonallergic rhinitis. This is the first clinical study to evaluate the use of HYT to treat patients with rhinitis. X. Lu et al. showed that Sequential treatments with Tongsai and Bufei Yishen Granules during acute exacerbation of chronic obstructive pulmonary disease- (AECOPD-) risk window (RW) periods can reduce inflammatory response and improve pulmonary function and shorten the recovery courses of AEs.

E. S. B. Barroqueiro et al. showed that babassu mesocarp extract (EE) has specific antimicrobial activity in vitro and has an important antiseptic effect in vivo possibly due to the antimicrobial and immunomodulatory activity. N. J. S. Lopez et al. evaluated the extrusion process as an alternative for improving the biological potential of sorghum bran: phenolic

compounds and antiradical and anti-inflammatory capacity. The extrusion process increased total phenol content in sorghum bran, which positively affected antiradical capacity.

In this issue, C.-Y. Cheng et al. reviewed the anti-inflammatory effects of traditional Chinese medicines against ischemic injury in in vivo models of cerebral ischemia. TCMs provide neuroprotective effects through downregulating ischemia-induced microglial activation and expression of proinflammatory cytokines, enzymes, and transcription factors.

These studies provide new insights to treat inflammatory diseases and help us understand better about the mechanism and function of CAMs.

Xiang Liu
Ying-Ju Lin
Yong Cheng

Hindawi Publishing Corporation
Evidence-Based Complementary and Alternative Medicine
Volume 2016, Article ID 2076921, 10 pages
http://dx.doi.org/10.1155/2016/2076921

Research Article

Intra-Articular Hyaluronic Acid Compared to Traditional Conservative Treatment in Dogs with Osteoarthritis Associated with Hip Dysplasia

Gabriel O. L. Carapeba,[1] Poliana Cavaleti,[2] Gabriel M. Nicácio,[1] Rejane B. Brinholi,[2] Rogério Giuffrida,[1,2] and Renata N. Cassu[1,2]

[1]*Postgraduate Program in Animal Science, Oeste Paulista University, 19067-175 Presidente Prudente, SP, Brazil*
[2]*Faculty of Veterinary Medicine, Oeste Paulista University, 19067-175 Presidente Prudente, SP, Brazil*

Correspondence should be addressed to Renata N. Cassu; renavarro@uol.com.br

Received 27 May 2016; Revised 15 August 2016; Accepted 28 August 2016

Academic Editor: Ying-Ju Lin

The purpose of this study was to compare the efficacy of the intra-articular (IA) hyaluronic acid injection to traditional conservative treatment (TCT) in dogs with osteoarthritis (OA) induced by hip dysplasia. Sixteen dogs were distributed into two groups: Hyal: IA injection of hyaluronic acid (5–10 mg), and Control: IA injection with saline solution (0.5–1.0 mL) in combination with a TCT using an oral nutraceutical (750–1000 mg every 12 h for 90 days) and carprofen (2.2 mg/kg every 12 h for 15 days). All dogs were assessed by a veterinarian on five occasions and the owner completed an assessment form (HCPI and CPBI) at the same time. The data were analyzed using unpaired t test, ANOVA, and Tukey's test ($P < 0.05$). Compared with baseline, lower scores were observed in both groups over the 90 days in the veterinarian evaluation, HCPI, and CPBI ($P < 0.001$). The Hyal group exhibited lower scores from 15 to 90 and 60 to 90 days, in the CBPI and in the veterinarian evaluation, respectively, compared to the Control group. Both treatments reduced the clinical signs associated with hip OA. However, more significant results were achieved with intra-articular hyaluronic acid injection.

1. Introduction

Hip dysplasia (HD) represents one of the orthopedic diseases with the highest incidence in the canine species, characterized by abnormal development of the hip joint, the etiology of which is multifactorial [1, 2]. HD is a degenerative joint disease that can progressively trigger the development of osteoarthritis (OA) of the affected joint [3], characterized by articular cartilage lesions, bone remodeling with the presence of osteophytes and inflammation [4].

The most common symptom of OA is joint pain, which involves peripheral and central sensitization mechanisms. The peripheral sensitization is triggered by injury and/or joint inflammation, which results in the release of neurotransmitters such as bradykinin, prostaglandins E2 and I2, serotonin, and leukotrienes. These primary neuromediators stimulate the release of neuropeptides such as calcitonin gene-related peptide (CGRP) and substance P in the lesion site [5]. The persistent and prolonged inflammatory stimulus results in central sensitization, which is related to hyperexcitability of spinal cord neurons and other central nervous system structures [6]. In addition to inflammation, the accumulation of stressors on the joint (e.g., overweight, joint instability, and excessive exercise) favors the destruction of cartilage, triggering alterations in the articular surface remodeling, synovial membrane changes, and an increased synovial fluid with decreased viscosity and lubrication properties [7, 8].

Although there is no curative intervention at present, the pharmacological treatment for OA is principally palliative and aims to relieve pain and improve function of the affected joint. In dogs, one of the principal conservative therapeutic approaches involves oral administration of nutraceuticals, whose formulation is primarily composed of glucosamine and chondroitin sulfate together with the use of nonsteroids

anti-inflammatory drugs (NSAIDs) [9, 10]. However, prolonged use of NSAIDs can be associated with side effects, especially in the digestive system and kidneys [11], so complementary and alternative medicine is increasingly offering concomitant therapeutic options.

Hyaluronic acid (HA) is a naturally occurring glycosaminoglycan and a component of synovial fluid and cartilage matrix. The molecular properties of HA favor viscosity and lubrication of cartilage, essential factors for proper joint performance [12]. In cases of degenerative joint disease drastic reduction in the concentration of HA occurs, compromising the viscosity of the synovial fluid [13]. Thus, one of the causes of pain and mobility impairment of the joint appears to be associated with the decreased protective effect of this viscoelastic medium on the pain receptors in the synovial tissue [14].

The preparations of HA currently available may be classified according to their molecular weight (MW) and formulation type, solutions of low MW (500–730 kDa), solutions of intermediate MW (800–2000 kDa), solutions of high MW (6000 kDa), cross-linked HA, and solutions of nonanimal stabilized HA (NASHA) [13]. The majority of exogenous HA remains in the joint for a few days; however, the clinical therapeutic effects of HA treatment may be seen between 5 and 13 weeks after injection, although improvements have also been observed after 14–26 weeks and sometimes even longer [15].

In humans, intra-articular (IA) injection of HA is an increasingly popular therapy for knee OA. Several clinical trials have reported the beneficial effects following IA injection of HA, with reduction in pain and improvement in joint function [15–17]. However, few studies have evaluated the clinical efficacy of HA administered through IA in the management of hip OA in man [18, 19].

The purpose of this study was to compare the clinical efficacy of intra-articular use of hyaluronic acid to TCT (nutraceutical/NSAID) administered orally in dogs with OA of the hip joint. The hypothesis of the study is to examine whether intra-articular HA injection is superior to TCT in pain relieve. The time expected for the maximal effect was at least 30 days after HA injection.

2. Methods

The study was performed following the guidelines of the Brazilian College of Animal Experimentation, and the experimental procedure was approved by the Institutional Animal Care Committee (protocol 1611-CEEA).

2.1. Animals. From August 2014 to July 2015, 16 client-owned dogs with HD/OA were enrolled. All procedures were performed with written consent of the owners. The age of the screened dogs varied from 1.5 to 15 years (12 ± 5 years) and the body weight from 07 to 35 kg (20.7 ± 7.8 kg). The study only included dogs with chronic pain (signs of pain for a period of at least three months) which had not been given any type of analgesic drug (NSAIDs or corticosteroids) or nutraceutical for at least eight weeks. In addition, the dogs only participated in the study if their owners reported at least two common clinical signs of dogs with HD/OA, such as difficulty in lying down or getting up, difficulty in jumping or refusing to jump, difficulty in going up or down stairs, or lameness. Animals were excluded if they presented lameness of both thoracic and pelvic limbs, presented lameness of neurologic etiology, showed neurological deficits, were pregnant, had a history of recurrent gastritis/gastric ulcers, or had severe systemic diseases. If OA of another major joint was suspected clinically, additional radiographs were also made.

The dogs included in the study ($n = 16$) were evaluated by laboratory tests (complete blood count, serum urea, creatinine, alanine aminotransferase enzymes, aspartate aminotransferase, and alkaline phosphatase) prior to initiation of treatment and monthly during the evaluation period (90 days).

2.2. Physical and Radiographic Evaluation. At the first evaluation, clinical data including age, weight, sex, duration of symptoms, previous or concomitant diseases, and current medications were recorded. As body weight may influence the clinical response to treatment, this variable was measured monthly. The severity of clinical signs was measured by a single veterinarian (blinded to treatment allocation) using an ordinal scoring system (Table 1) which included pain on palpation, the ability to jump and climb stairs, lameness, and stiffness of movements [20, 21].

A radiographic examination was performed to confirm the HD/OA. For correct positioning for the radiographic examination, the dogs were sedated with a combination of 0.03 mg/kg of acepromazine maleate 0.2% (Acepran, Vetnil, Brazil) and 0.5 mg/kg of morphine (Dimorf, Cristália, Brazil) intramuscularly (IM). In cases of insufficient analgesia for the correct positioning of the animal, intravenous (IV) propofol (Propovan, Cristália, Brazil) was administered to effect. Radiographic evaluations included the ventrodorsal and lateral views following the standards set by the *Orthopedic Foundation for Animals* (OFA). The degree of HD was measured according to the standard established by evaluation of hip radiographs, in which coxofemoral joints were classified into 5 classes, from A to E [22, 23]. Category A represents normal joints, while category E represents the most severely affected joints. All the dogs included in this study were classified as grade D or E. The radiological criteria of joint OA severities used in this study were based on the Takahashi scoring system [citar]: grade 0 (normal) = not affected; grade I (mild) = doubtful narrowing of joint space and possible osteophytic lipping; grade II (moderate): definite osteophytes and possible narrowing of joint space; grade III (severe): moderate multiple osteophytes, definite narrowing of joints space, some sclerosis, and possible deformity of bone contour; and grade IV (very severe): large osteophytes, marked narrowing of joint space, severe sclerosis, and definite deformity of bone contour [24].

2.3. Treatments. In a double-blind, controlled clinical trial the dogs were randomly assigned to receive IA hyaluronic acid (Hyal, $n = 8$) or saline solution (Control, $n = 8$). A random number generator (Research Randomizer, computer software, https://www.randomizer.org/) was used to assign

Table 1: Clinical scoring system for assessing dogs.

Criterion	Grade	Clinical evaluation
Pain on palpitation	0	No signs of pain on palpation of the affected joint
	1	Slight signs of pain on palpation of the affected joint, the dog turns its head in recognition
	2	Moderate signs of pain on palpation of the affected joint, the dog pulls the limb as a defense reaction
	3	Severe signs pain on palpation, the dog vocalizes or becomes aggressive
	4	The dog does not allow palpation
Lameness	0	Normal, no lameness
	1	Mild lameness, not very difficult to move
	2	Clear lameness, not moving freely
	3	Obvious lameness when walking
	4	Severe lameness preventing the dog from supporting weight on the affected limb
Ability to jump	0	Jumps normally
	1	Jumps with care
	2	Jumps with some difficulty
	3	Jumps or rises with great difficulty
	4	Does not try because of the difficulty/pain
Ability to climb stairs	0	Goes up and down the stairs normally
	1	Slightly careful, uses both paws successively
	2	Sometimes uses both feet at the same time, evidently does not move freely
	3	Goes up the stairs like a rabbit at all times, goes up the stairs with great difficulty
	4	Does not try to climb because of the difficulty/pain

the dogs to each of the two groups with block randomization. For the treatment allocation, the dogs received consecutive numbers based on the order of enrollment in the study. After the dogs were entered into the study by a veterinary surgeon, the assigned numbers were sent to a research assistant who prepared the injections according to the numbers received.

Each dog in the Hyal group received an IA injection of hyaluronic acid (Hyalovet, Hetacarpe, Brazil) at doses of 5 mg (animals weighing less than or equal to 10 kg) or 10 mg (animals weighing more than or equal to 11 kg) in both affected joints. The formulation injected was composed of purified HA, with a low MW (500–730 kDa) and a concentration of 10 mg/mL; it was not cross-linked by a chemical agent. An equivalent volume of 0.9 per cent saline solution was administered to the Control group. In addition, the dogs in the Control group were treated with an oral nutraceutical (Condroton, Vetnil, Brazil; every 12 h for 90 days) and carprofen (Rymadil, Bayer, Brazil; 2.2 mg/kg every 12 h for 15 days). For the nutraceutical, the dosing regimen was 750 and 1000 mg, respectively, for dogs weighting 10.0–20.0 and 21.0–50.0 kg. The nutraceutical formulation contained glucosamine, chondroitin sulfate, and collagen.

The dogs were positioned in lateral recumbency with the affected hip uppermost. The hair over the lateral aspect of the hip was clipped and the skin aseptically prepared. The articular access was guided by ultrasound, with the animals under inhalational anaesthesia. Arthrocentesis was performed through a craniolateral approach and confirmed through aspiration of synovial fluid. The hip infiltration was performed with the patient anaesthetized. All dogs were premedicated with IM acepromazine maleate 0.2% (0.03 mg/kg) associated with morphine (0.5 mg/kg), both in the same syringe. Twenty min later, the cephalic vein was catheterized and general anaesthesia was introduced using propofol. Orotracheal intubation was performed, and anaesthesia was maintained with isoflurane (Isoforine, Cristália, Brazil) in oxygen using a small animal rebreathing circuit (SAT 500, Takaoka, Brazil). Lactated Ringer's solution was administered at 10 mL/kg/h until recovery.

Twenty-four hours after the IA injection, the owners were asked by telephone to provide information on the behaviour of their dog during this period including questions on the presence of skin irritation or discomfort (such as licking or biting the injection site, any increase in the degree of lameness, greater difficulty in getting up or lying down, or the occurrence of vocalization).

2.4. Owner Assessment. In addition to the periodic evaluations performed by the veterinarian, the dogs were evaluated by the owners at home using two descriptive questionnaires: Helsinki Chronic Pain Index (HCPI) [25] and the Canine Brief Pain Inventory (CBPI) [26, 27] including the total pain scores (TPS) and those referring to pain severity scores (PSS) and pain interference scores (PIS).

Clinical improvement was associated with a decrease of at least 30% in the overall CBPI and/or HCPI posttreatment scores in comparison with the pretreatment values.

The evaluations performed by the veterinarian and the owners of the dogs were carried out prior to treatment (baseline) and 15, 30, 60, and 90 days after the IA injection. During the evaluation period (90 days), systemic analgesic therapy (carprofen, 2.2 mg/kg every 12 h for one week) was permitted in cases where the sum of the scores evaluated by the owner exceeded 50% of the total possible value evaluated by the CBPI and/or HCPI. In the case of alterations in the digestive system, such as appetite loss, anorexia, and/or episodes of vomiting, concomitant oral administration of the gastric mucosa protector, omeprazole (0.17 mg/kg every 24 hours), was permitted.

2.5. Adverse Effects. The manifestation of adverse effects such as pain, the presence of bruising at the injection site, the occurrence of vomiting, or diarrhea was evaluated.

2.6. Outcome Measures. The primary outcome measures were the CBPI and HCPI pain scales. Secondary outcome measures included veterinary assessment score, quality of life, and requirement for the rescue analgesia.

2.7. Statistical Analysis. The sample size was estimated to be a minimum of eight animals per group for a power test of

Table 2: Mixed model for repeated measurements of Helsinki Chronic Pain Index (HCPI) scores, Canine Brief Pain Inventory (CBPI, total) scores, and the scores evaluated by the veterinarian prior to treatment (i.e., baseline) and over time in dogs treated with intra-articular hyaluronic acid (Hyal, $n = 8$) or traditional conservative treatment (Control, $n = 8$).

Effect	F test	P
HCPI		
Time	20.88*	<0.001
Interaction time × treatment	1.80	0.18
CBPI		
Time	20.44*	<0.001
Interaction time × treatment	1.28	0.30
MedVet scores		
Time	22.68*	<0.001
Interaction time × treatment	4.62	0.003

*Significant differences over time ($P < 0.05$).

80%, alpha level of 5%, and a standard deviation (SD) of 12 to identify a reduction in the CBPI scores of 30% compared to baseline. SD was estimated from a pilot study.

The data were submitted to the Shapiro-Wilk and Kolmogorov-Smirnov normality tests to identify the distribution. For the variables weight, age, duration of symptoms, and overall clinical improvement, the unpaired t test was used to compare the groups. The sum of the scores evaluated by the veterinarian and the owners (CBPI and HCPI) was evaluated through analysis of variance (ANOVA) and Tukey's test to compare differences between groups and differences over time within the same group. Relationships between age, weight, and primary outcome measures at baseline and after treatment were examined using the Pearson Rank correlation statistic. The differences between treatments at each time, differences in time for each treatment, and interaction between treatment were performed using analysis of variance with the F test followed by Tukey's test using IBM SPSS Statistics Graphpad software. A P value less than 0.05 was considered significant (Table 2).

3. Results

A total of 40 dogs were screened to obtain 18 dogs eligible for inclusion in this study. Of the 22 dogs excluded, 18 dogs did not meet the inclusion criteria because of back pain associated with neurologic deficit ($n = 04$) and no hip OA, lack of OA in hip joints on radiographs ($n = 07$), lack of pain on manipulation of hip joints ($n = 3$), and abnormal laboratory results ($n = 4$). In addition, four of the owners refused to participate in the study. Two dogs were excluded from the study after enrollment because their owners did not complete the evaluations posttreatment.

There were no significant differences between groups in demographic and baseline data (Table 3). In the Hyal group, 50% (4/8) of the dogs were classified as severe degree of OA (grades III to IV) and 50% as moderate degree (grade II) of OA. In the Control group, 25% (2/8) of the dogs were classified as severe degree of OA (grades III to IV) and 75% as mild to moderate degree (grades I to II) of OA (Table 3).

Table 3: Baseline characteristics of the study population.

Patient data	Hyal ($n = 8$)	Control ($n = 8$)	P (value)
Body weight (kg)[a]	18 ± 8	22.7 ± 10	0.14
Age (years)[a]	8 ± 5	4.6 ± 2.3	0.09
Male/female	4/4	3/5	
Clinical severity			
Grade D	7/8	7/8	
Grade E	1/8	1/8	
Affected hip joint			
Bilateral	7/8	7/8	
Unilateral	1/8	1/8	
Breeds			
Labrador	1/8	3/8	
Crossbreed	2/8	2/8	
Boxer	1/8	2/8	
Border Collie	2/8	1/8	
Lhasa Apso	2/8		
Estimated duration of symptoms (years)[a]	1.6 ± 0.5	1.8 ± 0.8	0.13
HCPI at baseline[a]	26.2 ± 8	22.6 ± 6	0.35
CBPI at baseline[a]	41 ± 16	55 ± 16	0.19
Veterinary index at baseline[a]	5.3 ± 1.5	7.25 ± 2	0.11
Degree of OA at baseline[a]	2.6 ± 0.7	2.0 ± 0.7	0.19

[a]Values expressed as mean ± SD.

Compared with the baseline, lower scores were observed in both groups over the 90 days in the veterinarian evaluation ($P < 0.001$), the HCPI ($P < 0.001$), the total CBPI ($P < 0.001$), and the PIS-CBPI ($P < 0.001$ Hyal; $P = 0.019$: Control). In the comparison between groups, lower scores were observed from 60 to 90 days in the CBPI scores (total and PIS) in the Hyal group compared to the Control group. The Hyal group exhibited lower scores from 15 to 90 days compared with the Control group in the veterinarian evaluation (Tables 4 and 5 and Figure 1).

Overall, the scores (HCPI, CBPI, and veterinarian assessment) decreased around 30% from 15 to 90 days in the Control group. In the Hyal group, the greatest improvements (≥40%) in the CBPI scores (total, PSS, and PIS), and HCPI scores were noted from 30 to 90 and 60 to 90 days after injection, respectively.

Analgesic intervention was not required during the evaluation period.

Correlations with body weight, age, and clinical severity at trial entry were not significant. In the Hyal group, age was correlated with mean baseline HCPI score (SR = 0.90; $P = 0.002$) and HCPI score at the end of the trial (SR = 0.73; $P = 0.03$).

Clinical improvement was observed in 50% (4/8) of the animals in the Control group and 100% (8/8) of the animals

Table 4: Patient characteristics of sixteen dogs treated with intra-articular hyaluronic acid (Hyal, $n = 8$) or traditional conservative treatment (Control, $n = 8$).

Group/number of dog	Degree of OA	Weight (kg)	Age (years)	Breed	Improvement index CBPI (%)	Improvement index HCPI (%)
Hyal						
01	4	27	08	Labrador	34	27
02	2	19	02	Crossbreed	41	25
03	3	25	09	Boxer	69	31
04	2	22	1.5	Border Collie	79	98
05	2	12	15	Crossbreed	60	47
06	3	07	11	Lhasa Apso	49	0.5
07	2	09	11	Lhasa Apso	39	17
08	3	24	07	Border Collie	50	28
Control						
01	1	10	02	Crossbreed	51	28
02	2	30	05	Labrador	28	26
03	2	15	05	Crossbreed	10	20
04	3	28	07	Boxer	38	30
05	1	22	02	Border Collie	34	22
06	3	25	08	Labrador	23	32
07	2	24	02	Boxer	44	26
08	2	28	06	Labrador	19	27

Table 5: Helsinki Chronic Pain Index (HCPI) scores, Canine Brief Pain Inventory (CBPI) scores referring to total pain scores (TPS), pain severity scores (PSS), pain interference scores (PIS), and the scores evaluated by the veterinarian prior to treatment (i.e., baseline) and over time in dogs treated with intra-articular hyaluronic acid (Hyal, $n = 8$) or traditional conservative treatment (Control, $n = 8$).

Variables	Groups	Time of assessment					$^{*}P$ value
		Baseline	15 days	30 days	60 days	90 days	
HCPI score	Hyal	26 ± 8	19 ± 10*	19 ± 11*	17 ± 11*	16 ± 11*	$P < 0.001$
% change			28%	27%	40%	43%	
HCPI score	Control	22 ± 6	15 ± 3*	17 ± 3*	16 ± 4*	17 ± 5*	$P < 0.001$
% change			31%	22%	29%	24%	
CBPI TPS	Hyal	41 ± 16	25 ± 17*	22 ± 18*	20 ± 18$^{*\#}$	17 ± 16$^{*\#}$	$P < 0.001$
% change			36%	50%	54%	64%	
CBPI TPS	Control	55 ± 16	35 ± 12*	35 ± 13*	38 ± 11*	38 ± 11*	$P < 0.001$
% change			32%	31%	28%	28%	
$^{\#}P$ value					0.03	0.02	
CBPI PSS	Hyal	13 ± 5	10 ± 7	9 ± 8	9 ± 7	8 ± 7	
% change			30%	40%	40%	49%	
CBPI PSS	Control	18 ± 6	14 ± 5	14 ± 4	15 ± 5	15 ± 5	
% change			31%	33%	30%	27%	
CPBI PIS	Hyal	27 ± 12	15 ± 12*	12 ± 10*	11 ± 9$^{*\#}$	9 ± 9$^{*\#}$	$P < 0.001$
% change			30%	40%	40%	49%	
CPBI PIS	Control	34 ± 11	21 ± 8*	21 ± 6*	22 ± 7	22 ± 5	$P = 0.019$
% change			30%	30%	31%	32%	
$^{\#}P$ value					0.02	0.02	
Vet score	Hyal	5 ± 1	3 ± 2$^{*\#}$	2 ± 1$^{*\#}$	2 ± 1$^{*\#}$	2 ± 1$^{*\#}$	$P < 0.001$
% change			42%	56%	64%	57%	
Vet score	Control	7 ± 2	5 ± 1*	6 ± 2*	6 ± 2*	6 ± 1*	$P < 0.001$
% change			24%	20%	13%	13%	
$^{\#}P$ value			0.01	0.001	0.001	0.002	

Note: data are expressed as mean ± standard deviation (SD). *Significantly different from baseline values. $^{\#}$Significantly different from Control group. ANOVA with posttest Tukey-Kramer multiple comparisons test ($P < 0.05$).

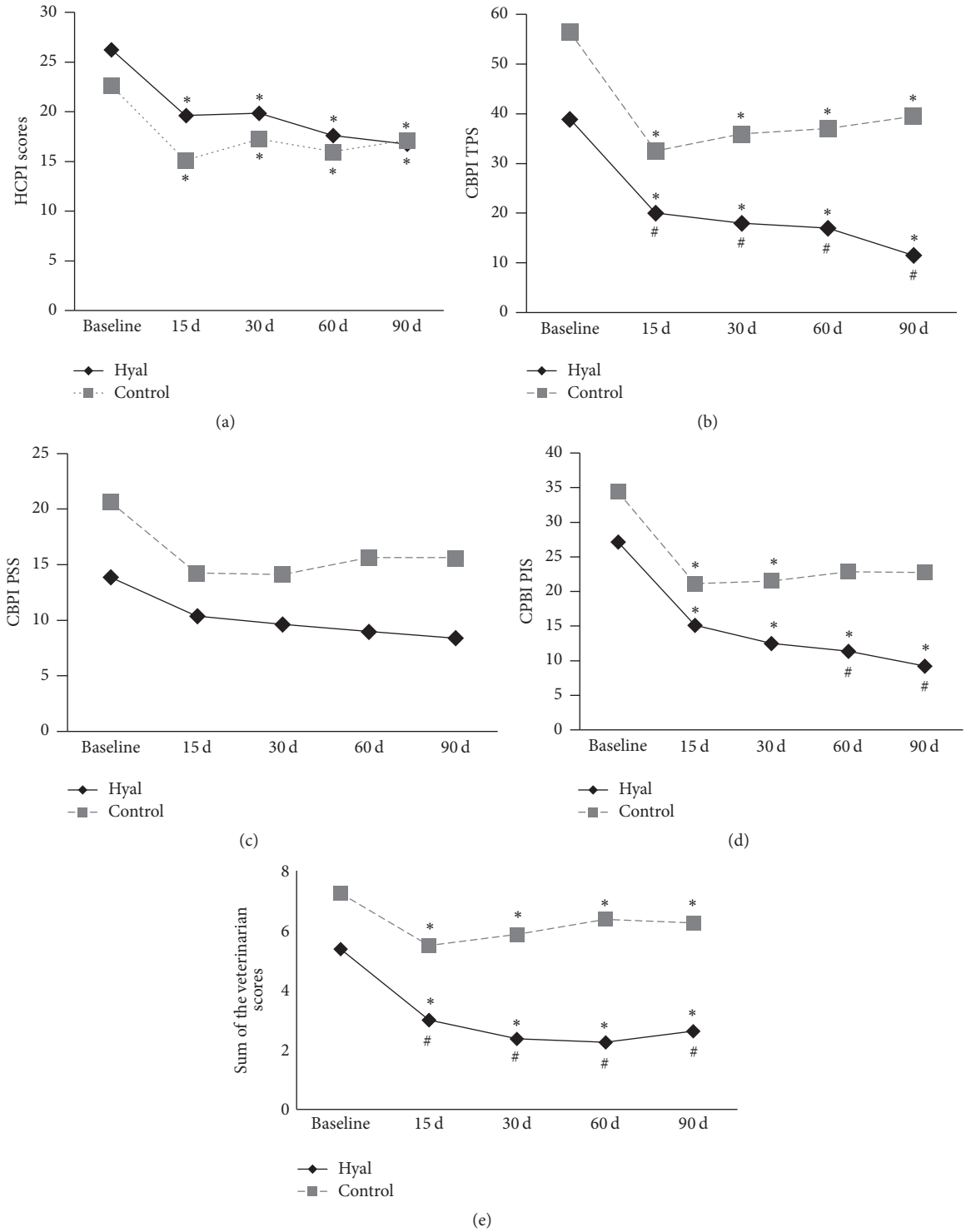

Figure 1: Helsinki Chronic Pain Index (HCPI) scores (a), Canine Brief Pain Inventory (CBPI) scores referring to total pain scores (TPS) (b), pain severity scores (PSS) (c), pain interference scores (PIS) (d), and the scores evaluated by the veterinarian (e) prior to treatment (i.e., baseline) and over time in dogs treated with intra-articular hyaluronic acid (Hyal, $n = 8$) or traditional conservative treatment (Control, $n = 8$). *Significantly different from baseline values. #Significantly different from Control group. ANOVA with posttest Tukey-Kramer multiple comparisons test ($P < 0.05$).

in the Hyal group, through the total-CBPI evaluation, and the difference was considered significant ($P = 0.028$). In the evaluation using the HCPI, the incidence of clinical improvement was observed in 25% (2/8) of the animals in the Control group and 50% (4/8) of the animals of the Hyal group for the evaluation with CBPI, with no difference between groups ($P = 0.396$).

The total indices evaluated by the owners using total CBPI showed an average of 56.4% and 29.6% clinical improvement in animals from the Hyal and Control groups, respectively, a statistical difference being detected between groups ($P = 0.010$). Using the HCPI, improvement indices were 34% and 24% in animals from the Hyal and Control groups, respectively, with no statistical difference between treatments ($P = 0.505$).

With respect to the overall impression of the dogs at the end of treatment, 75% of owners evaluated the quality of life as very good to excellent in the dogs of the Hyal group, while in the Control group the majority of owners (75%) evaluated the quality of life as good; a statistical difference was detected between the groups ($P = 0.046$).

Regarding adverse effects, three animals (two in the Hyal group and one in the Control group) demonstrated signs of pain in the first 24 h after the IA injection. Alterations in the digestive system were not observed, and the gastric mucosa protector was not required.

4. Discussion

This is the first study to compare the use of IA injection of HA with TCT in dogs with OA in the hip joint. Our results suggest that both treatments reduced the clinical signs of hip OA; however greater improvement was achieved in dogs with HA given by intra-articular injection, confirming the hypothesis of the study.

The HA dose administered was based on previous studies in dogs [20, 28]. There is no consensus in the current literature with respect to the required number of IA applications of HA to obtain satisfactory results. Studies developed with humans have reported success with a single IA application [29, 30] and with multiple applications at weekly intervals [15, 31]. In dogs undergoing surgical correction of patellar luxation, a single IA application of HA at the end of surgery resulted in similar effects to the application of two doses at weekly intervals [20]. In humans, similar results were reported by Kolarz et al. [32], who demonstrated that, in treatment with HA intra-articular injection, single or multiple applications resulted in similar beneficial effects in patients with signs of OA. In the current study, we opted for the single application of HA without the use of other associated medications due to the lack of published data on this treatment for dogs with HD/OA. However, the efficacy of single and multiple injections of HA in dogs with OA would be an interesting subject for further studies.

Clinical reports have demonstrated beneficial effects on pain, function, and patient global assessment especially 5–13 weeks following IA HA injection [31, 33]. The majority of studies have shown a percent improvement from baseline of 28–54% for pain and 9–32% for function [13, 15, 17]. Similarly, in the current study, the most significant decreases in the owner-based assessment scores (≤40%) were observed from 30 to 90 days (4 to 12 weeks) after HA injection. Clinical improvements in CBPI and in HCPI scores were seen in both treatment groups. However, significant differences in both CBPI (total and PIS scores) and HCPI scores were only seen from 60 to 90 days in the Hyal group in comparison to the Control group. These findings are in accordance with the results of other investigations that described a long-lasting benefit of HA [30, 31, 33]. In addition, it is possible that the treatment with carprofen given to the Control group could mask the differences between groups in the 30-day period following IA injection. The treatment prescribed for the Control group was based on the treatment commonly used by veterinarians to reduce clinical signs of HD in dogs. The anti-inflammatory chosen was carprofen, as it is one of the most widely studied NSAIDs in dogs with OA [34, 35], which several clinical studies have confirmed regarding the safety of this drug for periods exceeding 15 days of treatment [11, 34].

In the present study, the total indices evaluated by the owners of the dogs using the CBPI demonstrated a greater clinical improvement in animals treated with HA (56.4%) compared to the Control group (29.6%). Similar results have been reported in humans with knee OA, with reports of higher efficiency in the reduction of joint pain over 12 weeks in patients treated with HA compared to those treated with triamcinolone, both via IA [30].

It is known that factors such as body weight, age, and degree of cartilage degeneration can influence the efficacy of OA treatment [31]. In the current study, the randomization of dogs between treatments resulted in groups that were not completely homogeneous. Thus, there was a difference with regard to body weight, age, and degree of OA. In the Control group the sample consisted of a superior proportion of larger (<20 kg) and younger (≤7 years) dogs than the Hyal group. Body weight can influence degenerative joint disease by affecting the stresses on joints and smaller dogs may be better able to compensate for orthopedic disease compared to larger dogs [26]. Using TCT, only two of six larger dogs exhibited an overall clinical improvement with treatment. Interestingly, all the larger dogs treated with HA achieved an improvement of 30% or more at 12 weeks. This finding may be attributed to the viscoelastic properties of HA, which act as a lubricant and shock absorber [13]. These effects are related to a reduction in sensitivity to mechanical forces of stretch-activated channels present in the membrane of joint mechanonociceptors [20].

As expected, the older dogs exhibited a superior degree of OA (grades III and IV) compared to younger dogs. In general, the older dogs showed a clinical improvement with both treatments. However, a greater improvement was seen in the dogs treated with HA. This result can be explained by the various mechanisms of HA, including restoration of the elastic and viscous properties of the synovial fluid and anti-inflammatory, antinociceptive, and chondroprotective effects. Experimental animal models of OA have reported that intra-articular HA injections may decrease degradation of the cartilage matrix. Zhang et al. [36] showed that HA

injections provided better cartilage and synovial conditions than a placebo in rats submitted to surgically-induced OA. Another study demonstrated that cross-linked HA alone or in combination with ropivacaine or triamcinolone produced a significant improvement in knee articular cartilage in a rabbit model of collagenase-induced knee osteoarthritis [37].

Another important aspect is the correlation between clinical improvement indices and the quality of life for the dogs. In animals treated with HA, 75% of owners considered the quality of life of the animals after treatment to be very good to excellent. These results corroborate previous studies reported in humans, which attributed the best quality of life indices to patients who responded favorably to analgesic therapies, demonstrating a direct correlation between the relief of chronic pain and improved quality of life [15, 30].

One of the most relevant aspects of the present study refers to the advantages conferred by treatment with HA compared to TCT in dogs with HD/OA. From a clinical point of view, the most interesting factor concerns the possibility of using HA in isolation, without the need for additional analgesia 90 days after the IA administration, since NSAIDs may induce adverse effects when administered for prolonged periods, in addition to representing a risk factor for animals with a history of clotting disorders or renal and digestive diseases [11]. In parallel, the administration of a single IA injection of HA is a highly practical form of treatment, eliminating the daily oral administration of a nutraceutical or NSAID, a limiting factor in the treatment of dogs reluctant to swallow medication or that demonstrate aggressive behaviour. However, despite the favorable results obtained in this study, the therapeutic choice should be made on individual basis, carefully weighing the relative benefits and disadvantages of the treatment.

Although rare, complications of IA injections, such as joint infection, pain following injection, and skin pigment may occur. In the present study, no serious adverse events were noted. Of the 16 dogs evaluated, only three owners reported signs compatible with discomfort in the first 24 hours following the IA injection and this was of a temporary nature and did not represent clinical relevance. This result supports previous studies that reported minimal adverse effects following IA injection in humans [15, 31] and dogs [20, 28]. Another unfavorable aspect is related to the requirement of general anaesthesia for the hip infiltration, which may represent a limitation factor for some dogs.

Pain evaluation in animals is a difficult challenge, due to the impossibility of verbal expression, which makes the measurement of this parameter extremely subjective on the part of the evaluators. Many studies have been developed in order to improve the scales used in the evaluation of chronic pain, involving not only the evaluation by the researcher [21] but also the use of multifactorial questionnaires directed to the owners of the animals, taking into account behavioral change, walking ability, signs of pain, and quality of life [25–27]. In the present study, the experimental design was double-blind to minimize any bias in the results on the part of the researcher or the owners of the animals. In addition, the clinical evaluation of the dogs was performed by a veterinary orthopedic surgeon experienced in the evaluation of animals with OA, who has previously participated in other studies involving dogs with OA. In addition, as the pain scales are considered extremely subjective, in the present study, all the measurements were performed by the same trained observer, in an attempt to control the variability between different assessors.

The questionnaires used in the present study have been validated for evaluation of chronic pain in dogs with OA [25–27]. The results reported by the owners demonstrated greater differences between groups for evaluations using the CBPI. In dogs with OA, this questionnaire was capable of identifying clinical improvement in animals treated with NSAIDs compared to a placebo, suggesting it to be a viable method for evaluating the clinical evolution of dogs with OA [26, 27]. Differences were not found between the groups over time when using the HCPI. Similar results were observed by Teixeira [38] who used this questionnaire for the evaluation of clinical signs in dogs with HD subjected to different treatments. In this study, many of the owners demonstrated some degree of difficulty in completing HCPI questionnaire, which may have affected the outcome of the evaluation. Furthermore, although the owner-based questionnaires used in this study have been validated, it is possible that more reliable results could be obtained with an objective outcome measure such as kinetic force plates.

This study has some limitations. Among them, we can highlight the small number of animals evaluated. With a larger sample more reliable results could be demonstrated. Furthermore, the number of animals involved in the study was restricted due to the inclusion criteria and also the need for the owner's consent. Some of the owners refused to participate in the study due to the necessity of general anaesthesia in order to access the hip joint; many of the dogs were of an advanced age which increased the concern of the owners. Another limiting factor of the study is the large heterogeneity of the studied population. Although significant differences were not found in the demographic data, there was considerable individual variation with regard to body weight (07 to 35 kg), age (1.5 to 15 years), and breeds evaluated. Initially it was expected that body weight would be similar due to the higher incidence of the HD in large breeds. However, contrary to expectations, the breeds were diverse. Furthermore, despite the selection of animals with chronic pain associated with hip OA, the intensity of clinical signs and duration of disease progression differed between individuals. However, these differences are inherent in clinical studies, and form part of those variables that cannot be fully controlled and reveal the reality of clinical practice. In addition, our study design did not include a third group for evaluation of both treatments in combination. While HA and oral nutraceuticals have different mechanisms of action, simultaneous administration of the two drugs could result in a synergistic effect. Besides this, it is possible that saline in isolation might have had a positive effect, as reported by Gaustad et al. [39]. Thus, the inclusion of a fourth group using only TCT could lead to a better understanding of how the different treatments act in dogs with hip OA.

It was concluded that both treatments reduced the clinical signs of hip OA; however, the best results were obtained with

IA injection of HA, which may represent a viable alternative for dogs with OA induced by HD. Therefore, additional larger and long-term (up to one year) studies are needed to support these results. Additionally, future research should focus on cost effectiveness of therapy and relation between molecular weight and effectiveness.

Competing Interests

The authors declare that there is no conflict of interest regarding the publication of this manuscript.

Acknowledgments

This paper was supported by the CNPq (Conselho Nacional de Desenvolvimento Científico e Tecnológico). Special thanks are due to the owners of the dogs for their contribution.

References

[1] K. L. Tsai and K. E. Murphy, "Clinical and genetic assessments of hip joint laxity in the Boykin spaniel," *Canadian Journal of Veterinary Research*, vol. 70, no. 2, pp. 148–150, 2006.

[2] J. W. Alexander, "The pathogenesis of canine hip dysplasia," *Veterinary Clinics of North America: Small Animal Practice*, vol. 22, no. 3, pp. 503–511, 1992.

[3] G. K. Smith, P. D. Mayhew, A. S. Kapatkin, P. J. McKelvie, F. S. Shofer, and T. P. Gregor, "Evaluation of risk factors for degenerative joint disease associated with hip dysplasia in German shepherd dogs, golden retrievers, labrador retrievers, and rottweilers," *Journal of the American Veterinary Medical Association*, vol. 219, no. 12, pp. 1719–1724, 2001.

[4] S. A. Johnston, R. M. McLaughlin, and S. C. Budsberg, "Nonsurgical management of osteoarthritis in dogs," *Veterinary Clinics of North America: Small Animal Practice*, vol. 38, no. 6, pp. 1449–1470, 2008.

[5] H.-G. Schaible, M. Schmelz, and I. Tegeder, "Pathophysiology and treatment of pain in joint disease," *Advanced Drug Delivery Reviews*, vol. 58, no. 2, pp. 323–342, 2006.

[6] J. Kitagawa, K. Kanda, M. Sugiura et al., "Effect of chronic inflammation on dorsal horn nociceptive neurons in aged rats," *Journal of Neurophysiology*, vol. 93, no. 6, pp. 3594–3604, 2005.

[7] B. M. Daubs, M. D. Markel, and P. A. Manley, "Histomorphometric analysis of articular cartilage, zone of calcified cartilage, and subchondral bone plate in femoral heads from clinically normal dogs and dogs with moderate or severe osteoarthritis," *American Journal of Veterinary Research*, vol. 67, no. 10, pp. 1719–1724, 2006.

[8] Y.-K. Yim, H. Lee, K.-E. Hong et al., "Electro-acupuncture at acupoint ST36 reduces inflammation and regulates immune activity in collagen-induced arthritic mice," *Evidence-Based Complementary and Alternative Medicine*, vol. 4, no. 1, pp. 51–57, 2007.

[9] G. McCarthy, J. O'Donovan, B. Jones, H. McAllister, M. Seed, and C. Mooney, "Randomised double-blind, positive-controlled trial to assess the efficacy of glucosamine/chondroitin sulfate for the treatment of dogs with osteoarthritis," *The Veterinary Journal*, vol. 174, no. 1, pp. 54–61, 2007.

[10] F. Sauvé, M. Paradis, K. R. Refsal, M. Moreau, G. Beauchamp, and J. Dupuis, "Effects of oral administration of meloxicam, carprofen, and a nutraceutical on thyroid function in dogs with osteoarthritis," *Canadian Veterinary Journal*, vol. 44, no. 6, pp. 474–479, 2003.

[11] S. P. L. Luna, A. C. Basílio, P. V. M. Steagall et al., "Evaluation of adverse effects of long-term oral administration of carprofen, etodolac, flunixin meglumine, ketoprofen, and meloxicam in dogs," *American Journal of Veterinary Research*, vol. 68, no. 3, pp. 258–264, 2007.

[12] K. L. Goa and P. Benfield, "Hyaluronic acid: a review of its pharmacology and use as a surgical aid in ophthalmology, and its therapeutic potential in joint disease and wound healing," *Drugs*, vol. 47, no. 3, pp. 536–566, 1994.

[13] T. Iannitti, D. Lodi, and B. Palmieri, "Intra-articular injections for the treatment of osteoarthritis: focus on the clinical use of hyaluronic acid," *Drugs in R&D*, vol. 11, no. 1, pp. 13–27, 2011.

[14] K. Okazaki and Y. Iwamoto, "Progress of research in osteoarthritis. Gene expression and its regulatory mechanisms in the degenerative cartilage in osteoarthritis," *Clinical Calcium*, vol. 19, no. 11, pp. 1578–1585, 2009.

[15] A. A. C. Zóboli, M. U. Rezende, G. C. Campos, T. Pasqualin, R. Frucchi, and O. P. Camargo, "Prospective randomized clinical trial: single and weekly viscosupplementation," *Acta Ortopedica Brasileira*, vol. 21, no. 5, pp. 271–275, 2013.

[16] T. M. Duymus, S. Mutlu, B. Dernek, B. Komur, S. Aydogmus, and F. N. Kesiktas, "Choice of intra-articular injection in treatment of knee osteoarthritis: platelet-rich plasma, hyaluronic acid or ozone options," *Knee Surgery, Sports Traumatology, Arthroscopy*, 2016.

[17] E. Maheu, F. Rannou, and J.-Y. Reginster, "Efficacy and safety of hyaluronic acid in the management of osteoarthritis: evidence from real-life setting trials and surveys," *Seminars in Arthritis and Rheumatism*, vol. 45, no. 4, supplement, pp. S28–S33, 2016.

[18] E. Qvistgaard, R. Christensen, S. Torp-Pedersen, and H. Bliddal, "Intra-articular treatment of hip osteoarthritis: a randomized trial of hyaluronic acid, corticosteroid, and isotonic saline," *Osteoarthritis and Cartilage*, vol. 14, no. 2, pp. 163–170, 2006.

[19] S. Chandrasekaran, P. Lodhia, C. Suarez-Ahedo, S. P. Vemula, T. J. Martin, and B. G. Domb, "Symposium: evidence for the use of intra-articular cortisone or hyaluronic acid injection in the hip," *Journal of Hip Preservation Surgery*, vol. 3, no. 1, pp. 5–15, 2016.

[20] K. Nganvongpanit, B. Boonsri, T. Sripratak, and P. Markmee, "Effects of one-time and two-time intra-articular injection of hyaluronic acid sodium salt after joint surgery in dogs," *Journal of Veterinary Science*, vol. 14, no. 2, pp. 215–222, 2013.

[21] A. K. Hielm-Björkman, E. Kuusela, A. Liman et al., "Evaluation of methods for assessment of pain associated with chronic osteoarthritis in dogs," *Journal of the American Veterinary Medical Association*, vol. 222, no. 11, pp. 1552–1558, 2003.

[22] W. M. Adams, R. T. Dueland, J. Meinen, R. T. O'Brien, E. Giuliano, and E. V. Nordheim, "Early detection of canine hip dysplasia: comparison of two palpation and five radiographic methods," *Journal of the American Animal Hospital Association*, vol. 34, no. 4, pp. 339–347, 1998.

[23] G. Verhoeven, F. Coopman, L. Duchateau, J. H. Saunders, B. Van Rijssen, and H. Van Bree, "Interobserver agreement in the diagnosis of canine hip dysplasia using the standard ventrodorsal hip-extended radiographic method," *Journal of Small Animal Practice*, vol. 48, no. 7, pp. 387–393, 2007.

[24] M. Takahashi, K. Naito, M. Abe, T. Sawada, and A. Nagano, "Relationship between radiographic grading of osteoarthritis

and the biochemical markers for arthritis in knee Osteoarthritis," *Arthritis Research Therapy*, vol. 6, no. 1, pp. 208–212, 1998.

[25] A. K. Hielm-Björkman, H. Rita, and R.-M. Tulamo, "Psychometric testing of the Helsinki chronic pain index by completion of a questionnaire in Finnish by owners of dogs with chronic signs of pain caused by osteoarthritis," *American Journal of Veterinary Research*, vol. 70, no. 6, pp. 727–734, 2009.

[26] D. C. Brown, R. C. Boston, J. C. Coyne, and J. T. Farrar, "Ability of the Canine Brief Pain Inventory to detect response to treatment in dogs with osteoarthritis," *Journal of the American Veterinary Medical Association*, vol. 233, no. 8, pp. 1278–1283, 2008.

[27] D. C. Brown, R. C. Boston, J. C. Coyne, and J. T. Farrar, "Development and psychometric testing of an instrument designed to measure chronic pain in dogs with osteoarthritis," *American Journal of Veterinary Research*, vol. 68, no. 6, pp. 631–637, 2007.

[28] S. P. Franklin and J. L. Cook, "Prospective trial of autologous conditioned plasma versus hyaluronan plus corticosteroid for elbow osteoarthritis in dogs," *Canadian Veterinary Journal*, vol. 54, no. 9, pp. 881–884, 2013.

[29] C. Ertürk, M. A. Altay, N. Altay, A. M. Kalender, and İ. A. Öztürk, "Will a single periarticular lidocaine—corticosteroid injection improve the clinical efficacy of intraarticular hyaluronic acid treatment of symptomatic knee osteoarthritis?" *Knee Surgery, Sports Traumatology, Arthroscopy*, vol. 2, no. 1, pp. 56–62, 2014.

[30] A. Skwara, R. Ponelis, C. O. Tibesku, D. Rosenbaum, and S. Fuchs-Winkelmann, "Gait patterns after intraarticular treatment of patients with osteoarthritis of the knee-hyaluronan versus triamcinolone: a prospective, randomized, double blind, monocentric study," *European Journal of Medical Research*, vol. 14, no. 4, pp. 157–164, 2009.

[31] F. Rivera, "Single intra-articular injection of high molecular weight hyaluronic acid for hip osteoarthritis," *Journal of Orthopaedics and Traumatology*, vol. 17, no. 1, pp. 21–26, 2016.

[32] G. Kolarz, R. Kotz, and I. Hochmayer, "Long-term benefits and repeated treatment cycles of intra-articular sodium hyaluronate (Hyalgan) in patients with osteoarthritis of the knee," *Seminars in Arthritis and Rheumatism*, vol. 32, no. 5, pp. 310–319, 2003.

[33] D. Brzusek and D. Petron, "Treating knee osteoarthritis with intra-articular hyaluronans," *Current Medical Research and Opinion*, vol. 24, no. 12, pp. 3307–3322, 2008.

[34] S. Mansa, E. Palmér, C. Grøndahl, L. Lønaas, and G. Nyman, "Long-term treatment with carprofen of 805 dogs with osteoarthritis," *The Veterinary Record*, vol. 160, no. 13, pp. 427–430, 2007.

[35] M. Pollmeier, C. Toulemonde, C. Fleishman, and P. D. Hanson, "Clinical evaluation of firocoxib and carprofen for the treatment of dogs with osteoarthritis," *The Veterinary Record*, vol. 159, no. 17, pp. 547–551, 2006.

[36] F.-J. Zhang, S.-G. Gao, L. Cheng et al., "The effect of hyaluronic acid on osteopontin and CD44 mRNA of fibroblast-like synoviocytes in patients with osteoarthritis of the knee," *Rheumatology International*, vol. 33, no. 1, pp. 79–83, 2013.

[37] W.-Y. Tsai, J.-L. Wu, C.-C. Liu et al., "Early intraarticular injection of hyaluronic acid attenuates osteoarthritis progression in anterior cruciate ligament-transected rats," *Connective Tissue Research*, vol. 54, no. 1, pp. 49–54, 2013.

[38] L. R. Teixeira, *Owner assessment of chronic pain and gait analysis of dogs with hip dysplasia treated with acupuncture [Ph.D. thesis]*, São Paulo State University, São Paulo, Brazil, 2015.

[39] G. Gaustad, N. I. Dolvik, and S. Larsen, "Comparison of intra-articular injection of 2 ml of 0.9% NaCl solution with rest alone for treatment of horses with traumatic arthritis," *American Journal of Veterinary Research*, vol. 60, no. 9, pp. 1117–1121, 1999.

Hindawi Publishing Corporation
Evidence-Based Complementary and Alternative Medicine
Volume 2016, Article ID 8387975, 8 pages
http://dx.doi.org/10.1155/2016/8387975

Research Article

The Extrusion Process as an Alternative for Improving the Biological Potential of Sorghum Bran: Phenolic Compounds and Antiradical and Anti-Inflammatory Capacity

Norma Julieta Salazar Lopez,[1] Guadalupe Loarca-Piña,[2] Rocío Campos-Vega,[2] Marcela Gaytán Martínez,[2] Eduardo Morales Sánchez,[3] J. Marina Esquerra-Brauer,[1] Gustavo A. Gonzalez-Aguilar,[4] and Maribel Robles Sánchez[1]

[1]*Departamento de Investigación y Posgrado en Alimentos, Universidad de Sonora, 83000 Hermosillo, SON, Mexico*
[2]*Departamento de Investigación y Posgrado en Alimentos, Facultad de Química, Universidad Autónoma de Querétaro, 76010 Santiago de Querétaro, QRO, Mexico*
[3]*Instituto Politécnico Nacional, Centro de Investigación en Ciencia Aplicada y Tecnología Avanzada, 76090 Santiago de Querétaro, QRO, Mexico*
[4]*Centro de Investigación en Alimentación y Desarrollo, A.C., 83304 Hermosillo, SON, Mexico*

Correspondence should be addressed to Maribel Robles Sánchez; rsanchez@guayacan.uson.mx

Received 27 May 2016; Revised 1 August 2016; Accepted 14 August 2016

Academic Editor: Xiang Liu

Approximately 80% of sorghum phenolic compounds are linked to arabinoxylans by ester bonds, which are capable of resisting the digestion process in the upper gastrointestinal tract, compromising their bioaccessibility and biological potential. The aim of this study was to evaluate the effect of the extrusion process on the content of phenolic compounds in sorghum bran and its impact on phenolic compounds and antiradical and anti-inflammatory capacity. Results revealed that the extrusion process increased total phenol content in sorghum bran compared to nonextruded sorghum, particularly for extrusion at 180°C with 20% moisture content (2.0222 ± 0.0157 versus 3.0729 ± 0.0187 mg GAE/g +52%), which positively affected antiradical capacity measured by the DPPH and TEAC assays. The percentage of inhibition of nitric oxide (NO) production by RAW cells due to the presence of extruded sorghum bran extract was significantly higher than that of nonextruded sorghum bran extract ($90.2 \pm 1.9\%$ versus $76.2 \pm 1.3\%$). The results suggest that extruded sorghum bran could be used as a functional ingredient and provide advantages to consumers by reducing diseases related to oxidative stress and inflammation.

1. Introduction

Sorghum, the fifth most important cereal grown in the world, is resistant to semiarid climates, gluten-free, and a good source of phytochemical compounds that have been associated with antioxidant, anti-inflammatory, and antiproliferative capacities [1–4]. The biological potential of sorghum has been related to the presence of different hydroxycinnamic acids (HCAs) such as ferulic, ρ-coumaric, caffeic, and sinapic acids.

However, much of the biological potential of sorghum is not used by biological systems due to the structural properties of their phenolic acids. Approximately 80% of these compounds are linked by ester bonds to arabinoxylans (ARAs), located mainly in the cell walls of the pericarp and the aleurone layer [5, 6]. The linkage between HCAs and ARAs restricts their bioaccessibility and further bioavailability because ARAs are resistant to the digestion process in the upper gastrointestinal tract, which compromises their absorption. Therefore, it is necessary to find processes that

increase the bioaccessibility of the phenolic compounds prior to intake of this cereal.

The structure of arabinoxylans can be hydrolyzed by chemical processes, thermal processes, fermentation, enzymatic action, or a combination of these processes [7–11]. Rosa et al. [12] reported an increase in bioaccessibility of 86% of ferulic acid from the aleurone layer in wheat with the use of xylanase and ferulic esterase. Bartolomé and Gómez-Cordovés [13] found approximately 70% and 5% of ferulic acid and ρ-coumaric acid, respectively, released from barley using commercial enzyme preparations. However, enzymatic processes in sorghum can be more complicated than in wheat or barley because the sorghum arabinoxylan structure is more substituted, which is more difficult for the enzyme to gain access to the attached sites between ferulic acid and arabinose; therefore, chaperone enzymes are necessary [14–17]. Cardoso et al. [11] and Afify et al. [18] reported a loss of phenolic compound content and antioxidant capacity after the traditional processes of wet cooking and soaking of sorghum. On the other hand, Zielinski et al. [19] and Gumul and Korus [20] reported an increase in total phenolic content and hydroxycinnamic acids, mainly ferulic acid, in barley, rice, oats, wheat, and rye, after extrusion processes. These studies reveal that extrusion is a promising process in the production of functional foods based on cereals [19, 20].

Extrusion consists of heat and mechanical treatments under different conditions of low moisture, shear, and high pressure by producing structural alterations and changes in functional properties in a short time [21]. The effect of extrusion on the content of nutrients and nonnutritious components such as phenolic compounds depends on the process conditions and the food matrix [21]. The aim of this study was to evaluate the effect of the extrusion process under different temperature and moisture levels on the content of phenolic compounds and antiradical and anti-inflammatory capacity in sorghum bran.

2. Materials and Methods

2.1. Materials and Chemicals. Antibiotic-antimycotic, fetal bovine serum, sodium pyruvate, and Dulbecco's modified Eagle's medium (DMEM) were obtained from Gibco (Grand Island, NY, USA). All other reagents were purchased from Sigma-Aldrich (Saint Louis, Missouri, USA).

2.2. Sorghum Sample Preparation. Sorghum grains (*Sorghum bicolor* L. Moench), unpigmented variety (UDG110), were provided by the Produce Foundation, Mexico. The sorghum grains were decorticated using abrasive discs for 6 min and further ground using Pulvex 200 mill to pass through a 0.4 mm sieve. The sorghum bran was stored at −20°C until analysis.

2.3. Extrusion Procedure. The sorghum bran was allowed to hydrate for 8 h (20% and 30%) before extrusion and processed in an extruder (prototype) with a single screw with length of 45 cm and two jackets with length of 15 and 10 cm. The temperature of the first jacket was controlled to 60°C, while that of the second jacket was set to 110°C or 180°C. The screw speed was 15 rpm and the die diameter was 5 mm. The extrudates were dried in an oven at 60°C for 6 h. The dried products were ground and sieved with a 0.4 mm sieve and stored at −20°C until analysis.

2.4. Preparation of Sorghum Bran Extracts. Extruded sorghum bran (EB) or nonextruded sorghum bran (NEB) extracts were prepared as follows: 1 g of each sample was mixed with 15 mL of 80% aqueous methanol, sonicated for 1 h (100 W power output), and centrifuged at 1500 ×g for 15 min [6]. The supernatants were separated, and the residues were extracted twice for 30 min. Extracts were filtered through Whatman number 1 paper and evaporated to dryness in a rotary evaporator at 35°C, and samples were redissolved in 5 mL of 50% methanol for the analysis of total phenolic content, phenolic acid content, and antiradical capacity. The extracts were lyophilized and redissolved in DMSO for the cell culture tests.

2.5. Quantification of Phenolic Acids by UHPLC-DAD. The phenolic acid content in EB and NEB extracts was quantified using UHPLC system (Agilent Technologies, Germany) with a diode array detector. The separation was conducted on a Zorbax Eclipse Plus C18 rapid resolution column (50 mm × 2.1 mm i.d., 1.8 μm particle size). Column temperature was set to 30°C. A binary phase solvent system was used, A (0.1% acetic acid/water) and B (0.1% acetic acid/methanol), at a flow rate of 0.7 mL/min. The solvent gradient was as follows: initial 91% of A and 9% of B; 0–11 min, 9% to 14% B; and 11–15 min, 15% B. Detection of the acids was performed at 280 nm, and their quantitation was performed with curves established using external standards of caffeic, ρ-coumaric, ferulic, and sinapic acids. The results were expressed as μg phenolic acid per gram of dry weight [22].

2.6. Determination of Total Phenolic Content. The total phenolic content of the EB and NEB extracts was determined by the colorimetric method at 765 nm using the Folin–Ciocalteu reagent [23]. The results were expressed as mg of gallic acid equivalents (GAE) per gram of dry weight.

2.7. Antiradical Capacity

2.7.1. DPPH Assay. This assay is based on the measurement of the scavenging ability of antioxidants towards the stable radical DPPH relative to the DPPH scavenging ability of the water-soluble vitamin E analogue Trolox. Briefly, 3.9 mL aliquots of DPPH (0.0634 mM) solution were added to the test tubes, and 0.1 mL of sorghum bran extracts (EB or NEB) or Trolox standards (0 to 20 μM range) were added and shaken vigorously. The tubes were allowed to stand at 25°C for 60 min. A control reaction was prepared as above without any extract, and methanol was used for the baseline correction. Changes in the absorbance of the samples were measured at 515 nm. Radical scavenging activity was expressed as the percent inhibition. The final DPPH values were calculated by using a regression equation between the Trolox concentration and the percent inhibition and were expressed as micromoles of Trolox equivalents per gram of dry weight [24].

2.7.2. Trolox Equivalent Antioxidant Capacity (TEAC). The antiradical potential was determined using 2,2′-azino-bis(3-ethylbenzothiazoline-6-sulfonic acid) diammonium salt (ABTS) [25]. This assay is based on the ability of antioxidants to scavenge the blue-green $ABTS^{\bullet+}$ radical cation, relative to the $ABTS^{\bullet+}$ scavenging ability of the water-soluble vitamin E analogue Trolox. The $ABTS^{\bullet+}$ radical cation was generated by the interaction of 5 mL of 7 mM ABTS solution and 88 μL of 140 mM $K_2S_2O_8$ solution. The working solution was prepared with 1 mL of the active radical and 88 mL of ethanol for initial absorbance of 0.70 ± 0.2 at 734 nm using a Cary 50 Varian Spectrophotometer. After the addition of 2.9 mL of $ABTS^{\bullet+}$ solution to 0.1 mL of each extract or Trolox standards (0 to 20 μM range), the absorbance was monitored exactly 1 and 30 min after the initial mixing until the absorbance was stable. The percentage of absorbance inhibition at 734 nm was calculated and plotted as a function of that obtained for the extracts and the standard reference (Trolox). The final TEAC values were calculated by using a regression equation between the Trolox concentration and the percentage inhibition and expressed as micromoles of Trolox equivalents per gram of dry weight.

2.8. Anti-Inflammatory Capacity

2.8.1. Cell Culture. Mouse macrophage cell line RAW 264.7 was obtained from cryopreserved culture kindly provided by the Autonomous University of Queretaro, Mexico, which was originally from the ATCC (American Type Culture Collection). Macrophages were cultured in DMEM (Dulbecco's modified Eagle's medium) supplemented with 10% fetal bovine serum, 1% antibiotic-antimycotic, 1.5 g/L sodium bicarbonate, and 1 mL/L sodium pyruvate (1 mM) on a 60 mm plate and grown at 37°C and 5% CO_2 in a humidified atmosphere [26].

2.8.2. Effect of Sorghum Bran Extract on Cell Viability. RAW cells were cultured in 96-well plates at 1×10^4 cells/well at 37°C and 5% CO_2 for 24 h. Then, the culture medium was replaced by fresh medium in the absence (control viability 100%) and presence of different concentrations of extruded sorghum extract and nonextruded sorghum extract (extract equivalent to 4.3–10.1 mg sorghum/mL) previously lyophilized and dissolved in <1% DMSO. The culture was incubated for 24 h, and the medium was removed. The adhered cells were treated with 200 μL of MTT dissolved in DMEM free of fetal bovine serum and incubated for 2 h. The transformation of MTT to formazan by the action of the enzyme succinate dehydrogenase was evaluated at 570 nm. Cell viability was expressed as a percentage, calculated by the following equation: % cell viability = (absorbance of the sample/absorbance control cells) × 100 [26].

2.8.3. Determination of Nitric Oxide Production. Nitric oxide production was measured according to the method previously reported by Nguyen et al. [26] with slight modifications. Briefly, RAW cells were cultured in 96-well plates at a density of 2.5×10^5 cells/well at 37°C and 5% CO_2 for 24 h. Subsequently, the production of nitric oxide (NO) in cells was induced with lipopolysaccharide (LPS) (1 μg/mL) in the presence and absence of EB and NEB extracts for 24 h. NO production in the culture medium was assessed indirectly as nitrite by the Griess reaction. The supernatant medium (100 μL) was mixed with 100 μL of Griess reagent (1% sulfanilamide and 0.1% naphthylethylenediamine dihydrochloride) and incubated for 10 min. Absorbance was measured at 550 nm. The concentration of nitric oxide in the culture medium was determined based on a standard sodium nitrite curve.

2.9. Statistical Analysis. The effect of independent factors (moisture and temperature) and their interaction on the response variables was determined by ANOVA. Tukey's test was used for the comparison of the means. Statistical analyses were performed with the program JMP 5.0.1 (USA, SAS institute, Inc.). Values of $p < 0.05$ were accepted as statistically significant.

3. Results and Discussion

3.1. Total Phenolic and Phenolic Acid Content. Table 1 shows the total phenols and phenolic acid content of extruded and nonextruded sorghum bran. The extrusion process increased total phenol content in sorghum bran compared to nonextruded sorghum, particularly those extruded at 180°C and 20% moisture content (2.0222 ± 0.0157 versus 3.0729 ± 0.0187 mg GAE/g +52%).

The total hydroxycinnamic acids content increased in all extruded sorghum bran samples evaluated in this study compared to NEB. The EB samples treated at 180°C showed a higher total HCA content compared to the rest of the extruded samples. The amount of caffeic acid, ρ-coumaric acid, ferulic acid, and sinapic acid significantly increased after the extrusion process. Ferulic acid was the main phenolic acid found in the sorghum bran before and after the extrusion process. However, its concentration increased 2.7-fold with respect to NEB when heat treatment at 180°C was used.

The results obtained in this study, applying extrusion to sorghum bran, agree with those found by Zielinski et al. [19]. These authors observed an increase in the total phenolic and hydroxycinnamic acids, mainly ferulic and coumaric acids, in barley, rice, oats, and wheat as a result of extrusion at temperatures of 120°C, 160°C, and 200°C and 20% moisture. They suggested that heat treatment of cereals enhances the release of phenolic acids and their products from the cell walls. This last statement agrees with Ti et al. [27] who reported an increase of 12.6% in total phenolic content of rice bran as a consequence of the extrusion process. The release of phenol and other related compounds is a function of food matrix and extrusion conditions. Therefore, optimization of extrusion processes has to be established depending on the food matrix to have the highest release of bioactive compounds.

3.2. Antiradical Capacity. The effects on the antiradical capacity of sorghum before and after the extrusion processes measured by the DPPH and TEAC assays are shown in Figure 1. We observed that the antiradical capacities in both assays (DPPH and TEAC) were higher ($p < 0.05$) for

Table 1: Phenolic acid content and total phenols in sorghum bran extract before and after extrusion processes.

T°C	% M**	Phenolic acid content (μg/g)				Total HCAs***	Total phenols (mg GAE/g)
		Caffeic	Coumaric	Ferulic	Sinapic		
Nonextruded		14.9 ± 0.3^{c*}	8.7 ± 0.2^{e}	19.8 ± 0.2^{c}	3.4 ± 0.1^{d}	46.8 ± 0.5^{d}	2.0222 ± 0.0157^{d}
110	20	28.8 ± 0.2^{a}	21.5 ± 0.3^{a}	30.0 ± 0.9^{b}	5.0 ± 0.1^{c}	85.0 ± 0.7^{b}	2.4068 ± 0.1079^{c}
110	30	19.6 ± 0.2^{b}	19.7 ± 0.6^{b}	28.6 ± 0.3^{b}	4.6 ± 0.0^{c}	70.7 ± 2.3^{c}	2.1336 ± 0.0516^{d}
180	20	19.9 ± 0.8^{b}	17.3 ± 0.2^{c}	53.9 ± 1.6^{a}	7.7 ± 0.2^{a}	98.9 ± 1.3^{a}	3.0729 ± 0.0187^{a}
180	30	20.1 ± 0.9^{b}	14.9 ± 0.3^{d}	53.8 ± 1.1^{a}	6.5 ± 0.2^{b}	95.3 ± 2.4^{a}	2.6192 ± 0.0101^{b}

*Each value represents the mean of three replicates ± standard error. Different letters within each column indicate significant differences ($p < 0.05$).
**% M: % moisture.
***Total HCAs: total hydroxycinnamic acids.

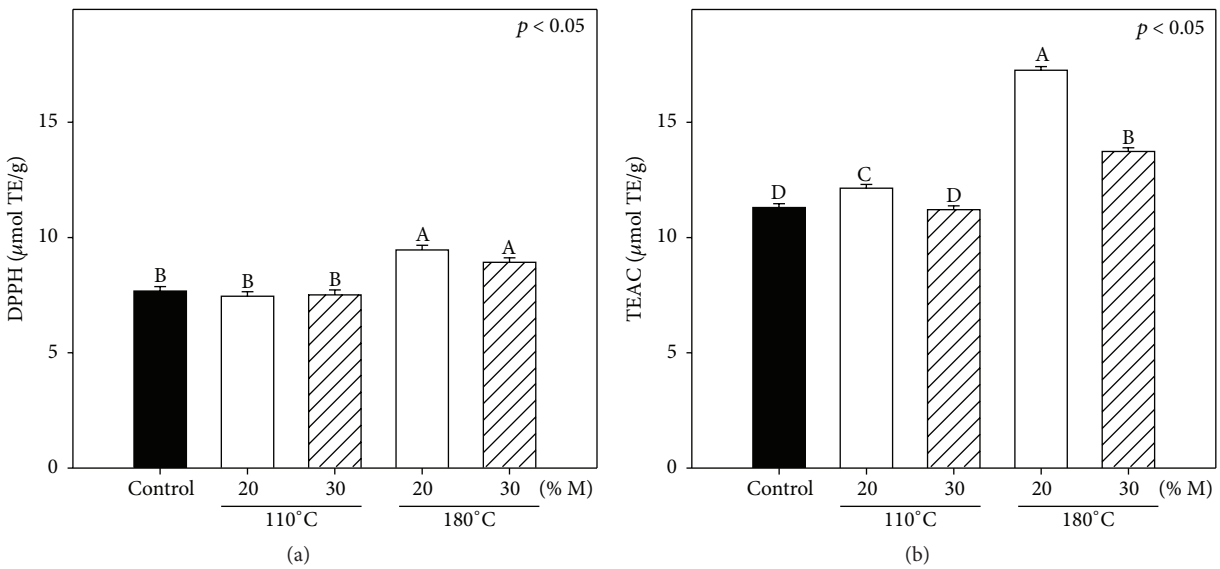

Figure 1: Antiradical capacity of sorghum bran before (control) and after extrusion processes: (a) DPPH and (b) TEAC. Each bar represents the mean of three replicates ± standard error. Different letters on bars represent significant differences ($p < 0.05$) between treatments including control.

sorghum bran extruded at 180°C, with 9.5 ± 0.4 and 17.3 ± 0.4 μg TE/g, than for nonextruded sorghum bran, with 7.7 ± 0.7 and 11.3±0.4 μg TE/g, respectively (Figures 1(a) and 1(b)). The antiradical capacity of extracts extruded at temperature of 110°C was lower ($p < 0.05$) than that of those extracts extruded at 180°C. This could be explained by the fact that temperatures above 170°C are sufficient to break down the chemical bond of lignin and ferulic acid [28] which could fragment the structure of arabinoxylans and consequently enhance the release of ferulic acid and increment the antiradical activity. Our results agreed with those reported by Ti et al. [27], where an increase of 19.7% in the antioxidant capacity of rice bran as a result of the extrusion process was observed.

To evaluate a possible association between changes in antioxidant capacity and total phenolic content (TPC), a correlation analysis was performed. A significant correlation was found between TPC and DPPH ($r^2 = 0.735$; $p < 0.05$) (Figure 2(a)) and between TPC and TEAC ($r^2 = 0.915$; $p < 0.05$) (Figure 2(b)). These findings suggest that total phenolic content is a good predictor of *in vitro* antiradical capacity. Shih et al. [29] reported a concomitant relationship between total phenolic content and antioxidant capacity (DPPH) in sweet potatoes after the extrusion process.

Additionally, a concomitant increase in antioxidant capacity and the content of phenolic acids, mainly ferulic acid, was previously reported in extruded rye [20]. The increase of phenolic compounds and antiradical capacity due to extrusion could be explained by the structural modification of the cell walls, where phenolic acids, such as ferulic and ρ-coumaric acids, are covalently linked to arabinoxylans favoring the release of these compounds. The increase in the efficacy of the extraction process can be accomplished by the modification of the bran matrix under conditions of high temperature, pressure, and shear [19, 27].

Extrusion processing of cereals provides advantages in terms of phenolic compound content and antioxidant capacity compared to the conventional wet cooking and soaking methods [11, 18].

In extruded corn flour, Mora-Rochin et al. [30] showed that the extrusion process has some advantages over the nixtamalization process. They evaluated the phenolic compound content and antioxidant capacity of corn tortillas and

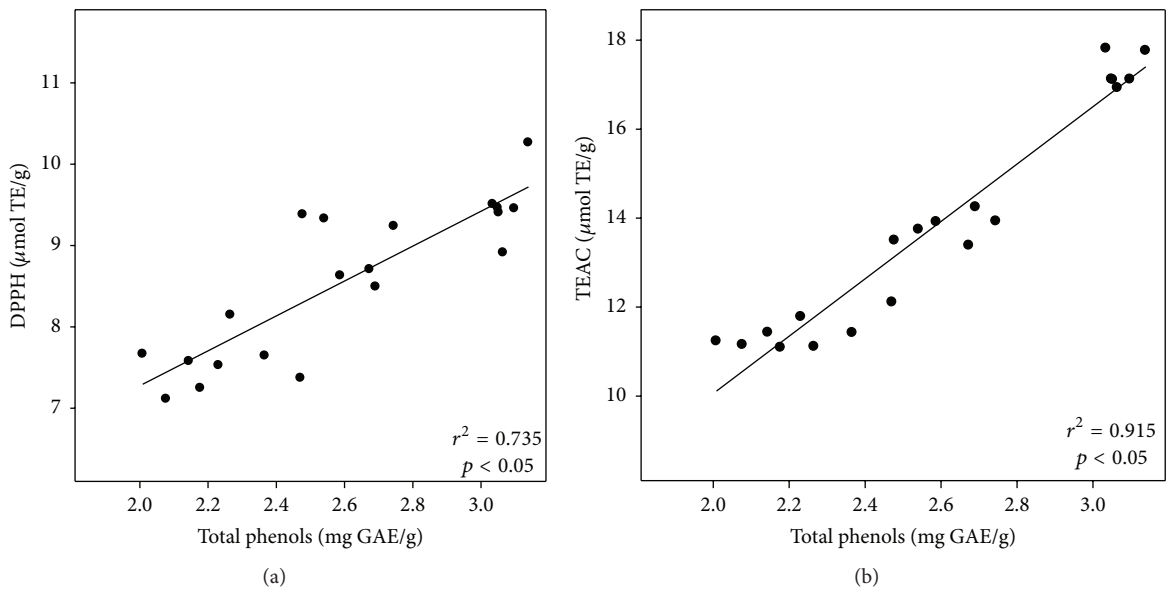

Figure 2: Correlations between the contents of total phenols in extruded sorghum bran and their antiradical capacity as determined by DPPH (a) and TEAC (b) assays.

observed that tortillas made with extruded corn flour retain a higher content of total phenolic compounds, ferulic acid, and antioxidant capacity compared to tortillas prepared with nixtamalized corn flour in the traditional method. Nevertheless, Dlamini et al. [10] reported that porridge obtained from African sorghum by traditional methods had higher antioxidant capacity that that of products cooked by extrusion.

The extrusion temperature of 180°C was a determining factor in the achievement of a higher total phenol content. However, further studies focusing on combined processes may be necessary to increase the biological potential of sorghum bran. These differences in the content of phenolic compounds and antioxidant capacity of extruded cereals, and also their nutritional value, depend on the conditions used in the extrusion process and the chemical composition of the food matrix [21].

3.3. Nitric Oxide Production. The inhibition of NO production by cell culture has been widely used as a biomarker to assess anti-inflammatory capacity because NO production is exacerbated by the action of the inducible nitric oxide synthase (iNOS), which is activated under conditions of oxidative stress, the presence of polysaccharides in Gram-negative bacteria, the tumor necrosis factor (TNF-α), and interleukin-1β which causes the activation of nuclear factor kappa B (NF-κB) and the production of proinflammatory cytokines [31–34]. NO production by RAW 264.7 macrophages in the presence of extruded and nonextruded sorghum bran extracts was evaluated. For this assay, the extrusion treatment with the higher content of total phenols and antiradical capacity was selected (180°C/20% moisture). Prior to nitric oxide evaluation, the possible cytotoxic effects of sorghum bran phenolic extracts were measured using the MTT assay. When extruded or nonextruded sorghum bran extracts were added to LPS-activated RAW 264.7, no significant ($p > 0.05$) effects on the cell viability (%) of the RAW 264.7 cells at 4.3–10.1 mg sorghum bran/mL were observed (Figure 3).

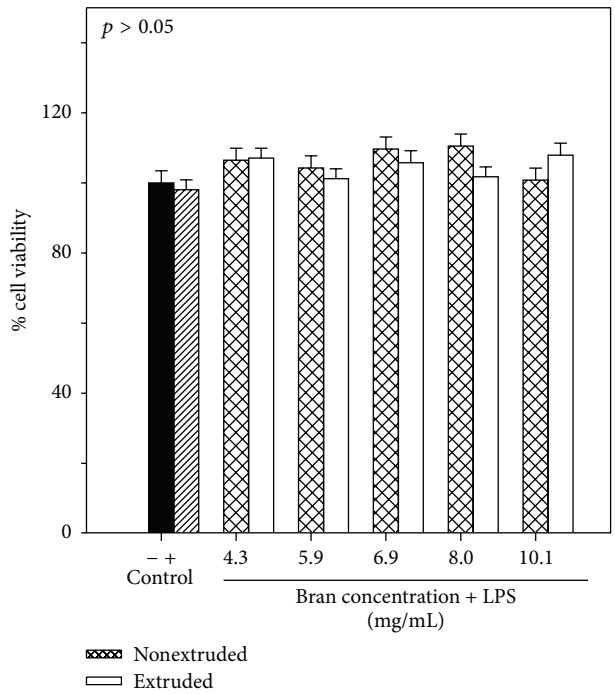

Figure 3: Cell viability (%) of RAW 264.7 cells treated with extruded sorghum bran (180°C/20% moisture) and nonextruded sorghum bran. Control (−) represents untreated cells and control (+) represents cells treated with LPS only. Each bar represents the mean of five replicates from three independent experiments ± standard error.

Figure 4 shows the effects of extruded or nonextruded sorghum bran on the production of nitric oxide by

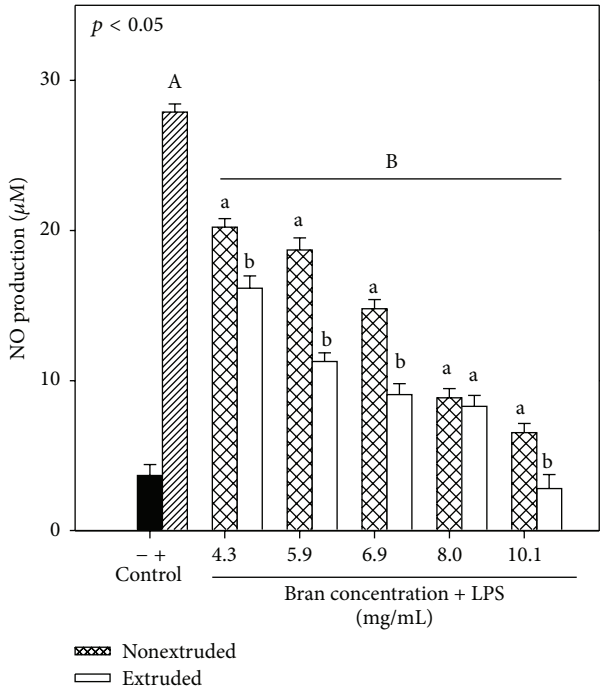

Figure 4: Nitric oxide production of RAW 264.7 cells treated with extruded sorghum bran at 180°C and 20% moisture and nonextruded sorghum bran. Control (−) represents untreated cell and control (+) represents cells treated with LPS only. Each bar represents the mean of five replicates from three independent experiments ± standard error. Bars with different letters in the same concentration are significantly different ($p < 0.05$). Capital letters represent significant differences ($p < 0.05$) between nonextruded and extruded treatments and positive control (LPS).

LPS-induced RAW 264.7 mouse macrophages. According to the concentrations of both extruded and nonextruded sorghum bran extracts selected for this study, it was observed that NO production was reduced significantly compared to the positive control (LPS-activated RAW 264.7). A dose-response effect on nitric oxide production in sorghum bran extracts evaluated was also observed. Using these results, the concentration of extract (extruded or nonextruded) was calculated, and the concentration at which there was 50% inhibition of nitric oxide production (EC_{50}) was obtained, showing lower EC_{50} for extruded sorghum bran (5.23 mg/mL) than that of nonextruded sorghum bran (6.58 mg/mL).

With respect to nitric oxide production, it was found that bran sorghum subjected to the extrusion process showed less nitric oxide production ($p < 0.05$). Considering the maximum concentration of the sorghum extracts (10.1 mg/mL), the percentage of inhibition of NO production by RAW cells due to the presence of extruded sorghum bran extract was significantly higher ($p < 0.05$) than that of nonextruded sorghum bran extract (90.2 ± 1.9% versus 76.2 ± 1.3%). These results agree with those reported by Shim et al. [35] who evaluated the anti-inflammatory capacity of ethanol extracts of sorghum measured as inhibition of NO production in LPS-induced RAW 264.7 cells.

Hwang et al. [36] reported that chloroform extracts of sorghum showed a significantly higher inhibitory effect on the production of NO, iNOS, TNFα, and IL-6 in LPS-induced RAW cells compared to the inhibitory effects of corn and barley extracts. However, these studies only evaluated anti-inflammatory capacity in sorghum grain without thermal processes. As far as we know, this is the first time that the anti-inflammatory capacity of extruded sorghum bran has been evaluated *in vitro*.

Several studies of sorghum grain have reported an association between phenolic compounds and anti-inflammatory capacity. In this context, Burdette et al. [4] observed a correlation between the anti-inflammatory capacity of sorghum extracts and their phenolic compound content and antioxidant capacity. Hwang et al. [36] established a relationship between the anti-inflammatory capacity and the content of flavonoids. Previous studies have shown that white sorghum variety is poor in flavonoid content. Therefore, the content of phenolic compounds and the antioxidant capacity apparently is provided mainly by the phenolic acid derivatives of cinnamic acid [37, 38].

Previous reports have indicated that the antioxidant capacity of cereal extracts is due to the presence of cinnamic acids, which are able to inhibit the pathway of nuclear factor-(NF-) κB. Kim et al. [39] evaluated the anti-inflammatory capacity of hydroxycinnamic acids isolated from corn bran in RAW 264.7 macrophages and observed inhibition of iNOS and NO production in connection to the NF-κB pathway. Yun et al. [40] and Shin et al. [41] evaluated the effect of sinapic acid (40 to 160 μM) and caffeic acid and its derivatives (25–100 μM) on anti-inflammatory capacity and reported that the inhibitory effects were due to the suppression of iNOS, COX-2, TNF-α, and IL-1β expression through the effect of the NF-κB pathway on RAW 264.7 macrophages. Other phenolic compounds such as quercetin and caffeic acid phenethyl ester also have been able to block the activation of NF-κB and, as a consequence, inhibit the production of iNOS and NO [32].

4. Conclusions

Applying the extrusion process to sorghum bran increased total phenol and cinnamic acid contents, which positively affected the antioxidant capacity and the inhibition of LPS-induced nitric oxide production in RAW macrophages. The extrusion process could be a good alternative for processing sorghum bran to increase its functionality. This improvement of extruded sorghum bran can be beneficial for people with diseases related to oxidative stress and inflammation. Additional studies examining the increase in bioaccessibility of phenolic compounds of extruded sorghum bran are in progress.

Competing Interests

The authors declare that there are no competing interests.

Acknowledgments

This work was performed with the support of PROINNOVA grant (Project no. 218169). Norma Julieta Salazar Lopez received scholarship from CONACyT (National Research and Technology Council), Mexico.

References

[1] F. Barros, J. M. Awika, and L. W. Rooney, "Interaction of tannins and other sorghum phenolic compounds with starch and effects on in vitro starch digestibility," *Journal of Agricultural and Food Chemistry*, vol. 60, no. 46, pp. 11609–11617, 2012.

[2] J. M. Awika, L. Yang, J. D. Browning, and A. Faraj, "Comparative antioxidant, antiproliferative and phase II enzyme inducing potential of sorghum (Sorghum bicolor) varieties," *LWT—Food Science and Technology*, vol. 42, no. 6, pp. 1041–1046, 2009.

[3] K. F. Benson, J. L. Beaman, B. Ou, A. Okubena, O. Okubena, and G. S. Jensen, "West African *Sorghum bicolor* leaf sheaths have anti-inflammatory and immune-modulating properties *in vitro*," *Journal of Medicinal Food*, vol. 16, no. 3, pp. 230–238, 2013.

[4] A. Burdette, P. L. Garner, E. P. Mayer, J. L. Hargrove, D. K. Hartle, and P. Greenspan, "Anti-inflammatory activity of select sorghum (*Sorghum bicolor*) brans," *Journal of Medicinal Food*, vol. 13, no. 4, pp. 879–887, 2010.

[5] L. Dykes and L. W. Rooney, "Sorghum and millet phenols and antioxidants," *Journal of Cereal Science*, vol. 44, no. 3, pp. 236–251, 2006.

[6] C. Chiremba, J. R. N. Taylor, L. W. Rooney, and T. Beta, "Phenolic acid content of sorghum and maize cultivars varying in hardness," *Food Chemistry*, vol. 134, no. 1, pp. 81–88, 2012.

[7] B. A. Acosta-Estrada, J. A. Gutiérrez-Uribe, and S. O. Serna-Saldívar, "Bound phenolics in foods, a review," *Food Chemistry*, vol. 152, pp. 46–55, 2014.

[8] S. D. McClendon, H.-D. Shin, and R. R. Chen, "Novel bacterial ferulic acid esterase from Cellvibrio japonicus and its application in ferulic acid release and xylan hydrolysis," *Biotechnology Letters*, vol. 33, no. 1, pp. 47–54, 2011.

[9] S. Mathew and T. E. Abraham, "Bioconversions of ferulic acid, an hydroxycinnamic acid," *Critical Reviews in Microbiology*, vol. 32, no. 3, pp. 115–125, 2006.

[10] N. R. Dlamini, J. R. N. Taylor, and L. W. Rooney, "The effect of sorghum type and processing on the antioxidant properties of African sorghum-based foods," *Food Chemistry*, vol. 105, no. 4, pp. 1412–1419, 2007.

[11] L. D. M. Cardoso, T. A. Montini, S. S. Pinheiro, H. M. Pinheiro-Sant'Ana, H. S. D. Martino, and A. V. B. Moreira, "Effects of processing with dry heat and wet heat on the antioxidant profile of sorghum," *Food Chemistry*, vol. 152, pp. 210–217, 2014.

[12] N. N. Rosa, C. Dufour, V. Lullien-Pellerin, and V. Micard, "Exposure or release of ferulic acid from wheat aleurone: impact on its antioxidant capacity," *Food Chemistry*, vol. 141, no. 3, pp. 2355–2362, 2013.

[13] B. Bartolomé and C. Gómez-Cordovés, "Barley spent grain: release of hydroxycinnamic acids (ferulic and p-coumaric acids) by commercial enzyme preparations," *Journal of the Science of Food and Agriculture*, vol. 79, no. 3, pp. 435–439, 1999.

[14] M. A. Verbruggen, B. A. Spronk, H. A. Schols et al., "Structures of enzymically derived oligosaccharides from sorghum glucuronoarabinoxylan," *Carbohydrate Research*, vol. 306, no. 1-2, pp. 265–274, 1998.

[15] J. Agger, A. Viksø-Nielsen, and A. S. Meyer, "Enzymatic xylose release from pretreated corn bran arabinoxylan: differential effects of deacetylation and deferuloylation on insoluble and soluble substrate fractions," *Journal of Agricultural and Food Chemistry*, vol. 58, no. 10, pp. 6141–6148, 2010.

[16] J. R. N. Taylor, T. J. Schober, and S. R. Bean, "Novel food and non-food uses for sorghum and millets," *Journal of Cereal Science*, vol. 44, no. 3, pp. 252–271, 2006.

[17] H.-D. Shin, S. McClendon, T. Le, F. Taylor, and R. R. Chen, "A complete enzymatic recovery of ferulic acid from corn residues with extracellular enzymes from Neosartorya spinosa NRRL185," *Biotechnology and Bioengineering*, vol. 95, no. 6, pp. 1108–1115, 2006.

[18] A. E.-M. M. R. Afify, H. S. El-Beltagi, S. M. A. El-Salam, and A. A. Omran, "Biochemical changes in phenols, flavonoids, tannins, vitamin E, β-carotene and antioxidant activity during soaking of three white sorghum varieties," *Asian Pacific Journal of Tropical Biomedicine*, vol. 2, no. 3, pp. 203–209, 2012.

[19] H. Zielinski, H. Kozlowska, and B. Lewczuk, "Bioactive compounds in the cereal grains before and after hydrothermal processing," *Innovative Food Science and Emerging Technologies*, vol. 2, no. 3, pp. 159–169, 2001.

[20] D. Gumul and J. Korus, "Polyphenol content and antioxidant activity of rye bran extrudates produced at varying parameters of extrusion process," *Food Science and Technology*, vol. 9, no. 4, pp. 1–11, 2006.

[21] S. Singh, S. Gamlath, and L. Wakeling, "Nutritional aspects of food extrusion: a review," *International Journal of Food Science and Technology*, vol. 42, no. 8, pp. 916–929, 2007.

[22] W. Guo and T. Beta, "Phenolic acid composition and antioxidant potential of insoluble and soluble dietary fibre extracts derived from select whole-grain cereals," *Food Research International*, vol. 51, no. 2, pp. 518–525, 2013.

[23] V. L. Singleton and J. A. Rossi, "Colorimetry of total phenolics with phosphomolybdic-phosphotungstic acid reagents," *American Journal of Enology and Viticulture*, vol. 16, pp. 144–158, 1965.

[24] R. A. Ortíz Cruz, J. L. Cárdenas López, G. A. González Aguilar et al., "Influence of sorghum kafirin on serum lipid profile and antioxidant activity in hyperlipidemic rats (*in vitro* and *in vivo* studies)," *BioMed Research International*, vol. 2015, Article ID 164725, 8 pages, 2015.

[25] R. Re, N. Pellegrini, A. Proteggente, A. Pannala, M. Yang, and C. Rice-Evans, "Antioxidant activity applying an improved ABTS radical cation decolorization assay," *Free Radical Biology and Medicine*, vol. 26, no. 9-10, pp. 1231–1237, 1999.

[26] P.-H. Nguyen, B. T. Zhao, J. H. Lee, Y. H. Kim, B. S. Min, and M. H. Woo, "Isolation of benzoic and cinnamic acid derivatives from the grains of Sorghum bicolor and their inhibition of lipopolysaccharide-induced nitric oxide production in RAW 264.7 cells," *Food Chemistry*, vol. 168, pp. 512–519, 2015.

[27] H. Ti, R. Zhang, M. Zhang et al., "Effect of extrusion on phytochemical profiles in milled fractions of black rice," *Food Chemistry*, vol. 178, pp. 186–194, 2015.

[28] C. Chiremba, L. W. Rooney, and T. Beta, "Microwave-assisted extraction of bound phenolic acids in bran and flour fractions from sorghum and maize cultivars varying in hardness," *Journal of Agricultural and Food Chemistry*, vol. 60, no. 18, pp. 4735–4742, 2012.

[29] M.-C. Shih, C.-C. Kuo, and W. Chiang, "Effects of drying and extrusion on colour, chemical composition, antioxidant activities and mitogenic response of spleen lymphocytes of sweet potatoes," *Food Chemistry*, vol. 117, no. 1, pp. 114–121, 2009.

[30] S. Mora-Rochin, J. A. Gutiérrez-Uribe, S. O. Serna-Saldivar, P. Sánchez-Peña, C. Reyes-Moreno, and J. Milán-Carrillo, "Phenolic content and antioxidant activity of tortillas produced from pigmented maize processed by conventional nixtamalization or extrusion cooking," *Journal of Cereal Science*, vol. 52, no. 3, pp. 502–508, 2010.

[31] F. Aktan, "iNOS-mediated nitric oxide production and its regulation," *Life Sciences*, vol. 75, no. 6, pp. 639–653, 2004.

[32] J. B. Calixto, M. F. Otuki, and A. R. S. Santos, "Anti-inflammatory compounds of plant origin. part i. action on arachidonic acid pathway, nitric oxide and nuclear factor κB (NF-κB)," *Planta Medica*, vol. 69, no. 11, pp. 973–983, 2003.

[33] T. Lawrence, "The nuclear factor NF-kappaB pathway in inflammation," *Cold Spring Harbor Perspectives in Biology*, vol. 1, no. 6, pp. 1–10, 2009.

[34] J. Ruland, "Return to homeostasis: downregulation of NF-κB responses," *Nature Immunology*, vol. 12, no. 8, pp. 709–714, 2011.

[35] T.-J. Shim, T. M. Kim, K. C. Jang, J.-Y. Ko, and D. J. Kim, "Toxicological evaluation and anti-inflammatory activity of a golden gelatinous sorghum bran extract," *Bioscience, Biotechnology and Biochemistry*, vol. 77, no. 4, pp. 697–705, 2013.

[36] J.-M. Hwang, K.-C. Choi, S.-J. Bang et al., "Anti-oxidant and anti-inflammatory properties of methanol extracts from various crops," *Food Science and Biotechnology*, vol. 22, no. 1, pp. 265–272, 2013.

[37] J. M. Awika and L. W. Rooney, "Sorghum phytochemicals and their potential impact on human health," *Phytochemistry*, vol. 65, no. 9, pp. 1199–1221, 2004.

[38] K. K. Adom and R. H. Liu, "Antioxidant activity of grains," *Journal of Agricultural and Food Chemistry*, vol. 50, no. 21, pp. 6182–6187, 2002.

[39] E. O. Kim, K. J. Min, T. K. Kwon, B. H. Um, R. A. Moreau, and S. W. Choi, "Anti-inflammatory activity of hydroxycinnamic acid derivatives isolated from corn bran in lipopolysaccharide-stimulated Raw 264.7 macrophages," *Food and Chemical Toxicology*, vol. 50, no. 5, pp. 1309–1316, 2012.

[40] K.-J. Yun, D.-J. Koh, S.-H. Kim et al., "Anti-inflammatory effects of sinapic acid through the suppression of inducible nitric oxide synthase, cyclooxygase-2, and proinflammatory cytokines expressions via nuclear factor-κB inactivation," *Journal of Agricultural and Food Chemistry*, vol. 56, no. 21, pp. 10265–10272, 2008.

[41] K.-M. Shin, I.-T. Kim, Y.-M. Park et al., "Anti-inflammatory effect of caffeic acid methyl ester and its mode of action through the inhibition of prostaglandin E_2, nitric oxide and tumor necrosis factor-α production," *Biochemical Pharmacology*, vol. 68, no. 12, pp. 2327–2336, 2004.

Hindawi Publishing Corporation
Evidence-Based Complementary and Alternative Medicine
Volume 2016, Article ID 5739434, 16 pages
http://dx.doi.org/10.1155/2016/5739434

Review Article

Anti-Inflammatory Effects of Traditional Chinese Medicines against Ischemic Injury in In Vivo Models of Cerebral Ischemia

Chin-Yi Cheng[1,2] and Yu-Chen Lee[3,4,5]

[1]*School of Chinese Medicine, College of Chinese Medicine, China Medical University, Taichung 40402, Taiwan*
[2]*Department of Chinese Medicine, Hui-Sheng Hospital, Taichung 42056, Taiwan*
[3]*Department of Chinese Medicine, China Medical University Hospital, Taichung 40447, Taiwan*
[4]*Research Center for Chinese Medicine & Acupuncture, China Medical University, Taichung 40402, Taiwan*
[5]*Graduate Institute of Acupuncture Science, China Medical University, Taichung 40402, Taiwan*

Correspondence should be addressed to Yu-Chen Lee; d5167@mail.cmuh.org.tw

Received 22 May 2016; Accepted 25 July 2016

Academic Editor: Xiang Liu

Inflammation plays a crucial role in the pathophysiology of acute ischemic stroke. In the ischemic cascade, resident microglia are rapidly activated in the brain parenchyma and subsequently trigger inflammatory mediator release, which facilitates leukocyte-endothelial cell interactions in inflammation. Activated leukocytes invade the endothelial cell junctions and destroy the blood-brain barrier integrity, leading to brain edema. Toll-like receptors (TLRs) stimulation in microglia/macrophages through the activation of intercellular signaling pathways secretes various proinflammatory cytokines and enzymes and then aggravates cerebral ischemic injury. The secreted cytokines activate the proinflammatory transcription factors, which subsequently regulate cytokine expression, leading to the amplification of the inflammatory response and exacerbation of the secondary brain injury. Traditional Chinese medicines (TCMs), including TCM-derived active compounds, Chinese herbs, and TCM formulations, exert neuroprotective effects against inflammatory responses by downregulating the following: ischemia-induced microglial activation, microglia/macrophage-mediated cytokine production, proinflammatory enzyme production, intercellular adhesion molecule-1, matrix metalloproteinases, TLR expression, and deleterious transcription factor activation. TCMs also aid in upregulating anti-inflammatory cytokine expression and neuroprotective transcription factor activation in the ischemic lesion in the inflammatory cascade during the acute phase of cerebral ischemia. Thus, TCMs exert potent anti-inflammatory properties in ischemic stroke and warrant further investigation.

1. Introduction

Stroke is the third leading cause of death in developed countries [1] and the major cause of severe long-term disability worldwide [1–3]. Approximately 15 million people experience stroke annually. Of these, one-third die and one-third experience permanent disabilities, thus imposing considerable social and economic burden [4]. Approximately 80%–85% of all stroke events are ischemic caused by cerebral arterial thrombosis or embolism [5, 6]. To date, recombinant tissue plasminogen activator (rtPA) is the only Food and Drug Administration-approved medical therapy for acute ischemic stroke. However, rtPA has severe disadvantages, including the narrow therapeutic time window of 4.5 h and potential risk of hemorrhagic transformation; therefore, the eligibility of rtPA is reduced to only 4%–7% in all the patients with acute ischemic stroke [5]. Thus, potential therapeutic strategies for ischemic stroke are urgently needed.

Increasing evidence has demonstrated that inflammation plays a pivotal role in the pathophysiology of acute ischemic stroke [3, 5, 7]. During acute ischemic stroke, the brain is injured by ischemia- and inflammation-related primary and secondary insults [5]. The primary injury occurs at the beginning of ischemia; it rapidly interrupts the cerebral blood flow to the ischemic core and subsequently causes a significant decrease in oxygen and glucose supply to

cerebral neurons [8, 9]. The secondary injury is attributed to the postischemic inflammatory cascade, which produces various proinflammatory mediators, including cytokines, chemokines, proteases, and cell adhesion molecules, leading to an exacerbated ischemic brain injury [10]. However, the postischemic inflammatory response has a disadvantage and an advantage, exacerbating ischemic brain damage in the early phase and triggering tissue regeneration in the delayed phase, respectively [1, 2].

The lack of effective and widely applicable therapeutic strategies for the treatment of ischemic stroke has triggered increasing interest in traditional medicines, particularly traditional Chinese medicine (TCM) [11, 12]. Several centuries ago, TCM was used in China to treat cerebrovascular disorders, including stroke. Evidence revealed that TCM preparation, Chinese herb medicine, and TCM-derived active compounds exert anti-inflammatory effects by inhibiting inflammatory mediators, leukocyte infiltration, and blood-brain barrier (BBB) disruption in experimental cerebral ischemia [13]. These potent effects of TCMs against cerebral ischemic injury highlight their potential in clinical applications. Therefore, this review summarized the origin and development of the postischemic inflammatory cascade and delineated the anti-inflammatory effects of TCMs (namely, TCM-derived active compounds, Chinese herbs, and TCM formulations) on the basis of the in vivo literature.

2. TCM-Mediated Downregulation of Microglial Activation

2.1. Activation of Microglia in the Initial Phase of Cerebral Ischemia. In the acute phase (min to h) of cerebral ischemia, ischemic injury triggers a rapid activation of resident microglia in the brain parenchyma [3, 14]. During cerebral ischemia, microglial morphology changes from a ramified to an amoeboid shape upon activation [15]. In the initial stage of ischemia, the injured neurons expose damage-associated molecular patterns (DAMPs), which are subsequently recognized by toll-like receptors (TLRs), such as TLR4, and other pattern recognition receptors on the surface of the reactive microglia; this recognition triggers microglia-mediated inflammatory mediators release, contributing to secondary damage after stroke [6, 10, 16]. Reactive microglia/macrophages can be detected as early as 2 h after cerebral ischemia and maintained up to 1 week after the ischemic insult [6]. Reactive microglia are divided into two phenotypes: the classically and alternatively activated phenotypes (M1 and M2, resp.) [17]. The M1 microglia produce proinflammatory mediators, such as cytokines [interleukin- (IL-) 1β, IL-6, IL-18, and tumor necrosis factor- (TNF-) α], chemokines [monocyte chemoattractant protein- (MCP-) 1, and macrophage inflammatory protein- (MIP-) 1α], interferon- (IFN-) γ, matrix metalloproteinase- (MMP-) 9, and reactive oxygen species (ROS) [18], exerting detrimental functions in the early phase. By contrast, the M2 microglia secrete anti-inflammatory mediators, such as IL-4, IL-10, IL-13, transforming growth factor- (TGF-) β, and insulin growth factor-1, exerting neuroprotective effects in the delayed phase [2, 3, 19]. In cerebral ischemia, microglial activation is accompanied by reactive astrogliosis, which also produces an excessive amount of cytokines and causes the exacerbation of ischemic brain injury [18].

2.2. The Effects and Mechanisms of TCMs on Inhibiting Microglial Activation in In Vivo Models of Cerebral Ischemia. Hsieh et al. reported that Paeonol, a common compound of *Paeonia suffruticosa* Andrews (Chinese name, Mu Dan Pi; Moutan cortex), reduces cerebral infarct and neurological deficits at 1.5 h of ischemia and 24 h of reperfusion. Paeonol exerts anti-infarct effect mainly by inhibiting microglial activation and IL-1β expression in the ischemic cortex in ischemia/reperfusion- (I/R-) injured rats [20]. Pretreatment with tetramethylpyrazine (TMP), an active compound isolated from *Ligusticum wallichii* Franch (Chuan Xiong), effectively reduces the cerebral volume by inhibiting myeloperoxidase (an inflammation marker) and ED1 (a microglia/macrophage marker) expression in the ischemic core 72 h after reperfusion. The effect of TMP against microglial activation-mediated neurotoxicity can be further attributed to the suppression of prostaglandin E2 (PGE2) in the ischemic core [21]. A later study reported that TMP provides neuroprotection against ischemic brain injury partially by inhibiting microglial activation and subsequently downregulating MCP-1 expression in the ischemic cortex 72 h after reperfusion [22]. Andrographolide, the major active compound derived from *Andrographis paniculata* (Chuan Xin Lian) protects against cerebral infarction and ameliorates neurological deficits 24 h after permanent middle cerebral artery occlusion (MCAo). Andrographolide exerts neuroprotective effects partially by inhibiting microglial activation and microglia-mediated IL-1β and TNF-α expression in the ischemic area [23]. Pretreatment with *Sophora japonica* L. (Huai Hua; intraperitoneal injection) effectively reduced the cerebral infarct area and neurological deficits at 1.5 h of ischemia and 24 h of reperfusion. The effects of *S. japonica* involve the suppression of microglial activation and microglia-mediated IL-1β expression in the ischemic cortex [24]. Lim et al. demonstrated that an intragastric administration of total isoflavones isolated from *Pueraria lobata* (Ge Gen; TIPL) significantly reduces the cerebral infarct volume at 2 h of ischemia and 48 h of reperfusion. The anti-inflammatory effect of TIPL is partially attributed to the inhibition of astrocyte and microglial activation in the hippocampal CA1 region 7 d after MCAo [25].

On the basis of these studies, the anti-inflammatory effects of TCMs against cerebral ischemic injury could be attributed to the downregulation of microglial activation and microglia-mediated proinflammatory cytokines production in the ischemic area during the initial phase of MCAo (Figure 1 and Table 1).

3. TCM-Mediated Suppression of Leukocyte Infiltration

3.1. The Process of Leukocyte Infiltration during Cerebral Ischemia. The microglial and astrocytic production of proinflammatory mediators rapidly increase the expression of

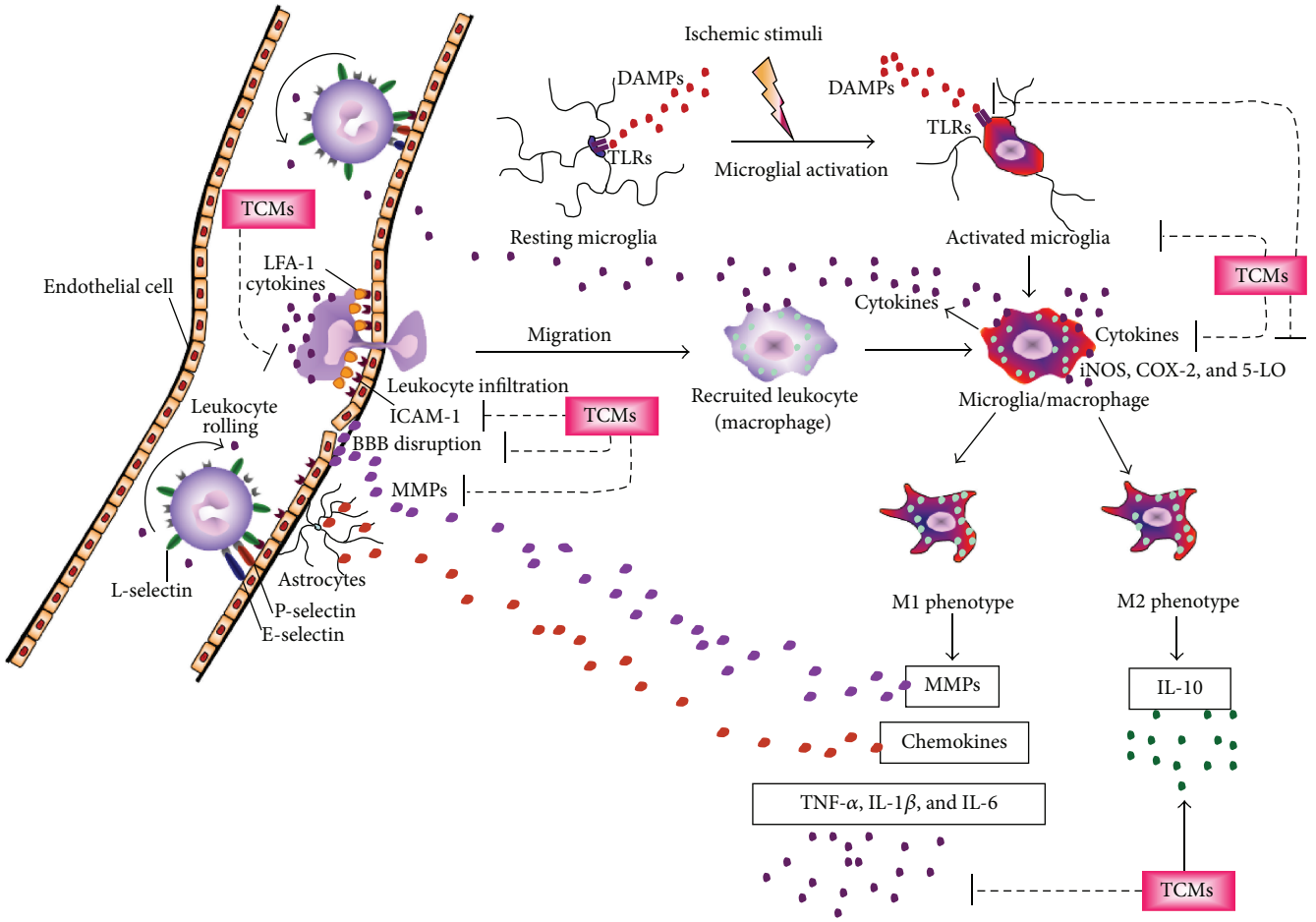

Figure 1: Schematic representation of the effects of traditional Chinese medicines on inflammation responses in the inflammatory cascade after cerebral ischemia. TCMs, traditional Chinese medicines; DAMPs, damage-associated molecular patterns; TLRs, toll-like receptors; LFA-1, leukocyte function-associated antigen-1 (CD11a/CD18); ICAM-1, intercellular adhesion molecule-1; MMPs, matrix metalloproteinases; iNOS, inducible nitric oxide synthase; COX-2, cyclooxygenase-2; 5-LO, 5-lipoxygenase; BBB, blood-brain barrier. Thick solid lines with arrowheads indicate activation, and thin dotted lines indicate inhibition.

adhesion molecules on the endothelium [26, 27]. During acute cerebral I/R injury, the peripheral leukocytes first roll, become activated, and consequentially attach to the endothelial cells in the ischemic lesion. Leukocyte-endothelial cell interactions in inflammation are mediated by various adhesion molecules, including selectins, integrins, intercellular adhesion molecule- (ICAM-) 1, and vascular cell adhesion molecule-1 [28]. Selectins, comprising L-selectin on leukocytes and E- and P-selectins on endothelial cells, are a family of lectin-like adhesion glycoproteins that regulate leukocyte rolling and recruitment [28, 29]. Integrins, including leukocyte function-associated antigen-1 (CD11a/CD18) expressed on all leukocytes and macrophage-1 (MAC-1; CD11b/CD18) expressed on neutrophils and monocytes, are transmembrane glycoproteins and mediate leukocyte-endothelium interactions [30]. In acute cerebral ischemia, the upregulation of integrins facilitates a firm adherence of leukocytes to endothelial ICAM-1; the leukocytes subsequently penetrate the endothelial basement membrane into the brain parenchyma. Thus, the tight junctions (TJs) between endothelial cells of the BBB are disrupted and become more permeable, leading to leukocyte infiltration [30]. This evidence revealed that circulating leukocytes adhere to the damaged endothelium as early as 4 h and achieve the peak at approximately 12–48 h after ischemic brain injury. Meanwhile, reactive microglia, platelets, and infiltrating leukocytes further release IL-1β, IL-6, TNF-α, ROS, MCP-1, MIP-1α, IL-8, and MMPs (mainly MMP-9) that exacerbate ischemic injury in MCAo [3, 5, 6].

3.2. The Effects and Mechanisms of TCMs on Inhibiting Leukocyte Infiltration in In Vivo Models of Cerebral Ischemia. Lu et al. reported that emodin, an active component of the rhizome of *Rheum palmatum* L. (Da Huang), effectively reduces the cerebral infarct size 6 h after MCAo. The neuroprotective effects of emodin can be attributed to ICAM-1 downregulation in the ischemic area in the early phase of cerebral ischemia [31]. Ferulic acid (FA), a major active compound in both *Angelica sinensis (Oliv.)* Diels (Dang Gui)

Table 1: TCMs downregulate microglial activation in the inflammatory cascade in ischemic stroke models.

TCMs	Isolated from the Chinese herb (Chinese name)	Anti-inflammatory actions	Models	References
Paeonol	Mu Dan	ED1↓, IL-1β↓	MCAo 1.5 h of ischemia followed by 24 h of reperfusion	[20]
Tetramethylpyrazine	Chuan Xiong	MPO↓, ED1↓, PGE2↓	MCAo 1.5 h of ischemia followed by 72 h of reperfusion	[21]
Tetramethylpyrazine	Chuan Xiong	MCP-1↓	MCAo 1.5 h of ischemia followed by 72 h of reperfusion	[22]
Andrographolide	Chuan Xin Lian	NF-κBp65↓, TNF-α↓, IL-1β↓, PGE2↓	Permanent MCAo 24 h of ischemia	[23]
Sophora japonica L	Huai Hua	ED1↓, IL-1β↓	MCAo 1.5 h of ischemia followed by 24 h of reperfusion	[24]
Isoflavones	Ge Gen	COX-2↓, GFAP↓, OX-42↓	MCAo 2 h of ischemia followed by 2 or 7 d of reperfusion	[25]

ED1, CD68 (macrophage marker); MPO, myeloperoxidase; PGE2, prostaglandin E2; MCP-1, monocyte chemoattractant protein-1; COX-2, cyclooxygenase-2; GFAP, glial fibrillary acidic protein; OX-42, CD11b (microglial activation marker).

and *Ligusicum chuanxiong* Hort. (Chuan Xiong), effectively reduces the cerebral infarct area and ameliorates the neurological deficit at 1.5 h of reperfusion and 24 h of reperfusion. FA exerts anti-inflammatory effects against cerebral I/R injury, at least partially, by inhibiting ICAM-1, mRNA, and Mac-1 mRNA expression in the ischemic striatum 2 h after reperfusion [32, 33]. Bu-yang Huan-wu decoction (BHD), composed of *Astragalus membranaceus* Bunge (Huang Qi), *A. sinensis (Oliv.)* Diels (Dang Gui), *Paeonia lactiflora* Pall (Shao Yao), *L. chuanxiong* (Chuan Xiong), *Prunus persica* (L.) Batsch (Tao Ren), *Carthamus tinctorius* L. (Hong Hua), and *Pheretima aspergillum* (Di Long), effectively ameliorates cerebral infarction and improves neurological deficits 24 h after transient MCAo. The effects of BHD against cerebral ischemic injury are partially attributed to the inhibition of CD11b (a marker of leukocyte and monocyte activation) expression in the ischemic area [34]. Persimmon leaf flavonoid isolated from *Diospyros kaki* L.F (Shi Zhi Ye) exerts anti-inflammatory effects by downregulating ICAM-1 expression in the ischemic area 2 h after cerebral ischemia and 24 h after reperfusion [35]. Liu et al. demonstrated that the oral administration of *Cordyceps sinensis* (Dong Chong Xia Cao) mycelium exerts neuroprotective effects against cerebral I/R injury by downregulating ICAM-1, IL-1β, and TNF-α expression and infiltrating polymorphonuclear leukocytes (PMNs) in the ischemic area 2 h after ischemia and 22 h after reperfusion [12]. The oral pretreatment with a herb formula, FuLing-BaiZhu-DangGui (FBD), composed of *Poria cocos* (Fu Ling), *Atractylodes macrocephala* (Bai Zhu), and *A. sinensis*, protects against cerebral I/R injury partially by inhibiting PMNs infiltration in the ischemic area 24 h after transient forebrain ischemia in mice. The anti-inflammatory properties of FBD can be further attributed to IL-1β, TNF-α, and IL-8 downregulation during the acute phase of cerebral ischemia [36]. Kong et al. reported that Borneol (Bing Pian), the resin of *Dryobalanops aromatica Gaertn*. F., effectively improves neurological deficits 24 h after forebrain ischemia. The beneficial effects of Borneol involve the reduction of leukocyte infiltration and ICAM-1 expression in the ischemic area [37].

These results indicate that TCMs provide beneficial effects against leukocyte infiltration mainly by downregulating ICAM-1 expression and activated leukocyte-induced cytokines, such as IL-1β, TNF-α, and IL-8, in the ischemic lesion in the acute phase of cerebral ischemia (Figure 1 and Table 2).

4. TCM-Mediated Stabilization of Blood-Brain Barrier Integrity

4.1. Blood-Brain Barrier Disruption during Cerebral Ischemia. Under normal conditions, leukocyte recruitment across the BBB into the brain parenchyma contributes to the maintenance of the central nervous system immune privilege [9]. The BBB comprising endothelial cells, the basement membrane, the astrocyte end-feet, and pericytes provides a highly selective permeability barrier that separates the blood cells from the brain interstitial fluid and maintains brain homeostasis [38]. However, during the acute phase of cerebral ischemia, the infiltrated leukocytes and reactive microglia synthesize and secrete MMPs (mainly MMP-2 and MMP-9) and ROS, thus increasing BBB permeability [72, 73]. Previous studies have reported that MMP-9 activation is initiated as early as 4 h, which reaches the maximum level at 24 h and persists for at least 5 d after cerebral ischemia [74, 75], whereas activated MMP-2 reaches the highest level 5 d after MCAo [75]. Active MMPs disrupt BBB integrity by degrading the

Table 2: TCMs suppress leukocyte infiltration in the inflammatory cascade in ischemic stroke models.

TCMs	Isolated from the Chinese herb (Chinese name)	Anti-inflammatory actions	Models	References
Emodin	Da Huang	ICAM-1↓, TNF-α↓, IL-1β↓	MCAo 6 h of ischemia	[31]
Ferulic acid	Dang Gui or Chuan Xiong	ICAM-1↓, ICAM-1 mRNA↓, MPO↓, NF-κBp50↓,	MCAo 1.5 h of ischemia followed by 2 or 24 h of reperfusion	[32, 33]
Bu-yang Huan-wu decoction	Huang Qi, Dang Gui, Shao Yao, Chuan Xiong, Tao Ren, Hong Hua, Di Long	CD11b↓	MCAo 0.5 h of ischemia followed by 24 h of reperfusion	[34]
Persimmon leaf flavonoid	Shi Zhi Ye	ICAM-1↓	MCAo 2 h of ischemia followed by 24 h of reperfusion	[35]
Cordyceps sinensis	Dong Chong Xia Cao	ICAM-1↓, TNF-α↓, IL-1β↓, NF-κBp50↓, iNOS↓, COX-2↓	MCAo 2 h of ischemia followed by 22 h of reperfusion	[12]
FuLing-BaiZhu-DangGui	Fu Ling, Bai Zhu, Dang Gui	TNF-α↓, IL-1β↓, IL-8↓, MPO↓, NF-κB↓	Repetitive BCCAo 10 min of ischemia (repeat 2 times) followed by 24 h of reperfusion	[36]
Borneol	Bing Pian	ICAM-1↓, TNF-α↓	MCAo 2 h of ischemia followed by 22 h of reperfusion	[37]

ICAM-1, intercellular adhesion molecule-1; BCCAo, bilateral common carotid artery occlusion.

extracellular matrix and TJs in endothelial cells and result in vascular and BBB leakage. The BBB disruption facilitates the entry of circulating leukocytes and intravascular fluid into the brain, which cause vasogenic edema and hemorrhagic transformation, leading to the exacerbation of cerebral infarction [6, 9, 76]. TJs, including claudin-5, occludin, and zonula occludens- (ZO-) 1, play a pivotal role in maintaining the structural and functional integrity of the BBB [77]. Previous studies have reported that decreased claudin-5, occludin, and ZO-1 expression is closely related to BBB disruption and ischemic brain edema formation [77, 78]. Thus, MMPs, claudin-5, occludin, and ZO-1 could present the potential targets for pharmacological intervention to stabilize BBB integrity in cerebral ischemic injury and the regulation of their activity may yield therapeutic effects.

4.2. The Effects and Mechanisms of TCMs on Ameliorating Blood-Brain Barrier Disruption in In Vivo Models of Cerebral Ischemia. Posttreatment methylophiopogonanone- (MO-) A, an active compound isolated from *Ophiopogon japonicus* (Mai Men Dong), effectively reduces the infarct volume and brain edema and improves neurological deficits 7 d after transient MCAo. The results indicate that MO-A protects against cerebral I/R injury mainly through its property to ameliorate BBB disruption through MMP-9 downregulation, and claudin-3 and claudin-5 upregulation in the ischemic cortex [38]. Tan et al. reported that pretreatment with ligustrazine, an active ingredient of *L. wallichii* Franchat (Chuan Xiong), effectively preserves BBB integrity by downregulating MMP-9 expression and upregulating claudin-5 and occludin expression in the ischemic area in a rat model of focal cerebral I/R injury [39]. Levo-tetrahydropalmatine (l-THP), a major active ingredient of *Rhizoma corydalis* (Yan Hu Suo), protects against cerebral I/R-induced BBB injury at 1.5 h of ischemia and 24 h of reperfusion. The protective effect of l-THP can be partially attributed to MMP-2 and MMP-9 downregulation and claudin-5, occludin, and ZO-1 upregulation in the ischemic area [40].

From these results, we conclude that MMP-9 downregulation and claudin-5, occludin, and ZO-1 upregulation are the potential effects of TCMs on the stabilization of BBB integrity to ameliorate inflammatory responses in the ischemic area during the acute and subacute phases of cerebral I/R injury (Figure 1 and Table 3).

5. TCM-Mediated Regulation of Proinflammatory Mediator Release

5.1. Toll-Like Receptor Stimulation on Microglia/Macrophages during Cerebral Ischemia. In the ischemic core, active microglia are indistinguishable from blood-derived macrophages, and the microglia/macrophages are apparent 3.5–12 h after transient focal cerebral ischemia [79]. Subsequently, active microglia/macrophages are distributed in the entire middle cerebral artery territory at 22–24 h and maintained for up to 1 week after cerebral ischemia [6]. During cerebral ischemic insult, the dying cells release DAMPs, including heat shock proteins (HSPs), β-amyloid, hyaluronan, high mobility group box 1 (HMGB1), heparin sulfate, and ATP, thus stimulating TLRs, which are expressed on microglia/macrophages. Thereafter, the microglia/macrophages transform into M1 and M2 phenotypes upon stimulation and secrete various

Table 3: TCMs stabilize blood-brain barrier integrity in the inflammatory cascade in ischemic stroke models.

TCMs	Isolated from the Chinese herb (Chinese name)	Anti-inflammatory actions	Models	References
Methylophiopogonanone A	Mai Men Dong	MMP-9↓, claudin-3↑, claudin-5↑	MCAo 2 h of ischemia followed by 7 d of reperfusion	[38]
Ligustrazine	Chuan Xiong	MMP-9↓, claudin-5↑, occludin↑	MCAo 1.5 h of ischemia followed by 22.5 h of reperfusion	[39]
Levo-tetrahydropalmatine	Yan Hu Suo	MMP-2↓, MMP-9↓ claudin-5↑, occludin↑, ZO-1↑	MCAo 1.5 h of ischemia followed by 24 h of reperfusion	[40]

MMP-9, matrix metalloproteinase-9; ZO-1, zonula occludens-1.

cytokines in response to ischemic injury [73, 80, 81]. TLRs are pivotal components in the innate immune system, and TLRs (mainly TLR2 and TLR4) stimulation in microglia/macrophages and T-lymphocytes also exerts strong regulatory effects on postischemic inflammatory responses [2, 73]. During cerebral ischemic injury, TLRs facilitate cytokine and chemokine release and trigger transcription factor activation by activating intercellular signaling pathways. According to recruitment of specific adaptors, TLR signaling can be classified into either myeloid differentiation primary response gene 88- (MyD88-) dependent or independent pathways [81]. The binding of HSPs, such as HSP60 and HSP70, or HMGB1 with TLR2 and TLR4 initiate the expression of nuclear factor- (NF-) κB, TNF-α, IL-1β, IL-6, inducible nitric oxide synthase (iNOS), and ICAM-1 by activating the MyD88-dependent signaling pathway and aggravating cerebral ischemic injury [82]. TLR2 and TLR4 levels markedly increase in the ischemic brain at 6 h, peak at 24 h, and decline at 72 h after MCAo [83].

5.2. The Effects and Mechanisms of TCMs on Suppressing Toll-Like Receptor Stimulation in In Vivo Models of Cerebral Ischemia. Zhou et al. reported that the anti-infarct effects of puerarin, a major isoflavonoid in *Radix puerariae* (Ge Gen), can be attributed to the downregulation of TLR4/MyD88/NF-κB/TNF-α signaling in the ischemic region 24 h after transient MCAo [41]. TMP exerts anti-inflammatory effects against neutrophil activation 3 d after permanent MCAo. The beneficial effects of TMP can be partially attributed to HMGB1 and TLR4 downregulation in the ischemic cortex [42].

5.3. M1 Microglia/Macrophages Releasing Proinflammatory Mediators during Cerebral Ischemia. The M1 microglia/macrophages produce proinflammatory cytokines, including TNF-α, IL-1β, IL-6, IL-8, IL-12, IL-18, IL-20, and IFN-γ, whereas the M2 microglia/macrophages release anti-inflammatory cytokines, including IL-4, IL-10, IL-13, and TGF-β [1]. TNF-α is a pleiotropic cytokine that possesses both neurotoxic and neuroprotective properties. In the early phase of the inflammatory response, TNF-α binds to TNF receptor 1 (TNFR1) and contributes to the detrimental effects, such as promoting BBB disruption, vasogenic edema, leukocyte infiltration, and endothelial cell apoptosis [6, 84, 85]. Furthermore, TNF-α/TNFR1 activates NF-κB signaling, which regulates the expression of cytokines; chemokines; adhesion molecules; and inducible enzymes, namely, iNOS and cyclooxygenase-2 (COX-2), thus exacerbating cerebral ischemic injury [6]. By contrast, in the late phase of postischemic inflammation, TNF-α/TNFR2 facilitates neuroprotection, synaptic plasticity, and tissue repair [6, 86]. TNF-α becomes predominant in the ischemic lesion 24–48 h after MCAo [87]. IL-1, including IL-1α and IL-1β, can bind to IL-1 receptor type 1 (IL-1R1) and majorly contribute to the exacerbation of ischemic brain injury [88]. IL-1β has been clearly implicated in the pathogenesis of cerebral ischemia [6]. Inactive proIL-1β is converted to biologically active IL-1β by an IL-1β-converting enzyme, which belongs to the cysteine protease family. IL-1β is initially upregulated at 1–3 h and peaks at 12–24 h after ischemic injury. The cytotoxic actions of IL-1β include facilitating the activation of microglia, infiltration of leukocytes, and production of other cytokines such as IL-6 [6, 89]. Conversely, IL-1 receptor antagonist, a member of the IL-1 family, binds to IL-1R1 and subsequently blocks the detrimental actions of IL-1, exerting neuroprotection in cerebral ischemia process [90]. The role of IL-6 in cerebral ischemia remains controversial. Some studies have reported that IL-6 aggravates cerebral infarction [91, 92], whereas other studies have reported the beneficial effects of IL-6 in preventing damaged neuron from undergoing apoptosis and promoting neuronal survival after cerebral ischemia [93, 94]. Moreover, IL-6 is predominantly expressed in the ischemic area 24–48 h following cerebral I/R injury [87]. IL-8, IL-12, IL-18, and IL-20 play a pivotal role in promoting cerebral ischemic injury [7, 16, 95, 96]. IL-18 is initiated within 24–48 h and peaks at 6 d in the ischemic region after cerebral ischemia [97]. IFN-γ contributes to the exacerbation of cerebral ischemia by increasing ischemia-induced glutamate release [98].

5.4. The Effects and Mechanisms of TCMs on Downregulating Proinflammatory Mediators in In Vivo Models of Cerebral Ischemia. Notoginseng saponins isolated from the root of *Panax notoginseng* (San Qi) provide beneficial effects

against cerebral I/R injury partially through IL-1β mRNA downregulation in the ischemic area after 22 h of reperfusion [43]. Chang et al. reported that pretreatment with puerarin effectively reduces the cerebral infarct size and neurobehavioral deficits 24 h after MCAo. The anti-infarct effect of puerarin is, at least partially, because of the inhibition of TNF-α and iNOS expression in the ischemic area [44]. Li et al. explored the effect of osthole, a major active ingredient in *Cnidium monnieri* (L.) Gusson (She Chuang Zi), on acute cerebral I/R injury and reported that pretreatment with osthole markedly reduces the brain infarct volume and ameliorates neurological scores 24 h after MCAo. The neuroprotective effects of osthole are accompanied by the downregulation of proinflammatory mediators, including TNF-α, IL-1β, COX-2, and iNOS, expressed in the ischemic cortex [45]. The caffeic acid ester (Caf) fraction from *Erigeron breviscapus* (Deng Zhan Hua) significantly reduces the cerebral infarct volume and improves neurobehavioral performance at 1 h of ischemia and 24 h of reperfusion. The inhibition of iNOS, TNF-α, and IL-1β mRNA expression is one of the mechanisms underlying the neuroprotective effects of Caf against cerebral infarction [46]. Pretreatment with arctigenin, an active agent from *Arctium lappa* (Nu Bang Zi), effectively inhibits microglial activation and subsequently downregulates TNF-α and IL-1β expression in the penumbra region 24 h after transient MCAo [47]. Lee et al. reported that schisandrin B isolated from *Fructus schisandrae* (Wu Wei Zi) markedly reduces the cerebral infarct size and neurological deficits 24 h after transient focal cerebral ischemia. The anti-inflammatory effect of schisandrin B involves the inhibition of TNF-α, IL-1β, MMP-2, and MMP-9 expression and suppression of microglial activation in the ischemic area [48]. Posttreatment with asiaticoside, an active compound isolated from *Centella asiatica* (L.) (Ji Xue Cao), attenuates memory deficits by suppressing iNOS, TNF-α, IL-1β, and IL-6 expression in the hippocampus 7 d after transient bilateral common carotid artery occlusion [49]. Chen et al. reported that posttreatment with magnolol, an active ingredient of *Magnolia officinalis* (Hou Pu), ameliorates cerebral infarction partially by dose-dependently inhibiting iNOS, TNF-α, IL-1β, and IL-6 expression in the ischemic area 24 h after transient global ischemia [50]. Posttreatment with danhong, extracted from Radix *salviae miltiorrhizae* (Dan Shen) and *Flos carthami* (Hong Hua), exerts beneficial effects in cerebral I/R injury, at least partially, through dose-dependent IL-1β and TNF-α downregulation in the ischemia area at 1.5 h of ischemia and 14 d of reperfusion [51]. Gastrodin, an active constituent of *Gastrodia elata* Blume (Tian Ma), exerts an initial anti-inflammatory effect by suppressing TNF-α and IL-1β expression in the ischemic hemispheres 6 h after cerebral I/R injury [52].

5.5. The Effects and Mechanisms of TCMs on Regulating Anti-Inflammatory Cytokines in In Vivo Models of Cerebral Ischemia. IL-4, IL-10, IL-13, and TGF-β reduce microglia/macrophages-induced proinflammatory cytokines, such as IL-8 [99]. Moreover, IL-4 promotes long-term recovery after ischemic stroke [100]. IL-10 can inhibit IL-1 and TNF-α expression [55] and prevent the downregulation of the antiapoptotic protein Bcl-2 expressed in ischemic brain lesion [101]. IL-4 mRNA generates as early as 1 h, reaches a peak at 3–24 h, and gradually declines 2 d following ischemic stroke [102]. Pretreatment with danshen, an aqueous extract of the root and rhizome of *Salvia miltiorrhiza* Bunge (Dan Shen), protects against cerebral I/R injury in association with decreased IL-10 and TNF-α mRNA and protein expression in the ischemic area 24 h after transient MCAO [53]. Guizhi fuling capsules, composed of *Cinnamomum cassia* Blume (Gui Zhi), *P. lactiflora* Pall (Shao Yao), *P. suffruticosa* Andrews (Mu Dan Pi), *P. persica* Batsch (Tao Ren), and *Poria cocos* Wolf (Fu Ling), protect against cerebral infarction through TNF-α and IL-1β mRNA and protein downregulation and IL-10 and IL-10 receptor (IL-10R) mRNA and protein upregulation in the ischemia area after 2 h of ischemia and 24 h of reperfusion [54]. Zhang et al. also reported that the Gualou Guizhi decoction composed of *Trichosanthis* radix (Tian Hua Fen), *Ramulus cinnamomi* (Gui Zhi), *P. lactiflora* (Shao Yao), *Glycyrrhiza* (Gan Zao), *Zingiber officinale* Roscoe (Sheng Jiang), and *Fructus jujubae* (Da Zao) exerts neuroprotection against cerebral I/R injury through IL-1, TNF-α, and NF-κB downregulation and IL-10 upregulation in the ischemic area in the subacute phase (7 d) after transient MCAo [55].

5.6. The Effects and Mechanisms of TCMs on Downregulating Proinflammatory Enzymes in In Vivo Models of Cerebral Ischemia. COX-2 and 5-lipoxygenase (5-LO) are rate-limiting enzymes that convert arachidonic acid to prostaglandins and leukotrienes [57]. In the delayed phase of cerebral ischemia, microglia/macrophages produce 5-LO, which converts arachidonic acid to leukotrienes. Leukotrienes are potent inflammatory mediators that trigger chemotaxis of leukocytes and BBB damage and subsequently cause vasogenic edema, thus exacerbating cerebral ischemia [103]. COX-2 and 5-LO expression is markedly enhanced in the ischemic cortex 24 h after cerebral I/R injury [57]. Guo et al. explored the anti-infarct effect of paeoniflorin (PF), the principle component of *P. radix* (Shao Yao), in the subacute phase of cerebral I/R injury and reported that PF protects against cerebral infarction mainly through TNF-α, IL-1β, iNOS, COX-2, and 5-LO downregulation in the ischemic area 14 d after reperfusion [56]. Chen et al. reported that pretreatment with PF effectively ameliorates the cerebral infarct volume and neurological deficits 24 h after reperfusion in a model of pharmacological preconditioning. The neuroprotective effects of PF against cerebral I/R injury are partially related to the inhibition of COX-2, 5-LO, and iNOS expression in the ischemic lesion [57].

According to the aforementioned studies, proinflammatory mediators, such as TLR4, TNF-α, IL-1β, IL-6, IL-18, COX-2, and 5-LO, are predominately expressed in the ischemic area 24 h after MCAo. TCMs effectively ameliorate cerebral I/R injury by downregulating TLR4, TNF-α, IL-1β, IL-6, iNOS, COX-2, and 5-LO expression and upregulating IL-10 expression in the ischemic area during the acute and subacute phases of cerebral ischemia (Figure 1 and Table 4).

Table 4: TCMs regulate the cytokine release in the inflammatory cascade in ischemic stroke models.

TCMs	Isolated from the Chinese herb (Chinese name)	Anti-inflammatory actions	Models	References
Puerarin	Ge Gen	TLR4↓, MyD88↓, NF-κBp65↓, TNF-α↓	MCAo 1.5 h of ischemia followed by 24 h of reperfusion	[41]
Tetramethylpyrazine	Chuan Xiong	TLR4↓, HMGB1↓, Nrf2↑, HO-1↑	Permanent MCAo 3 d of ischemia	[42]
Notoginseng	San Qi	IL-1β↓	MCAo 2 h of ischemia followed by 22 h of reperfusion	[43]
Puerarin	Ge Gen	TNF-α↓, iNOS↓	MCAo 1 h of ischemia followed by 24 h of reperfusion	[44]
Osthole	She Chuang Zi	TNF-α↓, IL-1β↓, COX-2↓, iNOS↓	Permanent MCAo 24 h of ischemia	[45]
Caffeic acid ester	Deng Zhan Hua	iNOS mRNA↓, TNF-α mRNA↓, IL-1β mRNA↓	MCAo 1 h of ischemia followed by 24 h of reperfusion	[46]
Arctigenin	Nu Bang Zi	TNF-α↓, IL-1β↓, OX-42↓	MCAo 2 h of ischemia followed by 24 h of reperfusion	[47]
Schisandrin B	Wu Wei Zi	TNF-α↓, IL-1β↓, MMP-2↓, MMP-9↓, OX-42↓	MCAo 2 h of ischemia followed by 24 h of reperfusion	[48]
Asiaticoside	Ji Xue Cao	iNOS↓, TNF-α↓, IL-1β↓, IL-6↓	BCCAo 10 min of ischemia (repeat 2 times) followed by 7 d of reperfusion	[49]
Magnolol	Hou Pu	iNOS↓, TNF-α↓, IL-1β↓, IL-6↓, NF-κBp65↓	BCCAo 1.5 h of ischemia followed by 24 h of reperfusion	[50]
Danhong injection	Dan Shen and Hong Hua	TNF-α↓, IL-1β↓	MCAo 1.5 h of ischemia followed by 14 d of reperfusion	[51]
Gastrodin	Tian Ma	TNF-α↓, IL-1β↓	MCAo 1 h of ischemia followed by 6 h of reperfusion	[52]
Danshen	Dan Shen	IL-10 mRNA↓, TNF-α mRNA↓, IL-10↓, TNF-α↓	MCAo 1 h of ischemia followed by 24 h of reperfusion	[53]
Guizhi fuling capsules	Gui Zhi, Shao Yao, Mu Dan, Tao Ren, Fu Ling	TNF-α mRNA↓, IL-1β mRNA↓, TNF-α↓, IL-1β↓, IL-10 mRNA↑, IL-10R mRNA↑, IL-10↑, IL-10R↑	MCAo 2 h of ischemia followed by 24 h of reperfusion	[54]
Gualou Guizhi decoction	Tian Hua Fen, Gui Zhi, Shao Yao, Gan Zao, Sheng Jiang, Da Zao	TNF-α↓, IL-1↓, NF-κBp65↓, IL-10↑	MCAo 2 h of ischemia followed by 7 d of reperfusion	[55]
Paeoniflorin	Shao Yao	TNF-α↓, IL-1β↓, iNOS↓, COX-2↓, 5-LO↓	MCAo 1.5 h of ischemia followed by 14 d of reperfusion	[56]
Paeoniflorin	Shao Yao	COX-2↓, 5-LO↓, iNOS↓	MCAo 1.5 h of ischemia followed by 24 h of reperfusion	[57]

TLR4, toll-like receptor 4; MyD88, myeloid differentiation primary response gene 88; HMGB1, high mobility group box 1; Nrf2, nuclear factor-erythroid 2-related factor 2; HO-1, heme oxygenase-1; iNOS, inducible nitric oxidase synthase; 5-LO, 5-lipoxygenase.

6. TCM-Mediated Regulation of Transcription Factor Activation

6.1. NF-κB Activation during Cerebral Ischemia. NF-κB is a classic transcription factor and plays a crucial role in the regulation of hundreds of genes involved in cell survival and death [104]. Thus, NF-κB can be activated via several intracellular signaling pathways associated with host defense, inflammation, and apoptosis [58]. In the brain, NF-κB regulates the expression of different sets of genes, such as antiapoptotic, proapoptotic, and proinflammatory genes, thereby playing a dual role in neuronal survival and death [63]. The NF-κB family includes five members, namely, p65 (RelA), RelB, c-Rel, p50/p105 (NF-κB1), and p52/p100 (NF-κB2), which form various homo- and heterodimeric complexes [2]. The most common form of NF-κB is the p65/p50 heterodimer [6]. Under an unstimulated condition, the inhibitor of NF-κB proteins (IκBs), including mainly IκBα, IκBβ, and IκBε, retain inactive NF-κB dimmers in the cytosol, whereas in response to various extracellular stimuli, including infection, proinflammatory cytokines, and antigen receptor engagement, the activated IκB kinase complexes phosphorylate IκB proteins, resulting in their ubiquitination and proteasomal degradation and consequently inducing the release of NF-κB for nuclear translocation and the activation of target gene transcription [6, 105]. During cerebral ischemia, the activated NF-κB dimers are subsequently translocated into the nucleus where they selectively bind to specific DNA sequences called κB sites; promoter domains present a large number of proinflammatory genes and subsequently cause TNF-α, IL-1β, IL-6, ICAM-1, PGE2, COX-2, and iNOS translation [6, 105, 106]. NF-κB activators include some proinflammatory cytokines, such as TNF-α and IL-1β, whose genes are regulated by NF-κB itself, inducing a positive feedback loop and resulting in the amplification of the inflammatory response and exacerbation of cerebral ischemic insults [107]. Previous studies have indicated that NF-κB activation occurs as early as 1 h, reaches a peak at 6 h, and sustains for at least 72 h in the cerebral ischemic area in rats [62, 107].

6.2. The Effects and Mechanisms of TCMs on Downregulating NF-κB Activation in In Vivo Models of Cerebral Ischemia. Wogonin, a flavonoid derived from *Scutellaria baicalensis* Georgi (Huang Qin), exerts neuroprotective effects by inhibiting the inflammatory activation of microglia in an in vitro cell culture model. The anti-inflammatory effects of wogonin are partially attributed to the downregulation of NF-κB-mediated iNOS and TNF-α expression in the ischemic hippocampal CA1 area in transient global cerebral ischemia in rats [58]. Tanshinone IIA (Ts IIA) and IIB, the key compounds of *S. miltiorrhiza* Bunge, effectively reduce the cerebral infarct volume and improve the neurological function 24 h after transient MCAo [59]. Dong et al. further reported that pretreatment with Ts IIA protects against cerebral infarction partially associated with the reduction of ROS-mediated NF-κB activation, leading to the inhibition of iNOS expression in the ischemic area 24 h after permanent MCAo [60]. Silymarin, a bioactive component isolated from *Silybum marianum* (Shui Fei Ji), provides neuroprotection against cerebral I/R injury by inhibiting oxidative and nitrosative stress in the ischemic area 24 h after cerebral ischemia. The antioxidative and antinitrosative effects of silymarin are partially attributed to the reduction of NF-κB-mediated iNOS, COX-2, ICAM-1, TNF-α, and IL-1β expression in the injured tissues [61]. In addition, Guan et al. reported that ruscogenin, a major effective compound isolated from *O. japonicus* Ker-Gawl, ameliorates cerebral I/R injury through the downregulation of NF-κB target genes, including *ICAM-1*, *iNOS*, *COX-2*, *TNF-α*, and *IL-1β*, in the ischemic area 24 h after reperfusion [62]. Hydroxysafflor yellow A, a major active component of *C. tinctorius* L. (Hong Hua), reduces cerebral infarction by suppressing cytosolic NF-κBp65 translocation to the nucleus and subsequently downregulates NF-κB-mediated TNF-α, IL-1β, and IL-6 expression in the ischemic area 24 h after permanent MCAo [63]. Chern et al. reported that 2-methoxystypandrone (2-MS), a major active component of *Polygonum cuspidatum* (Hu Zhang), attenuates the brain infarct size and improves the neurological function, at least partially, by preventing IκBα degradation and a reducing NF-κB-mediated iNOS and COX-2 expression in the peri-infarct cortex 24 h after transient MCAo. The anti-inflammatory effects of 2-MS can further contribute toward the preserving BBB integrity [64]. Previous studies have indicated that p38 mitogen-activated protein kinase (MAPK), one of the MAPK family members, upregulates NF-κB expression (p38 MAPK/NF-κB signaling) and subsequently causes the transcription of genes encoding proinflammatory cytokines, resulting in the exacerbation of cerebral infarction in the acute phase of transient MCAo [108–110]. In addition, activated p38 MAPK occurs in the ischemic area as early as 2 h and reaches a peak 24–48 h after reperfusion [110]. Piperlonguminine from *Piper longum* (Bi Bo) alkaloids protects against cerebral ischemic injury by inhibiting the activation of p38 MAPK/NF-κB signaling cascade in the ischemic region 24 h after permanent MCAo [65].

6.3. The Effects and Mechanisms of TCMs on Upregulating Peroxisome Proliferator-Activated Receptor Activation in In Vivo Models of Cerebral Ischemia. Peroxisome proliferator-activated receptors (PPARs) include PPARα, PPARγ, and PPARδ/β isoforms, which are members of the nuclear receptor superfamily and represent ligand-activated transcription factors. PPARγ is predominantly expressed in the central nervous system and binds to peroxisome proliferator response elements to regulate its target gene expression [66]. During cerebral ischemia, PPARγ is detected in the peri-infarct area as early as 4 h and is sustained for at least 14 d after ischemia [111]. PPARγ exerts neuroprotective effects against inflammatory mediators to initiate responses by inhibiting the activation of NF-κB signaling in the ischemic area after focal cerebral ischemia [66, 111]. Liu et al. reported that pretreatment with curcumin, a natural polyphenolic component of *curcuma longa* (Jiang Huang), markedly reduces the cerebral infarct volume by activating PPARγ signaling in the ischemic cortex 24 h after reperfusion. The effects of curcumin on the regulation of PPARγ signaling further contribute to the downregulation of NF-κBp65-mediated TNF-α, IL-1β,

iNOS, PGE2, and COX-2 expression [66]. Another study revealed that pretreatment with icariin, a natural flavonoid compound extracted from *Epimedium brevicornum maxim* (Yin Yang Huo), protects against cerebral I/R injury by activating PPARα and PPARγ and subsequently suppressing NF-κBp65-mediated IL-1β expression in the ischemic cortex at 2 h of ischemia and 24 h of reperfusion [67].

6.4. The Effects and Mechanisms of TCMs on Regulating Signal Transducer and Activator of Transcription Activation in In Vivo Models of Cerebral Ischemia. Signal transducer and activator of transcription (STAT) proteins are a family of transcription factors comprising seven members, namely, STAT1, STAT2, STAT3, STAT4, STAT5a, STAT5b, and STAT6 [112]. Some controversy exists on whether STAT signaling is neuroprotective or neurotoxic in cerebral ischemic injury [113]. Growing evidence has revealed that cytokines induce the activation of the receptor-associated Janus kinases (JAKs), including JAK1, JAK2, JAK3, and tyrosine kinase 2, which consequently activate STAT proteins; the activated STAT proteins undergo dimerization and translocation to the nucleus, thereby regulating the expression of proapoptotic and proinflammatory genes [114, 115]. Among STAT protein isoforms, STAT3 is the most-conserved isoform [68]. In the transient cerebral ischemic rat model, STAT3 is activated as early as 30 min and sustained 24 h after reperfusion, and activated STAT3 triggers cerebral I/R injury by amplifying inflammatory responses [116]. However, other studies have reported that activated STAT3 signaling provides neuroprotection by upregulating Bcl-2 and vascular endothelial growth factor expression in the peri-infarct area after transient cerebral ischemia [113, 117]. Kaempferol-3-O-rutinoside (KRS) and kaempferol-3-O-glucoside (KGS) are also the active components of *C. tinctorius* L. Both KRS and KGS markedly reduce the cerebral infarct volume at least partially associated with the inhibition of STAT3 and NF-κBp65 activation, and subsequently, proinflammatory mediators (TNF-α, IL-1β, iNOS, MMP-9, and ICAM-1) production in the cortical penumbra 24 h after transient MCAo [68]. Astragaloside IV [the active component of *Astragalus* (Huang Qi)] combined with Ginsenoside Rg1, Ginsenoside Rb1, and Notoginsenoside R1 (the active components of *P*. notoginseng) effectively restores cell survival partially related to the inhibition of JAK1/STAT1 and NF-κB signaling and consequently suppresses TNF-α, IL-1β, and ICAM-1 mRNA expression in the ischemic area 24 h after transient global cerebral ischemia [69]. By contrast, Li et al. reported that curcumin reduces cerebral infarction and attenuates neurological deficits by activating JAK2/STAT3 signaling and downregulating IL-1β and IL-8 in the injured region after 24 h of reperfusion [70].

6.5. The Effects and Mechanisms of TCMs on Regulating Nuclear Factor-Erythroid 2-Related Factor 2/Heme Oxygenase-1 and c-Jun N-Terminal Kinase/c-Jun/Activating Protein-1 Signaling in an In Vivo Model of Cerebral Ischemia. Nuclear factor-erythroid 2-related factor 2 (Nrf2), a potent cytoprotective transcription factor, induces the expression of genes encoding antioxidant and anti-inflammatory proteins [118]. Under stress, Nrf2 dissociates from its cytoplasmic inhibitory protein Kelch-like ECH-associated protein 1 and translocates into the nucleus, where it binds to an antioxidant response element and regulates target genes, including heme oxygenase-1 (HO-1). The Nrf2/HO-1 signaling pathway attenuates inflammatory responses in cerebral ischemia [71]. During transient focal cerebral ischemia, Nrf2 and HO-1 occur in the ischemic cortex as early as 6 h, up to a maximum 48 h and decline 72 h after cerebral I/R [119]. The activation of c-Jun N-terminal kinase (JNK), one of the MAPK family members, signaling plays a central role in ischemia-induced neuroinflammation. When stimulated, activated JNK translocates into the nucleus and phosphorylates c-Jun, the major component of activating protein-(AP-) 1, which comprises c-Jun and c-Fos proteins, leading to the expression of target genes encoding proinflammatory mediators. JNK/AP-1 signaling amplifies the inflammatory response during cerebral ischemia [71]. JNK/c-Jun/AP-1 signaling factors are predominantly expressed in the ischemic area 2 h after cerebral ischemia [120]. Kao et al. reported that TMP effectively reduces cerebral infarction by inhibiting microglia/macrophages activation in the ischemic cortex 72 h after permanent MCAo. The anti-inflammatory effects of TMP can be further attributed to the upregulation of Nrf2/HO-1 signaling and downregulation of JNK/c-Jun/AP-1 signaling in the ischemic cortex [71].

According to the aforementioned studies, NF-κB and JNK/AP-1 signaling induced in the ischemic brain may amplify inflammatory responses, whereas PPARs and Nrf2/HO-1 signaling are considered to prevent postischemic inflammation and yield potent effects against cerebral ischemic injury. JAK/STAT signaling plays a dual role in the regulation of proinflammatory mediators depending on the experimental models of brain ischemia. TCMs protect against cerebral ischemic injury by inhibiting deleterious transcription factors (NF-κB, JAK/STAT, and JNK/AP-1), activating neuroprotective transcription factors (PPARs and Nrf2/HO-1) and consequently regulating the expression of transcription factor-mediated proinflammatory genes (TNF-α, IL-1β, IL-6, IL-8, iNOS, COX-2, PGE2, MMP-9, and ICAM-1) in the ischemic area in the early stage (24–72 h) of cerebral ischemia (Figure 2 and Table 5).

7. Conclusions

After the onset of cerebral ischemia, resident microglia are rapidly activated (within a few minutes) and subsequently produce large amounts of cytokines, chemokines, and ROS, thus causing the initial ischemic injury. TCMs can exert neuroprotective effects against the initial ischemic injury by rapidly downregulating ischemia-induced microglial activation and microglia-mediated proinflammatory cytokine production in the ischemic region. The microglial production of proinflammatory mediators subsequently increase adhesion molecule expression, facilitate leukocyte-endothelial cell interactions, and activated leukocytes that penetrate the endothelial cell barrier into the brain parenchyma (as early as 4 h after the ischemic onset). The infiltrating leukocytes further release inflammatory mediators in the

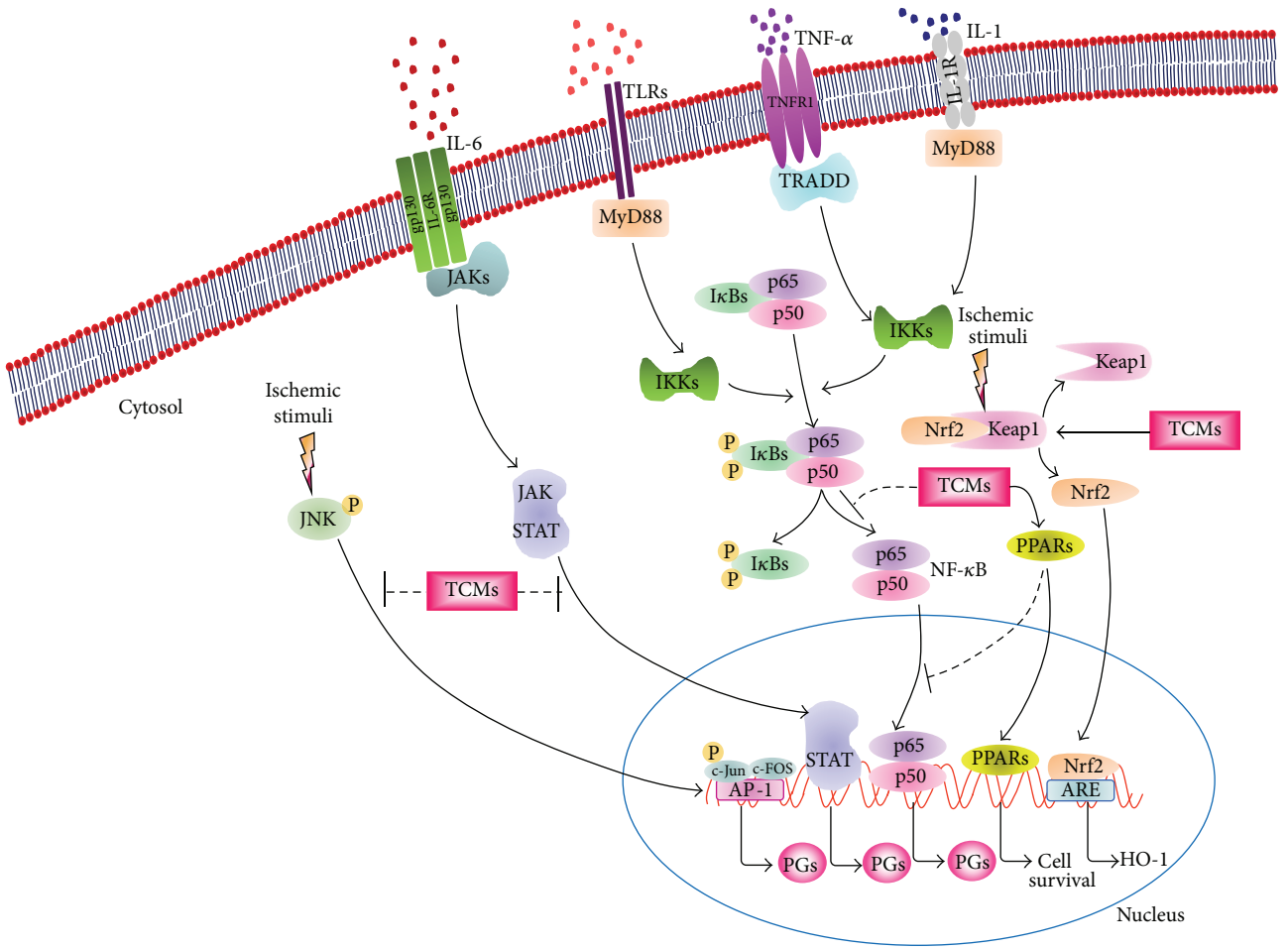

FIGURE 2: Schematic representation of the anti-inflammatory effects of traditional Chinese medicines through the regulation of transcription factors in the inflammatory cascade after cerebral ischemia. JAKs, Janus kinases; MyD88, myeloid differentiation primary response gene 88; TRADD, tumor necrosis factor receptor type 1-associated death domain; IκBs, inhibitor of NF-κB proteins; IKKs, IκB kinases; Nrf2, nuclear factor-erythroid 2-related factor 2; Keap1, Kelch-like ECH-associated protein 1; PPARs, peroxisome proliferator-activated receptors; STAT, signal transducer and activator of transcription; JNK, c-Jun N-terminal kinase; AP-1, activating protein-1; ARE, antioxidant response element; HO-1, heme oxygenase-1; PGs, proinflammatory genes. Thick solid lines with arrowheads indicate activation, and thin dotted lines indicate inhibition.

ischemic lesion, thus exacerbating ischemic injury. TCMs can effectively attenuate leukocyte infiltration by inhibiting ICAM-1 and activated leukocyte-induced cytokine expression in the ischemic region in the early phase of cerebral ischemia. Meanwhile, infiltrated leukocytes and activated microglia secrete MMPs, which cause the disruption of BBB integrity, worsening cerebral infarction. TCMs effectively inhibit MMPs expression and stabilize BBB integrity to ameliorate cerebral infarction. Increased TLRs stimulation in microglia/macrophages (activated microglia and recruited leukocytes) by the activation of intercellular signaling pathways robustly secretes various proinflammatory mediators (cytokines and enzymes) in the ischemic region 6–24 h after ischemia. TCMs can timely rescue the injured neurons by downregulating proinflammatory receptors (TLRs), cytokines, and enzymes and upregulating anti-inflammatory cytokine expression in the ischemic lesion. The proinflammatory transcription factors are subsequently activated by the secreted cytokines, whose genes are regulated by these transcription factors themselves, thus inducing a positive feedback loop, in which the inflammatory response is amplified and secondary brain injury is exacerbated 24–72 h after cerebral ischemia. TCMs protect against inflammatory response-induced secondary brain injury by inhibiting deleterious transcription factors, activating neuroprotective transcription factors, and consequently regulating the expression of transcription factor-mediated proinflammatory genes in the ischemic area. Therefore, TCMs provide promising anti-inflammatory therapeutic strategies in the acute phase of cerebral ischemia. However, further studies are needed to elucidate the precise mechanisms of TCMs against inflammatory responses in the ischemic cascade after stroke.

Competing Interests

The authors have declared that no competing interests exist.

Table 5: TCMs regulate transcription factors in the inflammatory cascade in ischemic stroke models.

TCMs	Isolated from the Chinese herb (Chinese name)	Anti-inflammatory actions	Models	References
Wogonin	Huang Qin	NF-κBp65↓, iNOS↓, TNF-α↓	4-VO 10 min of ischemia followed by 7 d of reperfusion	[58]
Tanshinone IIA	Dan Shen	NF-κBp65↓, iNOS↓	MCAo 2 h of ischemia followed by 24 h of reperfusion Permanent MCAo 24 h of ischemia	[59, 60]
Silymarin	Shui Fei Ji	NF-κBp65↓, iNOS↓, COX-2↓, ICAM-1↓, IL-1β↓, MPO↓	MCAo 1 h of ischemia followed by 24 h of reperfusion	[61]
Ruscogenin	Mai Men Dong	NF-κBp65↓, ICAM-1↓, iNOS↓, COX-2↓, TNF-α↓, IL-1β↓	MCAo 1 h of ischemia followed by 24 h of reperfusion	[62]
Hydroxysafflor yellow A	Hong Hua	NF-κBp65↓, TNF-α↓, IL-1β↓, IL-6↓	Permanent MCAo 24 h of ischemia	[63]
2-Methoxystypandrone	Hu Zhang	NF-κBp65↓, IκBα↑, iNOS↓, COX-2↓,	MCAo 40 min of ischemia followed by 24 h of reperfusion	[64]
Piperlonguminine	Bi Bo	NF-κBp65↓, p-p38 MAPK↓	Permanent MCAo 24 h of ischemia	[65]
Curcumin	Jiang Huang	PPARγ↑, NF-κBp65↓, IκBα↑, TNF-α↓, IL-1β↓, iNOS↓, PGE2↓, COX-2↓	MCAo 2 h of ischemia followed by 24 h of reperfusion	[66]
Icariin	Yin Yang Huo	PPARα↑, PPARγ↑, NF-κBp65↓, IL-1β↓	MCAo 2 h of ischemia followed by 24 h of reperfusion	[67]
Kaempferol-3-O-rutinoside and kaempferol-3-O-glucoside	Hong Hua	STAT3↓, NF-κBp65↓ TNF-α↓, IL-1β↓, iNOS↓, MMP-9↓, ICAM-1↓	MCAo 2 h of ischemia followed by 24 h of reperfusion	[68]
Astragaloside IV, ginsenoside Rg1, ginsenoside Rb1, notoginsenoside R1	Huang Qi and San Qi	JAK1↓, STAT1↓, NF-κBp65↓, p-IκBα↓ TNF-α mRNA↓, IL-1β mRNA↓, ICAM-1 mRNA↓	BCCAo 20 min of ischemia followed by 24 h of reperfusion	[69]
Curcumin	Jiang Huang	JAK2↑, STAT3↑, IL-1β↓, IL-8↓	MCAo 1.5 h of ischemia followed by 24 h of reperfusion	[70]
Tetramethylpyrazine	Chuan Xiong	Nrf2↑, HO-1↑, MPO↓, p-c-Jun↓, p-JNK↓, AP-1↓	Permanent MCAo 72 h of ischemia	[71]

4-VO, 4-vessel occlusion; IκBα, inhibitor of NF-κB protein α; PPARγ, peroxisome proliferator-activated receptor γ; STAT3, signal transducer and activator of transcription 3; JAK1, Janus kinase 1; AP-1, activating protein-1.

Acknowledgments

This study was supported by grants from China Medical University Hospital (DMR-105-007), Taichung, Taiwan.

References

[1] A. Siniscalchi, L. Gallelli, G. Malferrari et al., "Cerebral stroke injury: the role of cytokines and brain inflammation," *Journal of Basic and Clinical Physiology and Pharmacology*, vol. 25, no. 2, pp. 131–137, 2014.

[2] R. Jin, L. Liu, S. Zhang, A. Nanda, and G. Li, "Role of inflammation and its mediators in acute ischemic stroke," *Journal of Cardiovascular Translational Research*, vol. 6, no. 5, pp. 834–851, 2013.

[3] R. Jin, G. Yang, and G. Li, "Inflammatory mechanisms in ischemic stroke: role of inflammatory cells," *Journal of Leukocyte Biology*, vol. 87, no. 5, pp. 779–789, 2010.

[4] R.-D. Cheng, J.-J. Ren, Y.-Y. Zhang, and X.-M. Ye, "P2X4 receptors expressed on microglial cells in post-ischemic inflammation of brain ischemic injury," *Neurochemistry International*, vol. 67, no. 1, pp. 9–13, 2014.

[5] M. K. Tobin, J. A. Bonds, R. D. Minshall, D. A. Pelligrino, F. D. Testai, and O. Lazarov, "Neurogenesis and inflammation after ischemic stroke: what is known and where we go from here,"

Journal of Cerebral Blood Flow and Metabolism, vol. 34, no. 10, pp. 1573–1584, 2014.

[6] J. Y. Kim, M. Kawabori, and M. A. Yenari, "Innate inflammatory responses in stroke: mechanisms and potential therapeutic targets," *Current Medicinal Chemistry*, vol. 21, no. 18, pp. 2076–2097, 2014.

[7] S. E. Lakhan, A. Kirchgessner, and M. Hofer, "Inflammatory mechanisms in ischemic stroke: therapeutic approaches," *Journal of Translational Medicine*, vol. 7, article 97, 2009.

[8] E.-Y. Cho, S.-J. Lee, K.-W. Nam et al., "Amelioration of oxygen and glucose deprivation-induced neuronal death by chloroform fraction of bay leaves (Laurus nobilis)," *Bioscience, Biotechnology and Biochemistry*, vol. 74, no. 10, pp. 2029–2035, 2010.

[9] A. Simats, T. García-Berrocoso, and J. Montaner, "Neuroinflammatory biomarkers: from stroke diagnosis and prognosis to therapy," *Biochimica et Biophysica Acta—Molecular Basis of Disease*, vol. 1862, no. 3, pp. 411–424, 2016.

[10] J. Galea and D. Brough, "The role of inflammation and interleukin-1 in acute cerebrovascular disease," *Journal of Inflammation Research*, vol. 6, no. 1, pp. 121–128, 2013.

[11] V. L. Feigin, "Herbal medicine in stroke: does it have a future?" *Stroke*, vol. 38, no. 6, pp. 1734–1736, 2007.

[12] Z. Liu, P. Li, D. Zhao, H. Tang, and J. Guo, "Anti-inflammation effects of cordyceps sinensis mycelium in focal cerebral ischemic injury rats," *Inflammation*, vol. 34, no. 6, pp. 639–644, 2011.

[13] K. Sun, J. Fan, and J. Han, "Ameliorating effects of traditional Chinese medicine preparation, Chinese materia medica and active compounds on ischemia/reperfusion-induced cerebral microcirculatory disturbances and neuron damage," *Acta Pharmaceutica Sinica B*, vol. 5, no. 1, pp. 8–24, 2015.

[14] S. Rivest, "Regulation of innate immune responses in the brain," *Nature Reviews Immunology*, vol. 9, no. 6, pp. 429–439, 2009.

[15] H. W. Morrison and J. A. Filosa, "A quantitative spatiotemporal analysis of microglia morphology during ischemic stroke and reperfusion," *Journal of Neuroinflammation*, vol. 10, article 4, 2013.

[16] T. Shichita, M. Ito, and A. Yoshimura, "Post-ischemic inflammation regulates neural damage and protection," *Frontiers in Cellular Neuroscience*, vol. 8, article 319, 2014.

[17] Q. Zhao, X. Xie, Y. Fan et al., "Phenotypic dysregulation of microglial activation in young offspring rats with maternal sleep deprivation-induced cognitive impairment," *Scientific Reports*, vol. 5, article 9513, 2015.

[18] E. J. Walker and G. A. Rosenberg, "TIMP-3 and MMP-3 contribute to delayed inflammation and hippocampal neuronal death following global ischemia," *Experimental Neurology*, vol. 216, no. 1, pp. 122–131, 2009.

[19] Y. Lee, S.-R. Lee, S. S. Choi, H.-G. Yeo, K.-T. Chang, and H. J. Lee, "Therapeutically targeting neuroinflammation and microglia after acute ischemic stroke," *BioMed Research International*, vol. 2014, Article ID 297241, 9 pages, 2014.

[20] C.-L. Hsieh, C.-Y. Cheng, T.-H. Tsai et al., "Paeonol reduced cerebral infarction involving the superoxide anion and microglia activation in ischemia-reperfusion injured rats," *Journal of Ethnopharmacology*, vol. 106, no. 2, pp. 208–215, 2006.

[21] S.-L. Liao, T.-K. Kao, W.-Y. Chen et al., "Tetramethylpyrazine reduces ischemic brain injury in rats," *Neuroscience Letters*, vol. 372, no. 1-2, pp. 40–45, 2004.

[22] T.-K. Kao, Y.-C. Ou, J.-S. Kuo et al., "Neuroprotection by tetramethylpyrazine against ischemic brain injury in rats," *Neurochemistry International*, vol. 48, no. 3, pp. 166–176, 2006.

[23] S. J. Chan, W. S. F. Wong, P. T. H. Wong, and J.-S. Bian, "Neuroprotective effects of andrographolide in a rat model of permanent cerebral ischaemia," *British Journal of Pharmacology*, vol. 161, no. 3, pp. 668–679, 2010.

[24] C.-J. Lao, J.-G. Lin, J.-S. Kuo et al., "Microglia, apoptosis and interleukin-1β expression in the effect of Sophora Japonica L. on cerebral infarct induced by ischemia-reperfusion in rats," *American Journal of Chinese Medicine*, vol. 33, no. 3, pp. 425–438, 2005.

[25] D. W. Lim, C. Lee, I.-H. Kim, and Y. T. Kim, "Anti-inflammatory effects of total isoflavones from *Pueraria lobata* on cerebral ischemia in rats," *Molecules*, vol. 18, no. 9, pp. 10404–10412, 2013.

[26] A. C. C. da Fonseca, D. Matias, C. Garcia et al., "The impact of microglial activation on blood-brain barrier in brain diseases," *Frontiers in Cellular Neuroscience*, vol. 8, article 362, 2014.

[27] G. Trendelenburg, "Molecular regulation of cell fate in cerebral ischemia: role of the inflammasome and connected pathways," *Journal of Cerebral Blood Flow & Metabolism*, vol. 34, no. 12, pp. 1857–1867, 2014.

[28] G. Yilmaz and D. N. Granger, "Leukocyte recruitment and ischemic brain injury," *NeuroMolecular Medicine*, vol. 12, no. 2, pp. 193–204, 2010.

[29] J. Monteseirín, E. Llamas, H. Sánchez-Monteseirín et al., "IgE-mediated downregulation of L-selectin (CD62L) on lymphocytes from asthmatic patients," *Allergy*, vol. 56, no. 2, pp. 164–168, 2001.

[30] B. M. Famakin, "The immune response to acute focal cerebral ischemia and associated post-stroke immunodepression: a focused review," *Aging and Disease*, vol. 5, no. 5, pp. 307–326, 2014.

[31] J.-S. Lu, J.-X. Liu, W.-Y. Zhang, S.-W. Liang, D. Wang, and J. Fang, "Preventive effects of Emodin on cerebral ischemia injury and expression of the inflammatory factors in rats with cerebral ischemia," *Zhongguo Zhong Yao Za Zhi*, vol. 30, no. 24, pp. 1939–1943, 2005.

[32] C.-Y. Cheng, T.-Y. Ho, E.-J. Lee, S.-Y. Su, N.-Y. Tang, and C.-L. Hsieh, "Ferulic acid reduces cerebral infarct through its antioxidative and anti-inflammatory effects following transient focal cerebral ischemia in rats," *The American Journal of Chinese Medicine*, vol. 36, no. 6, pp. 1105–1119, 2008.

[33] C.-Y. Cheng, S.-Y. Su, N.-Y. Tang, T.-Y. Ho, S.-Y. Chiang, and C.-L. Hsieh, "Ferulic acid provides neuroprotection against oxidative stress-related apoptosis after cerebral ischemia/reperfusion injury by inhibiting ICAM-1 mRNA expression in rats," *Brain Research*, vol. 1209, pp. 136–150, 2008.

[34] H.-W. Wang, K.-T. Liou, Y.-H. Wang et al., "Deciphering the neuroprotective mechanisms of Bu-yang Huan-wu decoction by an integrative neurofunctional and genomic approach in ischemic stroke mice," *Journal of Ethnopharmacology*, vol. 138, no. 1, pp. 22–33, 2011.

[35] M. S. Miao, X. X. Zhang, M. Bai, and L. N. Wang, "Persimmon leaf flavonoid promotes brain ischemic tolerance," *Neural Regeneration Research*, vol. 8, no. 28, pp. 2625–2632, 2013.

[36] Z. Lin, D. Zhu, Y. Yan, and B. Yu, "Herbal formula FBD extracts prevented brain injury and inflammation induced by cerebral ischemia-reperfusion," *Journal of Ethnopharmacology*, vol. 118, no. 1, pp. 140–147, 2008.

[37] Q.-X. Kong, Z.-Y. Wu, X. Chu, R.-Q. Liang, M. Xia, and L. Li, "Study on the anti-cerebral ischemia effect of borneol and

its mechanism," *African Journal of Traditional, Complementary, and Alternative Medicines*, vol. 11, no. 1, pp. 161–164, 2014.

[38] M. Lin, W. Sun, W. Gong, Z. Zhou, Y. Ding, and Q. Hou, "Methylophiopogonanone a protects against cerebral ischemia/reperfusion injury and attenuates blood-brain barrier disruption," *PLoS ONE*, vol. 10, no. 4, Article ID e0124558, 2015.

[39] F. Tan, W. Fu, N. Cheng, D. I. Meng, and Y. Gu, "Ligustrazine reduces blood-brain barrier permeability in a rat model of focal cerebral ischemia and reperfusion," *Experimental and Therapeutic Medicine*, vol. 9, no. 5, pp. 1757–1762, 2015.

[40] X.-W. Mao, C.-S. Pan, P. Huang et al., "Levo-tetrahydropalmatine attenuates mouse blood-brain barrier injury induced by focal cerebral ischemia and reperfusion: involvement of Src kinase," *Scientific Reports*, vol. 5, Article ID 11155, 2015.

[41] F. Zhou, L. Wang, P. P. Liu et al., "Puerarin protects brain tissue against cerebral ischemia/reperfusion injury by inhibiting the inflammatory response," *Neural Regeneration Research*, vol. 9, no. 23, pp. 2074–2080, 2014.

[42] C.-Y. Chang, T.-K. Kao, W.-Y. Chen et al., "Tetramethylpyrazine inhibits neutrophil activation following permanent cerebral ischemia in rats," *Biochemical and Biophysical Research Communications*, vol. 463, no. 3, pp. 421–427, 2015.

[43] Y. H. Tang, S. P. Zhang, Y. Liang, and C. Q. Deng, "Effects of Panax notoginseng saponins on mRNA expressions of interleukin-1 β, its correlative factors and cysteinyl-aspartate specific protease after cerebral ischemia-reperfusion in rats," *Zhong Xi Yi Jie He Xue Bao*, vol. 5, no. 3, pp. 328–332, 2007.

[44] Y. Chang, C.-Y. Hsieh, Z.-A. Peng et al., "Neuroprotective mechanisms of puerarin in middle cerebral artery occlusion-induced brain infarction in rats," *Journal of Biomedical Science*, vol. 16, article 9, 2009.

[45] F. Li, Q. Gong, L. Wang, and J. Shi, "Osthole attenuates focal inflammatory reaction following permanent middle cerebral artery occlusion in rats," *Biological and Pharmaceutical Bulletin*, vol. 35, no. 10, pp. 1686–1690, 2012.

[46] S.-X. Wang, H. Guo, L.-M. Hu et al., "Caffeic acid ester fraction from erigeron breviscapus inhibits microglial activation and provides neuroprotection," *Chinese Journal of Integrative Medicine*, vol. 18, no. 6, pp. 437–444, 2012.

[47] T. Fan, W. L. Jiang, J. Zhu, and Y. Feng Zhang, "Arctigenin protects focal cerebral ischemia-reperfusion rats through inhibiting neuroinflammation," *Biological and Pharmaceutical Bulletin*, vol. 35, no. 11, pp. 2004–2009, 2012.

[48] T. H. Lee, C. H. Jung, and D.-H. Lee, "Neuroprotective effects of Schisandrin B against transient focal cerebral ischemia in Sprague-Dawley rats," *Food and Chemical Toxicology*, vol. 50, no. 12, pp. 4239–4245, 2012.

[49] S. Chen, Z.-J. Yin, C. Jiang et al., "Asiaticoside attenuates memory impairment induced by transient cerebral ischemia-reperfusion in mice through anti-inflammatory mechanism," *Pharmacology Biochemistry and Behavior*, vol. 122, pp. 7–15, 2014.

[50] J.-H. Chen, H.-C. Kuo, K.-F. Lee, and T.-H. Tsai, "Magnolol protects neurons against ischemia injury via the downregulation of p38/MAPK, CHOP and nitrotyrosine," *Toxicology and Applied Pharmacology*, vol. 279, no. 3, pp. 294–302, 2014.

[51] Z. Wang, F. Song, J. Li et al., "PET demonstrates functional recovery after treatment by danhong injection in a rat model of cerebral ischemic-reperfusion injury," *Evidence-Based Complementary and Alternative Medicine*, vol. 2014, Article ID 430757, 9 pages, 2014.

[52] Z. Peng, S. Wang, G. Chen et al., "Gastrodin alleviates cerebral ischemic damage in mice by improving anti-oxidant and anti-inflammation activities and inhibiting apoptosis pathway," *Neurochemical Research*, vol. 40, no. 4, pp. 661–673, 2015.

[53] X.-Y. Liang, H.-N. Li, X.-Y. Yang, W.-Y. Zhou, J.-G. Niu, and B.-D. Chen, "Effect of Danshen aqueous extract on serum hs-CRP, IL-8, IL-10, TNF-α levels, and IL-10 mRNA, TNF-α mRNA expression levels, cerebral TGF-β1 positive expression level and its neuroprotective mechanisms in CIR rats," *Molecular Biology Reports*, vol. 40, no. 4, pp. 3419–3427, 2013.

[54] T.-J. Li, Y. Qiu, J.-Q. Mao, P.-Y. Yang, Y.-C. Rui, and W.-S. Chen, "Protective effects of Guizhi-Fuling-capsules on rat brain ischemia/reperfusion injury," *Journal of Pharmacological Sciences*, vol. 105, no. 1, pp. 34–40, 2007.

[55] Y. Zhang, S. Zhang, H. Li et al., "Ameliorative effects of Gualou Guizhi decoction on inflammation in focal cerebral ischemic-reperfusion injury," *Molecular Medicine Reports*, vol. 12, no. 1, pp. 988–994, 2015.

[56] R.-B. Guo, G.-F. Wang, A.-P. Zhao, J. Gu, X.-L. Sun, and G. Hu, "Paeoniflorin protects against ischemia-induced brain damages in rats via inhibiting MAPKs/NF-κB-mediated inflammatory responses," *PLoS ONE*, vol. 7, no. 11, Article ID e49701, 2012.

[57] D.-M. Chen, L. Xiao, X. Cai, R. Zeng, and X.-Z. Zhu, "Involvement of multitargets in paeoniflorin-induced preconditioning," *Journal of Pharmacology and Experimental Therapeutics*, vol. 319, no. 1, pp. 165–180, 2006.

[58] H. Lee, Y. O. Kim, H. Kim et al., "Flavonoid wogonin from medicinal herb is neuroprotective by inhibiting inflammatory activation of microglia," *The FASEB Journal*, vol. 17, no. 13, pp. 1943–1944, 2003.

[59] B. Y. H. Lam, A. C. Y. Lo, X. Sun, H. W. Luo, S. K. Chung, and N. J. Sucher, "Neuroprotective effects of tanshinones in transient focal cerebral ischemia in mice," *Phytomedicine*, vol. 10, no. 4, pp. 286–291, 2003.

[60] K. Dong, W. Xu, J. Yang, H. Qiao, and L. Wu, "Neuroprotective effects of Tanshinone IIA on permanent focal cerebral ischemia in mice," *Phytotherapy Research*, vol. 23, no. 5, pp. 608–613, 2009.

[61] Y.-C. Hou, K.-T. Liou, C.-M. Chern et al., "Preventive effect of silymarin in cerebral ischemia-reperfusion-induced brain injury in rats possibly through impairing NF-κB and STAT-1 activation," *Phytomedicine*, vol. 17, no. 12, pp. 963–973, 2010.

[62] T. Guan, Q. Liu, Y. Qian et al., "Ruscogenin reduces cerebral ischemic injury via NF-κB-mediated inflammatory pathway in the mouse model of experimental stroke," *European Journal of Pharmacology*, vol. 714, no. 1–3, pp. 303–311, 2013.

[63] Y. Liu, Z. Lian, H. Zhu et al., "A systematic, integrated study on the neuroprotective effects of hydroxysafflor yellow a revealed by ^{1}H NMR-based metabonomics and the NF-κB pathway," *Evidence-Based Complementary and Alternative Medicine*, vol. 2013, Article ID 147362, 14 pages, 2013.

[64] C.-M. Chern, Y.-H. Wang, K.-T. Liou, Y.-C. Hou, C.-C. Chen, and Y.-C. Shen, "2-Methoxystypandrone ameliorates brain function through preserving BBB integrity and promoting neurogenesis in mice with acute ischemic stroke," *Biochemical Pharmacology*, vol. 87, no. 3, pp. 502–514, 2014.

[65] T. Yang, S. Sun, T. Wang et al., "Piperlonguminine is neuroprotective in experimental rat stroke," *International Immunopharmacology*, vol. 23, no. 2, pp. 447–451, 2014.

[66] Z.-J. Liu, W. Liu, L. Liu, C. Xiao, Y. Wang, and J.-S. Jiao, "Curcumin protects neuron against cerebral ischemia-induced inflammation through improving PPAR-gamma function,"

Evidence-Based Complementary and Alternative Medicine, vol. 2013, Article ID 470975, 10 pages, 2013.

[67] D. Xiong, Y. Deng, B. Huang et al., "Icariin attenuates cerebral ischemia-reperfusion injury through inhibition of inflammatory response mediated by NF-κB, PPARα and PPARγ in rats," *International Immunopharmacology*, vol. 30, pp. 157–162, 2016.

[68] L. Yu, C. Chen, L.-F. Wang et al., "Neuroprotective effect of kaempferol glycosides against brain injury and neuroinflammation by inhibiting the activation of NF-κB and STAT3 in transient focal stroke," *PLoS ONE*, vol. 8, no. 2, Article ID e55839, 2013.

[69] X.-P. Huang, H. Ding, J.-D. Lu, Y.-H. Tang, B.-X. Deng, and C.-Q. Deng, "Effects of the combination of the main active components of *Astragalus* and *Panax notoginseng* on inflammation and apoptosis of nerve cell after cerebral ischemia-reperfusion," *The American Journal of Chinese Medicine*, vol. 43, no. 7, pp. 1419–1438, 2015.

[70] L. Li, H. Li, and M. Li, "Curcumin protects against cerebral ischemia-reperfusion injury by activating JAK2/STAT3 signaling pathway in rats," *International Journal of Clinical and Experimental Medicine*, vol. 8, no. 9, pp. 14985–14991, 2015.

[71] T.-K. Kao, C.-Y. Chang, Y.-C. Ou et al., "Tetramethylpyrazine reduces cellular inflammatory response following permanent focal cerebral ischemia in rats," *Experimental Neurology*, vol. 247, pp. 188–201, 2013.

[72] H. Könnecke and I. Bechmann, "The role of microglia and matrix metalloproteinases involvement in neuroinflammation and gliomas," *Clinical and Developmental Immunology*, vol. 2013, Article ID 914104, 15 pages, 2013.

[73] T. Shichita, R. Sakaguchi, M. Suzuki, and A. Yoshimura, "Post-ischemic inflammation in the brain," *Frontiers in Immunology*, vol. 3, article 132, 2012.

[74] X. Dong, Y.-N. Song, W.-G. Liu, and X.-L. Guo, "MMP-9, a potential target for cerebral ischemic treatment," *Current Neuropharmacology*, vol. 7, no. 4, pp. 269–275, 2009.

[75] A. M. Romanic, R. F. White, A. J. Arleth, E. H. Ohlstein, and F. C. Barone, "Matrix metalloproteinase expression increases after cerebral focal ischemia in rats: inhibition of matrix metalloproteinase-9 reduces infarct size," *Stroke*, vol. 29, no. 5, pp. 1020–1030, 1998.

[76] S. E. Lakhan, A. Kirchgessner, D. Tepper, and A. Leonard, "Matrix metalloproteinases and blood-brain barrier disruption in acute ischemic stroke," *Frontiers in Neurology*, vol. 4, article 32, 2013.

[77] Y.-M. Zhang, H. Xu, H. Sun, S.-H. Chen, and F.-M. Wang, "Electroacupuncture treatment improves neurological function associated with regulation of tight junction proteins in rats with cerebral ischemia reperfusion injury," *Evidence-Based Complementary and Alternative Medicine*, vol. 2014, Article ID 989340, 10 pages, 2014.

[78] H. Jiao, Z. Wang, Y. Liu, P. Wang, and Y. Xue, "Specific role of tight junction proteins claudin-5, occludin, and ZO-1 of the blood-brain barrier in a focal cerebral ischemic insult," *Journal of Molecular Neuroscience*, vol. 44, no. 2, pp. 130–139, 2011.

[79] R. A. Taylor and L. H. Sansing, "Microglial responses after ischemic stroke and intracerebral hemorrhage," *Clinical and Developmental Immunology*, vol. 2013, Article ID 746068, 10 pages, 2013.

[80] R. Barakat and Z. Redzic, "Differential cytokine expression by brain microglia/macrophages in primary culture after oxygen glucose deprivation and their protective effects on astrocytes during anoxia," *Fluids and Barriers of the CNS*, vol. 12, article 6, 2015.

[81] Y.-C. Wang, S. Lin, and Q.-W. Yang, "Toll-like receptors in cerebral ischemic inflammatory injury," *Journal of Neuroinflammation*, vol. 8, article 134, 2011.

[82] Y. Wang, P. Ge, and Y. Zhu, "TLR2 and TLR4 in the brain injury caused by cerebral ischemia and reperfusion," *Mediators of Inflammation*, vol. 2013, Article ID 124614, 8 pages, 2013.

[83] X.-K. Tu, W.-Z. Yang, S.-S. Shi et al., "Spatio-temporal distribution of inflammatory reaction and expression of TLR2/4 signaling pathway in rat brain following permanent focal cerebral ischemia," *Neurochemical Research*, vol. 35, no. 8, pp. 1147–1155, 2010.

[84] A. Maddahi, L. S. Kruse, Q.-W. Chen, and L. Edvinsson, "The role of tumor necrosis factor-α and TNF-α receptors in cerebral arteries following cerebral ischemia in rat," *Journal of Neuroinflammation*, vol. 8, article 107, 2011.

[85] Q. Hua, X.-L. Zhu, P.-T. Li et al., "The inhibitory effects of cholalic acid and hyodeoxycholalic acid on the expression of TNFα and IL-1β after cerebral ischemia in rats," *Archives of Pharmacal Research*, vol. 32, no. 1, pp. 65–73, 2009.

[86] W. Chadwick, T. Magnus, B. Martin, A. Keselman, M. P. Mattson, and S. Maudsley, "Targeting TNF-α receptors for neurotherapeutics," *Trends in Neurosciences*, vol. 31, no. 10, pp. 504–511, 2008.

[87] A. Maddahi and L. Edvinsson, "Cerebral ischemia induces microvascular pro-inflammatory cytokine expression via the MEK/ERK pathway," *Journal of Neuroinflammation*, vol. 7, article 14, 2010.

[88] H. Boutin, R. A. LeFeuvre, R. Horai, M. Asano, Y. Iwakura, and N. J. Rothwell, "Role of IL-1α and IL-1β in ischemic brain damage," *The Journal of Neuroscience*, vol. 21, no. 15, pp. 5528–5534, 2001.

[89] G. P. Schielke, G.-Y. Yang, B. D. Shivers, and A. L. Betz, "Reduced ischemic brain injury in interleukin-1β converting enzyme- deficient mice," *Journal of Cerebral Blood Flow and Metabolism*, vol. 18, no. 2, pp. 180–185, 1998.

[90] K. N. Murray, A. R. Parry-Jones, and S. M. Allan, "Interleukin-1 and acute brain injury," *Frontiers in Cellular Neuroscience*, vol. 9, article 18, 2015.

[91] D. Acalovschi, T. Wiest, M. Hartmann et al., "Multiple levels of regulation of the interleukin-6 system in stroke," *Stroke*, vol. 34, no. 8, pp. 1864–1869, 2003.

[92] E. Tarkowski, L. Rosengren, C. Blomstrand et al., "Early intrathecal production of interleukin-6 predicts the size of brain lesion in stroke," *Stroke*, vol. 26, no. 8, pp. 1393–1398, 1995.

[93] T. Yamashita, K. Sawamoto, S. Suzuki et al., "Blockade of interleukin-6 signaling aggravates ischemic cerebral damage in mice: possible involvement of Stat3 activation in the protection of neurons," *Journal of Neurochemistry*, vol. 94, no. 2, pp. 459–468, 2005.

[94] S. A. Loddick, A. V. Turnbull, and N. J. Rothwell, "Cerebral interleukin-6 is neuroprotective during permanent focal cerebral ischemia in the rat," *Journal of Cerebral Blood Flow & Metabolism*, vol. 18, no. 2, pp. 176–179, 1998.

[95] M. Hedtjärn, A.-L. Leverin, K. Eriksson, K. Blomgren, C. Mallard, and H. Hagberg, "Interleukin-18 involvement in hypoxic-ischemic brain injury," *The Journal of Neuroscience*, vol. 22, no. 14, pp. 5910–5919, 2002.

[96] F. M. Domac and H. Misirli, "The role of neutrophils and interleukin-8 in acute ischemic stroke," *Neurosciences*, vol. 13, no. 2, pp. 136–141, 2008.

[97] S. Jander, M. Schroeter, and G. Stoll, "Interleukin-18 expression after focal ischemia of the rat brain: association with the late-stage inflammatory response," *Journal of Cerebral Blood Flow & Metabolism*, vol. 22, no. 1, pp. 62–70, 2002.

[98] K. L. Lambertsen, R. Gregersen, M. Meldgaard et al., "A role for interferon-gamma in focal cerebral ischemia in mice," *Journal of Neuropathology and Experimental Neurology*, vol. 63, no. 9, pp. 942–955, 2004.

[99] C. Marie, C. Pitton, C. Fitting, and J.-M. Cavaillon, "Regulation by anti-inflammatory cytokines (IL-4, IL-10, IL-13, TGFβ)of interleukin-8 production by LPS- and/ or TNFα-activated human polymorphonuclear cells," *Mediators of Inflammation*, vol. 5, no. 5, pp. 334–340, 1996.

[100] X. Liu, J. Liu, S. Zhao et al., "Interleukin-4 is essential for microglia/macrophage M2 polarization and long-term recovery after cerebral ischemia," *Stroke*, vol. 47, no. 2, pp. 498–504, 2016.

[101] N. Liu, R. Chen, H. Du, J. Wang, Y. Zhang, and J. Wen, "Expression of IL-10 and TNF-α in rats with cerebral infarction after transplantation with mesenchymal stem cells," *Cellular and Molecular Immunology*, vol. 6, no. 3, pp. 207–213, 2009.

[102] X. Zhao, H. Wang, G. Sun, J. Zhang, N. J. Edwards, and J. Aronowski, "Neuronal interleukin-4 as a modulator of microglial pathways and ischemic brain damage," *The Journal of Neuroscience*, vol. 35, no. 32, pp. 11281–11291, 2015.

[103] L.-S. Chu, S.-H. Fang, Y. Zhou et al., "Minocycline inhibits 5-lipoxygenase activation and brain inflammation after focal cerebral ischemia in rats," *Acta Pharmacologica Sinica*, vol. 28, no. 6, pp. 763–772, 2007.

[104] D. A. Ridder and M. Schwaninger, "NF-κB signaling in cerebral ischemia," *Neuroscience*, vol. 158, no. 3, pp. 995–1006, 2009.

[105] A. Oeckinghaus and S. Ghosh, "The NF-kappaB family of transcription factors and its regulation," *Cold Spring Harbor Perspectives in Biology*, vol. 1, no. 4, article a000034, 2009.

[106] F. Wan and M. J. Lenardo, "Specification of DNA binding activity of NF-kappaB proteins," *Cold Spring Harbor Perspectives in Biology*, vol. 1, no. 4, Article ID a000067, 2009.

[107] R. Berti, A. J. Williams, J. R. Moffett et al., "Quantitative real-time RT-PCR analysis of inflammatory gene expression associated with ischemia-reperfusion brain injury," *Journal of Cerebral Blood Flow and Metabolism*, vol. 22, no. 9, pp. 1068–1079, 2002.

[108] M. Jiang, J. Li, Q. Peng et al., "Neuroprotective effects of bilobalide on cerebral ischemia and reperfusion injury are associated with inhibition of pro-inflammatory mediator production and down-regulation of JNK1/2 and p38 MAPK activation," *Journal of Neuroinflammation*, vol. 11, article 167, pp. 1–17, 2014.

[109] L. Wang, Z. Li, X. Zhang et al., "Protective effect of shikonin in experimental ischemic stroke: attenuated TLR4, p-p38MAPK, NF-κB, TNF-α and MMP-9 expression, up-regulated claudin-5 expression, ameliorated BBB permeability," *Neurochemical Research*, vol. 39, no. 1, pp. 97–106, 2014.

[110] H. Liu, X. Wei, L. Kong et al., "NOD2 is involved in the inflammatory response after cerebral ischemia-reperfusion injury and triggers NADPH oxidase 2-derived reactive oxygen species," *International Journal of Biological Sciences*, vol. 11, no. 5, pp. 525–535, 2015.

[111] J.-H. Yi, S.-W. Park, R. Kapadia, and R. Vemuganti, "Role of transcription factors in mediating post-ischemic cerebral inflammation and brain damage," *Neurochemistry International*, vol. 50, no. 7-8, pp. 1014–1027, 2007.

[112] S. Dziennis and N. J. Alkayed, "Role of signal transducer and activator of transcription 3 in neuronal survival and regeneration," *Reviews in the Neurosciences*, vol. 19, no. 4-5, pp. 341–361, 2008.

[113] S. Dziennis, T. Jia, O. K. Rønnekleiv, P. D. Hurn, and N. J. Alkayed, "Role of signal transducer and activator of transcription-3 in estradiol-mediated neuroprotection," *The Journal of Neuroscience*, vol. 27, no. 27, pp. 7268–7274, 2007.

[114] X. Wang, Q. Liu, A. Ihsan et al., "JAK/STAT pathway plays a critical role in the proinflammatory gene expression and apoptosis of RAW264.7 cells induced by trichothecenes as don and T-2 toxin," *Toxicological Sciences*, vol. 127, no. 2, pp. 412–424, 2012.

[115] C. Schindler, D. E. Levy, and T. Decker, "JAK-STAT signaling: from interferons to cytokines," *The Journal of Biological Chemistry*, vol. 282, no. 28, pp. 20059–20063, 2007.

[116] C. Lei, J. Deng, B. Wang et al., "Reactive oxygen species scavenger inhibits STAT3 activation after transient focal cerebral ischemia-reperfusion injury in rats," *Anesthesia & Analgesia*, vol. 113, no. 1, pp. 153–159, 2011.

[117] H. Zhu, L. Zou, J. Tian, G. Du, and Y. Gao, "SMND-309, a novel derivative of salvianolic acid B, protects rat brains ischemia and reperfusion injury by targeting the JAK2/STAT3 pathway," *European Journal of Pharmacology*, vol. 714, no. 1–3, pp. 23–31, 2013.

[118] L. Li, X. Zhang, L. Cui et al., "Ursolic acid promotes the neuroprotection by activating Nrf2 pathway after cerebral ischemia in mice," *Brain Research*, vol. 1497, pp. 32–39, 2013.

[119] M. Li, X. Zhang, L. Cui et al., "The neuroprotection of oxymatrine in cerebral ischemia/reperfusion is related to nuclear factor erythroid 2-related factor 2 (Nrf2)-mediated antioxidant response: role of Nrf2 and hemeoxygenase-1 expression," *Biological and Pharmaceutical Bulletin*, vol. 34, no. 5, pp. 595–601, 2011.

[120] Y. Dong, H. D. Liu, R. Zhao et al., "Ischemia activates JNK/c-Jun/AP-1 pathway to up-regulate 14-3-3γ in astrocyte," *Journal of Neurochemistry*, vol. 109, supplement 1, pp. 182–188, 2009.

Hindawi Publishing Corporation
Evidence-Based Complementary and Alternative Medicine
Volume 2016, Article ID 9202675, 7 pages
http://dx.doi.org/10.1155/2016/9202675

Research Article

Hyeonggaeyeongyo-Tang for Treatment of Allergic and Nonallergic Rhinitis: A Prospective, Nonrandomized, Pre-Post Study

Min-Hee Kim,[1,2] Jaewoong Son,[1,2] Hae Jeong Nam,[3] Seong-Gyu Ko,[4] and Inhwa Choi[2,3]

[1]*Department of Clinical Korean Medicine, Graduate School, Kyung Hee University, Seoul, Republic of Korea*
[2]*Department of Otorhinolaryngology of Korean Medicine, Kyung Hee University Hospital at Gangdong, Seoul, Republic of Korea*
[3]*Department of Ophthalmology & Otorhinolaryngology, College of Korean Medicine, Kyung Hee University, Seoul, Republic of Korea*
[4]*Department of Preventive Medicine, College of Korean Medicine, Kyung Hee University, Seoul, Republic of Korea*

Correspondence should be addressed to Seong-Gyu Ko; epiko@khu.ac.kr and Inhwa Choi; inhwajun@hanmail.net

Received 27 May 2016; Revised 27 July 2016; Accepted 7 August 2016

Academic Editor: Xiang Liu

Hyeonggaeyeongyo-tang (HYT) is an ancient formula of oriental medicine traditionally used to treat rhinitis; however, clinical evidence has not yet been established. The aim of this study was to investigate the short-term and long-term efficacy and safety of HYT for chronic rhinitis. Adult subjects with chronic rhinitis symptoms were recruited. The subjects received HYT for 4 weeks and had follow-up period of 8 weeks. Any medicines used to treat nasal symptoms were not permitted during the study. The skin prick test was performed to distinguish the subjects with allergic rhinitis from those with nonallergic rhinitis. After treatment, the total nasal symptoms score and the Rhinoconjunctivitis Quality of Life Questionnaire score significantly improved in the whole subject group, in the allergic rhinitis group, and in the nonallergic rhinitis group, with no adverse events. This improvement lasted during a follow-up period of 8 weeks. Total IgE and eosinophil levels showed no significant difference after treatment in the allergic rhinitis group. HYT improved nasal symptoms and quality of life in patients with allergic rhinitis and nonallergic rhinitis. This is the first clinical study to evaluate the use of HYT to treat patients with rhinitis. This trial has been registered with the ClinicalTrials.gov Identifier NCT02477293.

1. Introduction

Rhinitis is defined by its clinical symptoms: rhinorrhea, nasal congestion, nasal itching, and sneezing. Anywhere from 10 to 40% of the population in industrialized countries has rhinitis based on epidemiologic surveys [1–4]. Chronic rhinitis (CR) is a chronic form of rhinitis and has been historically divided into allergic rhinitis (AR) and nonallergic rhinitis (NAR).

In Korea, several herbal medicines have been used to treat rhinitis. Hyeonggaeyeongyo-tang (HYT), also known as Keigai-rengyo-to or Jing Jie Lian Qiao Tang, is mixed herbal formula that has been used for hundreds of years in the treatment of rhinitis, rhinosinusitis, and acne. In an exploratory study, HYT was ranked first on the list of most commonly used herbal medications for treatment of allergic rhinitis in three Korean medical hospitals [5]. In another study, specialists in the Department of Otorhinolaryngology of Korean Medicine selected HYT as the third most preferred medicine to treat allergic rhinitis [6].

In animal studies, HYT has been shown to decrease the vascular permeability response to intradermal histamine and serotonin and to suppress a delayed type hypersensitivity response [7, 8]. Park and Hong reported that HYT has anti-inflammation effects for AR via the suppression of NF-κB activation and iNOS production in BALB/c mice [9]. Hong et al. reported that HYT reduces infiltration of inflammatory cells and mast cells into the nasal cavity and reduces the levels of cytokines and leukocytes in the blood in an ovalbumin-induced AR model [10]. In a clinical study, HYT has shown effectiveness in the treatment of adult patients with acne

Table 1: Study's flow chart.

Stage	Screening	Active treatment (4-week)			Follow-up (8-week)	
Visit	1	2	3	4	5	6
Weeks	−1	0	2	4	8	12
Informed consent	○					
Inclusion/exclusion criteria						
Skin prick test		○				
TNSS & RQLQ		○	○	○	○	○
Total IgE & eosinophil count†		○		○		
Vital sign	○	○	○	○	○	○
Laboratory tests for safety assessment*	○			○		
Adverse event			○	○	○	○

†Only for AR subjects; *complete blood cell counts, levels of aspartate transaminase, alanine transaminase, blood urea nitrogen, creatinine, and erythrocyte sedimentation rate.
TNSS, total nasal symptom score; RQLQ, Rhinoconjunctivitis Quality of Life Questionnaire; IgE, immunoglobulin E.

vulgaris [11]. To our knowledge, no other clinical studies have evaluated HYT for nasal symptoms thus far.

We conducted a prospective, nonrandomized, single-armed, pre-post study of Korean adults with rhinitis. The aim of this study was to investigate the short-term and long-term efficacy and the safety of HYT treatment for allergic and nonallergic rhinitis.

2. Methods

2.1. Study Design. This prospective, nonrandomized, single-armed, pre-post study was conducted at the Department of Otorhinolaryngology of Korean Medicine at Kyung Hee University Hospital at Gangdong. The study's flow chart is shown in Table 1. This study was approved by the Institutional Review Board of Kyung Hee University Hospital at Gangdong (KHNMC-OH-IRB 2015-04-009). Written informed consent was obtained from all subjects prior to enrollment.

2.2. Subjects. A total of 40 subjects with CR were enrolled. The inclusion criteria were as follows: (1) age of 18–65 years, (2) presence of one or more nasal symptoms (rhinorrhea, nasal congestion, nasal itching, and sneezing) for more than 12 weeks, and (3) moderate-to-severe rhinitis (at least one of the following moderate abnormality conditions: sleep disturbance; limitations in daily activity, physical exercise, or leisure activity; work/school limitations; and discomfort from several symptoms) [12]. The exclusion criteria were as follows: (1) treatment with nasal/oral corticosteroids within the past month; nasal cromolyn or tricyclic antidepressants within the past two weeks; or nasal/oral decongestants, nasal/oral antihistamines, or antileukotrienes within the past week, (2) presence of hypertension (systolic ≥ 180 mmHg or diastolic ≥ 100 mmHg) or severe anemia (hemoglobin ≤ 10 g/dL (male) and 9 g/dL (female)), (3) presence of abnormal liver function (aspartate transaminase (AST) or alanine transaminase (ALT) ≥ 100 IU/L) or abnormal renal function (blood urea nitrogen (BUN) ≥ 30 mg/dL or creatinine ≥ 1.8 mg/dL (male) and 1.5 mg/dL (female)), (4) presence of neoplasm, severe systemic inflammation, or other systemic diseases that affect rhinitis, (5) history of drug allergy, (6) history of anaphylaxis for allergic tests, and (7) pregnancy or lactation.

Table 2: The composition of herbal medicines in Hyeonggae-yeongyo-tang.

Component	Volume (g)
Schizonepeta tenuifolia	0.50
Forsythia fruit	0.50
Saposhnikovia radix	0.50
Angelicae gigantis radix	0.50
Cnidii rhizome	0.50
Paeoniae radix alba	0.50
Glycyrrhizae radix	0.50
Bupleuri radix	0.50
Ponciri fruit	0.50
Scutellariae radix	0.50
Gardeniae fruit	0.50
Angelicae dahuricae radix	0.83
Platycodi radix	0.83

2.3. Study Drug. Patients were treated with HYT extracted with water (Hanpoong Hyeonggaeyeongyo-tang granules, Hanpoong Pharm & Food Co., Ltd., Jeonju, Republic of Korea). It is a brown, bitter, herbal extract and was produced according to the Korean Good Manufacturing Practice (GMP) guidelines as permitted by the Korean Food & Drug Administration. HYT granules were sealed in opaque aluminum bags and administered to participants at doses of 3 g in accordance with standard guidelines for herbal prescription administration. The pharmacists instructed the subjects to dissolve HYT (3 g) from each package in water and take the solutions 30 minutes after each meal three times per day for 4 weeks. The composition of HYT is shown in Table 2. During the study, any medications that may have affected

nasal symptoms (antihistamines, corticosteroids, anticholinergics, antileukotriene drugs, decongestants, tricyclic antidepressants, phenothiazines, nonsteroidal anti-inflammatory drugs, or Korean herbal medicines that were judged by the researchers to affect nasal symptoms) were not permitted. Subjects that reported using any of these medications were excluded from the study.

2.4. Allergic Skin Prick Test. The skin prick test was performed according to routine procedure. Eleven common aeroallergens (*Dermatophagoides farinae*, *Dermatophagoides pteronyssinus*, dog fur, cat fur, grass mixture, tree mixture, mugwort, ragweed, *Alternaria tenuis*, *Aspergillus fumigatus*, and cockroach), negative controls (50% glycerin saline), and positive controls (0.1% histamine phosphate) were used (Allergopharma GmbH & Co. KG, Reinbek, Germany). The subjects who showed a positive reaction to the skin prick test were identified as AR, while subjects who showed no reaction to the skin prick test were identified as NAR.

2.5. Efficacy Assessment. Any change in the TNSS was considered the primary efficacy variable, while any change in the RQLQ was considered a secondary efficacy variable. The TNSS evaluates symptoms of rhinorrhea, nasal congestion, nasal itching, and sneezing on a 4-point scale. The total score range is from 0 to 12, where 0 = no symptoms, 1 = mild symptom(s) (present but bearable), 2 = moderate symptom(s) (present and uncomfortable), and 3 = severe symptom(s) (unbearable). Before and after medication we examined total serum IgE and eosinophil count for subjects with AR.

2.6. Safety Assessment. Before and after medication we assessed levels of AST/ALT, BUN/creatinine, complete blood counts (CBC) including white blood cell (WBC), red blood cell (RBC), hemoglobin, hematocrit, and platelet, and erythrocyte sedimentation rate (ESR) to ensure the subjects' safety. Throughout the trial all adverse events were noted in subjects' reports or in the case report forms.

2.7. Statistical Analysis. All statistical analyses were performed using the SPSS 21 (IBM Inc., Armonk, NY, USA), and values are presented as means ± standard deviations. A repeated-measures ANOVA test with Bonferroni post hoc test was performed to evaluate the changes of TNSS and RQLQ scores throughout the 12 weeks. Independent t-tests were performed in order to analyze the intergroup analysis at each period. Paired t-tests were used to compare values before and after medication in each group. In all tests, a value of $p < 0.05$ was considered statistically significant.

3. Results

3.1. Subjects. A total of 47 patients were screened, and 40 subjects with CR were included in this study. Seven patients were excluded because they had mild nasal symptoms. During the active treatment period, 2 subjects withdrew from the study because of personal reasons. During the follow-up period, 3 subjects were excluded because they used other medicines. There were 16 subjects who were identified as AR after skin prick test. All AR subjects showed positive reaction to at least one or more persistent allergens. There were no significant differences in sex, age, baseline TNSS, each nasal symptom score, and baseline RQLQ score between the AR group and the NAR group (Table 3).

Table 3: Demographic characteristics of the study population.

Number of subjects	40
Male/female (n)	15/25
Age (mean ± SD, years)	38.68 ± 12.86
Dropouts	
Personal reasons	2
Use of other medications	3
AR/NAR group (n)	16/24
Persistent allergens	
Dermatophagoides farinae	15
Dermatophagoides pteronyssinus	15
Cockroach	1
Dog fur	0
Cat fur	5
Aspergillus fumigatus	2
Alternaria tenuis	3
Seasonal allergens	
Grass mixture	1
Mugwort	6
Tree mixture	3
Ragweed	1

SD, standard deviations; AR, allergic rhinitis; NAR, nonallergic rhinitis.

Table 4: Mean TNSS from baseline to week 12.

	Week 0	Week 4	Week 8	Week 12
All subjects	7.53 ± 1.95	5.10 ± 2.81*	5.63 ± 2.57*	5.43 ± 3.09*
AR	8.31 ± 1.58	5.50 ± 3.29*	6.19 ± 3.08*	6.00 ± 3.44*
NAR	7.00 ± 2.02	4.83 ± 2.48*	5.25 ± 2.15*	5.04 ± 2.84*

Mean ± standard deviation, repeated-measures ANOVA test, and Bonferroni post hoc test.
*Significant difference ($p < 0.05$) compared with week 0 (baseline) in each group (no significant difference between week 4, week 8, and week 12 in each group).
TNSS, total nasal symptom score; AR, allergic rhinitis; NAR, nonallergic rhinitis.

3.2. TNSS. A statistically significant decrease in TNSS was observed after medication (week 4), and this decrease lasted for the follow-up period in the whole subject group (CR), the AR group, and the NAR group. There was no significant between-group difference at any time point (Table 4 and Figures 1(a) and 1(c)). All nasal symptoms, rhinorrhea, nasal congestion, nasal itching, and sneezing, showed significant improvement during treatment. There was no significant

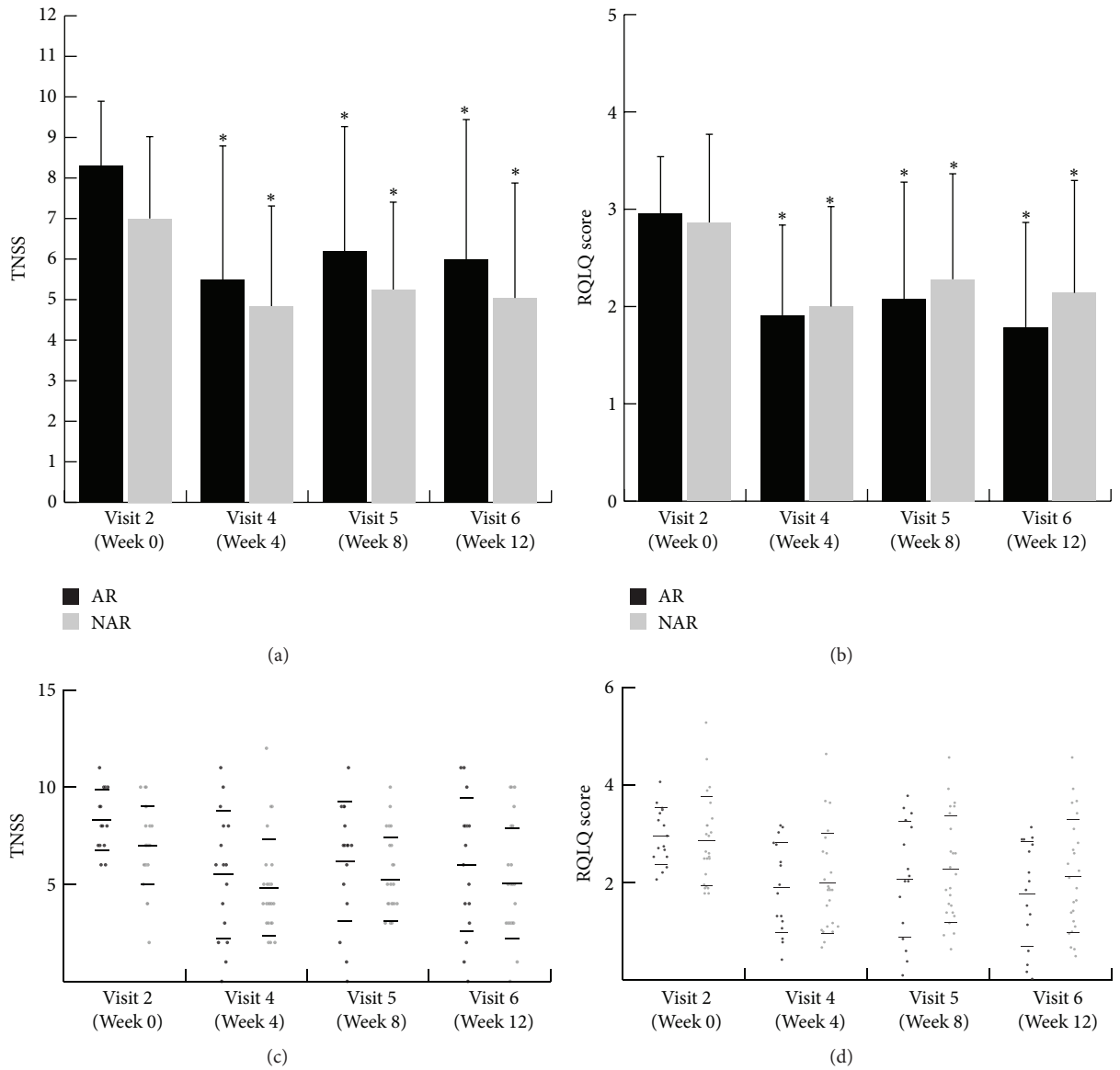

Figure 1: Effects of HYT on the AR group and the NAR group. (a and c) Mean TNSS at each visit. (b and d) Mean RQLQ score at each visit. *Significant difference ($p < 0.05$) compared with week 0 (baseline) in each group (repeated-measures ANOVA test and Bonferroni post hoc test). HYT, Hyeonggaeyeongyo-tang; AR, allergic rhinitis; NAR, nonallergic rhinitis; TNSS, total nasal symptom score; RQLQ, Rhinoconjunctivitis Quality of Life Questionnaire.

difference in any of the nasal symptoms between the AR group and the NAR group (Table 5).

3.3. RQLQ. The RQLQ showed a statistically significant decrease after medication and this improvement lasted for follow-up period in the whole subject group (CR), the AR group, and the NAR group. There was no significant between-group difference at any time point (Table 6 and Figures 1(b) and 1(d)).

3.4. Serum Total IgE and Eosinophil Count. There was no significant change in total serum IgE or eosinophil count after treatment in the AR group (Table 7).

3.5. Safety. There were no serious adverse events observed or reported during the study. The only minor adverse events observed during treatment were dyspepsia ($n = 3$) and xerostomia ($n = 2$), but these events disappeared during the follow-up period. There were statistically significant differences in BUN, RBC, hemoglobin, and hematocrit after treatment. However, all these changes were in normal ranges and there was no subject who showed abnormal value after treatment assessment (Table 8).

4. Discussion

CR is chronic form of rhinitis and has been classified as AR and NAR. Approximately 50% of CR patients are classified

Table 5: Nasal symptom score from baseline to week 4 in AR and NAR group.

	Week 0	Week 4	p value
Rhinorrhea			
AR	2.06 ± 0.93	1.44 ± 1.09	0.036*
NAR	1.88 ± 0.90	1.29 ± 0.95	0.001*
Nasal congestion			
AR	1.69 ± 0.95	1.00 ± 0.89	0.029*
NAR	1.92 ± 0.88	1.42 ± 0.72	0.043*
Nasal itching			
AR	2.50 ± 0.63	1.56 ± 1.03	0.001*
NAR	1.54 ± 0.98	0.92 ± 1.02	0.002*
Sneezing			
AR	2.06 ± 0.44	1.50 ± 0.97	0.045*
NAR	1.67 ± 0.96	0.96 ± 0.86	0.001*

Mean ± standard deviation and paired t-test.
*Significant difference ($p < 0.05$) between week 0 (baseline) and week 4 in each group.
TNSS, total nasal symptom score; AR, allergic rhinitis; NAR, nonallergic rhinitis.

Table 6: Mean RQLQ scores from baseline to week 12.

	Week 0	Week 4	Week 8	Week 12
All subjects	2.90 ± 0.79	1.96 ± 0.98*	2.20 ± 1.12*	2.00 ± 1.13*
AR	2.96 ± 0.58	1.91 ± 0.93*	2.08 ± 1.19*	1.78 ± 1.08*
NAR	2.86 ± 0.91	2.00 ± 1.03*	2.28 ± 1.09*	2.14 ± 1.16*

Mean ± standard deviation, repeated-measures ANOVA test, and Bonferroni post hoc test.
*Significant difference ($p < 0.05$) compared with week 0 (baseline) in each group (no significant difference between week 4, week 8, and week 12 in each group).
RQLQ, Rhinoconjunctivitis Quality of Life Questionnaire; AR, allergic rhinitis; NAR, nonallergic rhinitis.

Table 7: Total serum IgE and eosinophil count in the AR group.

	Week 0	Week 4	p value
Total IgE (IU/mL)	287.93 ± 321.26	233.21 ± 183.23	0.486
Eosinophil count (/μL)	271.25 ± 211.03	281.25 ± 244.29	0.847

Mean ± standard deviation and paired t-test.
IgE, immunoglobulin E; AR; allergic rhinitis.

as having AR, and the others are classified as having NAR [13]. AR is characterized by a specific IgE response against relevant aeroallergens. NAR encompasses all forms of rhinitis in which a specific IgE response against relevant aeroallergens is absent.

The main medications currently used for allergic and nonallergic rhinitis are antihistamines, nasal steroids, nasal decongestants, and leukotriene receptor antagonists [14, 15]. In many cases of CR, symptoms are prolonged for years throughout all seasons; therefore, it is necessary to find the medicine which has no adverse effects for long-term medication and has long lasting effects. However, long-term use of many of the medications used for the treatment of CR can cause adverse effects. Antihistamines are the most widely used treatment for both AR and NAR. Antihistamines have limited efficacy in treating nasal congestion and commonly cause adverse effects such as sedation and weight gain [16, 17]. Nasal decongestants are useful for nasal obstruction, but using them for more than a week is not recommended because of adverse effects and drug tolerance [18]. For these reasons, traditional Chinese medicines which are made with natural herbs have recently gained much interest [19].

In this study, HYT improved nasal symptoms and quality of life in patients with AR and NAR after 4 weeks of medication, and these effects lasted 8 weeks after the end of medication. Each rhinitis patient has different symptoms based on his or her type of rhinitis and environmental factors. Some patients mainly have watery rhinorrhea and sneezing symptoms, while others mainly have nasal obstruction symptoms. In our study, both rhinorrhea and nasal obstruction were improved in patients with AR and NAR.

Other studies reported that HYT has anti-inflammation effects for AR by the suppression of NF-κB activation and iNOS production in BALB/c mice [9]. In several previous studies, main components of HYT, *Schizonepeta tenuifolia*, *Forsythia* fruit, *Saposhnikovia divaricata*, and *Bupleurum falcatum*, were observed to have antioxidant and anti-inflammatory activities [20–23]. These antioxidant and anti-inflammatory activities could be the reason of the effect of HYT in patients with AR and NAR.

In a previous animal study, HYT had antiallergic effects, inhibiting the increase of the levels of IL-4, IL-13, leukemia inhibitory factor (LIF), eosinophils, neutrophils, monocytes, basophils, lymphocytes, and WBC in ovalbumin-induced AR model [10]. Based on previous studies, we hypothesized that IgE and eosinophils will be suppressed in patients with AR; however, current study showed no decrease in IgE and eosinophils in AR patients. By referring to previous clinical study that reported changes of serum IgE, cytokines, IL-4 stimulated prostaglandin E2 (PGE2), and polymorphonuclear leukocyte (PMN) after 12-week administration of oriental herbal medicine, duration of medication needed to be longer in our study to observe the changes of serum IgE and eosinophils [24, 25].

There were statistically significant differences in BUN, RBC, hemoglobin, and hematocrit after treatment. However, all these changes were in normal ranges and there was no subject who showed abnormal value after treatment assessment. A clinical study with long-term medication for at least 8 weeks and the safety assessment would be necessary to confirm the long-term safety of HYT and to observe antiallergic effects in laboratory tests.

Our study has several limitations. First, this study is pre-post study that was conducted with a nonrandomized and no-control-group design. Second, our sample size was relatively small. Third, the medication period was relatively short for safety assessment.

Despite these limitations, this study has a meaning as the first clinical study for HYT in CR. From this study, we suggest that HYT could be investigated as a medicine for patients with AR and NAR. A clinical study with a randomized, double-blind, placebo-controlled design, larger sample size, and long-term medication should be performed to obtain

Table 8: The laboratory tests for safety assessment.

	Normal ranges	Week 0	Week 4	p value
AST	0~40 (U/L)	21.50 ± 6.84	24.45 ± 14.47	0.148
ALT	0~40 (U/L)	18.84 ± 11.39	22.95 ± 22.43	0.167
BUN	8~23 (mg/dL)	13.24 ± 3.94	11.73 ± 3.26	0.005*
Creatinine	0.6~1.2 (mg/dL)	0.74 ± 0.15	0.73 ± 0.16	0.354
CBC				
WBC	4.0~10.0 ($\times 10^3/\mu$L)	6.76 ± 1.33	6.45 ± 1.38	0.116
RBC	4.2~6.3 ($\times 10^6/\mu$L)	4.66 ± 0.51	4.57 ± 0.48	0.019*
Hemoglobin	13~17 (g/dL)	13.93 ± 1.60	13.64 ± 1.53	0.002*
Hematocrit	36~48 (%)	41.64 ± 4.24	40.87 ± 4.01	0.011*
Platelet	150~350 ($\times 10^3/\mu$L)	261.95 ± 46.21	261.49 ± 51.24	0.890
ESR	~20 (mm/h)	12.62 ± 8.97	11.49 ± 8.30	0.290

Mean ± standard deviation and paired t-test.
*Significant difference ($p < 0.05$) between week 0 (baseline) and week 4.
AST, aspartate transaminase; ALT, alanine transaminase; BUN, blood urea nitrogen; CBC, complete blood count; WBC, white blood cell; RBC, red blood cell; ESR, erythrocyte sedimentation rate.

more accurate knowledge about HYT treatment for rhinitis and to observe its mechanism.

Competing Interests

The authors declare that there are no competing interests regarding the publication of this paper.

Authors' Contributions

Min-Hee Kim and Jaewoong Son contributed equally to this work.

Acknowledgments

This study was funded by a grant from the Traditional Korean Medicine R&D Project, Ministry of Health & Welfare, Republic of Korea (HI12C1889 and HI13C0530).

References

[1] E. Middleton Jr., "Chronic rhinitis in adults," *Journal of Allergy and Clinical Immunology*, vol. 81, no. 5, pp. 971–975, 1988.

[2] M. F. Mullarkey, J. S. Hill, and D. R. Webb, "Allergic and nonallergic rhinitis: their characterization with attention to the meaning of nasal eosinophilia," *The Journal of Allergy and Clinical Immunology*, vol. 65, no. 2, pp. 122–126, 1980.

[3] R. A. Settipane and P. Lieberman, "Update on nonallergic rhinitis," *Annals of Allergy, Asthma & Immunology*, vol. 86, no. 5, pp. 494–507, 2001.

[4] C. Bachert, P. van Cauwenberge, J. Olbrecht, and J. van Schoor, "Prevalence, classification and perception of allergic and non-allergic rhinitis in Belgium," *Allergy*, vol. 61, no. 6, pp. 693–698, 2006.

[5] B.-H. Jang, I.-H. Choi, K.-S. Kim et al., "Current status of allergic rhinitis patients in Korean Medicine hospitals-exploratory study based on electronic medical records of 3 hospitals," *The Journal of Korean Medical Ophthalmology & Otolaryngology & Dermatology*, vol. 27, no. 1, pp. 117–129, 2014.

[6] N.-K. Kim, D.-H. Lee, E.-S. Seo et al., "Treatment packages of persistent allergic rhinitis for developing PRCT protocols: an expert survey," *The Journal of Oriental Medical Preventive*, vol. 17, no. 3, pp. 143–153, 2013.

[7] T.-S. Yu, Y.-S. Jin, and G.-M. Jeong, "Study of the effects of Hyunggaeyeungyotang on the Anti-allergic effect in rats and mice," *The Journal of Korean Oriental Pediatrics*, vol. 4, no. 1, pp. 19–30, 1990.

[8] E.-J. Park and S.-Y. Shin, "Effects of Hyunggyeyungyotang and Kamihyunggyeyungyotang administration on the anti-inflammation, analgesia and anti-allergic reaction in mice," *The Journal of Korean Oriental Pediatrics*, vol. 11, no. 1, pp. 249–273, 1997.

[9] J.-H. Park and S.-U. Hong, "The effects of hyunggaeyungyo-tang of suppression of iNOS production on mice with allergic rhinitis," *The Journal of Korean Medicine Ophthalmology and Otolaryngology and Dermatology*, vol. 25, no. 1, pp. 12–21, 2012.

[10] S. H. Hong, S. R. Kim, H.-S. Choi et al., "Effects of hyeonggaeyeongyo-tang in ovalbumin-induced allergic rhinitis model," *Mediators of Inflammation*, vol. 2014, Article ID 418705, 9 pages, 2014.

[11] K. S. Kim and Y.-B. Kim, "Anti-inflammatory effect of *Keigai-rengyo-to* extract and acupuncture in male patients with acne vulgaris: a randomized controlled pilot trial," *The Journal of Alternative and Complementary Medicine*, vol. 18, no. 5, pp. 501–508, 2012.

[12] J. Bousquet, N. Khaltaev, A. A. Cruz et al., "Allergic rhinitis and its impact on asthma (ARIA) 2008," *Allergy*, vol. 63, supplement 86, pp. 8–160, 2008.

[13] T. L. Smith, "Vasomotor rhinitis is not a wastebasket diagnosis," *Archives of Otolaryngology—Head & Neck Surgery*, vol. 129, no. 5, pp. 584–587, 2003.

[14] E. O. Meltzer, M. S. Blaiss, M. J. Derebery et al., "Burden of allergic rhinitis: results from the Pediatric Allergies in America survey," *Journal of Allergy and Clinical Immunology*, vol. 124, no. 3, pp. S43–S70, 2009.

[15] G. Ciprandi, "Treatment of nonallergic perennial rhinitis," *Allergy*, vol. 59, no. 76, pp. 16–23, 2004.

[16] M. K. Church, M. Maurer, C. Bindslev-Jensen et al., "Risk of first-generation H_1-antihistamines: a GA^{2}LEN position paper," *Allergy*, vol. 65, no. 4, pp. 459–466, 2010.

[17] F. E. R. Simons, "H1-Antihistamines: more relevant than ever in the treatment of allergic disorders," *Journal of Allergy and Clinical Immunology*, vol. 112, no. 4, pp. S42–S52, 2003.

[18] P. Graf, "Adverse effects of benzalkonium chloride on the nasal mucosa: allergic rhinitis and rhinitis medicamentosa," *Clinical Therapeutics*, vol. 21, no. 10, pp. 1749–1755, 1999.

[19] R. Y. P. Chan and W. T. Chien, "The effects of two Chinese herbal medicinal formulae vs. placebo controls for treatment of allergic rhinitis: a randomised controlled trial," *Trials*, vol. 15, article 261, 2014.

[20] B.-S. Wang, G.-J. Huang, H.-M. Tai, and M.-H. Huang, "Antioxidant and anti-inflammatory activities of aqueous extracts of *Schizonepeta tenuifolia* Briq," *Food and Chemical Toxicology*, vol. 50, no. 3-4, pp. 526–531, 2012.

[21] H. S. Kang, J. Y. Lee, and C. J. Kim, "Anti-inflammatory activity of arctigenin from Forsythiae Fructus," *Journal of Ethnopharmacology*, vol. 116, no. 2, pp. 305–312, 2008.

[22] J. M. Chun, H. S. Kim, A. Y. Lee, S. Kim, and H. K. Kim, "Anti-inflammatory and antiosteoarthritis effects of saposhnikovia divaricata ethanol extract: in vitro and in vivo studies," *Evidence-Based Complementary and Alternative Medicine*, vol. 2016, Article ID 1984238, 8 pages, 2016.

[23] W. H. Park, S. Kang, Y. Piao et al., "Ethanol extract of *Bupleurum falcatum* and saikosaponins inhibit neuroinflammation via inhibition of NF-κB," *Journal of Ethnopharmacology*, vol. 174, pp. 37–44, 2015.

[24] S.-H. Yang, C.-L. Yu, Y.-L. Chen, S.-L. Chiao, and M.-L. Chen, "Traditional Chinese medicine, Xin-yi-san, reduces nasal symptoms of patients with perennial allergic rhinitis by its diverse immunomodulatory effects," *International Immunopharmacology*, vol. 10, no. 8, pp. 951–958, 2010.

[25] S.-H. Yang and C.-L. Yu, "Antiinflammatory effects of Buzhong-yi-qi-tang in patients with perennial allergic rhinitis," *Journal of Ethnopharmacology*, vol. 115, no. 1, pp. 104–109, 2008.

Hindawi Publishing Corporation
Evidence-Based Complementary and Alternative Medicine
Volume 2016, Article ID 2859652, 7 pages
http://dx.doi.org/10.1155/2016/2859652

Research Article

Immunomodulatory and Antimicrobial Activity of Babassu Mesocarp Improves the Survival in Lethal Sepsis

Elizabeth S. B. Barroqueiro, Dayanna S. Prado, Priscila S. Barcellos, Tonicley A. Silva, Wanderson S. Pereira, Lucilene A. Silva, Márcia C. G. Maciel, Rodrigo B. Barroqueiro, Flávia R. F. Nascimento, Azizedite G. Gonçalves, and Rosane N. M. Guerra

Centro de Ciências Biológicas e da Saúde, Laboratorio de Imunofisiologia, Universidade Federal do Maranhão, Cidade Univesitária Dom Delgado, No. 1966, Avenida dos Portugueses, 6080-580 São Luís, MA, Brazil

Correspondence should be addressed to Rosane N. M. Guerra; roguerra@globo.com

Received 24 May 2016; Accepted 26 July 2016

Academic Editor: Yong Cheng

Attalea speciosa syn *Orbignya phalerata* Mart. (babassu) has been used in the treatment of inflammatory and infectious diseases. *Aim of the study*. To investigate the antimicrobial and immunological activity of babassu mesocarp extract (EE). *Material and Methods.* The *in vitro* antimicrobial activity was evaluated by disk diffusion assay and by determination of the minimum inhibitory concentration (MIC) to *Escherichia coli*, *Pseudomonas aeruginosa*, *Enterococcus faecalis*, *Staphylococcus aureus,* and methicillin-resistant *Staphylococcus aureus* (MRSA). The flavonoids and phenolic acids content were determined by chromatography. The *in vivo* assays were performed in Swiss mice submitted to sepsis by cecal ligation and puncture (CLP). The mice received EE subcutaneously (125 or 250 mg/Kg), 6 hours after the CLP. The number of lymphoid cells was quantified and the cytokines production was determined by ELISA after 12 h. *Results.* EE was effective as antimicrobial to *E. faecalis*, *S. aureus*, and MRSA. EE is rich in phenolic acids, a class of compounds with antimicrobial and immunological activity. An increased survival can be observed in those groups, possibly due to a significant inhibition of TNF-α and IL-6. *Conclusions.* The EE showed specific antimicrobial activity *in vitro* and an important antiseptic effect *in vivo* possibly due to the antimicrobial and immunomodulatory activity.

1. Introduction

Babassu (*Attalea speciosa* syn *Orbignya phalerata* Mart.) is the generic name of Brazilian native oleaginous palm trees from Arecaceae family. The mesocarp is obtained from the fruits and dried and ground into a powder, called babassu mesocarp flour. This product is widely commercialized either as a food supplement for adults and children or as medicine in the treatment of inflammatory and infectious diseases [1, 2].

A number of biological activities have been attributed to babassu mesocarp, such as anti-inflammatory [3], healing [4], antitumor [5, 6], antithrombotic [7], and antimicrobial properties [8]. In addition, the mesocarp is able to induce the release of hydrogen peroxide by macrophages suggesting an immunological effect on macrophage activation [9] and acts on cytokine production indicating an immunomodulatory effect [10].

Sepsis is a complex syndrome and still continues to be a major cause of morbidity and mortality among critically ill patients and at the intensive care units worldwide [11]. The significant morbidity and mortality associated with sepsis have continued to be powerful incentives for attempts to develop novel therapeutic strategies for this disease [12, 13]. The initial control of infection is very important to avoid the development of sepsis. The progression from a local to a systemic inflammatory and infective response is the result of the activation of circulating cells that release proinflammatory cytokines, such as interleukin 1 (IL-1), TNF-α, IL-6, and IL-8, into the circulation [14]. An increased production of chemokines is responsible for the recruitment of leukocytes to the inflammatory focus. Additionally, the release of anti-inflammatory cytokines seems to counterbalance the actions of proinflammatory mediators, either by reducing the synthesis and release of these mediators or

by antagonizing their effects [15]. The goal of these mechanisms is to increase microbicidal activity and to control infection and systemic inflammatory response [16–18].

Antibiotic drugs generally interfere with the infection but not with the inflammatory response, a fact that might explain the high mortality rate observed in patients with septic shock [19, 20].

The progressive resistance of pathogenic microorganisms to multiple drugs [21–23] has encouraged the search for new agents, especially those derived from natural products. Therefore, the objective of the present study was to evaluate the *in vitro* and *in vivo* antimicrobial activity of babassu mesocarp extract in mice with sepsis by cecal ligation and puncture (CLP).

2. Material and Methods

2.1. Plant Material. All assays were carried out using flour prepared from *Attalea speciosa* fruits in our laboratory. The fruits were collected in Pedreiras, Maranhão, Brazil. A voucher specimen (number 1135/SLS017213) has been deposited at the Ático Seabra Herbarium, Federal University of Maranhão. Mesocarp, obtained manually, was dried at 45°C, 24 h, and ground to obtain the mesocarp flour.

2.2. Preparation of the Babassu Ethanol Extract (EE). The babassu mesocarp flour (500 g) was air-dried at room temperature, powdered, and extracted in 2000 mL ethanol PA (Merck, Brazil), for 72 h. The extract was filtered and concentrated under low pressure at 24°C. The extract obtained was stored (10°C) prior to antimicrobial studies. The final yield was 7.9% (w/w).

2.3. Chemical Screening. The analysis of polyphenols and flavonoids was performed accordingly as previously described [24]. The total concentration of polyphenols was determined by Folin-Ciocalteu method using gallic acid as standard. The extract samples were serially diluted to a final volume of 2 mL. To each dilution 300 μL of sodium carbonate (1.9 M) and 100 μL of Folin were added. The solutions were incubated during one hour in the dark and the absorbances were measured at 760 nm. The content of total phenolic compounds was determined by the following formula: Abs $\times f \times$ dilution, considering f as the calibration factor to gallic acid [25].

The flavonoid concentration was measured with aluminum chloride at 425 nm using quercetin as standard. All samples were tested in triplicate. The phenolic acids concentration was determined from the difference between the flavonoids and total phenol concentration [26]. All results were expressed as similarity index (%)

2.4. In Vitro Assay to Antibacterial Activity. The dry EE was dissolved in phosphate-buffered saline, pH 7.2, to a final concentration of 500 mg/mL, sterilized by filtration (0.22 μm). The reference strains were used for the *in vitro* antibacterial assay: *Escherichia coli* (ATCC 25922), *Pseudomonas aeruginosa* (ATCC 27853), *Enterococcus faecalis* (ATCC 29212), and *Staphylococcus aureus* (ATCC 25923). The antibacterial activity of EE was also evaluated against a strain of methicillin-resistant *Staphylococcus aureus* (MRSA) isolated from tracheal secretion from patients, which was susceptible to vancomycin and resistant to cefoxitin, cefazolin, clindamycin, erythromycin, ciprofloxacin, gentamicin, and tetracycline.

2.4.1. Disk Diffusion Method (Kirby-Bauer). The bacterial inoculum was adjusted to final concentration of 1.5×10^8 CFU/mL (0.5, McFarland) and seeded onto a Mueller-Hinton agar plate. Sterile filter paper disks (6 mm) were placed on the plate and impregnated with 10 μL of the EE at concentrations of 250 or 500 mg/mL. Disks impregnated with oxacillin (1 μg) and cefoxitin (30 μg) were used as positive controls. The plates were incubated at 35°C for 24 h [27].

2.4.2. Determination of the Minimum Inhibitory Concentration (MIC) of EE. For the determination of MIC, a serial dilution of EE ranging from 500 to 0.9 mg/mL was added to tubes containing broth cultures of each strain, prepared in brain heart infusion [BHI (1.5×10^8 UFC/mL, 0.5 on McFarland scale)], and incubated at 35°C, for 24 h. Tubes containing only BHI plus bacteria were used as positive controls and those ones containing BHI plus EE were considered as negative controls. The MIC is defined as the lowest concentration of the EE at which the microorganism tested does not demonstrate visible growth [28].

2.5. In Vivo Antimicrobial Activity: Sepsis

2.5.1. Animals. Female Swiss mice weighing 25 ± 5 g were obtained from the Central Animal House of the Federal University of Maranhão.

2.5.2. Sepsis Induction. Polymicrobial sepsis was induced by cecal ligation and puncture (CLP). Briefly, following anesthesia with sodium pentobarbital (50–65 mg/Kg, by intraperitoneal route i.p.), a small mid-abdominal incision was made and the cecum was exposed. A distended portion of the cecum just distal to the ileocecal valve was isolated and ligated with a silk suture in a manner not to disrupt bowel continuity. The ligated portion of the cecum was punctured eight times with an 18-gauge hypodermic needle. The abdomen was then closed in two layers and the animals were allowed to recover [15, 29].

2.5.3. Experimental Design. The animals were randomly assigned to the experimental groups. Sham: the cecum was not perforated and the mice were not treated. The other 3 groups were given subcutaneously NaCl solution (CLP), EE 125 mg/Kg (EE125), or EE 250 mg/Kg (EE250). Animals were cared for in accordance with the guidelines of the Brazilian College of Animal Experimentation and the experimental protocol was approved by the Ethics Committee (protocol 23115011476/2007-50).

To evaluate the lifespan, the number of remaining animals was recorded every 12 h until the 5th day.

Table 1: Antimicrobial activity of babassu mesocarp ethanolic extract evaluated by disk diffusion assay.

Bacterial strains	Zones of inhibition (mm)	
	EE250[a]	EE500
Enterococcus faecalis (ATCC 29212)	12.4 ± 0.2[b]	14.4 ± 0.4
Staphylococcus aureus (ATCC 25923)	15.0 ± 0.3	18.5 ± 0.9
MRSA (hospital strain)	15.3 ± 0.3	17.4 ± 0.3
Escherichia coli (ATCC 25922)	0	0
Pseudomonas aeruginosa	0	0

[a]EE babassu mesocarp ethanolic extract at concentrations of 250 and 500 mg/mL.
[b]The diameters of zones of inhibition (mm) are expressed as mean ± SD (n = 3); a diameter less than 7 mm was considered inactive; and the diameters of zones of inhibition (mm) are expressed as mean ± SD (n = 3).

2.5.4. Colony-Forming Units (CFU). Bacterial counts were performed on aseptically obtained peritoneal fluid. At 12 h after CLP, mice were sacrificed and the skin of abdomen was cut open in the midline without injury to the muscle. Sterile phosphate-buffered saline (PBS) (2 mL) was injected into and aspirated out of the peritoneal cavities. Samples were serially diluted in PBS and cultured on Mueller-Hinton agar dishes (Difco Laboratories, Detroit). Colony-forming units were counted after overnight incubation at 37°C. The results were expressed as $\log_{10}$ of the number of colony-forming units per peritoneal cavity.

2.5.5. Cytokines Assay. Serum TNF-α, IFN-γ, and IL-6 were measured by ELISA method in accordance with the manufacturer's instructions (eBiosciences, USA).

2.6. Statistical Analysis. All data were expressed as mean ± standard error (X ± SE). Statistical significance was determined using ANOVA followed by Newman-Keuls test, Student's t-test. Kaplan-Meier curve and the log-rank statistical test were applied to compare the curves and for the evaluation of lifespan. Values with $p < 0.05$ were considered significant.

3. Results

3.1. The In Vitro Antimicrobial Activity of EE. The EE at the two tested concentrations inhibited the growth of *Enterococcus faecalis* (ATCC 29212), *Staphylococcus aureus* (ATCC 25923), and the MRSA strains. On the other hand, the same concentrations of EE have no effect on *Escherichia coli* (ATCC 25922) or *Pseudomonas aeruginosa* (ATCC 27853) strains (Table 1).

The MIC was determined only for the effective EE doses and bacteria strains. The MIC was 31.2 mg/mL for *S. aureus* (ATCC 25923) and MRSA and 7.8 mg/mL for *E. faecalis* (ATCC 29212). The highest concentration of EE (500 mg/mL) completely inhibited the growth of *S. aureus* (ATCC 25923), MRSA, and *E. faecalis* (ATCC 29212) (Table 2).

3.2. Chemical Composition of the EE. The predominance of phenolic compounds was detected. The extract contained 56% total polyphenols, including 55% phenolic acids and 1% flavonoids.

Table 2: Minimum inhibitory concentration of babassu mesocarp ethanolic extract.

Bacterial strains	MIC[a] (mg/mL)
Enterococcus faecalis (ATCC 29212)	7.8[b]
Staphylococcus aureus (ATCC 25923)	32.1
MRSA (hospital strain)	32.1

[a]MIC: minimum inhibitory concentration.
[b]Values represent the mean of triplicates (n = 3).

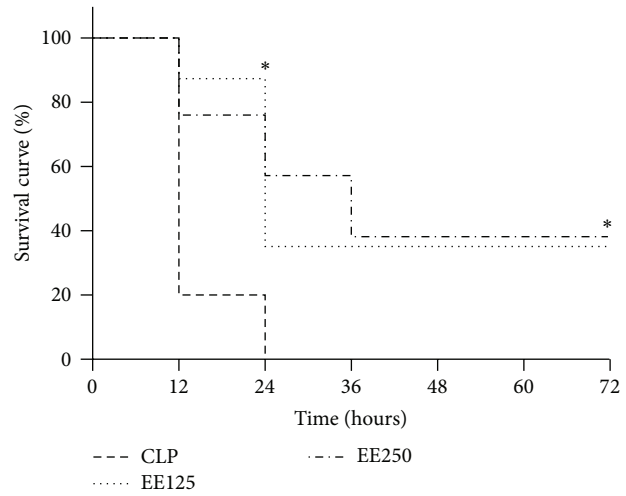

Figure 1: Effect of treatment with ethanolic extract (EE) of babassu mesocarp on the survival of mice with lethal sepsis induced by cecal ligation and puncture (CLP). The animals were treated with EE at doses of 125 mg/Kg (EE125) or 250 mg/Kg (EE250) 6 h after the induction of sepsis by cecal ligation and puncture and compared to animals that have received saline (CLP). The animals were examined at intervals of 12 h until day 10. The results are expressed as mean ± SEM (5 animals/group). (∗) $p < 0{,}05$ in comparison to the CLP group.

3.3. Effect of Babassu Mesocarp on Survival in CLP-Induced Mice Sepsis. As shown in Figure 1, the survival in all groups submitted to sepsis was 100%, after surgery (T0). As shown in Figure 1 at the control group (CLP) the mortality was 80%, 12 hours after sepsis induction and, after 24 h, all animals of this group were dead. The onset of death was markedly delayed in mice that have received EE treatment. The survival in EE125 and EE250 groups was, respectively, 90% and 80%, after 12 hours and 40% and 60%, 24 h after the sepsis induction. In the EE125 group, survival remained constant (40%) until 10th day. In the EE250 group the survival rate only decreased to 40% after 36 h and remained unchanged thereafter.

3.4. Effect of EE on Cell Distribution on Peritoneum and Lymphoid Organs. Sepsis by cecal perforation frequently induces an expressive increase in cell migration to the peritoneal cavity, as it was shown by the comparison between the group without sepsis (Sham) and group CLP, but the

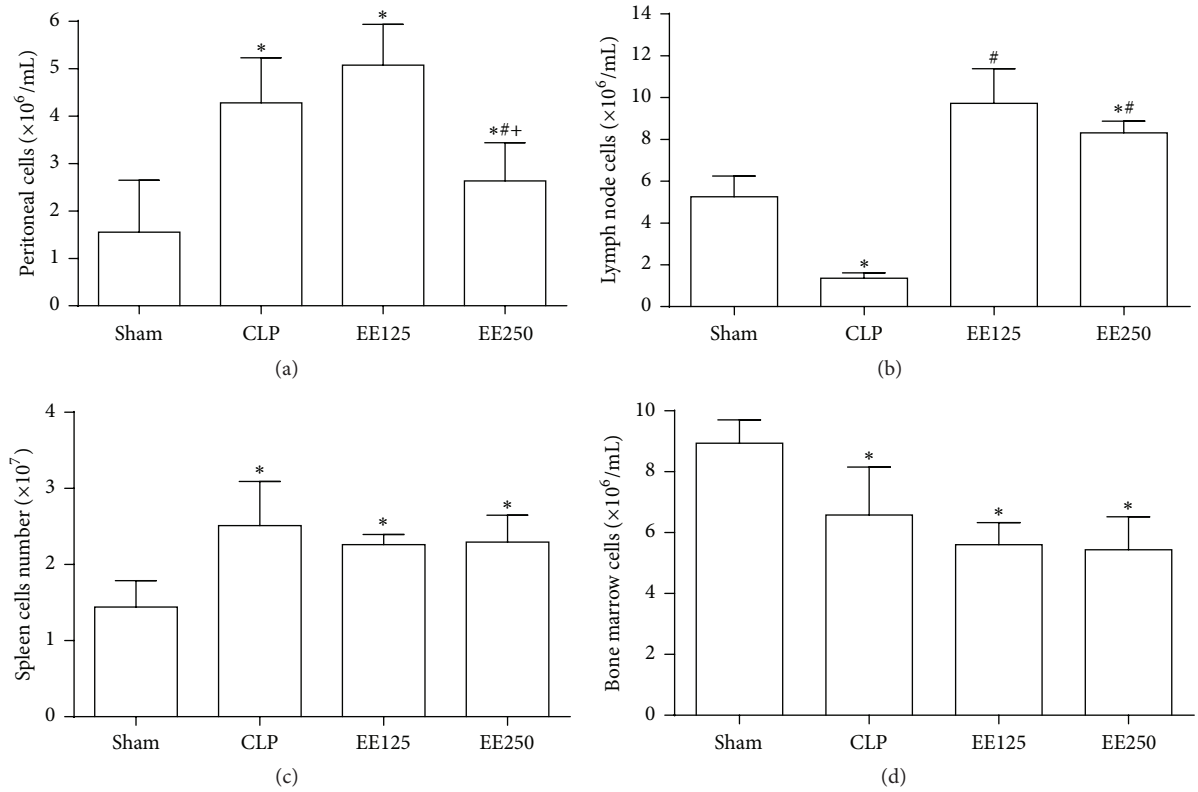

Figure 2: Effect of treatment with ethanolic extract (EE) of babassu mesocarp on the number of lymphoid cells. The animals were treated with EE at doses of 125 (EE125) or 250 mg/Kg (EE250) 6 h after the induction of sepsis by cecal ligation and puncture, sacrificed 12 h after the procedure, and compared to the untreated animals without (Sham) or with sepsis (CLP). The number of cells in the peritoneum (a), lymph nodes (b), bone marrow (c), and spleen (d) was quantified. The results are expressed as mean ± SEM (5 animals/group). (∗) $p < 0{,}05$ in comparison to the Sham group; (#) $p < 0{,}05$ in comparison to CLP group; and (+) $p < 0{,}05$ in comparison to EE250.

treatment with 250 mg/Kg of EE inhibited this cellular influx, in comparison to the other groups with sepsis (CLP and EE125) (Figure 2(a)). On the other hand, the EE treatment, irrespective of the dose, significantly increased the number of mesenteric lymph node cells, when compared to the cell numbers found in untreated groups without (Sham) or with sepsis (CLP) (Figure 2(b)). The treatment with EE has no effect on the number of splenocytes (Figure 2(c)) and bone marrow cells (Figure 2(d)).

3.5. Cytokine Production. Treatment with EE inhibited the production of TNF-α, irrespective of the dose. In addition, treatment with EE125, but not with EE250, inhibited the production of IL-6. The production of IFN-γ was not affected by treatment with the extract (Figure 3).

4. Discussion

The medicinal potential of babassu (*Attalea speciosa*) has been recognized based on preclinical trials showing its biological activity. Phytochemical screening demonstrated a predominance of phenolic acids. Previous chemical studies using *O. phalerata* extracts also identified the presence of triterpenes, glycosylated triterpenes, tannins, sugars, saponins, and steroids [26].

The EE showed an effective antimicrobial *in vitro* activity against the Gram-positive bacteria *E. faecalis*, *S. aureus,* and MRSA. However, no activity was observed against *E. coli* and *P. aeruginosa*, which indicates a selective and specific antibacterial action of EE.

The MIC and minimum bactericidal concentration (MBC) were only determined for strains against which antimicrobial activity was observed in the disk diffusion assay. A higher MIC was observed for *E. faecalis*, although similar MBC were obtained for *E. faecalis*, *S. aureus,* and the hospital strain of *S. aureus* MRSA. The antimicrobial activity to Gram-positive bacteria for other vegetal extracts obtained from native and exotic species of the Brazilian flora was described previously [30–32]. The antimicrobial activity for *S. aureus* and MRSA was also reported previously [8], but the antimicrobial activity of babassu mesocarp to *E. faecalis* was not reported before.

E. faecalis is part of the commensal Gram-positive microbial flora of the gastrointestinal tract of humans and other mammals [33]. This microorganism is associated with nosocomial infections and may cause endocarditis and urinary infections. These bacteria are generally resistant to a wide variety of antibiotics, a fact that contributes to their high pathogenicity [34, 35].

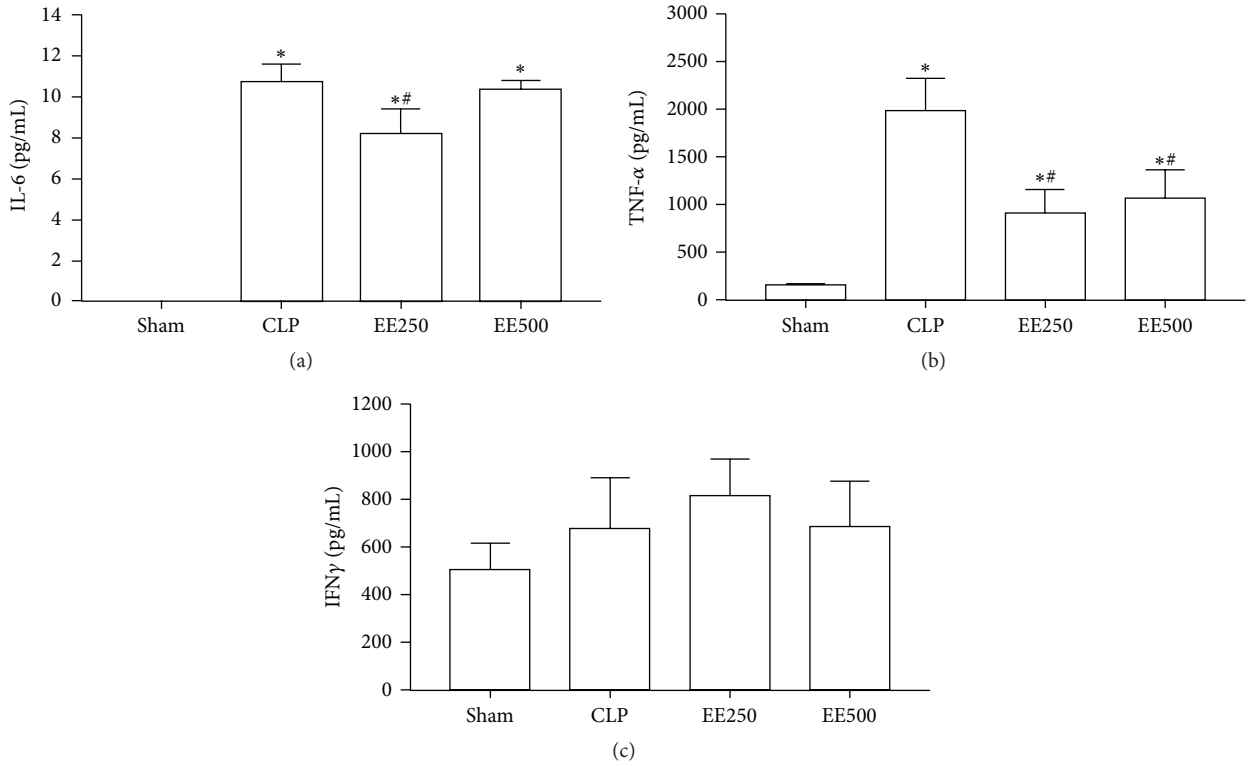

Figure 3: Effect of treatment with ethanolic extract (EE) of babassu mesocarp on the production of cytokines. The animals were treated with EE at doses of 125 (EE125) or 250 mg/Kg (EE250) 6 h after the induction of sepsis by cecal ligation and puncture and compared to the untreated group also submitted to the inductions of sepsis (CLP) or not (Sham). The animals were sacrificed 12 h after the procedure and serum was obtained for the measurement of IL-6 (a), TNF-α (b), and IFN-γ (c) by ELISA assay. The results are expressed as mean ± SEM (5 animals/group). (∗) $p < 0{,}05$ in comparison to the SHAM group and (#) $p < 0{,}05$ in comparison to the CLP group.

Antimicrobial compounds of plant origin with a restricted action against specific bacteria species and/or strains are desired not only due to their efficacy in the infection control, but also because they permit the maintenance of the normal microbiota. One important finding of this study was the sensitivity of the hospital strain of MRSA to the babassu mesocarp extract, since therapeutic options for patients infected with MRSA are limited. MRSA strains are always resistant to all cephalosporins, including fourth-generation drugs, as well as to carbapenems, irrespective of the result of the antibiogram [36]. The glycopeptide antibiotics vancomycin and teicoplanin are often the only choice for the treatment of infections caused by these microorganisms.

An increasing resistance of *E. faecalis* to traditional antibiotics has been frequently reported in some Brazilian hospitals [37]. In addition, the growing resistance of these strains to vancomycin [37, 38] has encouraged studies aimed at the discovery of new therapeutic agents that act rapidly on the control of these microorganisms.

The presence of phenolic acids in the extract suggests a direct relationship with its antimicrobial activity since an antimicrobial action of these compounds has been attributed to their ability to form complexes with extracellular polysaccharides and proteins, rupturing the bacterial cell wall and inhibiting the enzymatic systems responsible for the synthesis of cell wall components [11, 39]. Since the pharmacological action of a plant species employed as a phytotherapeutic agent involves the interaction between its different chemical components [40], the antimicrobial activity of EE observed in this study may also be attributed to the synergistic action of phenolic compounds, specifically phenolic acids, and flavonoids present in the extract.

In view of the restricted number of active products available for the control of MRSA and of the growing resistance of *E. faecalis*, babassu mesocarp might be used as a potential target for prospecting bioactive compounds with controlled antibiotic action.

Due to this antibacterial action, the effect of EE treatment on *in vivo* bacterial systemic infection was evaluated using the CLP model which mimics the events that occur in sepsis in humans in terms of both surgical trauma and the involved microbiota [15, 29].

The CLP model reproduces a type of infection mainly caused by *Escherichia coli*, Gram-negative bacteria [15], but evaluates the possible coexistence of other bacteria colonizing the abdominal cavity, in this case Gram-positive bacteria. CLP alone triggers a series of proinflammatory events that are characteristic of a systemic inflammatory response, including cell and tissue injury, neutrophil migration, reduction in the number of cells in adjacent lymph nodes and spleen, and increased production of proinflammatory cytokines and other mediators. This set

of events eventually results in multiple organ failure and death.

Treatment with EE was initiated 6 h after the induction of sepsis to evaluate the therapeutic effect of the extract. The results showed that treatment with the babassu extract did not affect bacterial counts but increased the survival of the animals and immunoregulated the proinflammatory cytokine production. Similar results were previously described by Maciel et al. [29] studying the effect of *Syzygium jambolanum* in sepsis. They showed an increased survival in lethal sepsis more associated with the anti-inflammatory effect than with the antibiotic activity of the extract.

Mice from EE250 group showed inhibition of peritoneal cell migration and a lower production of TNF-α and IL-6 when compared to the control group. IL-6, TNF-α, and IL-8 exert an inflammatory action and an increased level of these cytokines is frequently found in septic shock caused by Gram-negative bacteria as observed in the CLP model [18, 19, 21, 36].

Proinflammatory cytokines such as TNF-α, IL-6, IL-1, and IFN-γ play an important role during the course of sepsis, interfering with the prognosis, progression, and intensity of tissue damage, and are associated with the aggravation and lethality of sepsis [11, 18]. TNF-α is the first cytokine in the blood circulation in human sepsis and promotes leukocytes recruitment to the inflammatory focus. Additionally, TNF-α is associated with an increase in the production of chemokines and adhesion molecules that are involved in the recruitment, proliferation, and survival of cells at sites of injury [19]. Taken together, these data suggest that the lower production of TNF-α observed in animals treated with EE250 might be associated with the inhibition of cell migration to the peritoneum. This hypothesis is supported by the increased number of cells detected on adjacent lymph nodes observed in the EE250 group.

Babassu mesocarp flour has a potent activating effect on macrophages as shown previously [3]. The treatment with EE125 was more effective in decreasing the IL-6 production and increased the cellular influx to the peritoneal cavity, in contrast to the treatment with the high dose EE250 that had no effect on IL-6 production, but efficiently reduced the cellular influx to peritoneal cavity. The differences between the doses can be related to the efficacy of the compounds present in babassu mesocarp to regulate the IL-6 production and the expression of receptors that can be associated with cellular migration [41, 42] and with the EE effect on the outcome and survival in experimental sepsis.

Taken together, the present results show that the efficacy of EE in increasing the lifespan in mice with sepsis by CLP is related to an immunomodulatory effect on the inflammatory process, mediated by cytokines. The immunomodulatory effect of babassu mesocarp on inflammation has been reported in other studies [3, 9, 10]. The present results confirm this property and also indicate that this action is possibly related to the capacity of compounds present in the extract to inhibit the production of TNF-α and IL-6 cytokines.

In conclusion the present study showed that the EE has a relevant and selective bacteriostatic action *in vitro* against the Gram-positive bacteria *Staphylococcus aureus* and *Enterococcus faecalis*, but not against the Gram-negative bacteria *Escherichia coli* and *Pseudomonas aeruginosa*. Besides the EE increases the survival of animals submitted to the lethal sepsis, activity possibly related to a decrease in TNF-α and IL-6 production and a consequent inhibition of systemic inflammation.

Competing Interests

The authors declare that they have no competing interests.

Acknowledgments

The authors thank CNPq for the financial support (Proc. no. 562248/2008) and for the researcher fellowship to Flávia R. F. Nascimento and Rosane N. M. Guerra and master fellowship to Wanderson S. Pereira. The authors thank CAPES for the master fellowship to Dayanna S. Prado, Priscila S. Barcellos, Tonicley A. Silva, and Lucilene A. Silva. The authors are also grateful to FAPEMA and UFMA.

References

[1] M. J. Balick, "The economic utilization of the babassu palm: a conservation strategy for sustaining tropical forest resources," *Journal of the Washington Academy of Sciences*, vol. 77, no. 4, pp. 215–222, 1987.

[2] M. H. S. L. Souza, C. A. Monteiro, P. M. S. Figueredo, F. R. F. Nascimento, and R. N. M. Guerra, "Ethnopharmacological use of babassu (*Orbignya phalerata* Mart) in communities of babassu nut breakers in Maranhão, Brazil," *Journal of Ethnopharmacology*, vol. 133, no. 1, pp. 1–5, 2011.

[3] F. R. F. Nascimento, E. S. B. Barroqueiro, A. P. S. Azevedo et al., "Macrophage activation induced by Orbignya phalerata Mart," *Journal of Ethnopharmacology*, vol. 103, no. 1, pp. 53–58, 2006.

[4] C. P. Batista, O. J. M. Torres, J. E. F. Matias et al., "Effect of watery extract of *Orbignya phalerata* (babassu) in the gastric healing in rats: morfologic and tensiometric study," *Acta Cirurgica Brasileira*, vol. 21, no. 3, pp. 26–32, 2006.

[5] M. N. Rennó, G. M. Barbosa, P. Zancan et al., "Crude ethanol extract from babassu (*Orbignya speciosa*): cytotoxicity on tumoral and non-tumoral cell lines," *Anais da Academia Brasileira de Ciencias*, vol. 80, no. 3, pp. 467–476, 2008.

[6] T. S. Fortes, E. M. S. Fialho, A. S. Reis et al., "Desenvolvimento do tumor de Ehrlich em camundongos após tratamento *in vitro* com mesocarpo de babaçu," *Revista de Ciências da Saúde*, vol. 11, pp. 101–105, 2009.

[7] A. P. S. Azevedo, J. C. Farias, G. C. Costa et al., "Anti-thrombotic effect of chronic oral treatment with *Orbignya phalerata* Mart.," *Journal of Ethnopharmacology*, vol. 111, no. 1, pp. 155–159, 2007.

[8] N. Caetano, A. Saraiva, R. Pereira, D. Carvalho, M. C. B. Pimentel, and M. B. S. Maia, "Determinação de atividade antimicrobiana de extratos de plantas de uso popular como antiflamatório," *Brazilian Journal of Pharmacognosy*, vol. 12, pp. 132–135, 2002.

[9] B. P. da Silva and J. P. Parente, "An anti-inflammatory and immunomodulatory polysaccharide from *Orbignya phalerata*," *Fitoterapia*, vol. 72, no. 8, pp. 887–893, 2001.

[10] R. N. M. Guerra, V. M. G. Silva, L. S. A. França et al., "Babassu aqueous extract (BAE) as an adjuvant for T helper

(Th)1-dependent immune responses in mice of a Th2 immune response-prone strain," *BMC Immunology*, vol. 12, article 13, 2011.

[11] A. Matsuda, A. Jacob, R. Wu et al., "Novel therapeutic targets for sepsis: regulation of exaggerated inflammatory responses," *Journal of Nippon Medical School*, vol. 79, no. 1, pp. 4–18, 2012.

[12] M. S. Rangel-Frausto, "The epidemiology of bacterial sepsis," *Infectious Disease Clinics of North America*, vol. 13, no. 2, pp. 299–312, 1999.

[13] R. Daniels, "Surviving the first hours in sepsis: Getting the basics right (an intensivist's perspective)," *Journal of Antimicrobial Chemotherapy*, vol. 66, supplement 2, pp. ii11–ii23, 2011.

[14] B. Cai, E. A. Deitch, and L. Ulloa, "Novel insights for systemic inflammation in sepsis and hemorrhage," *Mediators of Inflammation*, vol. 2010, Article ID 642462, 10 pages, 2010.

[15] C. F. Benjamim, J. S. Silva, Z. B. Fortes, M. Aparecida Oliveira, S. H. Ferreira, and F. Q. Cunha, "Inhibition of leukocyte rolling by nitric oxide during sepsis leads to reduced migration of active microbicidal neutrophils," *Infection and Immunity*, vol. 70, no. 7, pp. 3602–3610, 2002.

[16] H. MacArthur, T. C. Westfall, D. P. Riley, T. P. Misko, and D. Salvemini, "Inactivation of catecholamines by superoxide gives new insights on the pathogenesis of septic shock," *Proceedings of the National Academy of Sciences of the United States of America*, vol. 97, no. 17, pp. 9753–9758, 2000.

[17] A. A. Giacometti, O. Cirioni, R. Ghiselli et al., "Potential therapeutic role of cationic peptides in three experimental models of septic shock," *Antimicrobial Agents and Chemotherapy*, vol. 46, no. 7, pp. 2132–2136, 2002.

[18] I. Cinel and S. M. Opal, "Molecular biology of inflammation and sepsis: a primer," *Critical Care Medicine*, vol. 37, no. 1, pp. 291–304, 2009.

[19] M. G. Davies and P.-O. Hagen, "Systemic inflammatory response syndrome," *British Journal of Surgery*, vol. 84, no. 7, pp. 920–935, 1997.

[20] J. A. Sales Júnior, C. M. David, R. Hatum et al., "Sepse Brasil: estudo epidemiológico da sepse em Unidades de Terapia Intensiva brasileiras," *Revista Brasileira de Terapia Intensiva*, vol. 18, no. 1, pp. 9–17, 2006.

[21] H. Ma, J. Kou, D. Zhu, Y. Yan, and B. Yu, "Liu-Shen-Wan, a traditional Chinese medicine, improves survival in sepsis induced by cecal ligation and puncture via reducing TNF-α levels, MDA content and enhancing macrophage phagocytosis," *International Immunopharmacology*, vol. 6, no. 8, pp. 1355–1362, 2006.

[22] R. P. M. Antunes, E. O. Lima, M. S. V. Pereira et al., "*In vitro* antimicrobial activity and determination of the minimum inhibitory concentration (MIC) of natural and synthetic compounds against bacteria and leveduriform fungi," *Brazilian Journal of Pharmacognosy*, vol. 16, pp. 517–524, 2006.

[23] F. P. de Oliveira, E. de Oliveira Lima, J. P. de Siqueira Júnior, E. L. de Souza, B. H. C. Santos, and H. M. Barreto, "Effectiveness of *Lippia sidoides* Cham. (*Verbenaceae*) essential oil in inhibiting the growth of *Staphylococcus aureus* strains isolated from clinical material," *Revista Brasileira de Farmacognosia*, vol. 16, no. 4, pp. 510–516, 2006.

[24] M. B. Falkenberg, R. I. Santos, and C. M. O. Simões, "Introdução a fitoquímica experimental," in *Farmacognosia: da Planta ao Medicamento*, C. O. M. Simões, E. P. Schenkel, G. Gosmann, J. C. P. Mello, L. A. Mentz, and P. R. Petrovick, Eds., Porto Alegre/Florianópolis, pp. 163–179, Universidade/UFRGS/Ed. da UFSC, 5th edition, 2004.

[25] V. L. Singleton and J. A. Rossi Jr., "Colormetry of total phenolics with phosphomolybdic-phosphotungstic acid reagents," *American Journal of Enology and Viticulture*, vol. 16, pp. 144–158, 1965.

[26] R. G. Woisky and A. Salatino, "Analysis of propolis: some parameters and procedures for chemical quality control," *Journal of Apicultural Research*, vol. 37, no. 2, pp. 99–105, 1998.

[27] CLSI-Clinical and Laboratory Standards Institute, "Performance standards for antimicrobial susceptibitity testing: eighteenth informational supplement," CLSI Document M 100-D18, 2008.

[28] I. Phillips, "A guide to sensitivity testing," *Journal of Antimicrobial Chemotherapy*, vol. 27, pp. 1–50, 1991.

[29] M. C. G. Maciel, J. C. Farias, M. J. Maluf et al., "*Syzygium jambolanum* treatment improves survival in lethal sepsis induced in mice," *BMC Complementary and Alternative Medicine*, vol. 8, article 57, 2008.

[30] M. F. Agra, P. F. Freitas, and J. M. Barbosa-Filho, "Synopsis of the plants known as medicinal and poisonous in Northeast of Brazil," *Brazilian Journal of Pharmacognosy*, vol. 17, no. 1, pp. 114–140, 2007.

[31] I. B. Suffredini, M. L. Barradas Paciencia, A. D. Varella, and R. N. Younes, "Antibacterial activity of Brazilian Amazon plant extracts," *Brazilian Journal of Infectious Diseases*, vol. 10, no. 6, pp. 400–402, 2006.

[32] J. F. Packer and M. M. S. Da Luz, "Evaluation and research method for natural products inhibitory activity," *Brazilian Journal of Pharmacognosy*, vol. 17, no. 1, pp. 102–107, 2007.

[33] S. G. B. Amyes, "Enterococci and streptococci," *International Journal of Antimicrobial Agents*, vol. 29, no. 3, pp. S43–S52, 2007.

[34] P. Courvalin, "Vancomycin resistance in gram-positive cocci," *Clinical Infectious Diseases*, vol. 42, supplement 1, pp. S25–S34, 2006.

[35] J. Marrow, J. K. Whittington, M. Mitchell, L. L. Hoyer, and C. Maddox, "Prevalence and antibiotic-resistance characteristics of *Enterococcus* spp. isolated from free-living and captive raptors in central illinois," *Journal of Wildlife Diseases*, vol. 45, no. 2, pp. 302–313, 2009.

[36] Y. Tang, X. Xu, H. Song et al., "Early diagnostic and prognostic significance of a specific Th1/Th2 cytokine pattern in children with haemophagocytic syndrome," *British Journal of Haematology*, vol. 143, no. 1, pp. 84–91, 2008.

[37] A. Çiftci, A. Findik, T. Içа, B. Bas, E. E. Onuk, and S. Güngördü, "Slime production and antibiotic resistance of *Enterococcus faecalis* isolated from arthritis in chickens," *Journal of Veterinary Medical Science*, vol. 71, no. 6, pp. 849–853, 2009.

[38] A. L. Reale, M. L. Depetri, C. Culasso et al., "Vancomycin-resistant enterococci: prevalence and factors associated with intestinal colonization in oncology patients from Hospital de Niños de Córdoba," *Revista Argentina de Microbiologia*, vol. 41, no. 2, pp. 92–96, 2009.

[39] M. M. Cowan, "Plant products as antimicrobial agents," *Clinical Microbiology Reviews*, vol. 12, no. 4, pp. 564–582, 1999.

[40] P. J. Houghton, M.-J. Howes, C. C. Lee, and G. Steventon, "Uses and abuses of *in vitro* tests in ethnopharmacology: visualizing an elephant," *Journal of Ethnopharmacology*, vol. 110, no. 3, pp. 391–400, 2007.

[41] N. C. Riedemann, R.-F. Guo, T. A. Neff et al., "Increased C5a receptor expression in sepsis," *The Journal of Clinical Investigation*, vol. 110, no. 1, pp. 101–108, 2002.

[42] N. C. Riedemann, T. A. Neff, R.-F. Guo et al., "Protective effects of IL-6 blockade in sepsis are linked to reduced C5a receptor expression," *Journal of Immunology*, vol. 170, no. 1, pp. 503–507, 2003.

Hindawi Publishing Corporation
Evidence-Based Complementary and Alternative Medicine
Volume 2016, Article ID 1359105, 17 pages
http://dx.doi.org/10.1155/2016/1359105

Research Article

Sequential Treatments with Tongsai and Bufei Yishen Granules Reduce Inflammation and Improve Pulmonary Function in Acute Exacerbation-Risk Window of Chronic Obstructive Pulmonary Disease in Rats

Xiaofan Lu,[1,2] Ya Li,[3,4,5] Jiansheng Li,[2,3,6] Haifeng Wang,[3,6] Zhaohuan Wu,[2,3] Hangjie Li,[2,3] and Yang Wang[2,3]

[1]*Dongzhimen Hospital, Beijing University of Chinese Medicine, Beijing 100700, China*
[2]*Institute for Geriatrics, Henan University of Chinese Medicine, Zhengzhou, Henan 450046, China*
[3]*Collaborative Innovation Center for Respiratory Diseases Diagnostics, Treatment and New Drug Research and Development in Henan Province, Zhengzhou, Henan 450046, China*
[4]*Institute for Respiratory Diseases and the Level Three Laboratory of Respiration Pharmacology of Chinese Medicine, the First Affiliated Hospital, Henan University of Chinese Medicine, Zhengzhou, Henan 450000, China*
[5]*Central Laboratory, the First Affiliated Hospital, Henan University of Chinese Medicine, Zhengzhou, Henan 450000, China*
[6]*Department of Respiratory Diseases, the First Affiliated Hospital of Henan University of Chinese Medicine, Zhengzhou, Henan 450000, China*

Correspondence should be addressed to Jiansheng Li; li_js8@163.com

Received 14 April 2016; Accepted 15 June 2016

Academic Editor: Ying-Ju Lin

Background. Sequential treatments of Chinese medicines for acute exacerbation of chronic obstructive pulmonary disease (AECOPD) risk window (RW) have benefits for preventing reoccurrences of AEs; however, the effects on pulmonary function, pulmonary, and systemic inflammatory biomarkers remain unclear. *Methods*. Cigarette-smoke/bacterial infections induced rats were randomized into Control, COPD, AECOPD, Tongsai Granule/normal saline (TSG/NS), moxifloxacin + salbutamol/NS (MXF+STL/NS), TSG/Bufei Yishen Granule (BYG), MXF+STL/STL, and TSG+MXF+STL/BYG+STL groups and given corresponding medicine(s) in AE- and/or RW phase. Body temperature, pulmonary function, blood cytology, serum amyloid A (SAA) and C-reactive protein (CRP), pulmonary histomorphology and myeloperoxidase (MPO), polymorphonuclear (PMN) elastase, interleukins IL-1β, IL-6, and IL-10, and tumor necrosis factor- (TNF-) α expressions were determined. *Results*. Body temperature, inflammatory cells and cytokines, SAA, CRP, and pulmonary impairment were higher in AECOPD rats than stable COPD, while pulmonary function declined and recovered to COPD level in 14–18 days. All biomarkers were improved in treated groups with shorter recovery times of 4–10 days, especially in TSG+MXF+STL/BYG+STL group. *Conclusion*. Sequential treatments with Tongsai and Bufei Yishen Granules, during AECOPD-RW periods, can reduce inflammatory response and improve pulmonary function and shorten the recovery courses of AEs, especially the integrated Chinese and Western medicines.

1. Background

Chronic obstructive pulmonary disease (COPD) is commonly accompanied by acute exacerbations (AEs), which significantly contribute to morbidity and mortality [1]. Acute exacerbations are usually caused by pathogen infection-related inflammation and other insults. Proinflammatory stimuli in the lung recruit inflammatory cells, such as neutrophils, eosinophils, macrophages, and lymphocytes. These cells can secrete proinflammatory cytokines, chemokines,

and proteases, leading to the destruction of pulmonary parenchyma and remodeling of multiple components of airway epithelium and contributing to the pathogenesis of AECOPD and the development of emphysema [2, 3]. Previous studies have shown that the concentrations of C-reactive protein (CRP), interleukins IL-6 and IL-1, tumor necrosis factor- (TNF-) α, and myeloperoxidase (MPO) and the number of polymorphonuclear (PMN) cells are positively correlated with the severity and poor prognosis of AECOPD [4–7]. However, in the subsequent remission stage, inflammatory indicators presented unstable trends. The numbers of white blood cells (WBCs) and neutrophils in the sputum and blood were increased 24 h after infection and were significantly decreased 3 days after the patients received medication, but the numbers did not fully recover until 10–40 days after infections [8–12]. This unstable period is defined as the AECOPD risk window (RW), which begins approximately 7–21 days after exacerbation in AECOPD patients but does not recover to the baseline of the stable phase and is characterized by decreased body temperature, incompletely recovered pulmonary function, decreased inflammation, and increased risk of subsequent exacerbations. The recurrences of AEs during this period may require readmissions and may increase mortality [13]. A similar variable period was also observed in a sequential COPD-AE-RW rat model, where the levels of inflammatory indicators, such as the number of WBCs and neutrophils and serum amyloid A (SAA) and CRP levels, varied rapidly for 5 days in the AE phase, but the changes were mild in the subsequent 10 days of the RW phase [14, 15].

In traditional Chinese medicine (TCM), COPD is classified as FEIZHANG disease, for which the treatments are based on syndrome differentiation. At different stages of AE and stable phases of COPD, the syndromes are completely different [16]. Generally, the primary syndrome in the AE period is phlegm-heat obstructing lungs, whereas lung-kidney qi deficiency is present in the stable phase. In the risk window period, pathogenesis is presented as a syndrome of lingering pathogen infection due to a deficiency in vital qi, in which the qi deficiency is superior to the excess pathogenic syndrome and is characterized by alleviated clinical symptoms, incomplete recovery of pulmonary function, and high risk of AE recurrence and rehospitalization [17]. Clinically, the method of clearing heat and dissipating phlegm is applied to the phlegm-heat obstructing lung syndrome, which is mainly induced by bacteria and/or viruses and is characterized by fever, cough, and spitting yellow phlegm, as well as pharyngalgia and chest distress [18, 19]. For the stable phase and risk window period, the main treatment principle is to reinforce the deficiency in vital qi because most or all of the excess syndromes have disappeared. In previous studies, Tongsai Granule was confirmed to clear heat-phlegm, relieve cough and breathlessness, and depress the systemic inflammation in AECOPD patients, including serum IL-1β, IL-6, and IL-8 levels [20, 21]. Furthermore, it also inhibited the expression of matrix metalloproteinases MMP-2 and MMP-9, type III precollagen (PCIII), transforming growth factor- (TGF-) β, laminin (LN), and hyaluronic acid (HA) in AECOPD rats [22, 23]. Bufei Yishen Granule was also shown to improve lung function and reduce the incidence and duration of AE in COPD patients after a 6-month treatment and even in a 12-month follow-up without treatment [24]; the results were confirmed in a rat model [25, 26].

In this study, we attempted to explore the effects of sequential treatments with Tongsai Granule (TSG) and Bufei Yishen Granule (BYG) in the AE-RW period in a rat model by observing improvements in pulmonary function, inflammatory biomarker levels, and pulmonary histomorphology.

2. Methods

2.1. Animals. Thirty-two male and 32 female 2-month-old Sprague-Dawley rats, weighing 200 ± 20 grams (g), were provided by the Experimental Animal Center of Henan Province (Special Pathogen Free, SCXK (Henan) 2005-0001) and accommodated in individual ventilated cases for 7 days in the facility in the First Affiliated Hospital, Henan University of Traditional Medicine, Zhengzhou, Henan, China, before experiments were performed. The room temperature was maintained at 25 ± 1°C, the relative humidity was 50 ± 10%, with 10 to 15 gas changes per hour, the ammonia concentration was ≤14 mg/m^3, and the noise was ≤60 db. The rats had free access to sterilized feed and water.

2.2. Cigarette. Hongqi Canal® Filter cigarettes (tobacco type, tar 10 mg, nicotine content 1.0 mg, and carbon monoxide 11 mg) were provided by Henan Zhongyan Industry Company (Zhengzhou, Henan).

2.3. Bacteria. *Klebsiella pneumoniae* (KP; strain: 46114) was provided by the National Center For Medical Culture Collections (Beijing, China) and was prepared at a concentration of 6×10^8 and 6×10^{14} colony forming units (CFU) per milliliter (mL) in suspension before bacteria challenges.

2.4. Drugs. Tongsai Granule consists of Ting Li Zi (*Lepidium apetalum* Willd.) 12 g, Di Long (*Pheretima aspergillum* (E. Perrier)) 12 g, Chuan Bei Mu (*Fritillaria cirrhosa* D. Don) 12 g, Da Huang (*Rheum officinale* Baill.) 6 g, Ma Huang (*Ephedra sinica* Stapf.) 9 g, Chi Shao (*Paeonia anomala* subsp. *veitchii* (Lynch) D. Y. Hong and K. Y. Pan) 12 g, Mai Dong (*Ophiopogon japonicus* (Thunb.) Ker Gawl.) 12 g, and Ai Di Cha (*Ardisia japonica* (Thunb.) Blume) 15 g [22]. Bufei Yishen Granule consists of Ren Shen (*Panax ginseng* C. A. Mey.) 9 g, Huang Qi (*Astragalus membranaceus* (Fisch.) Bunge) 15 g, Gou Qi (*Lycium chinense* Mill.) 12 g, Shan Zhu Yu (*Cornus officinalis* Siebold and Zucc.) 12 g, Yin Yang Huo (*Epimedium rotundatum* K. S. Hao) 9 g, Wu Wei Zi (*Schisandra chinensis* (Turcz.) Baill.) 9 g, and Ai Di Cha (*Ardisia japonica* (Thunb.) Blume) 9 g [27]. These drugs were prepared by the Department of Pharmacology in the First Affiliated Hospital, Henan University of Chinese Medicine, Zhengzhou, China. Moxifloxacin (MXF) hydrochloride tablets (0.4 g/tablet, Bayer, Germany) and salbutamol (STL) sulfate tablets (2 mg/tablet, Yabang, Jiangsu, China) were crushed and prepared as 10 mg/mL and 1 mg/mL solutions, respectively, before administrations.

Table 1: Protocol for treatments during the acute exacerbation and risk window phases in COPD rats.

Group	AE phase (Day −1, 0, Day 2 to Day 6)				RW phase (Day 7 to Day 16)		
	NS	TSG	MXF	STL	NS	BYG	STL
Control	+	−	−	−	+	−	−
COPD	+	−	−	−	+	−	−
AECOPD	+	−	−	−	+	−	−
TSG/NS	−	+	−	−	+	−	−
MXF+STL/NS	−	−	+	+	+	−	−
TSG/BYG	−	+	−	−	−	+	−
MXF+STL/STL	−	−	+	+	−	−	+
TSG+MXF+STL/BYG+STL	−	+	+	+	−	+	+

Note: +: treated with this medicine; −: not treated with this medicine. AE: acute exacerbation; AECOPD: acute exacerbation of chronic obstructive pulmonary disease; BYG: Bufei Yishen Granule; COPD: chronic obstructive pulmonary disease; MXF: moxifloxacin; NS: normal saline; RW: risk window; TSG: Tongsai Granule; STL: salbutamol.

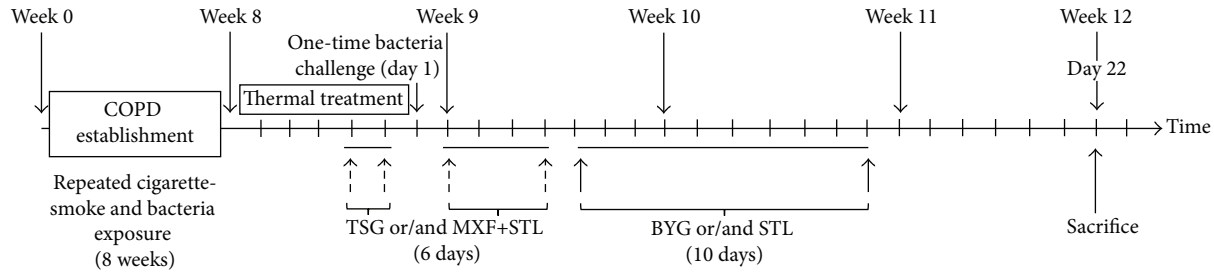

Figure 1: Experimental flow and key time points for the administrations. Week 1 through week 8: COPD model preparation period. Day 1: the rats were challenged with *Klebsiella pneumonia* solution (6×10^{14} CFU/mL) after a 5-day thermal treatment. Tongsai Granule (TSG) or/and moxifloxacin (MXF) were administered to the AECOPD rats 2 days before and 4 days after challenge. Bufei Yishen Granule (BYG) and/or salbutamol (SLT) were administered over the next 10 days. The rats were sacrificed at the end of week 12 (Day 22). BYG: Bufei Yishen Granule; COPD: chronic obstructive pulmonary disease; MXF: moxifloxacin; RW: risk window; TSG: Tongsai Granule; STL: salbutamol.

2.5. Model Preparation. After adaptive accommodation for 7 days, the COPD model was established by cigarette-smoke and KP exposure, as previously reported [28]. The rats were housed in a sealed chamber and exposed to tobacco smoke (3,000 ± 500 parts per million (ppm)) generated by a smoke machine (BUXCO, NC, USA) for two 30-minute exposures per day for 8 weeks, with three-hour intervals. A KP solution prepared at 6×10^8 CFU/mL was slowly dropped into both nostrils in an alternating fashion at 0.1 mL/animal every 5 days for 8 weeks. The AECOPD rat model of phlegm-heat syndrome was established at week 9 according to previous reports [15, 29]. In the first 5 days of week 9, the rats were exposed to a heated ventilated chamber (39.0 ± 0.5°C) twice for 30 min at three-hour intervals. They were then intratracheally challenged with the KP solution (0.1 mL/animal, 6×10^{14} CFU) on the 6th day of week 9 (Day 1) after being anesthetized with chloral hydrate (0.28 g/kg body weight). All animals were sacrificed on Day 22 (Figure 1).

2.6. Grouping and Administrations. Sixty-four rats were randomized into Control, COPD, AECOPD, TSG/normal saline (TSG/NS), MXF+STL/NS, TSG/BYG, MXF+STL/STL, and TSG+MXF+STL/BYG+STL groups using a random number table (4 males and 4 females per group). Rats were administered intragastrically according to the protocol presented in Table 1 from the 4th day (Day −1) of week 9 to Day 16, excluding Day 1 (the challenge day). The sequential treatments with Western medicine were designed according to the "Global Strategy for the Diagnosis, Management, and Prevention of Chronic Obstructive Pulmonary Disease" *(update 2014)* [16].

The equivalent doses of TSG (7.2 g/kg/d), BYG (4.44 g/kg/d), MXF (27 mg/kg/d), and STL (0.41 mg/kg/d) were calculated using the following formula according to published references: $D_{rat} = D_{human} \times (K_{rat}/K_{human}) \times (W_{rat}/W_{human})^{2/3}$; D: dose; K: body shape index; $K = A/W^{2/3}$ (A: surface area/m^2, W: body weight/kg); W: body weight [30].

2.7. General Status. Body weights were recorded on weeks 4 and 8 and then weekly from week 9 to week 12.

2.8. Pulmonary Function Tests. Peak expiratory flow (PEF) was measured with an unrestrained Whole Body Plethysmograph (uWBP) system (Buxco, NY, USA) at the end of week 4 and week 8 and each weekend from week 9 to week 12. Forced expiratory volume 0.3 s (FEV0.3) and forced vital capacity (FVC) was determined with a FinePoint™ Pulmonary Function Test system (Buxco, NY, USA) on Day 22 after the animals were anesthetized and prior to sacrifice.

2.9. Blood Cytological Analysis and Serum Inflammatory Biomarkers Detection. The numbers of white blood cells (WBCs), neutrophils, monocytes, and lymphocytes in tail vein blood were analyzed with a hemocyte analyzer every 2 days from Day 0 to Day 22. CRP and SAA levels were also detected in the serum of the vein blood by enzyme-linked immunosorbent assay (ELISA) (Boster, Wuhan, China).

Whole blood was collected from the aorta abdominalis after the animals were anesthetized and sacrificed on Day 22. MPO, PMN elastase, IL-1β, IL-6, IL-10, and TNF-α levels in the serum were detected by ELISA (Boster, Wuhan, China).

2.10. Lung Tissue Sectioning and Bronchoalveolar Lavaging. All animals were sacrificed by exsanguination of the abdominal aorta after blood was collected. The trachea was cannulated, and the heart/lung block was removed from the thoracic cavity. The right extrapulmonary bronchus was ligated with sutures, and the right lung lobes were removed. The left lung lobe was lavaged with normal saline, and the recovered bronchoalveolar lavage fluid (BALF) was used to determine the total cell number, numbers of specific cell types, and cytokine levels. The lavaged left lung lobe was perfusion-fixed with 10% neutral buffered formalin via the trachea at a constant pressure of 30 cm fixative for 2 h, and it was immersed in the same fixative for at least 24 h before further processing.

2.11. BALF Cytological Analysis and Inflammatory Biomarkers Detection. Total cell numbers were determined manually using a hemocytometer, and the numbers of different cell types, such as neutrophils, macrophages, and lymphocytes, were determined under inverted and upright microscopes (Olympus, Japan). The left BALF was centrifuged, and the supernatant was collected to determine IL-1β, TNF-α, IL-6, IL-10, MPO, and PMN elastase levels by ELISA (Boster, Wuhan, China).

2.12. Pulmonary Morphology and Morphometry. Randomly orientated, serial sections of the formalin-fixed left lung lobe were processed using routine methods and embedded in paraffin. The tissue slices (4 μm) were deparaffinized and stained with hematoxylin-eosin (HE) for histopathology. The slides were blinded, and the alveolar cavity and density of alveoli were determined as follows: Mean linear intercept (MLI) (μm) = L/N_s. After a cross (+) was drawn through the center of each photo, the number of alveolar septa (N_s) lying on the cross was counted, and then the total length of the cross (L) was measured: mean alveolar numbers (MAN) (/mm^2) = N_a/A. The number of pulmonary alveoli in each visual field (N_a) and the area of the visual field (A) were measured [31].

2.13. Statistical Analysis. The data are presented as the means ± standard errors (SE). Chi-square test was applied to the mortality data. For repeated measurements, such as body weight, body temperature, cytological analysis, SAA and CRP levels, and PEF, repeated measures of a general linear regression equation were applied. One-Way ANOVA was applied to the FEV0.3, FVC, FEV0.3/FVC, levels of inflammatory factors in the BALF and serum, and pulmonary morphometry results. Statistical analyses were performed with SPSS Statistics 19.0 software (IBM, CA, USA). A two-tailed $P < 0.05$ indicated statistical significance.

Table 2: Mortalities of the rats in each group.

Group	N	Number of deaths	Mortality (%)
Control	8	0	0
COPD	8	1	12.5
AECOPD	8	2	25*
TSG/NS	8	0	0
MXF+STL/NS	8	0	0
TSG/BYG	8	0	0
MXF+STL/STL	8	0	0
TSG+MXF+STL/BYG+STL	8	0	0

Note: AE: acute exacerbation; AECOPD: acute exacerbation of chronic obstructive pulmonary disease; BYG: Bufei Yishen Granule; COPD: chronic obstructive pulmonary disease; MXF: moxifloxacin; NS: normal saline; TSG: Tongsai Granule; STL: salbutamol. * $P < 0.05$ versus Control group.

3. Results

3.1. Mortality. Two rats in COPD and AECOPD groups died as a result of pulmonary abscesses during the preparation period of the COPD model. Another rat in AECOPD group died for the same reason on Day 3, 48 h after bacterial challenge (Table 2).

3.2. Body Weight. As shown in Figure 2, the body weights of COPD rats were decreased from week 8 to week 12 compared with Control group ($P < 0.05$). After challenge with the KP solution, body weights of AECOPD group decreased from week 9 to week 12 compared with COPD group ($P < 0.05$). Body weights in the treated groups showed increasing trends after bacteria challenge compared with AECOPD group, and the body weights of TSG/BYG and TSG+MXF+STL/BYG+STL groups were significantly higher than those of AECOPD group at week 11 and week 12 ($P < 0.05$) (Figure 2(a)).

Body weight gain in COPD rats was lower than that in Control rats during COPD model preparation period ($P < 0.05$); it was higher in TSG/BYG and TSG+MXF+STL/BYG+STL groups than in AECOPD group in AE-RW-COPD period, and it was even higher in TSG+MXF+STL/BYG+STL group than in TSG/BYG and MXF+STL/STL groups ($P > 0.05$) (Figures 2(b) and 2(c)).

3.3. Body Temperature. As shown in Figure 3(a), the variations in body temperature in COPD group were approximately the same as those in the Control group. Twenty-four hours after bacterial challenge, body temperatures in AECOPD group increased sharply compared with those in COPD group ($P < 0.05$); the temperatures rapidly decreased over the next 4 days, fluctuated more smoothly in the subsequent days, and finally were synchronized with COPD group on Day 16 ($P < 0.05$). Compared with AECOPD group, body

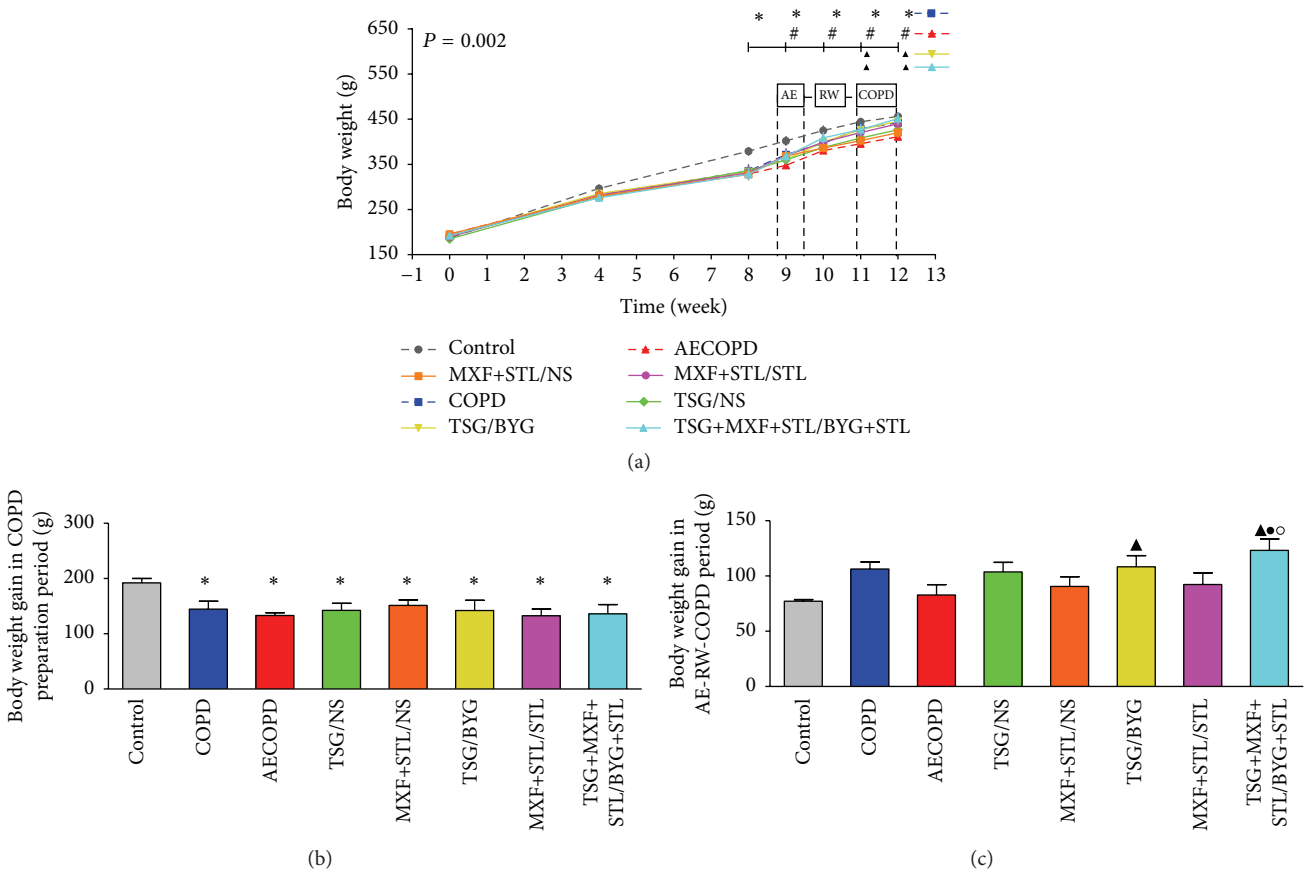

Figure 2: Temporal changes in body weights (a) over the 12-week experimental period; body weight gain in COPD preparation period (b) and AE-RW-COPD periods (c) in each group. AE: acute exacerbation; BYG: Bufei Yishen Granule; COPD: chronic obstructive pulmonary disease; MXF: moxifloxacin; NS: normal saline; RW: risk window; TSG: Tongsai Granule; STL: salbutamol. $N = 6$. Repetitive measurement deviation analysis of body weights: $P = 0.002$. $^{*}P < 0.05$, versus Control group; $^{\#}P < 0.05$, versus the COPD group; $^{\blacktriangle}P < 0.05$, versus AECOPD group; $^{\bullet}P < 0.05$, versus TSG/BYG group; $^{\circ}P < 0.05$, versus MXF+STL/STL group.

temperatures of the treated groups decreased on Day 2 and sharply decreased over the next 2 days ($P < 0.05$) (Figures 3(b), 3(c), 3(d), and 3(e)). Then, the curve shifted below that of COPD group on Day 6 and presented a mild decline in the subsequent days (Figures 3(b), 3(c), 3(d) and 3(e)). Moreover, the temperatures of TSG+MXF+STL/BYG+STL group were even lower than those in TSG/BYG group on Day 14 ($P < 0.05$) (Figure 3(e)).

3.4. Pulmonary Function. PEF in COPD group was significantly lower than in the Control group from week 4 to week 12 ($P < 0.05$) (Figure 4(a)). PEF was significantly reduced in AECOPD group 24 hours after bacterial challenge ($P < 0.05$), showed an increasing trend over the next 3 weeks, and recovered to the baseline values of COPD group at week 12. There was a slight increase in PEF in the treated groups compared with AECOPD group beginning at week 9, which returned to the baseline level of COPD group at week 11, approximately 1 week earlier than AECOPD group. PEF was higher in TSG/BYG and MXF+STL/STL groups than in TSG/NS and MXF+STL/NS groups at week 12 ($P < 0.05$).

As shown in Figures 4(b), 4(c), and 4(d), FVC, FEV0.3, and FEV0.3/FVC were decreased in COPD group compared with Control group, respectively ($P < 0.05$), and were substantially decreased in AECOPD group. All of the above-mentioned parameters were higher in the treated groups than in AECOPD group and were much higher in TSG/BYG and MXF+STL/STL groups than in the TSG/NS and MXF+STL/NS groups ($P < 0.05$).

3.5. Cell Types in the Peripheral Blood. As shown in Figures 5(a), 5(b) and 5(c), there were more WBCs in COPD group than in Control group throughout the experiment ($P < 0.05$), and the numbers of monocytes and neutrophils were increased in the first 2–8 days ($P < 0.05$). After challenge with the KP solution, the indicators mentioned above were highly elevated in AECOPD group ($P < 0.05$), decreased rapidly over the next 4 days, presented a smooth decreasing trend in the subsequent days, and returned to the baseline levels of COPD group on Day 16. For the treated groups, all indicators were reduced to different extents compared with AECOPD group on Day 2; they declined rapidly over

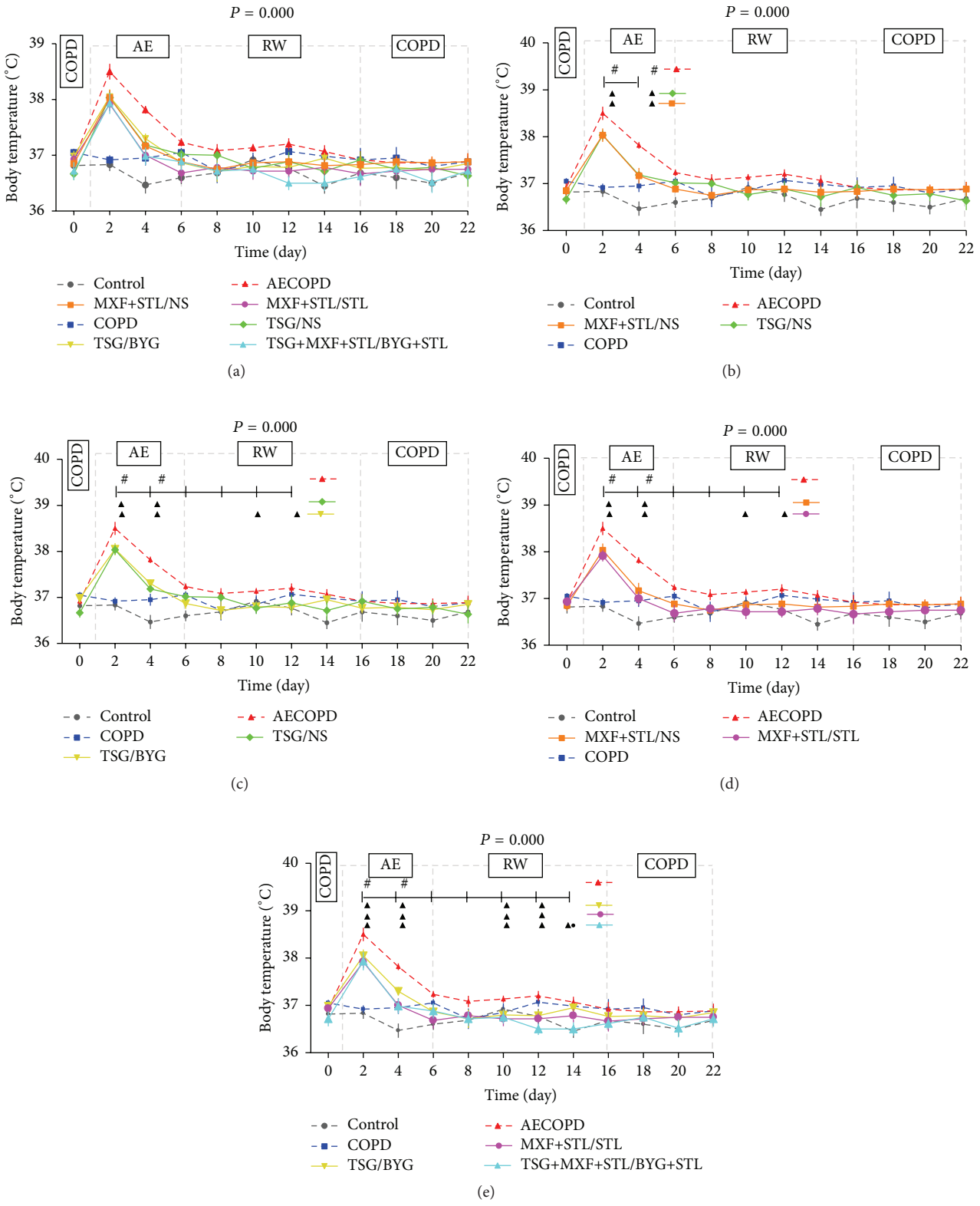

Figure 3: Temporal changes in body temperature (a) in rats administered sequential/nonsequential treatments. Panels (b), (c), (d), and (e) were split from panel (a) and indicate the comparison of sequential and nonsequential treatments with traditional Chinese medicine, Western medicine, or integrated medicines. AE: acute exacerbation; BYG: Bufei Yishen Granule; COPD: chronic obstructive pulmonary disease; MXF: moxifloxacin; NS: normal saline; RW: risk window; TSG: Tongsai Granule; STL: salbutamol. $N = 6$. Repetitive measurement deviation analysis of the body temperatures: $P = 0.000$. $^{\#}P < 0.05$, versus COPD group; $^{\blacktriangle}P < 0.05$, versus AECOPD group; $^{\bullet}P < 0.05$, versus TSG/BYG group. Bacteria challenge was performed on Day 1.

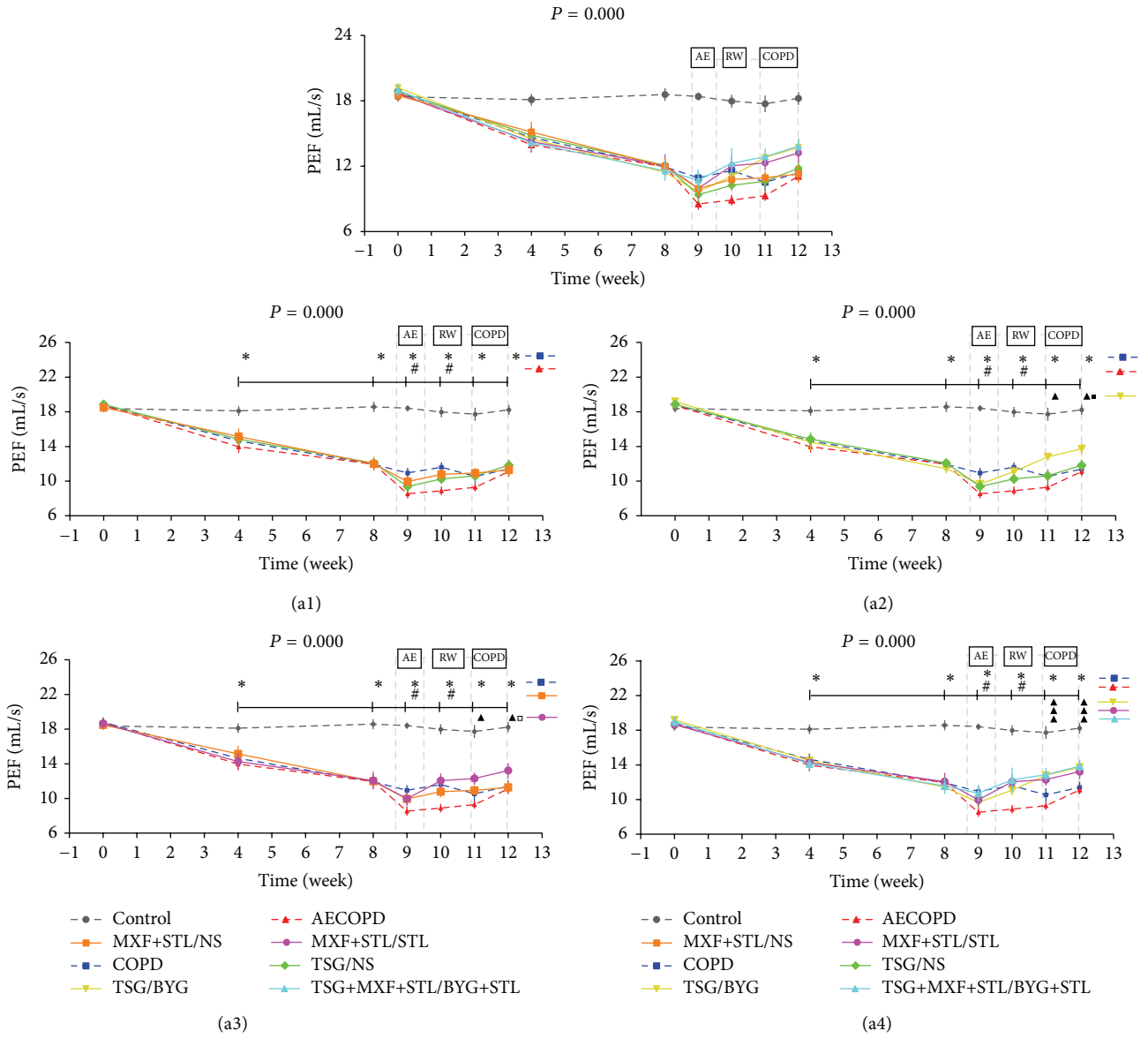

(a)

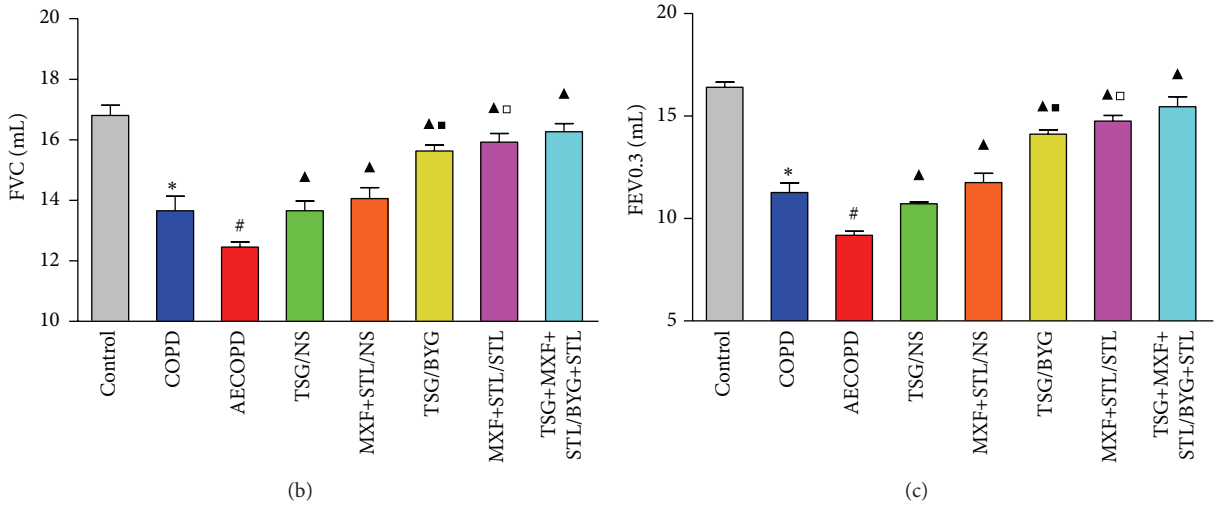

(b) (c)

Figure 4: Continued.

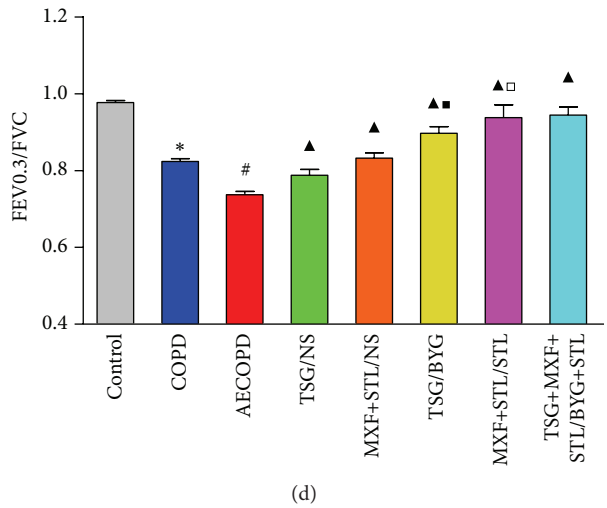

(d)

Figure 4: Changes in peak expiratory flow (PEF) (a) and forced vital capacity (FVC) (b), forced expiratory volume at 0.3 s (FEV0.3) (c), and FEV0.3/FVC (d) in rats treated with sequential/nonsequential treatments. Panels (a1)–(a4) from panel (a) indicate the comparisons of the sequential and nonsequential treatments with traditional Chinese medicine, Western medicine, or integrated medicines, respectively. AE: acute exacerbation; BYG: Bufei Yishen Granule; COPD: chronic obstructive pulmonary disease; MXF: moxifloxacin; NS: normal saline; RW: risk window; TSG: Tongsai Granule; STL: salbutamol. $N = 6$. Repetitive measurement deviation analysis of PEF: $P = 0.000$. $^{*}P < 0.05$, versus Control group; $^{\#}P < 0.05$, versus COPD group; $^{\blacktriangle}P < 0.05$, versus AECOPD group; $^{\blacksquare}P < 0.05$, versus TSG/NS group; $^{\square}P < 0.05$, versus MXF+STL/NS group. Bacterial challenge was performed on the 6th day of week 9.

the next 2 days, changed more smoothly in the subsequent days, and returned to the levels of COPD group or decreased further on Days 8–12. In addition, the numbers of WBCs, neutrophils, and monocytes were decreased in MXF+STL/NS group compared with TSG/NS group on Day 2, and the numbers of WBCs in MXF+STL/STL and TSG+MXF+STL/BYG+STL groups were even lower than those in TSG/BYG group ($P < 0.05$). Meanwhile, the numbers of neutrophils and monocytes were significantly reduced in TSG+MXF+STL/BYG+STL group compared with TSG/BYG group ($P < 0.05$). Additionally, the numbers of WBCs in TSG/BYG and MXF+STL/STL groups were reduced compared with TSG/NS and MXF+STL/NS group from Day 12 to Day 20, respectively ($P < 0.05$). The number of neutrophils in TSG/BYG group was reduced compared with TSG/NS group from Day 18 to 22 and was reduced in MXF+STL/STL group compared with MXF+STL/NS group on Day 12 ($P < 0.05$).

As shown in Figure 5(d), the number of lymphocytes in each group did not differ throughout the course of AE-RW-COPD.

3.6. Cell Types in Bronchoalveolar Lavage Fluid. The numbers of neutrophils, macrophages, and lymphocytes were significantly increased in COPD group compared with Control group, and the numbers of neutrophils and lymphocytes were increased in AECOPD group compared with COPD group ($P < 0.05$) (Figure 6). Moreover, the numbers of neutrophils, macrophages, and lymphocytes were significantly decreased in the treated groups compared with AECOPD group ($P < 0.05$). The macrophage population was reduced even more in TSG/BYG and MXF+STL/STL groups compared with TSG/NS and MXF+STL/NS groups, respectively, whereas the macrophage counts in TSG+MXF+STL/BYG+STL and TSG/BYG groups were lower than in MXF+STL/STL group ($P < 0.05$).

3.7. C-Reactive Protein and Serum Amyloid A Levels in Serum. As shown in Figure 7, CRP and SAA levels in COPD groups were higher than in Control group from Day 0 to Day 22 ($P < 0.05$). After challenge with the KP solution, they were highly elevated in AECOPD group on Day 2, sharply decreased on Days 4 and 6, presented a steady recovery trend in the subsequent days, and reverted to the baseline levels of COPD group on Day 16 ($P < 0.05$). CRP and SAA levels in the treated groups were lower than those in AECOPD group on Day 2, rapidly decreased over the next 4 days, changed steadily in the subsequent days, and were restored to the levels in COPD group or further decreased on Day 10–Day 14. On Day 2, the CRP and SAA levels in MXF+STL/NS group were reduced compared with TSG/NS group, and they were even lower in MXF+STL/STL and TSG+MXF+STL/BYG+STL groups compared with TSG/BYG group ($P < 0.05$). During the RW and COPD periods, the CRP and SAA levels in MXF+STL/NS group were significantly reduced compared with TSG/NS group on Day 10 and Day 6 ($P < 0.05$), and they were significantly reduced in the 2 sequential treatment groups, TSG/BYG and MXF+STL/STL, compared with TSG/NS group and MXF+STL/NS groups from Day 12–Day 22, respectively. In particular, the CRP levels in TSG+MXF+STL/BYG+STL group were much lower than those in TSG/BYG and/or MXF+STL/STL groups on Days 6–12, whereas the SAA levels on Day 6, Day 14, and Day 16 were significantly decreased ($P < 0.05$).

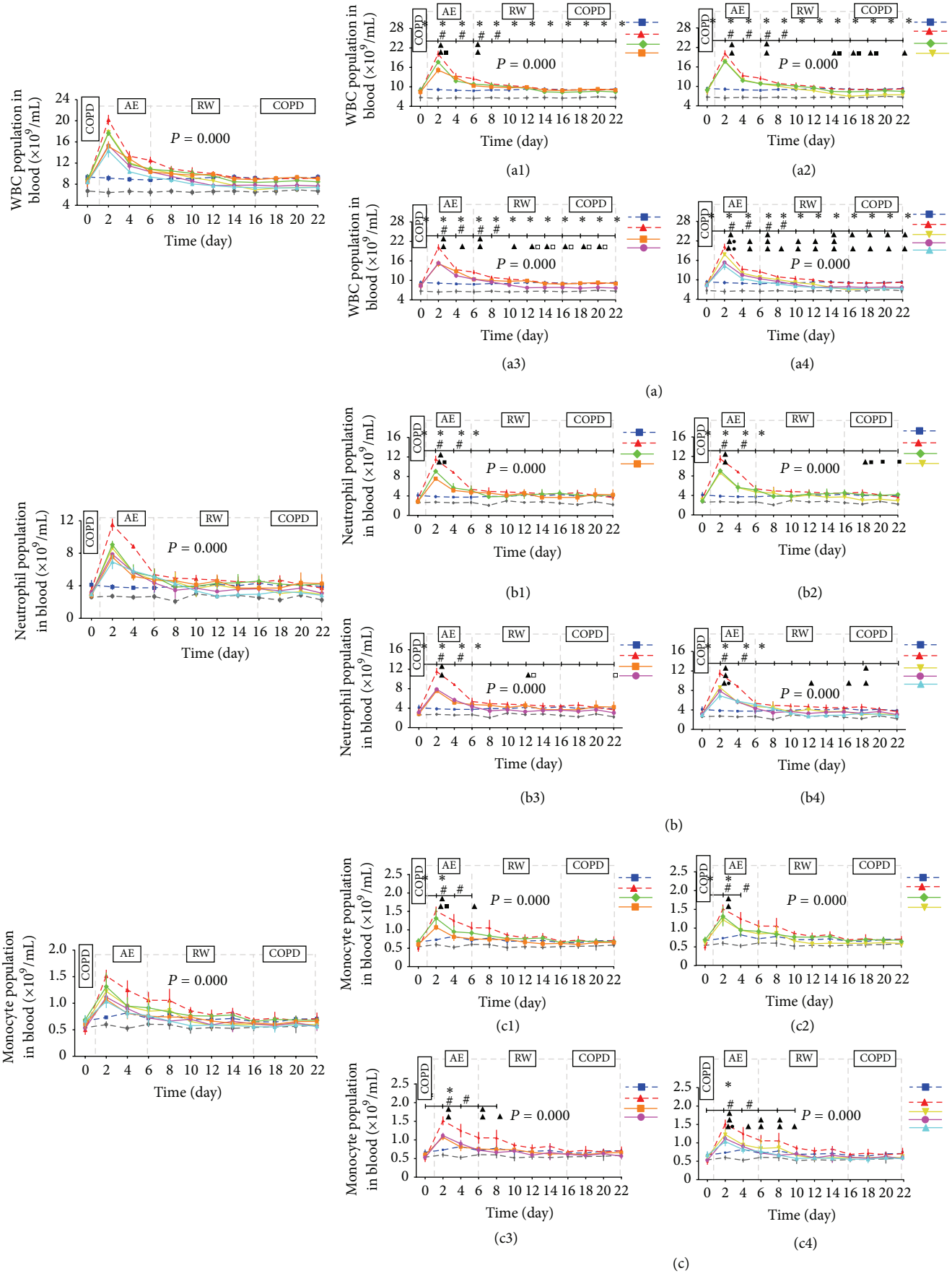

Figure 5: Continued.

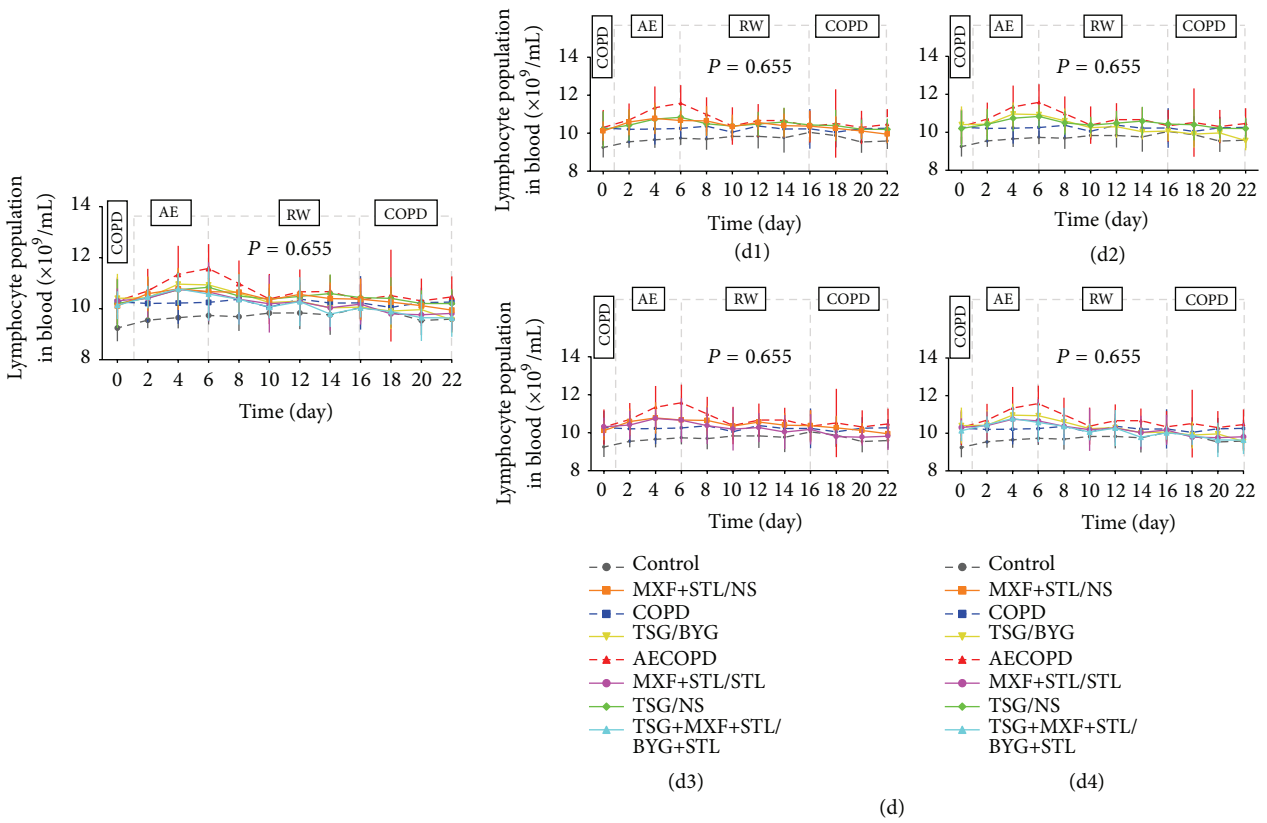

Figure 5: Temporal changes in the numbers of white blood cells (WBCs) (a), neutrophils (b), monocytes (c), and lymphocytes (d) in rats administered sequential/nonsequential treatments. Panels (a1)–(a4), (b1)–(b4), (c1)–(c4), and (d1)–(d4) from panels (a), (b), (c), and (d) indicate the comparisons of sequential and nonsequential treatments with traditional Chinese medicine, Western medicine, or integrated medicines, respectively. AE: acute exacerbation; BYG: Bufei Yishen Granule; COPD: chronic obstructive pulmonary disease; MXF: moxifloxacin; NS: normal saline; RW: risk window; TSG: Tongsai Granule; STL: salbutamol. $N = 6$. Repetitive measurement deviation analysis of the numbers of WBCs, neutrophils, and monocytes: $P = 0.000$; lymphocytes: $P = 0.655$. $^{*}P < 0.05$, versus Control group; $^{\#}P < 0.05$, versus COPD group; $^{\blacktriangle}P < 0.05$, versus AECOPD group; $^{\blacksquare}P < 0.05$, versus TSG/NS group; $^{\square}P < 0.05$, versus MXF+STL/NS group; $^{\bullet}P < 0.05$, versus TSG/BYG group. Bacterial challenge was performed on Day 1.

3.8. Inflammatory Factors in Serum and Bronchoalveolar Lavage Fluid. MPO, PMN elastase, IL-1β, TNF-α, and IL-6 and IL-10 levels in serum and BALF of COPD group were significantly increased compared with Control group ($P < 0.05$) (Figure 8). Similarly, MPO, PMN elastase, and IL-6 and IL-10 levels in serum and BALF and the IL-1β and TNF-α levels in BALF of AECOPD group were much higher than those in COPD group ($P < 0.05$). Serum and BALF levels of all inflammatory factors in the treated groups were reduced compared with those of AECOPD group ($P < 0.05$).

For the treated groups, serum IL-1β, TNF-α, IL-6, MPO, and PMN elastase levels and BALF MPO and PMN elastase levels were decreased in TSG/BYG and MXF+STL/STL groups compared with those in TSG/NS and MXF+STL/NS groups ($P < 0.05$). Serum levels of the above-mentioned indicators and BALF PMN elastase, IL-1β, and IL-6 were significantly reduced in TSG+MXF+STL/BYG+STL group compared with TSG/BYG and MXF+STL/STL groups ($P < 0.05$). BALF TNF-α in MXF+STL/STL group was significantly higher than those in TSG/BYG and TSG+MXF+STL/BYG+STL groups ($P < 0.05$). Serum IL-10 in TSG/BYG and MXF+STL/STL groups were significantly increased compared with TSG/NS and MXF+STL/NS groups, respectively ($P < 0.05$), and BALF IL-10 in TSG/BYG group was significantly increased compared with TSG/NS and MXF+STL/STL groups ($P < 0.05$).

3.9. Pulmonary Morphology and Morphometry. No obvious pathological impairments were observed in Control group (Figure 9(a)). Marked chronic bronchiolar and pulmonary inflammation and obstruction, airway wall thickening and hyperplasia, and alveolar destruction were observed in COPD rats (Figure 9(b)), particularly in those suffering from acute exacerbation (Figure 9(c)). However, the impairments were reduced to different degrees in the treated groups (Figures 9(d), 9(e), 9(f), 9(g), and 9(h)), of which TSG/BYG, MXF+STL/STL, and TSG+MXF+STL/BYG+STL groups had fewer impairments (Figures 9(f), 9(g), and 9(h)). As shown in Figures 9(i) and 9(j), MLI in COPD group was significantly increased compared with Control group, whereas MAN was significantly decreased ($P < 0.05$). MLI in AECOPD group was even higher than in COPD group,

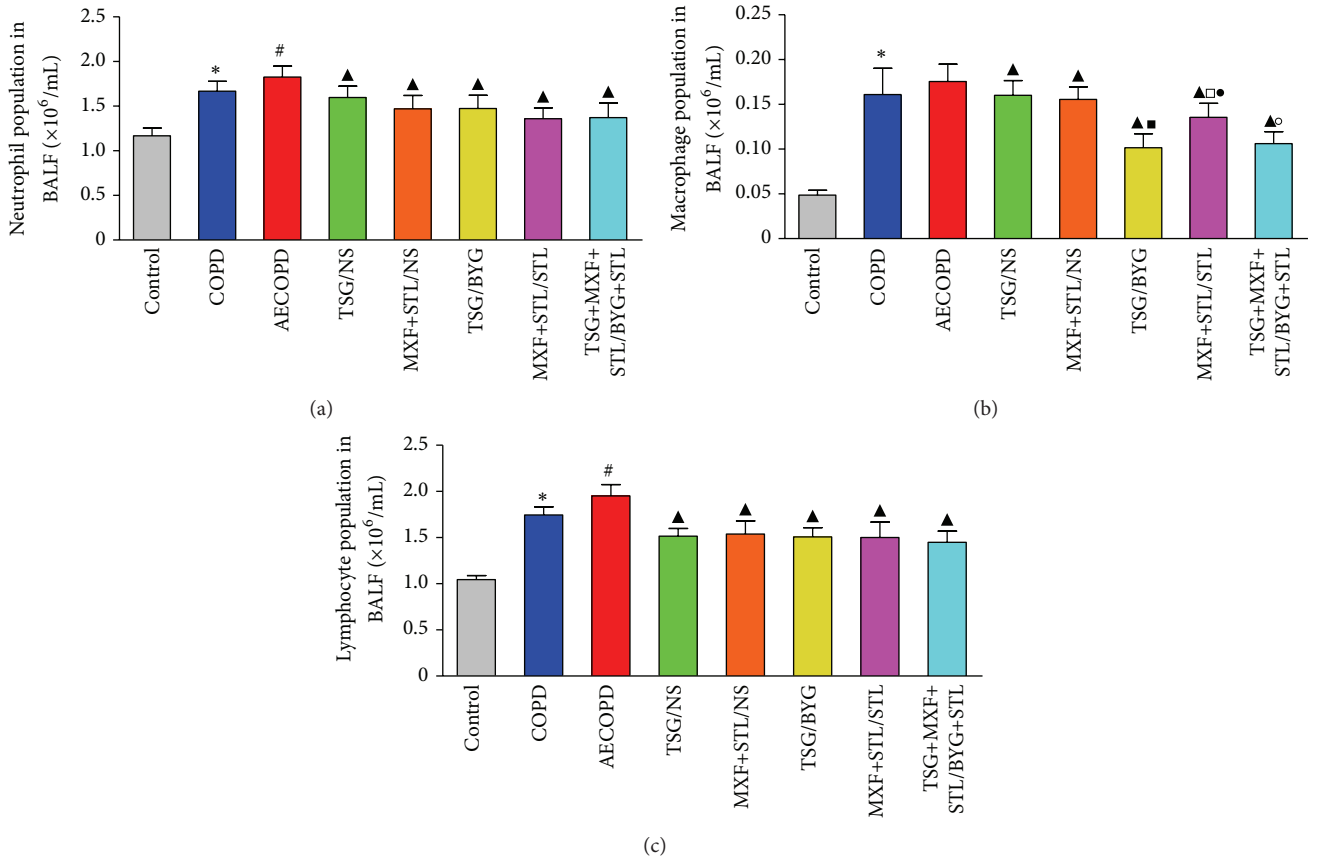

FIGURE 6: Changes in the numbers of neutrophils (a), macrophages (b), and lymphocytes (c) in the bronchoalveolar lavage fluid from rats administered sequential/nonsequential treatments. AE: acute exacerbation; BYG: Bufei Yishen Granule; COPD: chronic obstructive pulmonary disease; MXF: moxifloxacin; NS: normal saline; RW: risk window; TSG: Tongsai Granule; STL: salbutamol. $N = 6$. $^{*}P < 0.05$, versus Control group; $^{\#}P < 0.05$, versus COPD group; $^{\blacktriangle}P < 0.05$, versus AECOPD group; $^{\blacksquare}P < 0.05$, versus TSG/NS group; $^{\square}P < 0.05$, versus MXF+STL/NS group; $^{\bullet}P < 0.05$, versus TSG/BYG group; $^{\circ}P < 0.05$, versus MXF+STL/STL group.

and MAN was lower than in COPD group ($P < 0.05$). Furthermore, all of the treated groups had reduced variations compared with AECOPD group ($P < 0.05$). MLI in TSG/BYG and MXF+STL/STL groups was significantly reduced compared with TSG/NS and MXF+STL/NS groups, respectively, and MLI in TSG+MXF+STL/BYG+STL group was further decreased compared with TSG/BYG and MXF+STL/STL groups ($P < 0.05$). MAN in TSG/BYG and MXF+STL/STL groups was elevated compared with TSG/NS and MXF+STL/NS groups and was even higher in TSG+MXF+STL/BYG+STL group than in TSG/BYG and MXF+STL/STL groups ($P < 0.05$).

4. Discussion

This is the first study to discuss the therapeutic effects of sequential treatments with Tongsai and Bufei Yishen Granules during the AE-RW period in a rat model of AECOPD. The major findings of this study indicate that sequential treatments in the AE and RW phases improved pulmonary function, reduced systemic inflammation, and shortened the recovery time, especially the sequential treatment with the combination of Chinese and Western medicines.

In TCM, COPD belongs to the category of FEIZHANG disease, which is characterized as deficient root and excessive superficial throughout the course of disease. The lungs and kidneys govern innate and postnatal qi of the body, and the deficiency of the lung and kidney qi will result in breathlessness, cough, and sputum production and is considered as one of the most common syndromes, the lung-kidney qi deficiency syndrome, in the stable phase of COPD. During the acute exacerbation of COPD, pathogenesis is mainly considered an invasion of external pathogenic factors, including wind-cold and wind-heat, which can develop into phlegm-dampness and phlegm-heat syndromes; phlegm-heat is the most important syndrome in the AE stage. The main features of phlegm-heat syndrome are fever, cough, and yellow/white sticky phlegm production [19]. Thus, we treated the COPD rats with a 5-day wind-heat exposure before bacterial challenge to mimic the syndrome of phlegm-heat. During the risk window, syndrome of intermingled deficiency and excess is the main pattern of pathogenesis, which is characterized by reduced phlegm-stasis complicated by the deficiency of lung-kidney qi [17]. Therefore, we treated the AE rats with Tongsai and Bufei Yishen Granules to clear the heat and expel the phlegm in the AE phase and

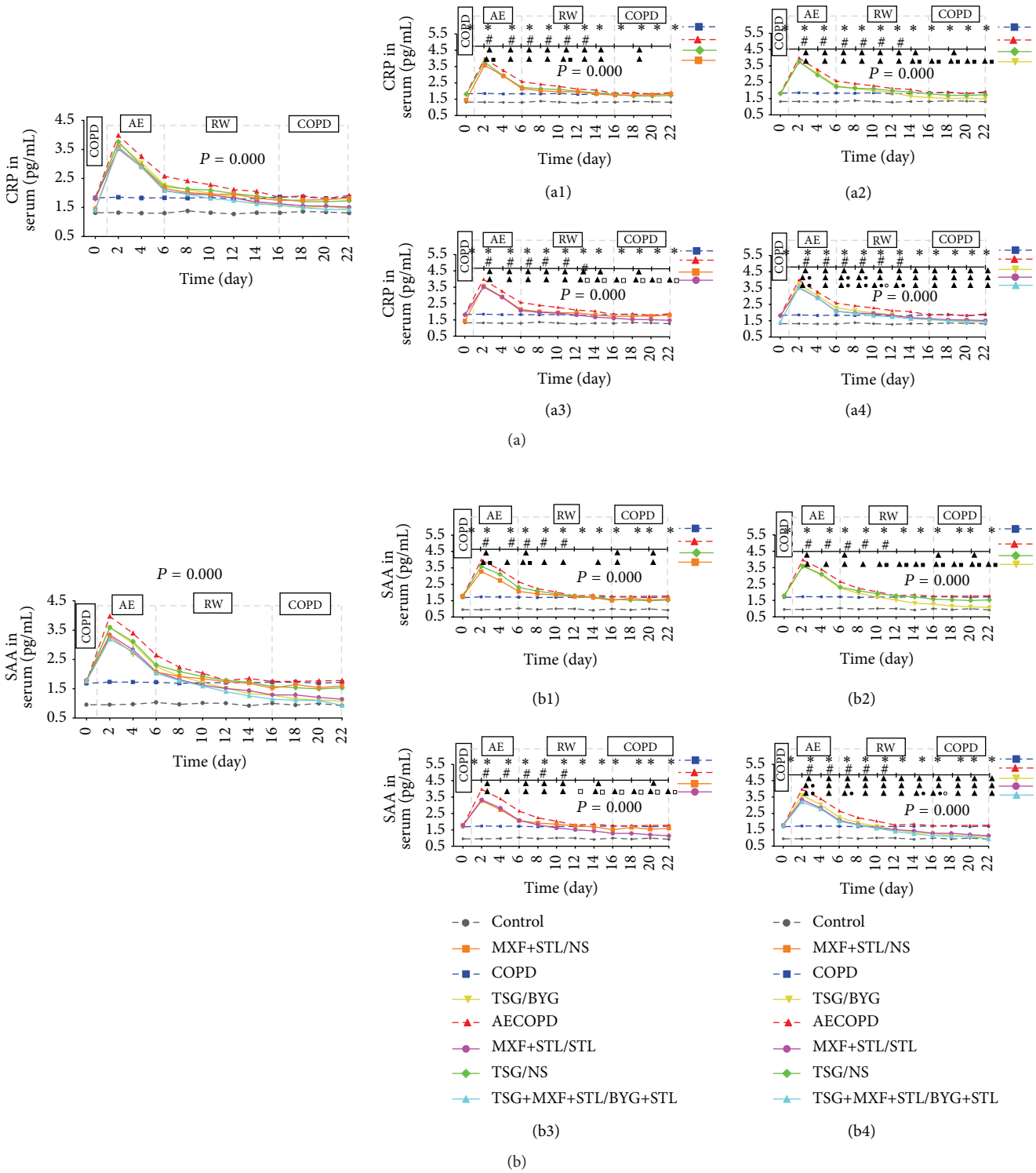

Figure 7: Temporal changes in C-reactive protein (CRP) (a) and serum amyloid A (SAA) levels (b) in rats administered sequential/nonsequential treatments. Panels (a1)–(a4) and (b1)–(b4) from panels (a) and (b) indicate the comparisons of the sequential and nonsequential treatment with traditional Chinese medicine, Western medicine, or integrated medicines, respectively. AE: acute exacerbation; BYG: Bufei Yishen Granule; COPD: chronic obstructive pulmonary disease; MXF: moxifloxacin; NS: normal saline; RW: risk window; TSG: Tongsai Granule; STL: salbutamol. $N = 6$. Repetitive measurement deviation analysis of CRP and SAA levels: $P = 0.000$. $^{*}P < 0.05$, versus Control group; $^{\#}P < 0.05$, versus COPD group; $^{\blacktriangle}P < 0.05$, versus AECOPD group; $^{\blacksquare}P < 0.05$, versus TSG/NS group; $^{\square}P < 0.05$, versus MXF+STL/NS group; $^{\bullet}P < 0.05$, versus TSG/BYG group; $^{\circ}P < 0.05$, versus MXF+STL/STL group. Bacterial challenge was performed on Day 1.

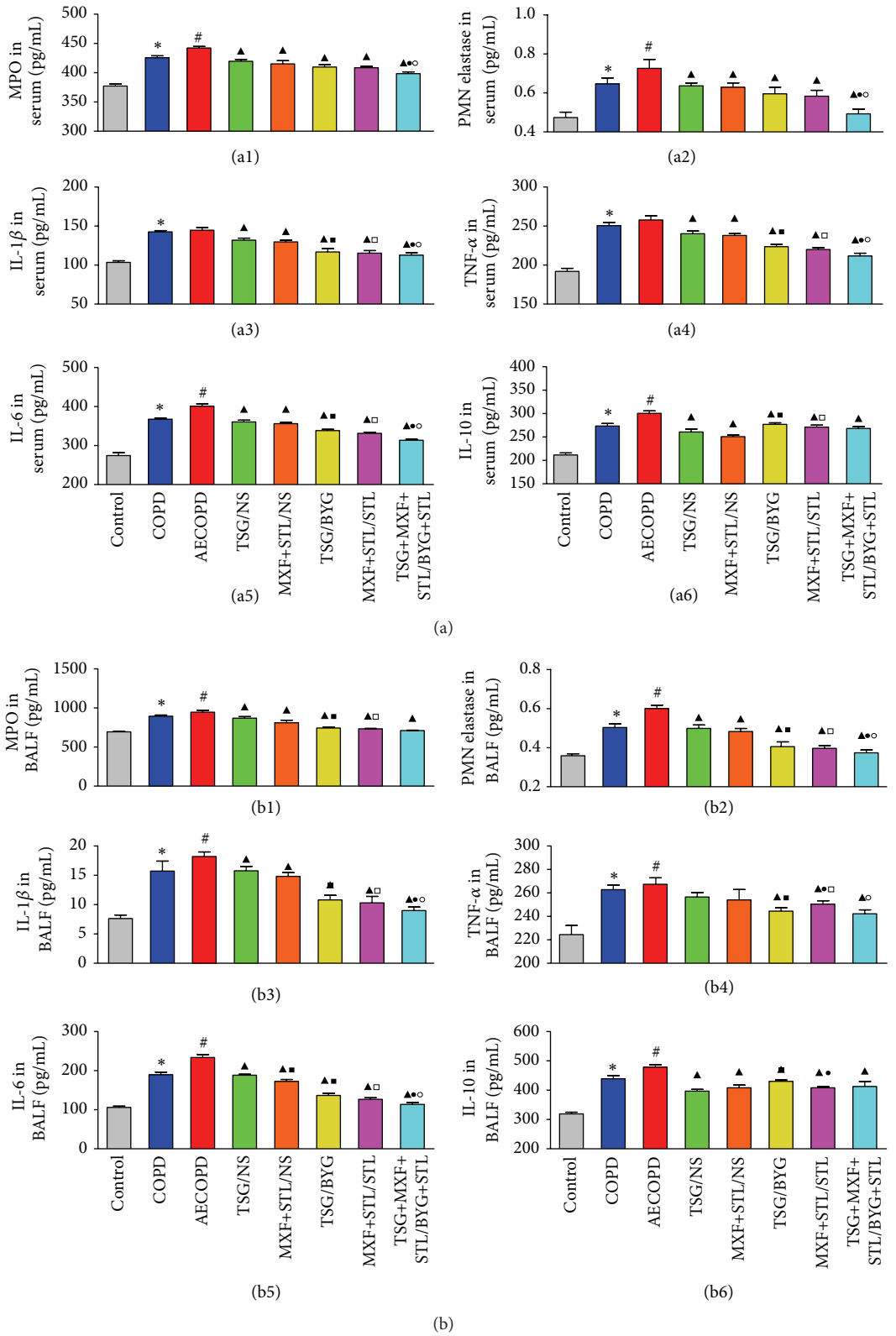

Figure 8: Changes in MPO (a1, b1), PMN elastase (a2, b2), IL-1β (a3, b3), TNF-α (a4, b4), IL-6 (a5, b5), and IL-10 (a6, b6) levels in the serum (a) and BALF (b) from sequentially/nonsequentially treated COPD rats. AE: acute exacerbation; BYG: Bufei Yishen Granule; COPD: chronic obstructive pulmonary disease; IL: interleukin; MPO: myeloperoxidase; MXF: moxifloxacin; NS: normal saline; PMN: polymorphonuclear; RW: risk window; TNF: tumor necrosis factor; TSG: Tongsai Granule; STL: salbutamol. $N = 6$. $^{*}P < 0.05$, versus Control group; $^{\#}P < 0.05$, versus COPD group; $^{\blacktriangle}P < 0.05$, versus AECOPD group; $^{\blacksquare}P < 0.05$, versus TSG/NS group; $^{\square}P < 0.05$, versus MXF+STL/NS group; $^{\bullet}P < 0.05$, versus TSG/BYG group; $^{\circ}P < 0.05$, versus MXF+STL/STL group.

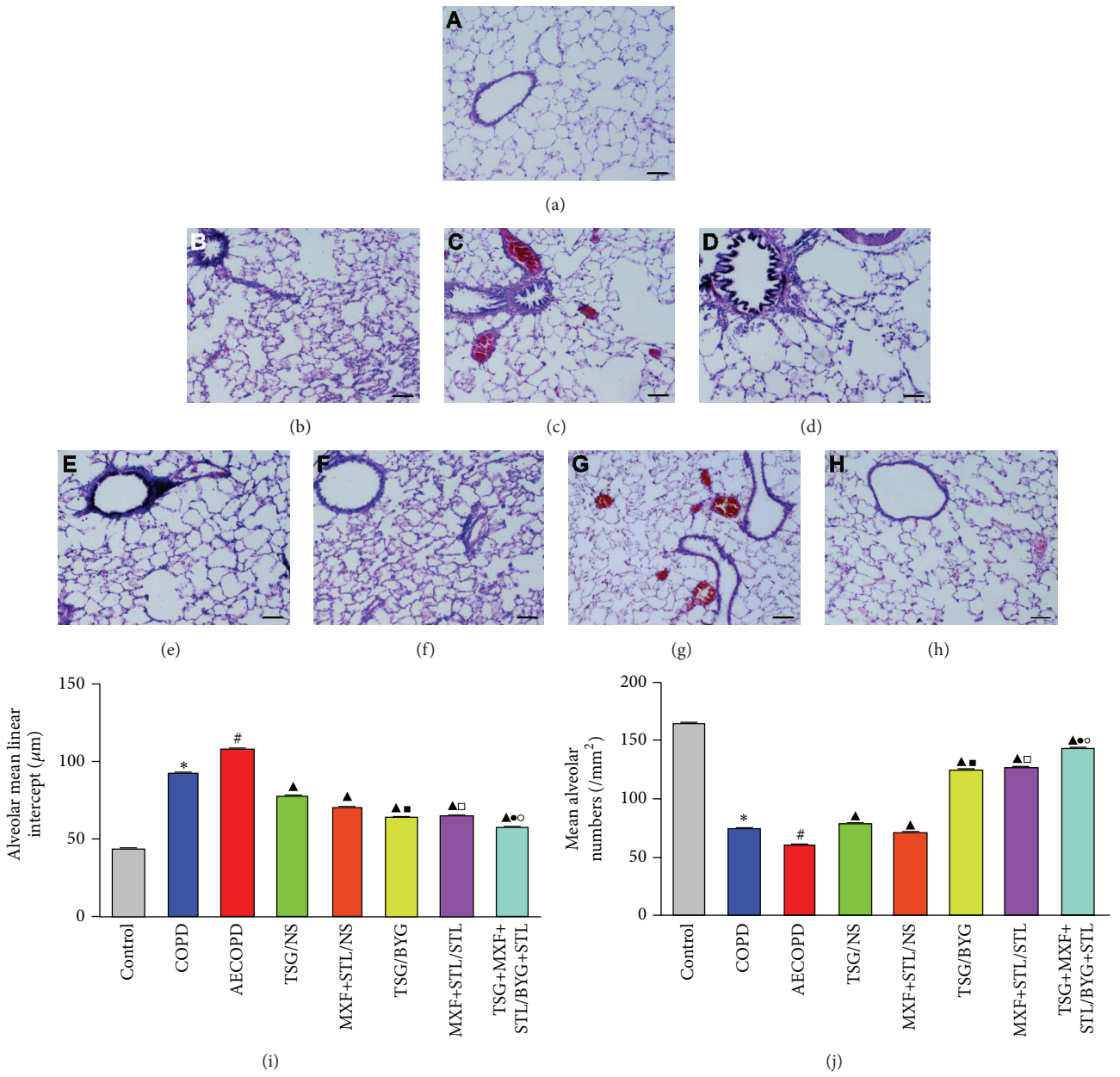

Figure 9: Representative images of the pathology in lung tissues from rats administered sequential/nonsequential treatments. (a) Control group; (b) chronic obstructive pulmonary disease (COPD) group, (c) acute exacerbation of COPD (AECOPD) group; (d) TSG/NS group; (e) MXF+STL/NS group; (f) TSG/BYG group; (g) MXF+STL/STL group; (h) TSG+MXF+STL/BYG+STL group. H&E stained, magnification: ×100. (i) Mean linear intercept (MLI); (j) mean alveolar numbers (MAN). AE: acute exacerbation; BYG: Bufei Yishen Granule; COPD: chronic obstructive pulmonary disease; MXF: moxifloxacin; NS: normal saline; RW: risk window; TSG: Tongsai Granule; STL: salbutamol. $N = 6$. $^{*}P < 0.05$, versus Control group; $^{\#}P < 0.05$, versus COPD group; $^{\blacktriangle}P < 0.05$, versus AECOPD group; $^{\blacksquare}P < 0.05$, versus TSG/NS group; $^{\square}P < 0.05$, versus MXF+STL/NS group; $^{\bullet}P < 0.05$, versus TSG/BYG group; $^{\circ}P < 0.05$, versus MXF+STL/STL group.

reinforce the lung-kidney qi in the RW phase. According to our previous study, the AE phase lasts for approximately 5 days after *Klebsiella pneumoniae* challenge, followed by an approximately 10-day RW phase [14, 15]. To ensure that all rats were sacrificed in the stable phase of COPD, we stopped the administration at 7 days after RW, on Day 22.

Acute exacerbations of COPD are often followed by subsequent clinical pulmonary deterioration, which is associated with fever and a decrease in lung function, particularly in patients with frequent exacerbations [32]. Additionally, previous studies have demonstrated that COPD exacerbations are mainly associated with aggravated airway inflammation, such as increased numbers of inflammatory cells, including WBCs and neutrophils, and increased levels of acute inflammatory biomarkers, including IL-1β, IL-6, TNF-α, IL-10, CRP, and SAA [8, 11, 33–36]. Neutrophils are the predominant effector

cells activated during an acute inflammatory response, and the levels of relevant MPO and PMN elastase are also elevated [8, 11, 37, 38]. Currently, CRP and SAA levels are the most common indicators used to assess systemic inflammation and curative effects [33, 39] because they show similar variation tendencies [40]. Clinical reports indicate that 24 hours after AE, pulmonary function decreases whereas the number of WBCs and neutrophils and CRP and SAA levels increase. Pulmonary function was significantly improved 72 h after patients received medication but did not fully recover until 40 days following infection [9, 10]. Pulmonary function tests, including FVC, FEV0.3, FEV0.3/FVC, and PEF, were also decreased in similar manners in COPD rat model, whereas the levels of the above-mentioned inflammatory factors were increased [41–44].

Our data indicate that body temperature and inflammatory status, including the numbers of WBCs, neutrophils, and monocytes and CRP and SAA levels, were markedly elevated in the AE rats 24 h postbacterial challenge and decreased over the next 4–6 days, whereas the PEF decreased. All of the above-mentioned targets were improved in the treated groups at different levels, and the recovery times were shortened to 2–4 days, especially with the sequential treatment with integrated Chinese and Western medicines. Tongsai Granule and/or moxifloxacin combined with salbutamol improved lung function and decreased systemic inflammation in the AE phase.

In the RW phase, all of the above-mentioned biomarkers were markedly decreased in the treated groups compared with AECOPD rat; recovery time was also decreased. PEF and inflammatory biomarkers were lower in the sequential treatment groups, such as TSG/BYG and MXF+STL/STL treatments, than in nonsequentially treated groups at different time points from Day 12 to Day 22. The recovery times were reduced from 10 days to 4–6 days in the sequentially treated groups compared with 6–8 days in the nonsequentially treated groups. The concentrations of IL-6, IL-8, IL-10, TNF-α, and CRP in plasma could be used for calculating the degree and process of systemic inflammation [45]. After sacrifice and 7 days after treatment, serum and BALF inflammatory factors levels, such as IL-1β, IL-6, TNF-α, IL-10, MPO, and PMN elastase, were decreased in the sequentially treated groups compared with the nonsequentially treated groups, especially in TSG+MXF+STL/BYG+STL group. These results indicate that the treatments could reduce the systemic inflammation, and the curative effects of the sequential treatments are better than the nonsequential treatments, especially the combination of TCM and Western medicines. Moreover, as an anti-inflammatory cytokine, the value of IL-10 in sequential treatment was higher than nonsequential groups, and it was even higher in BALF in TCM sequential treatment group than Western medicine group, which may imply that TSG/BYG had greater anti-inflammatory capability.

Histopathologically, chronic bronchitis, airway obstruction, alveolar structure destruction, and emphysema are the main pulmonary impairments in COPD patients. In this study, marked inflammatory cell infiltration, bronchiolar stenosis, and alveolar expansion and destruction were observed in the COPD and AECOPD rats and were improved in the treated groups at different levels. MLI and MAN, size of the alveolar cavity, and density of alveoli [31] also indicated that the level of emphysema was greater in COPD rats than in controls, particularly in AECOPD rats. All the 5 treatments alleviated emphysema, but the sequential integrated Chinese and Western medicine treatments showed a better response.

5. Conclusions

Sequential treatments with Tongsai and Bufei Yishen Granules in the AE-RW period can alleviate inflammation and shorten the recovery time in AECOPD rats, and sequential, integrated TCM and Western medicine treatments have more beneficial effects than TCM or Western medicine alone. This study may provide a basis for further research and the clinical applications of sequential treatments.

Abbreviations

AE: Acute exacerbation
BALF: Bronchoalveolar lavage fluid
BYG: Bufei Yishen Granule
CFU: Colony forming units
COPD: Chronic obstructive pulmonary disease
CRP: C-reactive protein
FEV0.3: Forced expiratory volume in 0.3 s
FVC: Forced vital capacity
KP: *Klebsiella pneumonia*
IL: Interleukin
MPO: Myeloperoxidase
MXF: Moxifloxacin
PEF: Peak expiratory flow
PMN: Polymorphonuclear
RW: Risk window
SAA: Serum amyloid A
STL: Salbutamol
TCM: Traditional Chinese medicine
TNF: Tumor necrosis factor
TSG: Tongsai Granule.

Ethical Approval

The study protocol was approved by the Ethics Committee of the First Affiliated Hospital, Henan University of Chinese Medicine, Zhengzhou, Henan, China.

Competing Interests

The authors declare that they have no competing interests.

Authors' Contributions

Xiaofan Lu participated in the design of the study, the animal experiments, and the statistical analysis of the data and drafted the paper. Ya Li participated in the statistical analysis of the data and drafted the paper. Jiansheng Li conceived and participated in the design of the study. Haifeng Wang participated in the design of the study. Yang Wang participated in the animal experiments and the lung function measurements. Zhaohuan Wu participated in the animal

experiments and performed the ELISA tests. Hangjie Li participated in the animal experiments and helped collect the blood samples. All authors read and approved the final paper. Xiaofan Lu and Ya Li Equal contributors.

Acknowledgments

This study was funded by the National Natural Science Foundation of China (81302921) and the China National Scientific Research Foundation of Traditional Chinese Medicine Clinical Research Base Construction (no. JDZX2012028). The authors thank Ms. Weihong Liu, Si Shen, and Xiaoxiao Wang for their technological assistance in the animal experiments and pathological analysis.

References

[1] M. Decramer, W. Janssens, and M. Miravitlles, "Chronic obstructive pulmonary disease," *The Lancet*, vol. 379, no. 9823, pp. 1341–1351, 2012.

[2] S. Sethi and T. F. Murphy, "Infection in the pathogenesis and course of chronic obstructive pulmonary disease," *The New England Journal of Medicine*, vol. 359, no. 22, pp. 2355–2365, 2008.

[3] J. J. Soler-Cataluña, M. Á. Martínez-García, P. Román Sánchez, E. Salcedo, M. Navarro, and R. Ochando, "Severe acute exacerbations and mortality in patients with chronic obstructive pulmonary disease," *Thorax*, vol. 60, no. 11, pp. 925–931, 2005.

[4] C. Chang, Z. Guo, N. Shen et al., "Dynamics of inflammation resolution and symptom recovery during AECOPD treatment," *Scientific Reports*, vol. 4, article 5516, 2014.

[5] J.-J. Fu, V. M. McDonald, K. J. Baines, and P. G. Gibson, "Airway IL-1β and systemic inflammation as predictors of future exacerbation risk in asthma and COPD," *Chest*, vol. 148, no. 3, pp. 618–629, 2015.

[6] R. Tkacova, Z. Kluchova, P. Joppa, D. Petrasova, and A. Molcanyiova, "Systemic inflammation and systemic oxidative stress in patients with acute exacerbations of COPD," *Respiratory Medicine*, vol. 101, no. 8, pp. 1670–1676, 2007.

[7] T. Yange, L. Ya, L. Jiansheng et al., "Effects of therapies for regulating and reinforcing lung and kidney on osteoporosis in rats with chronic obstructive pulmonary disease," *Journal of Traditional Chinese Medicine*, vol. 35, no. 2, pp. 175–183, 2015.

[8] T. M. Eagan, J. K. Damås, T. Ueland et al., "Neutrophil gelatinase-associated lipocalin: a biomarker in COPD," *Chest*, vol. 138, no. 4, pp. 888–895, 2010.

[9] A. Koutsokera, T. S. Kiropoulos, D. J. Nikoulis et al., "Clinical, functional and biochemical changes during recovery from COPD exacerbations," *Respiratory Medicine*, vol. 103, no. 6, pp. 919–926, 2009.

[10] A. Mohan, D. Prasad, A. Sharma et al., "Delayed resolution of inflammatory response compared with clinical recovery in patients with acute exacerbations of chronic obstructive pulmonary disease," *Respirology*, vol. 17, no. 7, pp. 1080–1085, 2012.

[11] A. Papi, C. M. Bellettato, F. Braccioni et al., "Infections and airway inflammation in chronic obstructive pulmonary disease severe exacerbations," *American Journal of Respiratory and Critical Care Medicine*, vol. 173, no. 10, pp. 1114–1121, 2006.

[12] M. A. Sze, P. A. Dimitriu, M. Suzuki et al., "Host response to the lung microbiome in chronic obstructive pulmonary disease," *American Journal of Respiratory and Critical Care Medicine*, vol. 192, no. 4, pp. 438–445, 2015.

[13] W. Haifeng, L. Jiansheng, L. Suyun et al., "Effect of sequential treatment with syndrome differentiation on acute exacerbation of chronic obstructive pulmonary disease and 'AECOPD Risk-Window': study protocol for a randomized placebo-controlled trial," *Trials*, vol. 13, article 40, 2012.

[14] J.-S. Li and H.-F. Wang, "Sequential syndrome differentiation by eliminating pathogen and strengthening vital Qi on the basis of acute exacerbation of chronic obstructive pulmonary disease risk window," *Zhongguo Zhong Xi Yi Jie He Za Zhi*, vol. 31, no. 9, pp. 1276–1280, 2011.

[15] X. Mei, J.-S. Li, H.-Y. Zhou, C.-X. Qiao, S.-Y. Li, and Y.-X. Zhang, "A comparative study of inflammatory factor expression of phlegm-heat syndrome and phlegm-dampness syndrome model with acute exacerbation of chronic obstructive pulmonary disease," *Zhonghua Wei Zhong Bing Ji Jiu Yi Xue*, vol. 25, no. 6, pp. 343–346, 2013.

[16] Global Initiative for Chronic Obstructive Lung Disease, "Global strategy for diagnosis, management, and prevention of COPD," 2016, http://www.goldcopd.org.

[17] Z. Hailong, L. Jiansheng, W. Haifeng et al., "Clinical investigation on distribution of syndrome in AECOPD-RW," *World Science and Technology-Modernization of Traditional (Chinese) Medicine*, vol. 7, pp. 1587–1592, 2014.

[18] Committee of Lung Disease Branch Department of China Association of Chinese Medicine, "Syndrome diagnostic criteria of Traditional Chinese Medicine of chronic obstructive pulmonary disease (2011 version)," *Zhong Yi Za Zhi*, vol. 53, pp. 177–178, 2012.

[19] Committee of Lung Disease Branch Department of China Association of Chinese Medicine, "Diagnosis and treatment guideline of traditional Chinese medicine for chronic obstructive pulmonary disease (2011 version)," *Zhong Yi Za Zhi*, vol. 53, pp. 80–84, 2012.

[20] S. Y. Li, X. K. Cheng, J. S. Li, L. J. Ma, and C. H. Li, "Effect of Tongse grain of TCM on cytokine in patients with chronic obstructive pulmonary disease," *Liaoning University of Traditional Chinese Medicine*, vol. 30, pp. 624–625, 2003.

[21] S. Y. Li, J. S. Li, L. J. Ma, C. H. li, and X. K. Cheng, "Effects of tongsai granules on extracellular matrixes and adhesion molecule in the patient of senile chronic obstructive pulmonary diseases at the acute exacerbation stage," *Journal of Traditional Chinese Medicine*, vol. 44, no. 12, pp. 906–908, 2003.

[22] J. S. Li, S. Y. Li, Y. H. Wang, Y. W. Zhao, and L. F. Kong, "Changes of matrix metalloproteinase of lung tissue in the acute exacerbations of COPD rat models and the effect of Tongse granule," *Chinese Journal of Gerontology*, vol. 25, pp. 174–175, 2005.

[23] S. Li, J. Li, L. Kong et al., "Effect of Tongsai granule on the extracellular matrix of lung tissue in the acute exacerbation of rats with chronic obstructive pulmonary disease," *Journal of Traditional Chinese Medicine*, vol. 50, pp. 453–456, 2009.

[24] S.-Y. Li, J.-S. Li, M.-H. Wang et al., "Effects of comprehensive therapy based on traditional Chinese medicine patterns in stable chronic obstructive pulmonary disease: a four-center, open-label, randomized, controlled study," *BMC Complementary and Alternative Medicine*, vol. 12, article197, 2012.

[25] Y. Tian, Y. Li, J. Li et al., "Bufei Yishen granule combined with acupoint sticking improves pulmonary function and morphormetry in chronic obstructive pulmonary disease rats,"

BMC Complementary and Alternative Medicine, vol. 15, no. 1, article 266, 2015.

[26] L. Yang, J. Li, Y. Li et al., "Identification of metabolites and metabolic pathways related to treatment with Bufei Yishen formula in a rat COPD model using HPLC Q-TOF/MS," *Evidence-Based Complementary and Alternative Medicine*, vol. 2015, Article ID 956750, 9 pages, 2015.

[27] J. S. Li, Y. Li, S. Y. Li et al., "Long-term effects of Tiaobu Feishen therapies on systemic and local inflammation responses in rats with stable chronic obstructive pulmonary disease," *Zhong Xi Yi Jie He Xue Bao*, vol. 10, no. 9, pp. 1039–1048, 2012.

[28] Y. Li, S.-Y. Li, J.-S. Li et al., "A rat model for stable chronic obstructive pulmonary disease induced by cigarette smoke inhalation and repetitive bacterial infection," *Biological and Pharmaceutical Bulletin*, vol. 35, no. 10, pp. 1752–1760, 2012.

[29] J.-S. Li, S.-Y. Li, Y.-X. Zhang, C.-X. Qiao, and H.-Y. Zhou, "A comparative study of biological indicators of phlegm-heat syndrome and phlegm-dampness syndrome model with acute exacerbation of chronic obstructive pulmonary disease," *Zhongguo Wei Zhong Bing Ji Jiu Yi Xue*, vol. 22, no. 5, pp. 267–270, 2010.

[30] Y. Li, J.-S. Li, W.-W. Li et al., "Long-term effects of three Tiao-Bu Fei-Shen therapies on NF-κB/TGF-β1/smad2 signaling in rats with chronic obstructive pulmonary disease," *BMC Complementary and Alternative Medicine*, vol. 14, article 140, 2014.

[31] J. Feng, A. A.-P. Chiang, Q. Wu et al., "Sleep-related hypoxemia aggravates systematic inflammation in emphysematous rats," *Chinese Medical Journal*, vol. 123, no. 17, pp. 2392–2399, 2010.

[32] P. Almagro, B. Barreiro, A. Ochoa de Echagüen et al., "Risk factors for hospital readmission in patients with chronic obstructive pulmonary disease," *Respiration*, vol. 73, no. 3, pp. 311–317, 2006.

[33] S. Bozinovski, A. Hutchinson, M. Thompson et al., "Serum amyloid A is a biomarker of acute exacerbations of chronic obstructive pulmonary disease," *American Journal of Respiratory and Critical Care Medicine*, vol. 177, no. 3, pp. 269–278, 2008.

[34] A. Duvoix, J. Dickens, I. Haq et al., "Blood fibrinogen as a biomarker of chronic obstructive pulmonary disease," *Thorax*, vol. 68, no. 7, pp. 670–676, 2013.

[35] J. R. Hurst, W. R. Perera, T. M. A. Wilkinson, G. C. Donaldson, and J. A. Wedzicha, "Systemic and upper and lower airway inflammation at exacerbation of chronic obstructive pulmonary disease," *American Journal of Respiratory and Critical Care Medicine*, vol. 173, no. 1, pp. 71–78, 2006.

[36] T.-G. Jia, J.-Q. Zhao, and J.-H. Liu, "Serum inflammatory factor and cytokines in AECOPD," *Asian Pacific Journal of Tropical Medicine*, vol. 7, no. 12, pp. 1005–1008, 2014.

[37] A. S. Cowburn, A. M. Condliffe, N. Farahi, C. Summers, and E. R. Chilvers, "Advances in neutrophil biology: clinical implications," *Chest*, vol. 134, no. 3, pp. 606–612, 2008.

[38] R. A. O'Donnell, C. Peebles, J. A. Ward et al., "Relationship between peripheral airway dysfunction, airway obstruction, and neutrophilic inflammation in COPD," *Thorax*, vol. 59, no. 10, pp. 837–842, 2004.

[39] W. R. Perera, J. R. Hurst, T. M. A. Wilkinson et al., "Inflammatory changes, recovery and recurrence at COPD exacerbation," *European Respiratory Journal*, vol. 29, no. 3, pp. 527–534, 2007.

[40] G. R. Husebø, P. S. Bakke, M. Aanerud et al., "Predictors of exacerbations in chronic obstructive pulmonary disease—results from the bergen COPD cohort study," *PLoS ONE*, vol. 9, no. 10, Article ID e109721, 2014.

[41] B.-L. Luo, R.-C. Niu, J.-T. Feng, C.-P. Hu, X.-Y. Xie, and L.-J. Ma, "Downregulation of secretory leukocyte proteinase inhibitor in chronic obstructive lung disease: the role of TGF-β/Smads signaling pathways," *Archives of Medical Research*, vol. 39, no. 4, pp. 388–396, 2008.

[42] C. Wang, X. Liu, Q. Peng, L. Fang, C. Wang, and Z. Li, "Role of Foxp3/Treg and RORγt/Th17 cell imbalance in rat model of chronic obstructive pulmonary disease," *Zhonghua Wei Zhong Bing Ji Jiu Yi Xue*, vol. 26, no. 12, pp. 860–864, 2014.

[43] C.-Y. Wang, X.-G. Liu, C.-B. Wang, Q.-X. Ji, L. Fang, and Z. L. Ze Geng, "Regulation of Thl/Th2 cells by T cell-mediated transcription factor in rats with chronic obstructive pulmonary disease," *Sichuan Da Xue Xue Bao Yi Xue Ban*, vol. 45, no. 6, pp. 941–945, 2014.

[44] C. Zhang, S. Cai, P. Chen et al., "Inhibition of tumor necrosis factor-alpha reduces alveolar septal cell apoptosis in passive smoking rats," *Chinese Medical Journal*, vol. 121, no. 7, pp. 597–601, 2008.

[45] N. V. Zotova, V. A. Chereshnev, and E. Y. Gusev, "Systemic inflammation: methodological approaches to identification of the common pathological process," *PLoS ONE*, vol. 11, no. 5, Article ID e0155138, 2016.

Hindawi Publishing Corporation
Evidence-Based Complementary and Alternative Medicine
Volume 2016, Article ID 4312538, 10 pages
http://dx.doi.org/10.1155/2016/4312538

Research Article

Qingchang Wenzhong Decoction Ameliorates Dextran Sulphate Sodium-Induced Ulcerative Colitis in Rats by Downregulating the IP10/CXCR3 Axis-Mediated Inflammatory Response

Tang-you Mao,[1,2] Rui Shi,[2] Wei-han Zhao,[1,2] Yi Guo,[1,2] Kang-li Gao,[1,2] Chen Chen,[1,2] Tian-hong Xie,[1,2] and Jun-xiang Li[2]

[1]*Beijing University of Chinese Medicine, No. 11, North Third Ring East Road, Beijing 100029, China*
[2]*Gastroenterology Department, Dongfang Hospital, Beijing University of Chinese Medicine, No. 6, 1st Section, Fangxingyuan, Fangzhuang, Beijing 100078, China*

Correspondence should be addressed to Jun-xiang Li; lijunxiang1226@163.com

Received 30 January 2016; Revised 12 May 2016; Accepted 30 May 2016

Academic Editor: Ying-Ju Lin

Qingchang Wenzhong Decoction (QCWZD) is an effective traditional Chinese medicine prescription. Our previous studies have shown that QCWZD has significant efficacy in patients with mild-to-moderate ulcerative colitis (UC) and in colonic mucosa repair in UC rat models. However, the exact underlying mechanism remains unknown. Thus, this study was conducted to determine QCWZD's efficacy and mechanism in dextran sulphate sodium- (DSS-) induced UC rat models, which were established by 7-day administration of 4.5% DSS solution. QCWZD was administered daily for 7 days, after which the rats were euthanized. Disease activity index (DAI), histological score (HS), and myeloperoxidase (MPO) level were determined to evaluate UC severity. Serum interferon gamma-induced protein 10 (IP10) levels were determined using ELISA kits. Western blotting and real-time polymerase chain reaction were, respectively, used to determine colonic protein and gene expression of IP10, chemokine (cys-x-cys motif) receptor (CXCR)3, and nuclear factor- (NF-) κB p65. Intragastric QCWZD administration ameliorated DSS-induced UC, as evidenced by decreased DAI, HS, and MPO levels. Furthermore, QCWZD decreased the protein and gene expression of IP10, CXCR3, and NF-κB p65. Overall, these results suggest that QCWZD ameliorates DSS-induced UC in rats by downregulating the IP10/CXCR3 axis-mediated inflammatory response and may be a novel UC therapy.

1. Introduction

Ulcerative colitis (UC), a major phenotype of inflammatory bowel diseases (IBD), is characterized by chronic nonspecific inflammation of the colorectal mucosa and a relapsing-remitting course [1, 2]. The number of patients with UC in Asia is increasing annually, and the incidence of UC has increased more than 3 times in the last 10 years in China [3]. Although the exact pathogenesis of UC remains unclear, it is well known that intestinal mucosal immune system disorders, intestinal mucosal barrier defects, persistent intestinal infections, and genetic and environmental factors are involved in the development of UC [4, 5]. Persistent intestinal infections in particular are a major cause of UC [6], and alleviation of infection has become the main approach in the treatment of UC.

Interferon gamma- (IFN-γ-) induced protein 10 (IP10) is an endogenous chemokine belonging to the CXC subfamily. Previous studies have demonstrated that the amounts of IP10 in the serum and colon tissue of UC patients were significantly higher than the corresponding amounts in healthy individuals [7]. Thus, inhibiting IP10 expression can effectively resolve the clinical symptoms of UC. Furthermore, blocking of IP10 expression was shown to alleviate spontaneous colitis induced by IL-10 knockout in mice [8, 9]. IP10 expression was shown to increase in multiple cells such as

Table 1: DAI scoring criteria.

Types	0	1	2	3	4
Percent weight loss	0	1%–5%	5%–10%	10%–15%	>15%
Stool consistency	Normal	/	Mushy	/	Diarrhoea
Haematochezia level	Negative	/	Positive	/	Blood traces visible in stool

monocytes, natural killer (NK) cells, T helper (Th)1 cells, and endothelial cells (ECs) under stimulation by intestinal IFN-γ and tumour necrosis factor- (TNF-) α [10].

Chemokine (cys-x-cys motif) receptor 3 (CXCR3) is the specific binding protein of IP10, and it is mainly expressed by epithelial and endothelial cells, as well as lymphoid cells such as memory T cells, NK cells, B cells, neutrophils, and monocytes. Upon binding to IP10, CXCR3 is activated, which increases the chemotactic activity of CXCR3-positive cells and contributes to its transfer to local inflammatory lesions [11]. Finally, the intestinal mucosa produces large amounts of inflammatory cytokines [12, 13], which not only further stimulate IP10, thus recruiting more immune cells and forming a vicious cycle, but also directly or indirectly damage the intestinal mucosal barrier and the intestinal mucosa [14, 15] and promote the occurrence and development of UC [16]. Therefore, the IP10/CXCR3-mediated inflammatory response plays an important role in the pathogenesis of UC, and inhibiting the IP10/CXCR3 axis to block excessive inflammation may be a new approach for treatment of UC.

At present, an effective treatment for UC is lacking. Amino salicylic acid, steroid hormones, and immunosuppressive drugs are the main treatments for UC, and the primary goals of these treatments are to induce remission and prevent a relapse [17, 18]. However, these treatments are associated with numerous problems such as drug intolerance, side effects, requirement of a prolonged treatment course, and high recurrence rate. Thus, there is an urgent need for the development of novel and effective drugs for treatment of UC [19].

Qingchang Wenzhong Decoction (QCWZD) is a new and effective traditional Chinese medicine prescription formulated by Li Jun-Xiang, a professor at the Beijing University of Chinese Medicine. Our previous studies have shown significant clinical efficacy of QCWZD in patients with mild-to-moderate UC [20, 21]. Furthermore, in rat models of UC, QCWZD reduced damage to colonic epithelial cells, repaired the colonic mucosa, and downregulated proinflammatory cytokines [22, 23]. However, the exact mechanism of action is yet to be elucidated. Therefore, the present study sought to further explore the molecular mechanism underlying QCWZD's protective effects in rat models of UC.

2. Materials and Methods

2.1. Preparation of QCWZD and Mesalazine. QCWZD granules were purchased from the Pharmacy Department of Dongfang Hospital, Beijing University of Chinese Medicine (Beijing, China). The QCWZD granules contained Qingchang Wenzhong ingredients in equal weights: Huanglian (coptis), 6 g; Pao Jiang (ginger), 10 g; Kushen (matrine), 15 g; Qingdai (indigo), 6 g; Diyutan (sanguisorba carbon), 30 g; Muxiang (wood), 6 g; Sanqi (pseudoginseng), 6 g; and Gancao (licorice), 6 g. Mesalazine was purchased from Losan Pharma GmbH, Germany.

2.2. Experimental Animals. All the experimental procedures were approved by the Animal Ethics Committee of Beijing University of Chinese Medicine, in accordance with guidelines issued by Regulations of Beijing Laboratory Animal Management. Fifty male Sprague-Dawley rats (weighing 180–220 g; SPF Biological Technology Co., Ltd., Beijing, China) were housed in a specific pathogen-free animal room with temperature maintained at 20–24°C, 50–60% humidity, and a light-controlled environment (12/12 h light/dark cycle), with free access to food and sterile tap water. All animals were allowed to adapt for 7 days before the experiments were started.

2.3. Induction of Colitis by DSS and Experimental Procedure. Colitis was induced using 4.5% (w/v) DSS (MW, 36–50 KDa, MP Biomedical, California, USA) added to distilled water. Fresh DSS solution was administered every day. The rats in the DSS (DSS, $n = 10$), low-dose QCWZD (low, 0.3 g/kg/day, p.o., $n = 10$), high-dose QCWZD (high, 1.2 g/kg/day, p.o., $n = 10$), and mesalazine (mesalazine, 0.03 g/kg/day, p.o., $n = 10$) groups were administered 4.5% DSS solution from day 1 to day 7. The control group rats received only distilled water. All rats were killed after deep anaesthesia with 10% chlorine hydrate solution (3.5 mL/kg, i.p.), and blood samples were collected from the abdominal aorta. Colon samples (8 cm in length) were removed and cut into 6 segments, each measuring 0.5 cm, starting from the anus and cut at 1 cm intervals. One of every two sections was fixed in 10% neutral buffered formalin for histological analysis, and the other one was placed into a freezer tube and stored at −80°C until used.

2.4. Analysis of Disease Activity Index. All rats were checked daily for colitis by evaluating their weight, faecal occult blood, and stool consistency. The disease activity index (DAI) was evaluated daily in a blinded manner by nonproject team members (Table 1) as previously described [24]. DAI was calculated using the following formula: DAI = (percent weight loss score + stool consistency score + haematochezia level score)/3.

2.5. Histological Analysis. After being fixed with 10% neutral buffered formalin for 24 h, the tissues were embedded in paraffin blocks and sectioned to obtain a thickness of 6 μm.

Table 2: Histological score criteria.

Histological changes	0	1	2	3
Inflammatory cell infiltration	No	Mild	Moderate	Severe
Granuloma	No	Mild	Moderate	Severe
Lesion depth	Mucosa	Submucosa	Muscular layer	Serosa

Thereafter, the sections were stained with haematoxylin and eosin (HE), and the histological score (HS) was determined using an optical microscope (Table 2). Each sample was randomly selected from 3 perspectives, and the average score was calculated as previously described [25]. The analysis was performed by nonproject team members under the guidance of a pathologist.

2.6. Assay for Myeloperoxidase (MPO) Activity. Frozen colons that were dissected 1 cm above the anus were homogenized in phosphate-buffered saline and centrifuged at 20,000 ×g. Then, myeloperoxidase (MPO) activity in the colonic tissue was detected using chemical colorimetry (NANODROP 2000, Thermo, USA) as previously described [26].

2.7. Measurement of Serum IP10 Level Using ELISA. After blood samples were collected from the abdominal aorta of rats, IP10 levels in the serum were tested using rat ELISA kits (MULTISKAN MK3, Thermo, USA).

2.8. Western Blotting for Detection of IP10, CXCR3, and NF-κB p65 Expression in the Colon. Western blot analysis was performed as described previously [27]. Proteins were isolated from ice-cold colon tissues, and protein concentrations were determined using the bicinchoninic acid (BCA) assay (Cwbiotech, Beijing, China). The proteins were then separated using 10% SDS-PAGE for 1.5 h before being transferred to polyvinylidene fluoride (PVDF) membranes. The membranes were probed with IP10 (1 : 5000), CXCR3 (1 : 5000), NF-κB p65 (1 : 2000), and GAPDH (1 : 1000) antibodies (TDY Biotech, Beijing, China). Each membrane was washed three times for 10 min and incubated with goat polyclonal secondary antibody to rabbit antibodies (111-035-003, Jackson Laboratory, USA). Finally, densitometry was performed to quantitate protein band intensities by using the Gel Image System ver. 4.00 (Tanon, China).

2.9. Real-Time Polymerase Chain Reaction for IP10, CXCR3, and NF-κB p65 mRNA Expression. Evaluation of mRNA expression was performed by using real-time polymerase chain reaction as previously described [28]. Total RNA was extracted from the colon tissue samples by using extraction kits (CWbio, Beijing, China). After reverse transcription, PCR amplification was performed using the TRIzol method (TRIzol reagent; Invitrogen Life Technologies, Carlsbad, CA, USA). The real-time PCR primer sequences for target genes were as follows: 5′-GCGGCTAGTCCTAACTGTCC-3′/5′-GAATTGGGAAGCCTTGCTGC-3′ for IP10, 5′-TCACTTCCTCTGTTCACGGC-3′/5′-AGGAGGCTGTAGAGGACTGG-3′ for CXCR3, 5′-CAGACACCTTTGCACTTGGC-3′/5′-CTTGAGTAGGACCCCGAGGA-3′ for NF-κB p65, and 5′-CCCATCTATGAGGGTTACGC-3′/5′-TTTAATGTCACGCACGATTTC-3′ for GAPDH (CWbio, Beijing, China). For real-time PCR, the cycling conditions were 95°C for 10 min and 45 × (95°C for 10 s, 59°C for 60 s), followed by a melting curve analysis-based assay with conditions of 95°C for 15 s and 72°C for 15 s and increase in temperature to 95°C for 15 s. Relative expression was assessed by calculating the expression relative to that of GAPDH by using the $2^{-\Delta\Delta Ct}$ method.

2.10. Statistical Analysis. All data are expressed as mean ± standard deviation (SD) values. SPSS v18.0 (IBM Corp., Armonk, NY, USA) was used for statistical analyses. The data were compared between groups using one-way analysis of variance (ANOVA), followed by Student's *t*-tests. $P < 0.05$ was considered statistically significant.

3. Results

3.1. Effect of QCWZD on Body Weight and DAI in UC Rats. All animals tolerated the entire experiment well, and no deaths occurred. After free access to 4.5% DSS for 4 days, body weight started to decrease in the DSS group. By the 8th day, the weight loss was significantly higher than that in the control group (DSS group versus control group: 221.70 ± 10.35 g versus 310.00 ± 10.21 g, $P < 0.01$). Both the low-dose (256.90 ± 10.96 g) and high-dose QCWZD (246.70 ± 10.140 g) groups showed significant attenuation of body weight loss ($P < 0.05$, resp.), similar to the mesalazine group (269.10 ± 12.260 g versus 221.70 ± 10.35 g, $P < 0.05$) (Figure 1(a)). There were no significant differences between low-dose and high-dose QCWZD ($P > 0.05$), possibly because of the small sample size.

On the 8th day, the DSS group showed a significantly increased DAI score (2.13 ± 0.42) compared to that of the control group (0.10 ± 0.32; $P < 0.01$, Figure 1(b)). The DAI scores in the low-dose group (1.47 ± 0.88), high-dose group (1.27 ± 0.96), and mesalazine group (1.28 ± 0.78) were significantly lower than that in the DSS group ($P < 0.05$, $P < 0.01$, resp., Figure 1(b)).

Subsequently, we separately analysed the categorical data of DAI according to each category. As shown in Figure 1(c), the haematochezia level (3.00 ± 1.41), stool consistency (2.60 ± 0.97), and percent weight loss (0.80 ± 1.03) in the DSS group were significantly higher than those in the control group (0.20 ± 0.63, 0.00 ± 0.00, and 0.10 ± 0.32, $P < 0.05$ and $P < 0.01$, resp., Figure 1(c)). The haematochezia level in the low-dose group (2.20 ± 1.16), high-dose group (2.20 ± 1.16), and mesalazine group (1.80 ± 1.14) was significantly lower than that in the DSS group ($P < 0.05$, $P < 0.01$, resp., Figure 1(c)). The stool consistency (2.20 ± 1.75 in the low-dose

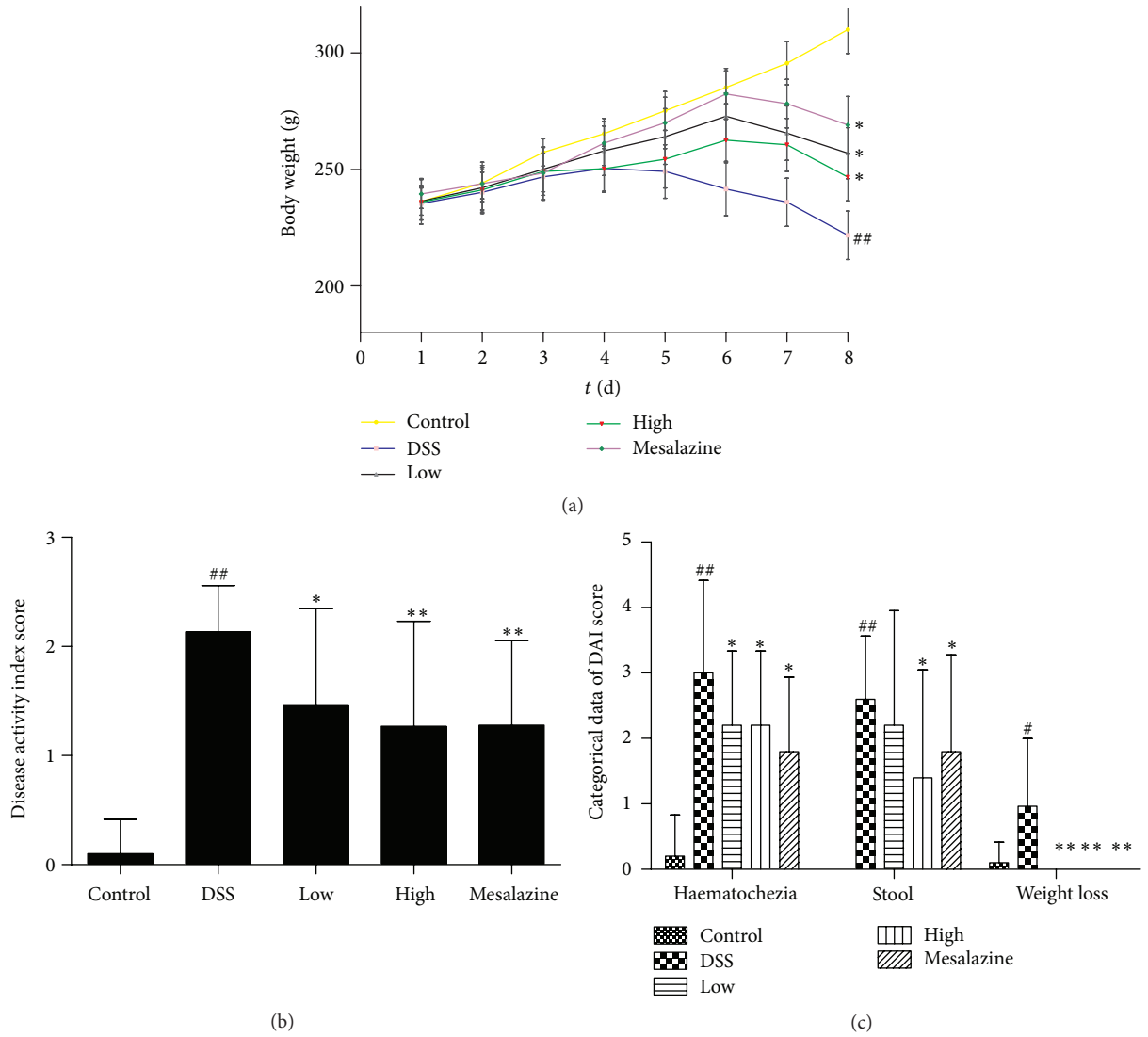

Figure 1: Effect of QCWZD on body weight (a), DAI score (b), and categorical data of DAI (c) in UC rats. Control: blank control group; DSS: DSS-treated group; low: low-dose QCWZD group; high: high-dose QCWZD group; mesalazine: mesalazine group; haematochezia: haematochezia level; stool: stool consistency; and weight: percent weight loss. Data are presented as the mean ± SD. $^{\#\#}P < 0.01$, $^{\#}P < 0.05$ versus the control group; $^{**}P < 0.01$, $^{*}P < 0.05$ versus the DSS group ($n = 10$ per group).

group, 1.40 ± 1.65 in the high-dose group, and 1.80 ± 1.48 in the mesalazine group) and percent weight loss (0.00 ± 0.00 in the low-dose, high-dose, and mesalazine groups) showed the same tendency ($P < 0.05$ and $P < 0.01$, resp., Figure 1(c)).

3.2. QCWZD Improved Histopathology in Rats. Compared with the control group (Figure 2(a)), the DSS group showed severely damaged crypts and epithelial integrity, and remarkable inflammatory cell infiltration in the mucosa (Figure 2(b)). After intrarectal administration of QCWZD and mesalazine, mild infiltration of inflammatory cells, crypt regeneration, and epithelial restoration were observed (Figures 2(c), 2(d), and 2(e)). Similarly, as shown in Figure 2(f), the histological score reached a significantly higher value in the DSS group (8.13 ± 0.37) than in the control group ((2.15±0.23), $P < 0.01$). In contrast to the DSS group, the low- and high-dose QCWZD groups and the mesalazine group showed protection against histological damage (4.64 ± 0.60, 3.71 ± 0.46, and 3.97 ± 0.40, resp., $P < 0.05$) (Figure 2(f)).

3.3. QCWZD Decreased Colonic MPO Activity in DSS-Induced UC Rats. To determine the degree of infiltration by neutrophil granulocytes in the colonic tissue, the activity of MPO was detected by chemical colorimetry. Compared with the control group (0.98 ± 0.06), the DSS group showed significantly higher MPO activity (1.43 ± 0.16, $P < 0.05$). As expected, the difference was significantly less when the groups given QCWZD (1.19 ± 0.22 in the low-dose group, 1.07 ± 0.11 in the high-dose group, $P < 0.05$, $P < 0.01$, resp.)

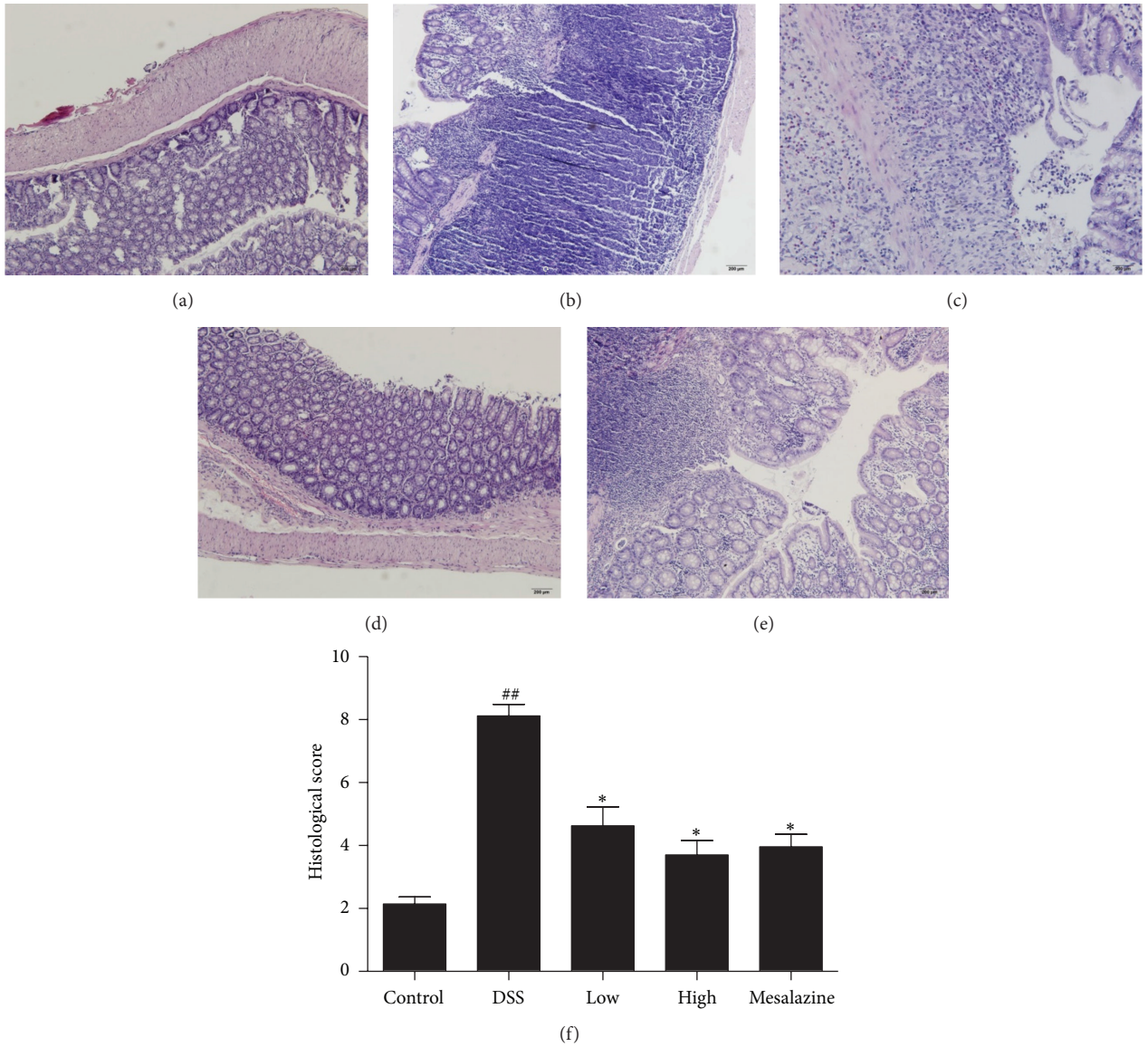

Figure 2: QCWZD ameliorated histological damage (a–e) and reduced the histological score (f) in rats. (a) Control: blank control group; (b) DSS: DSS group; (c) low: low-dose QCWZD group; (d) high: high-dose QCWZD group; and (e) mesalazine: mesalazine group. $^{\#\#}P < 0.01$ versus the control group; $^{*}P < 0.05$ versus the DSS group ($n = 10$ per group).

and mesalazine (1.03 ± 0.09, $P < 0.01$) were compared to the DSS group (Figure 3).

3.4. Effects of QCWZD on Serum IP10 Level. The serum IP10 level was determined in the control rats and DSS-induced UC rats treated with distilled water, low- and high-dose QCWZD groups, and mesalazine group. As shown in Figure 4, DSS significantly elevated IP10 levels in serum compared with those in the control group (552.8 ± 158.5 ng/mL in the DSS group versus 367.8 ± 44.30 ng/mL, $P < 0.01$). The low-dose QCWZD group (313.0 ± 72.69 ng/mL), the high-dose QCWZD group (266.7 ± 89.99 ng/mL), and the mesalazine group (270.0 ± 98.34 ng/mL) showed significant inhibition of DSS-induced elevation of serum IP10 level (versus the DSS group, all $P < 0.01$) (Figure 4).

3.5. QCWZD Regulated Colonic IP10 and IP10 mRNA Expression in DSS-Induced UC Rats. We also investigated whether or not QCWZD had a regulatory effect on IP10 expression in the colon. IP10 levels in the colon were significantly increased in the DSS group ($P < 0.01$ versus the control group). Additionally, high-dose QCWZD and mesalazine produced a dramatically reduced effect on IP10 expression (Figure 5(a)).

Furthermore, we measured IP10 gene expression to confirm the effects of QCWZD on the colon. As shown in Figure 5(b), induction of colitis significantly elevated colonic

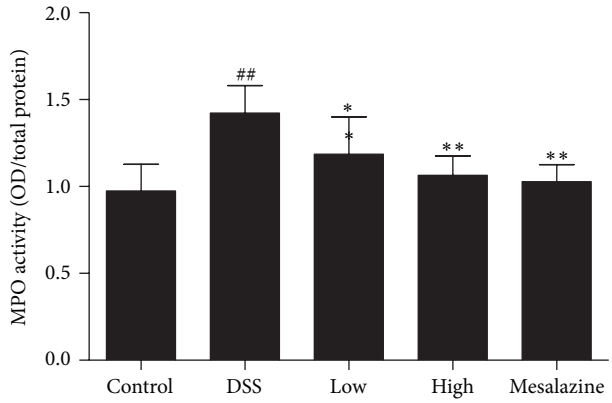

Figure 3: QCWZD decreased colonic MPO activity in rats with DSS-induced UC. Control: blank control group; DSS: DSS group; low: low-dose QCWZD group; high: high-dose QCWZD group; mesalazine: mesalazine group. $^{\#\#}P < 0.01$ versus the control group; $^{**}P < 0.01$, $^{*}P < 0.05$ versus the DSS group ($n = 10$ per group).

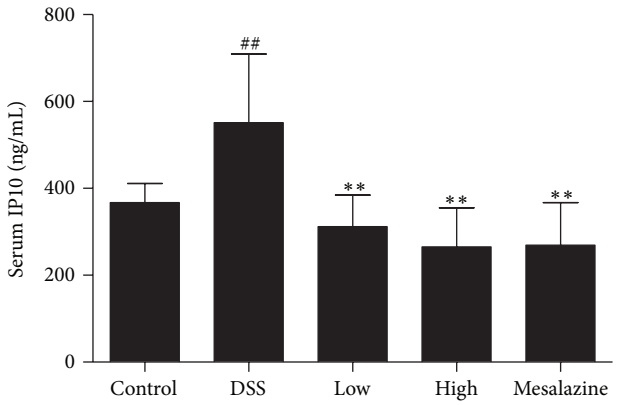

Figure 4: Effects of QCWZD on serum IP10 level. Control: blank control group; DSS: DSS group; low: low-dose QCWZD group; high: high-dose QCWZD group; mesalazine: mesalazine group. $^{\#\#}P < 0.01$ versus the control group; $^{**}P < 0.05$ versus DSS group ($n = 10$ per group).

IP10 gene expression compared with that in the control group ($P < 0.01$). Treatment with QCWZD and mesalazine for 7 days decreased IP10 gene expression in a dose-dependent manner ($P < 0.05$, $P < 0.01$, resp.) compared to that in the DSS group.

3.6. QCWZD Decreased Colonic CXCR3 and CXCR3 mRNA Expression in Rats with DSS-Induced UC. Because CXCR3 specifically binds to IP10, its levels were analysed by western blot. Compared to the control group, the DSS group showed increased CXCR3 expression ($P < 0.01$); the QCWZD and mesalazine groups showed alleviation of the effects of DSS on CXCR3 expression in rats with DSS-induced UC (versus the DSS group, $P < 0.05$ and $P < 0.01$, resp., Figure 6(a)). The expression of the CXCR3 gene was measured as described above. Gene expression in the DSS group was increased compared to that in the control group ($P < 0.01$, Figure 6(b)). Remarkably, QCWZD and mesalazine both greatly decreased CXCR3 gene expression (versus the DSS group, $P < 0.05$ and $P < 0.01$, resp., Figure 6(b)).

3.7. QCWZD Suppressed the Increase in Colonic NF-κB p65 and NF-κB p65 mRNA Expression in Rats with DSS-Induced UC. Because the cytokines TNF-α and IL-6 produced by CXCR3-positive cells contribute to the activation of NF-κB, we examined the effect of CXCR3 on NF-κB p65 activation. We found distinctly increased NF-κB p65 and NF-κB p65 mRNA expression in the DSS group compared to that in the control group ($P < 0.01$, Figures 7(a) and 7(b)). Nevertheless, NF-κB p65 and NF-κB p65 mRNA expression was significantly reduced in DSS-induced UC rats treated with QCWZD and mesalazine ($P < 0.05$, resp., Figures 7(a) and 7(b)).

4. Discussion

In the present study, to observe the anti-inflammatory effects of QCWZD, we generated an ulcerative colitis model in rats by allowing them to drink 4.5% DSS freely for 7 days; this model is widely used because of its similarities to human UC. DSS is a polysaccharide extracted from sucrose synthesis. Although the exact mechanism by which it induces UC remains unclear, it may be related to the negative charge of DSS, which may affect the synthesis of colonic epithelial DNA, inhibit the proliferation of epithelial cells, and damage the intestinal mucosal barrier [29].

In our study, faecal occult blood began to appear on the 2nd day and the animals' body weight started to decrease on the 4th day in the DSS group. With time, gross blood began to appear in the stool and the body weight continued to decrease, and the DAI score increased and reached the maximum value on the 8th day. In the histological analysis, we found that the number of inflammatory cells (mainly neutrophils) was increased in the colonic tissue of rats that received DSS and that the crypts and epithelial integrity were severely damaged. Correspondingly, the histological score increased to a significantly higher value in the DSS group than in the control group. After administration of QCWZD and mesalazine, the body weight loss, DAI score, and histological score were significantly decreased and improved (Figures 1 and 2). These results suggest that QCWZD has prominent therapeutic effects on rats with DSS-induced ulcerative colitis.

After observing a definite effect, we further explored the therapeutic mechanism of QCWZD in rats with DSS-induced UC. Persistent intestinal infection plays an important role in the pathogenesis and development of UC [30, 31], and the IP10/CXCR3 axis that regulates the infiltration of immune cells to sites of inflammatory injury plays an essential role in the inflammatory response. Previous studies showed that both IP-10 expression in colonic tissue and IP10 levels in serum were higher in patients with UC than in healthy controls [16, 32], and that anti-IP-10 antibodies alleviated acute colitis and enhanced crypt cell survival in mice with UC induced by DSS [8]. Thus, anti-IP-10 therapy may provide an important direction for the treatment of UC. A recent phase

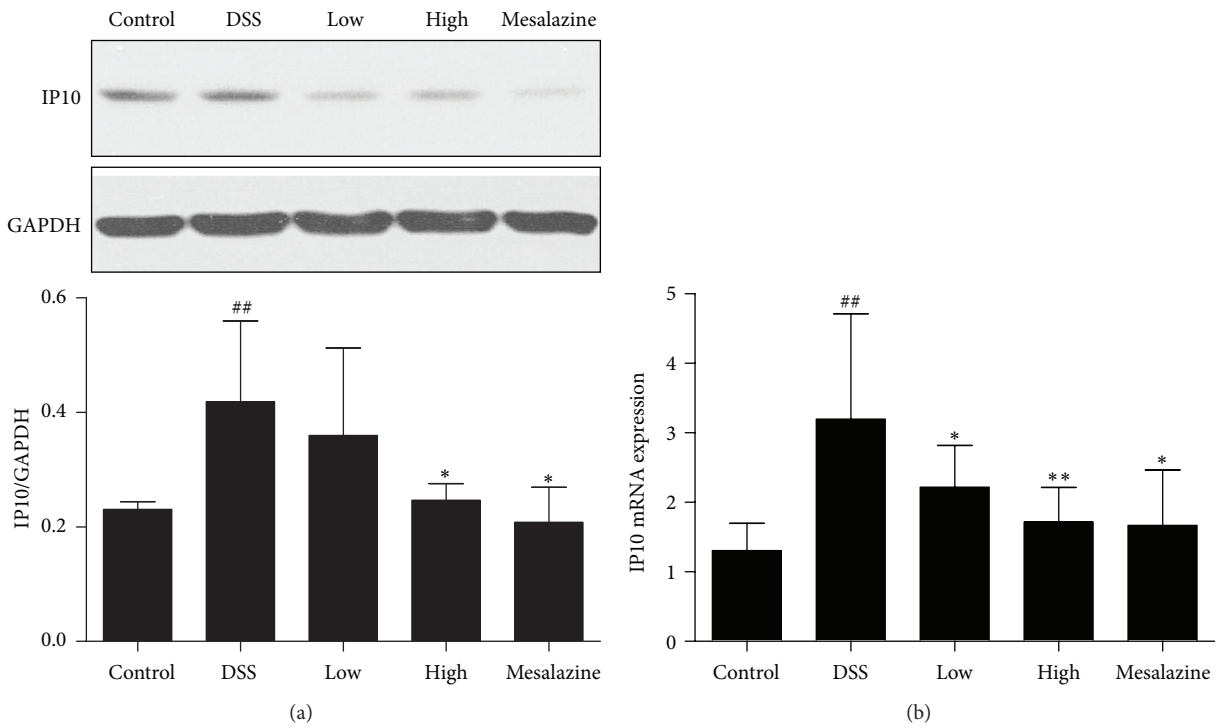

Figure 5: QCWZD regulated colonic IP10 (a) and IP10 mRNA (b) expression in DSS-induced UC rats. Control: blank control group; DSS: DSS group; low: low-dose QCWZD group; high: high-dose QCWZD group; and mesalazine: mesalazine group. $^{\#\#}P < 0.01$ versus control group; $^{**}P < 0.01$, $^{*}P < 0.05$ versus DSS group ($n = 10$ per group).

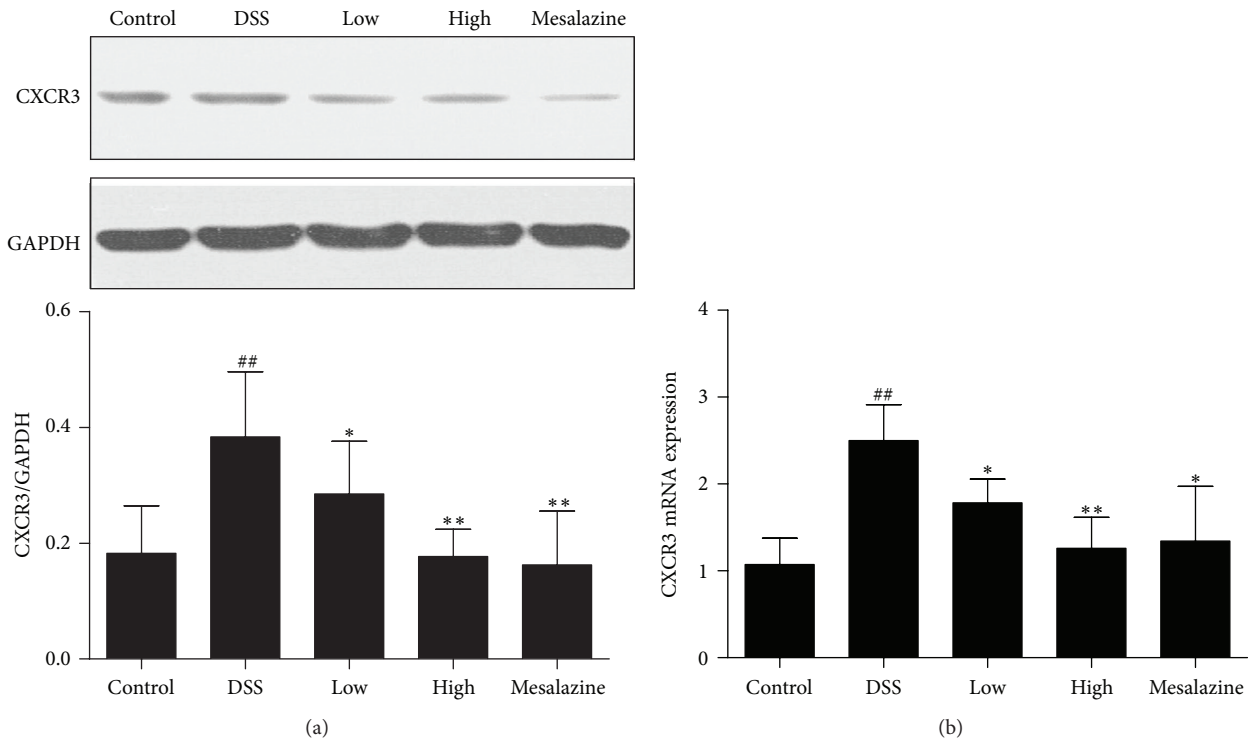

Figure 6: QCWZD inhibited colonic CXCR3 (a) and CXCR3 mRNA (b) expression in rats with DSS-induced UC. Control: blank control group; DSS: DSS group; low: low-dose QCWZD group; high: high-dose QCWZD group; and mesalazine: mesalazine group. $^{\#\#}P < 0.01$ versus control group; $^{**}P < 0.01$, $^{*}P < 0.05$ versus DSS group ($n = 10$ per group).

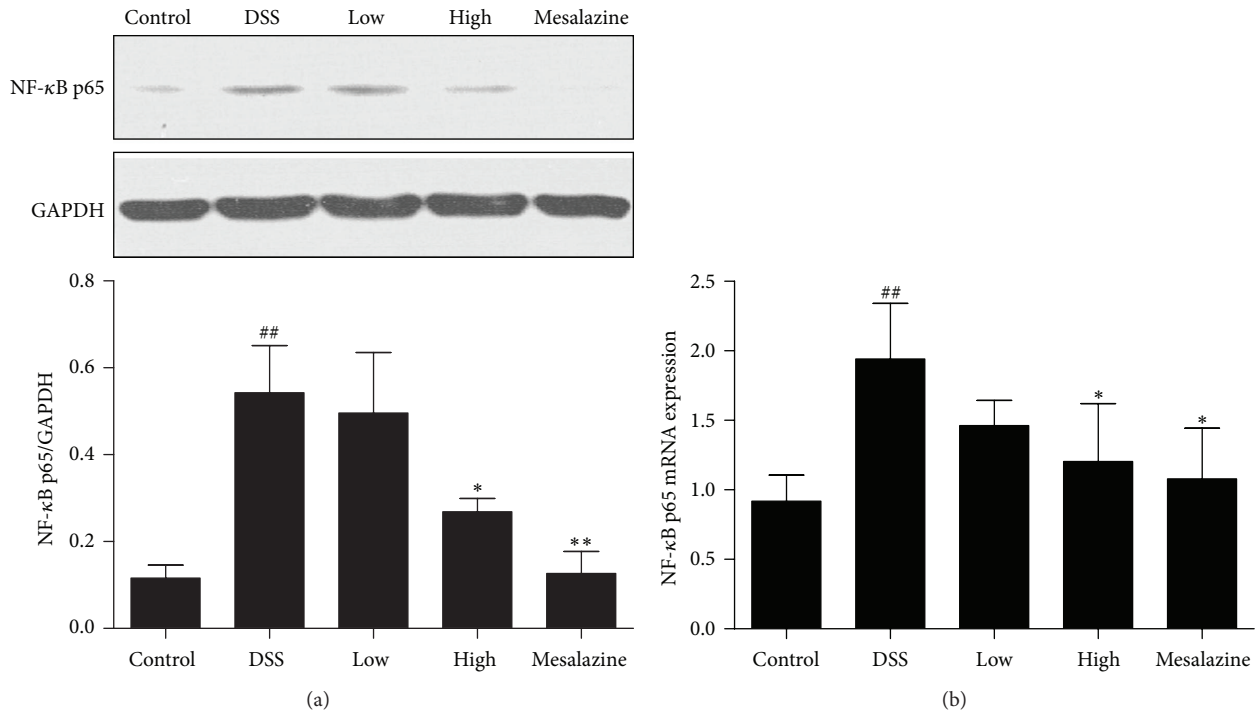

Figure 7: QCWZD suppressed the increase in colonic NF-κB p65 (a) and NF-κB p65 mRNA (b) levels in rats with DSS-induced UC. Control: blank control group; DSS: DSS group; low: low-dose QCWZD group; high: high-dose QCWZD group; and mesalazine: mesalazine group. $^{\#\#}P < 0.01$ versus control group; $^{**}P < 0.01$, $^{*}P < 0.05$ versus DSS group ($n = 10$ per group).

II study for UC [7] showed that anti-IP-10 therapy with BMS-936557 effectively relieved clinical symptoms and increased histological improvement in patients with moderate-to-severe UC. Although robust efficacy was demonstrated, the drug dose response and safety profile require further research. Therefore, it is necessary to identify a new method to evaluate the therapeutic value of targeting the IP/CXCR3 axis for UC. In this regard, traditional Chinese medicine has been proven to have a curative effect in the treatment of ulcerative colitis [5, 33]. Previous studies have shown significant clinical efficacy of QCWZD in patients with UC, but the specific mechanism is not clear. Thus, we designed the present study to determine whether or not QCWZD exerts an anti-inflammatory effect through IP/CXCR3 axis. In the present study, abnormally high expression of IP10 and CXCR3 was observed in the colonic mucosa of rats with DSS-induced UC, and treatment with QCWZD and mesalazine dose-dependently decreased IP10 and CXCR3 expression (Figures 4, 5, and 6).

An increase in neutrophils is a key feature in the pathogenesis of UC [34, 35]. Coupling of IP10 to CXCR3 in the colon leads to activation of CXCR3, which promotes recruitment of neutrophils to the inflammatory site, whereas CXCR3 blockade limits neutrophil accumulation in the inflamed site. Therefore, we evaluated the expression of MPO in colon tissues, which reflects the degree of mucosal neutrophil infiltration [36, 37]. As expected, DSS significantly increased MPO activity in the colon tissue, and QCWZD treatment partially reversed this effect (Figure 3).

In addition to promoting the recruitment of neutrophils, the IP/CXCR3 axis increases the chemotactic activity of CXCR3-positive cells, which are directly and indirectly involved in the generation and recruitment of inflammatory cytokines [38] such as TNF-α and MCP-1, thereby damaging the intestinal mucosal barrier and colon mucosa [39, 40]. NF-κB is an upstream regulator for TNF-α and MCP-1, which can in turn activate NF-κB [41]. NF-κB activation is involved in inflammatory recruitment [42]; therefore, we investigated whether or not the IP10/CXCR3 axis plays a role in NF-κB activation in the development of UC. Overexpression of NF-κB p65 has been identified in the colonic mucosa and is positively correlated with the increase in IP10/CXCR3. In the present study, QCWZD and mesalazine played a major role in decreasing NF-κB p65 expression (Figure 7). Although other signalling pathways may also activate NF-κB or proinflammatory cytokine genes, the proinflammatory effect of IP10/CXCR3 axis in UC is at least partly related to the induction of NF-κB. NF-κB activation is an important way that the IP10/CXCR3 axis exerts its proinflammatory effect.

In the present study, using a DSS-induced rat colonic mucosal injury as a model, we found that QCWZD significantly improved the body weight, DAI score, HS, and MPO activity in DSS-induced UC rats. The protective effects of QCWZD may be attributed to its significant regulation of the IP10/CXCR3 axis-mediated inflammatory response. QCWZD can reverse the dysregulated expression of serum and colonic IP10 and IP10 mRNA, reduce colonic CXCR3 and CXCR3 mRNA production, and thereby inhibit activation

of the IP10/CXCR3 axis, in turn decreasing the generation and recruitment of inflammatory cytokines and promoting epithelial cell proliferation and repair of injured mucosa.

5. Conclusions

Our results show that intragastric administration of QCWZD can ameliorate DSS-induced UC in rats. The protective mechanism may be attributed to significant downregulation of the IP10/CXCR3 axis-mediated inflammatory response. Our results suggest that QCWZD may be a novel therapeutic option for UC.

Competing Interests

The authors declare that there is no conflict of interests regarding the publication of this paper.

Authors' Contributions

Tang-you Mao and Rui Shi contributed equally to this work.

Acknowledgments

This study was supported by the National Science Foundation of China (Grant no. 81403369) and the self-selected topic of the Beijing University of Chinese Medicine (Grant no. 2015-JYB-XS172).

References

[1] S. Danese and C. Fiocchi, "Ulcerative colitis," *The New England Journal of Medicine*, vol. 365, no. 18, pp. 1713–1725, 2011.

[2] H. M. Zhao, X. Y. Huang, F. Zhou et al., "Si Shen Wan inhibits mRNA expression of apoptosis-related molecules in p38 MAPK signal pathway in mice with colitis," *Evidence-Based Complementary and Alternative Medicine*, vol. 2013, Article ID 432097, 8 pages, 2013.

[3] APDW 2004 Chinese IBD Working Group, "Retrospective analysis of 515 cases of Crohn's disease hospitalization in China: nationwide study from 1990 to 2003," *Journal of Gastroenterology and Hepatology*, vol. 21, no. 6, pp. 1009–1015, 2006.

[4] A. Kaser, S. Zeissig, and R. S. Blumberg, "Inflammatory bowel disease," *Annual Review of Immunology*, vol. 28, pp. 573–621, 2010.

[5] X. P. Li, Y. J. Xu, C. L. Zhang et al., "Protective effect of Calculus *Bovis Sativus* on dextran sulphate sodium-induced ulcerative colitis in mice," *Evidence-Based Complementary and Alternative Medicine*, vol. 2015, Article ID 469506, 8 pages, 2015.

[6] H. Matsuoka, H. Ikeuchi, M. Uchino et al., "Clinicopathological features of ulcerative colitis-associated colorectal cancer pointing to efficiency of surveillance colonoscopy in a large retrospective Japanese cohort," *International Journal of Colorectal Disease*, vol. 28, no. 6, pp. 829–834, 2013.

[7] L. Mayer, W. J. Sandborn, Y. Stepanov et al., "Anti-IP-10 antibody (BMS-936557) for ulcerative colitis: a phase II randomised study," *Gut*, vol. 63, no. 3, pp. 442–450, 2014.

[8] S. Sasaki, H. Yoneyama, K. Suzuki et al., "Blockade of CXCL10 protects mice from acute colitis and enhances crypt cell survival," *European Journal of Immunology*, vol. 32, no. 11, pp. 3197–3205, 2002.

[9] U. P. Singh, S. Singh, R. Singh, Y. Cong, D. D. Taub, and J. W. Lillard Jr., "CXCL10-producing mucosal $CD4^+$ T cells, NK cells, and NKT cells are associated with chronic colitis in IL-$10^{-/-}$ mice, which can be abrogated by anti-CXCL10 antibody inhibition," *Journal of Interferon and Cytokine Research*, vol. 28, no. 1, pp. 31–43, 2008.

[10] K. Van Raemdonck, P. E. Van den Steen, S. Liekens, J. Van Damme, and S. Struyf, "CXCR3 ligands in disease and therapy," *Cytokine & Growth Factor Reviews*, vol. 26, no. 3, pp. 311–327, 2015.

[11] M. Liu, S. Guo, J. M. Hibbert et al., "CXCL10/IP-10 in infectious diseases pathogenesis and potential therapeutic implications," *Cytokine & Growth Factor Reviews*, vol. 22, no. 3, pp. 121–130, 2011.

[12] J.-M. Xu and G.-P. Shi, "Emerging role of mast cells and macrophages in cardiovascular and metabolic diseases," *Endocrine Reviews*, vol. 33, no. 1, pp. 71–108, 2012.

[13] B.-G. Xiao, W.-H. Zhu, and C.-Z. Lu, "The presence of GM-CSF and IL-4 interferes with effect of TGF-β1 on antigen presenting cells in patients with multiple sclerosis and in rats with experimental autoimmune encephalomyelitis," *Cellular Immunology*, vol. 249, no. 1, pp. 30–36, 2007.

[14] T. Y. Ma, G. K. Iwamoto, N. T. Hoa et al., "TNF-α-induced increase in intestinal epithelial tight junction permeability requires NF-κB activation," *American Journal of Physiology—Gastrointestinal and Liver Physiology*, vol. 286, no. 3, pp. G367–G376, 2004.

[15] P. K. Kim and C. S. Deutschman, "Inflammatory responses and mediators," *Surgical Clinics of North America*, vol. 80, no. 3, pp. 885–894, 2000.

[16] A. E. Ostvik, A. V. B. Granlund, M. Bugge et al., "Enhanced expression of CXCL10 in inflammatory bowel disease: potential role of mucosal toll-like receptor 3 stimulation," *Inflammatory Bowel Diseases*, vol. 19, no. 2, pp. 265–274, 2013.

[17] A. Kornbluth, D. B. Sachar, and Practice Parameters Committee of the American College of Gastroenterology, "Ulcerative colitis practice guidelines in adults: American college of gastroenterology, practice parameters committee," *American Journal of Gastroenterology*, vol. 105, no. 3, pp. 501–523, 2010.

[18] C. Mowat, A. Cole, A. Windsor et al., "Guidelines for the management of inflammatory bowel disease in adults," *Gut*, vol. 60, no. 5, pp. 571–607, 2011.

[19] D. Laharie, A. Bourreille, J. Branche et al., "Ciclosporin versus infliximab in patients with severe ulcerative colitis refractory to intravenous steroids: a parallel, open-label randomised controlled trial," *The Lancet*, vol. 380, no. 9857, pp. 1909–1915, 2012.

[20] S. B. Wei, *Clinical Research on the Treatment of Ulcerative Colitis with Qingchang Wenzhong Decoction*, Beijing University of Chinese Medicine, Beijing, China, 2014 (Chinese).

[21] J. W. Chen, *Clinical Effect of Qingchang Wenzhong on the Treatment of Ulcerative Colitis*, Beijing University of Chinese Medicine, Beijing, China, 2015 (Chinese).

[22] L. J. Liu, Y. L. Wang, R. Shi et al., "Effect of Qingchang Wenzhong decoction on colonic mucosa of TNBS-induced colitis rats," *Global Traditional Chinese Medicine*, vol. 7, no. 3, pp. 187–191, 2014.

[23] L. J. Liu, Y. L. Wang, S. B. Wei, M. J. Yang, and J. X. Li, "Effects of Qingchang Wenzhong decoction on intestinal mucosa barrier

in colitis rats induced by TNBS," *China Journal of Traditional Chinese Medicine and Pharmacy*, vol. 30, no. 9, pp. 3266–3269, 2015.

[24] S. Sasaki, I. Hirata, K. Maemura et al., "Prostaglandin E_2 inhibits lesion formation in dextran sodium sulphate-induced colitis in rats and reduces the levels of mucosal inflammatory cytokines," *Scandinavian Journal of Immunology*, vol. 51, no. 1, pp. 23–28, 2000.

[25] L. A. Dieleman, M. J. H. J. Palmen, H. Akol et al., "Chronic experimental colitis induced by dextran sulphate sodium (DSS) is characterized by Th1 and Th2 cytokines," *Clinical and Experimental Immunology*, vol. 114, no. 3, pp. 385–391, 1998.

[26] A. Mallakin, L. W. Kutcher, S. A. McDowell et al., "Gene expression profiles of Mst1r-deficient mice during nickel-induced acute lung injury," *American Journal of Respiratory Cell and Molecular Biology*, vol. 34, no. 1, pp. 15–27, 2006.

[27] F. Huang, C. Y. Kao, S. Wachi, P. Thai, J. Ryu, and R. Wu, "Requirement for both JAK-mediated PI3K signaling and ACT1/TRAF6/TAK1-dependent NF-κB activation by IL-17A in enhancing cytokine expression in human airway epithelial cells," *Journal of Immunology*, vol. 179, no. 10, pp. 6504–6513, 2007.

[28] S. A. Bustin, "Absolute quantification of mrna using real-time reverse transcription polymerase chain reaction assays," *Journal of Molecular Endocrinology*, vol. 25, no. 2, pp. 169–193, 2000.

[29] Y. Araki, K. I. Mukaisyo, H. Sugihara, Y. Fujiyama, and T. Hattori, "Increased apoptosis and decreased proliferation of colonic epithelium in dextran sulfate sodium-induced colitis in mice," *Oncology Reports*, vol. 24, no. 4, pp. 869–874, 2010.

[30] S. Watanabe, M. Yamakawa, T. Hiroaki, S. Kawata, and O. Kimura, "Correlation of dendritic cell infiltration with active crypt inflammation in ulcerative colitis," *Clinical Immunology*, vol. 122, no. 3, pp. 288–297, 2007.

[31] M. Zhao and F. Gao, "New progress in the pathogenesis of ulcerative colitis," *Progress in Modern Biomedicine*, vol. 10, no. 16, pp. 3160–3165, 2010.

[32] S. Schroepf, R. Kappler, S. Brand et al., "Strong overexpression of CXCR3 axis components in childhood inflammatory bowel disease," *Inflammatory Bowel Diseases*, vol. 16, no. 11, pp. 1882–1890, 2010.

[33] Y. Hao, K. Nagase, K. Hori et al., "Xilei San ameliorates experimental colitis in rats by selectively degrading proinflammatory mediators and promoting mucosal repair," *Evidence-Based Complementary and Alternative Medicine*, vol. 2014, Article ID 569587, 10 pages, 2014.

[34] L. A. Boxer, "Role of neutrophils in genetic disorders of phagocyte function leading to IBD," *Journal of Pediatric Gastroenterology and Nutrition*, vol. 46, supplement 1, p. E17, 2008.

[35] Y. Xu, N. H. Hunt, and S. Bao, "The role of granulocyte macrophage-colony-stimulating factor in acute intestinal inflammation," *Cell Research*, vol. 18, no. 12, pp. 1220–1229, 2008.

[36] J. Zhao, T. Hong, M. Dong, Y. Meng, and J. Mu, "Protective effect of myricetin in dextran sulphate sodium-induced murine ulcerative colitis," *Molecular Medicine Reports*, vol. 7, no. 2, pp. 565–570, 2013.

[37] D. Lau, H. Mollnau, J. P. Eiserich et al., "Myeloperoxidase mediates neutrophil activation by association with CD11b/CD18 integrins," *Proceedings of the National Academy of Sciences of the United States of America*, vol. 102, no. 2, pp. 431–436, 2005.

[38] M. F. Neurath, S. Finotto, and L. H. Glimcher, "The role of TH1/TH2 polarization in mucosal immunity," *Nature Medicine*, vol. 8, no. 6, pp. 567–573, 2002.

[39] S. Molesworth-Kenyon, A. Mates, R. Yin, R. Strieter, J. Oakes, and R. Lausch, "CXCR3, IP-10, and Mig are required for $CD4^+$ T cell recruitment during the DTH response to HSV-1 yet are independent of the mechanism for viral clearance," *Virology*, vol. 333, no. 1, pp. 1–9, 2005.

[40] P. Romagnani, F. Annunziato, L. Lasagni et al., "Cell cycle-dependent expression of CXC chemokine receptor 3 by endothelial cells mediates angiostatic activity," *Journal of Clinical Investigation*, vol. 107, no. 1, pp. 53–63, 2001.

[41] X. Zhang, J. Han, K. Man et al., "CXC chemokine receptor 3 promotes steatohepatitis in mice through mediating inflammatory cytokines, macrophages and autophagy," *Journal of Hepatology*, vol. 64, no. 1, pp. 160–170, 2016.

[42] G. C. Farrell, D. van Rooyen, L. Gan, and S. Chitturi, "NASH is an inflammatory disorder: pathogenic, prognostic and therapeutic implications," *Gut and Liver*, vol. 6, no. 2, pp. 149–171, 2012.

Hindawi Publishing Corporation
Evidence-Based Complementary and Alternative Medicine
Volume 2016, Article ID 9580234, 14 pages
http://dx.doi.org/10.1155/2016/9580234

Research Article

Vascular Protective Role of Samul-Tang in HUVECs: Involvement of Nrf2/HO-1 and NO

Eun Sik Choi,[1,2] Yun Jung Lee,[1,2] Chang Seob Seo,[3] Jung Joo Yoon,[1,2] Byung Hyuk Han,[1,2] Min Cheol Park,[4] Dae Gill Kang,[1,2] and Ho Sub Lee[1,2]

[1]*College of Oriental Medicine and Professional Graduate School of Oriental Medicine, Wonkwang University, 460 Iksandae-ro, Iksan, Jeonbuk 54538, Republic of Korea*
[2]*Hanbang Body-Fluid Research Center, Wonkwang University, 460 Iksandae-ro, Iksan, Jeonbuk 54538, Republic of Korea*
[3]*K-Herb Research Center, Korea Institute of Oriental Medicine, 1672 Yuseong-daero, Yuseong-gu, Daejeon 34054, Republic of Korea*
[4]*Department of Oriental Medical Ophthalmology & Otolaryngology & Dermatology, College of Oriental Medicine, Wonkwang University, 460 Iksandae-ro, Iksan, Jeonbuk 54538, Republic of Korea*

Correspondence should be addressed to Dae Gill Kang; dgkang@wku.ac.kr and Ho Sub Lee; host@wku.ac.kr

Received 11 January 2016; Revised 19 April 2016; Accepted 5 May 2016

Academic Editor: Ying-Ju Lin

Samul-Tang (Si-Wu-Tang, SMT), composed of four medicinal herbs, is a well-known herbal formula treating hematological disorder or gynecologic disease. However, vascular protective effects of SMT and its molecular mechanisms on the vascular endothelium, known as the central spot of vascular inflammatory process, are not reported. The aim of this study was to investigate vascular protective effects of SMT water extract in human umbilical vein endothelial cells (HUVECs). Water extract of SMT was prepared and identified by HPLC-PDA analysis. Expression of cell adhesion molecules (CAMs) and heme oxygenase-1 (HO-1) and translocation of nuclear factor-kappa B (NF-κB) and nuclear factor-erythroid 2-related factor 2 (Nrf2) were determined by western blot. Nuclear localization of NF-κB and Nrf2 was visualized by immunofluorescence and DNA binding activity of NF-κB was measured. ROS production, HL-60 monocyte adhesion, and intracellular nitric oxide (NO) were also measured using a fluorescent indicator. SMT suppressed NF-κB translocation and activation as well as expression of CAMs, monocyte adhesion, and ROS production induced by TNF-α in HUVECs. SMT treated HUVECs showed upregulation of HO-1 and NO which are responsible for vascular protective action. Our study suggests that SMT, a traditionally used herbal formula, protects the vascular endothelium from inflammation and might be used as a promising vascular protective drug.

1. Introduction

Patients with vascular dysfunction are more likely to develop several complications like hypertension, congestive heart failure, angina pectoris, thrombosis, and atherosclerosis and these are pathologically related to each other. Recent studies suggest that the vascular endothelium, the inner lumen of blood vessels, is emphasized as the central spot of vascular inflammatory process [1]. The endothelium regulates vascular tone, proliferation, and permeability of inflammatory inducers or infiltration of leukocytes [2]. For inflammatory cascade to occur, selectins and CAMs (cellular adhesion molecules) are required which are expressed by inflammatory cytokines such as TNF-α [3] and ROS/NF-κB pathway plays as a key mediator [4, 5]. TNF-α increases production of ROS (reactive oxygen species), stimulating redox signaling pathways resulting in atherogenesis [6], and stimulates NF-κB (nuclear factor-kappa B), a transcription factor mediating the expression of inflammatory genes such as CAMs [7].

Conversely, some genes including HO-1 (heme oxygenase-1) are involved in vascular protection against inflammatory process. HO-1 is an enzyme that catalyzes degradation of heme to ferric iron, CO (carbon monoxide), and biliverdin [8], which is converted to bilirubin by biliverdin reductase [9]. Metabolites (ferric iron, CO, and bilirubin) produced by HO-1 are known to have antioxidative, anti-inflammatory, and antiatherogenic effects [10, 11]. In addition, HO-1 expression can also suppress atherosclerosis resulting from

environmental factors such as smoking and air pollution [12]. NO (nitric oxide) is known as a vasodilator that can relax smooth muscle but also exerts antiatherogenic actions to inhibit adhesion of leukocyte and platelet on the endothelium [13].

Samul-Tang (SMT), also known as Si-Wu-Tang or the four-agent decoction, is a well-known herbal prescription traditionally used to treat women's illnesses such as anemia [14], dysmenorrhea [15, 16], and postpartum weakness resulting from hematological disorders defined as blood deficiency and blood stasis in traditional Korean medicine. SMT is recorded in several formularies including *Treasured Mirror of Eastern Medicine* (*Donguibogam*) and consists of 4 medical herbs: Angelicae Gigantis Radix (*Angelica gigas* Nakai, root), Cnidii Rhizoma (*Ligusticum officinale* Makino, rhizome), Rehmanniae Radix Preparata (*Rehmannia glutinosa* Gaertn. DC., rhizome, steamed and dried), and Paeoniae Radix (*Paeonia lactiflora* Pall., root). Recently, pharmacological studies were performed with SMT and it was proven to exert hematopoietic [17, 18], antipruritic [19], and antidermatitis [20] effects. To our knowledge, though tonifying effects of SMT are well known [21], vascular protective effects of SMT and its molecular mechanisms are not reported yet. Here, we report effects of SMT water extracts as a complementary or alternative therapeutic drug on vascular inflammation in human umbilical vein endothelial cells (HUVECs).

2. Materials and Methods

2.1. Plant Materials. The four crude herbs forming SMT were purchased from Omniherb (Yeongcheon, Korea) in February 2008. The origin of each herbal medicine was taxonomically identified by Professor Je Hyun Lee, Dongguk University, Gyeongju, Korea. A voucher specimen (2008-KE25-1~KE25-4) has been deposited at the K-Herb Research Center, Korea Institute of Oriental Medicine.

2.2. Chemicals and Reagents. Ferulic acid and 5-hydroxymethyl-2-furaldehyde (5-HMF) were purchased from Sigma-Aldrich (St. Louis, MO, USA). Albiflorin and paeoniflorin were the products of Wako (Osaka, Japan). Nodakenin was purchased from NPC BioTechnology Inc. (Daejeon, Korea). The purity of all reference standards was ≥98.0%. HPLC-grade methanol, acetonitrile, and water were obtained from J.T.Baker (Phillipsburg, NJ, USA). Glacial acetic acid, analytical reagent grade, was purchased from Junsei (Tokyo, Japan). RPMI 1640, fetal bovine serum, TNF-α, tissue culture reagents, 2′,7′-bis(2-carboxyethyl)-5(6)-carboxyfluorescein acetoxy-methylester (BCECF-AM), DAF-FM diacetate, and CM-H_2DCFDA, Alexa Fluor 488 and 594 conjugated second antibodies were purchased from Invitrogen (San Diego, CA). Biotin 3′ End DNA Labeling Kit, LightShift® Chemiluminescent EMSA Kit, Biodyne® Precut Nylon Membranes, Lipofectamine LTX reagent, and *Renilla*-Firefly Luciferase Dual Assay Kit were purchased from Pierce Biotechnology (Rockford, USA). Primary antibodies, including mouse anti-ICAM-1, goat anti-VCAM-1, rabbit anti-E-selectin, mouse anti-NF-κB, mouse anti-p-IκB-α, rabbit anti-HO-1, and rabbit anti-Nrf2, were purchased from Santa Cruz Biotechnology (CA, USA). Donkey anti-goat IgG-H+I were purchased from Bethyl (Montgomery, USA) and goat anti-rabbit IgG and goat anti-mouse IgG were purchased from Enzo (Farmingdale, USA).

2.3. Preparation of SMT Decoction. SMT extract was deposited at the Herbarium of the K-Herb Research Center, Korea Institute of Oriental Medicine (Daejeon, Korea). SMT (18.76 g) is composed of four herbs, Angelica Gigantis Radix (*Angelica gigas* Nakai, root, 4.69 g), Cnidii Rhizoma (*Ligusticum officinale* Makino, rhizome, 4.69 g), Rehmanniae Radix Preparata (*Rehmannia glutinosa* (Gaertn.) DC., rhizome, steamed and dried, 4.69 g), and Paeoniae Radix (*Paeonia lactiflora* Pall., root, 4.69 g). Totally, 2.0 kg of SMT was extracted in distilled water at 100°C for 2 h using an electric extractor (COSMOS-660; Kyungseo Machine Co., Incheon, Korea). The solution was filtered using a standard sieve (number 270, 53 μm; Chung Gye Sang Gong Sa, Seoul, Korea), evaporated to dryness at 40°C under vacuum (Eyela N-11, Tokyo, Japan), and freeze-dried (PVTFD10RS, ilShinBioBase, Yangju, Korea) and retained at −70°C until required. The amount of water extract was 667.3 g (yield: 33.3%).

2.4. High-Performance Liquid Chromatography (HPLC) Analysis of SMT. The chromatographic analysis was performed using the Shimadzu Prominence LC-20A series (Shimadzu Co., Kyoto, Japan) consisting of a solvent delivery unit (LC-20AT), online degasser (DGU-$20A_3$), column oven (CTO-20A), autosample injector (SIL-20AC), and photodiode array detector (PDA, SPD-M20A). The data were acquired and processed by LCsolution software (Version 1.24). All analytes were separated on a Phenomenex Gemini C18 (250 × 4.6 mm, 5 μm, Torrance, CA, USA) and maintained at 40°C. The mobile phases consisted of 1.0% (v/v) aqueous acetic acid (A) and 1.0% (v/v) acetic acid in acetonitrile (B). The gradient flow was as follows: 5–60% B for 0–40 min, 60–100% B for 40–45 min, 100% B for 45–50 min, and 100–5% B for 50–55 min. The flow-rate was kept 1.0 mL/min and injection volume was 10 μL. The analytes were detected at 230 nm for albiflorin and paeoniflorin, 280 nm for 5-HMF, 320 nm for ferulic acid, and 330 nm for nodakenin. For quantitative analysis, lyophilized SMT extract (200 mg) was dissolved in 20 mL of distilled water and then the solution was filtered through a 0.2 μm GHP syringe filter (SmartPor, PALL Life Sciences, Ann Arbor, MI, USA) before HPLC injection.

2.5. Cell Cultures. Human umbilical vein endothelial cells (HUVECs) and HL-60, human promyelocytic leukemia cell line, were purchased from the American Type Culture Collection (ATCC, Manassas, VA). Cells were cultured with RPMI 1640 containing 10% fetal bovine serum and penicillin-streptomycin and maintained in a humidified incubator containing 5% CO_2 at 37°C.

2.6. Western Blot Analysis. Cell homogenates were separated on 10% SDS-polyacrylamide gel electrophoresis and transferred to nitrocellulose paper. Blots were then washed with

H_2O, blocked with 5% skimmed milk powder in tris-buffered saline Tween-20 (TBS-T) (10 mM tris-HCl, pH 7.6, 150 mM NaCl, and 0.05% Tween-20) for 1 h, and incubated with the appropriate primary antibody at dilutions recommended by the supplier. Then the membrane was washed, and primary antibodies were detected with secondary antibodies conjugated to horseradish peroxidase, and the bands were visualized with enhanced chemiluminescence (Amersham Bioscience, Buckinghamshire, UK). Protein expression levels were determined by analyzing the signals captured on the nitrocellulose membranes using the ChemiDoc image analyzer (Bio-Rad Laboratories, Hercules, CA).

2.7. Preparation of Cytoplasmic and Nucleus Extracts. The cells were scraped in cold PBS on ice and centrifuged at 13,000 rpm for 10 min at 4°C. Nuclear and cytoplasmic extracts were extracted with NE-PER Nuclear and Cytoplasmic Extraction Reagents (Pierce Biotechnology). After cytosolic protein was extracted with cytoplasmic extraction reagents I and II, nuclear pellet was then resuspended with 100 μL of nuclear extraction reagent. Nuclear protein extracts were immediately transferred to a clean prechilled tube and all extracts were stored at −80°C until use.

2.8. Monocyte-HUVEC Adhesion Assay. In adhesion assay, 1.2×10^6 of HUVECs were seeded in 24-well plates. HUVECs were grown to confluence in 24-well culture plates, pretreated with SMT for 30 min, and stimulated with TNF-α for 6 h. Then the HL-60 cells were labeled with 10 μM BCECF-AM for 1 h at 37°C and washed twice with growth medium. This was followed by adding 2.5×10^5 of the labeled HL-60 cells to the HUVEC and incubating them in a CO_2 incubator for 1 h. The nonadherent HL-60 cells were removed from the plate by washing with PBS, and the HL-60 cells bound to the HUVEC were measured by fluorescence microscopy and then lysed with 50 mM tris-HCI, pH 8.0, containing 0.1% SDS. The fluorescent intensity was measured using a spectrofluorometer (Infinite F200 PRO, TECAN) at excitation and emission wavelengths of 485 and 535 nm, respectively.

2.9. Intracellular ROS Production Assay. The fluorescent probe, CMH_2DCFDA, was used to determine the intracellular generation of ROS. Briefly, the confluent HUVECs in the 24-well culture plates were pretreated with SMT for 30 min. After removing from the wells, the HUVECs were incubated with 20 μM CM-H_2DCFDA for 6 h and then stimulated with TNF-α. The fluorescence intensity was measured by spectrofluorometer (Infinite F200 PRO, TECAN) and examined under a fluorescence microscope (Eclipse Ti, Nikon).

2.10. Intracellular NO and Nitrite Production Assay. The fluorescent probe, DAF-FM diacetate, was used to determine the intracellular generation of NO. The confluent HUVECs in the 6-well culture plates were pretreated with DAF-FM for 1 h. After removing excess probe from the wells, the HUVECs were treated with SMT for 30 min. The fluorescence intensity was measured by a spectrofluorometer (Infinite F200 PRO, TECAN) and examined under a fluorescence microscope (Eclipse Ti, Nikon). Nitrites were measured with 50 μL of cell cultured medium, Griess assay solution, 50 μL of 1% solution of sulfanilamide diluted in 5% phosphoric acid, 50 μL of 0.1% N-1-napthylethylenediamine dihydrochloride (NED) diluted in sterile water. Sodium nitrite (1–100 μM) was used to set standard curve. Absorbance was read at 540 nm using a spectrometer (Infinite F200 PRO, TECAN).

2.11. Electrophoretic Mobility Shift Assay (EMSA). EMSA for NF-κB was performed in the nuclear fraction using LightShift Chemiluminescent EMSA Kit (Pierce Biotechnology, Rockford, IL) following the manufacturer's protocol. Briefly, DNA was biotin-labeled using the biotin 3′ end-labeling kit (Pierce Biotechnology), ds NF-κB oligonucleotide (5′-AGTTGAGGGGACTTTCCCAGGC-3′ and 3′-TCAACTCCCCTGAAAGGGTCCG-5′) incubated in a tube with terminal deoxynucleotidyl transferase (TdT) buffer, and ultrapure water at 37°C for 30 minutes. To extract labeled DNA, chloroform : isoamyl alcohol (24 : 1) was added and centrifuged at 13,000 rpm. The top aqueous phase containing the labeled DNA was further used and each binding reaction contained 1x binding buffer (100 mM tris, 500 mM KCl, and 10 mM dithiothreitol, pH 7.5), 2.5% glycerol, 5 mM $MgCl_2$, 50 ng/mL poly(dI–dC), 0.05% NP-40, 2.5 mg of nuclear extract, and 20 to 50 fmol of biotin end-labeled target DNA. The contents were incubated at room temperature for 20 minutes. To this reaction mixture, loading buffer was added, subjected to gel electrophoresis on a native polyacrylamide gel, and transferred to a nylon membrane. After transfer was completed, DNA was cross-linked to the membrane at 120 mJ/cm^2 using a UV cross-linker equipped with 254 nm bulb. The biotin end-labeled DNA was detected using streptavidin-HRP conjugate and a chemiluminescent substrate. The membrane was developed using ChemiDoc (Bio-Rad).

2.12. Luciferase Promoter Assay. Sixty to seventy percent confluent cells were transiently cotransfected with the plasmids using Lipofectamine LTX (Invitrogen, Carlsbad, CA) according to the manufacturer's protocol. Briefly, transfection mixture containing 5 μg of the pGL3-NF-κB-Luc or *Renilla* and 5 μL of media was mixed with the Lipofectamine LTX reagent and added to the cells. After 48 h, the cells were treated with SMT for 30 min and stimulated with TNF-α for 6 h and then lysed. The luciferase activities were determined using *Renilla*-Firefly Luciferase Dual Assay Kit (Thermo Scientific, Rockford, IL). The luciferase assay activity was normalized with respect to the *Renilla* activity and was expressed as a percentage of the activity of the control.

2.13. Immunofluorescence Microscopy. For localization of NF-κB and Nrf2, HUVECs were grown on cover glass and treated as described in all figures' captions. Cells were then fixed in 1% formaldehyde and permeabilized with 0.1% Triton X-100. The cells were probed with NF-κB or Nrf2 antibody followed by Alexa Fluor 488 or 594 conjugated secondary antibody, respectively. To visualize the nuclei, cells were then treated with 1 μg/mL of DAPI for 10 min. Cells were finally washed three times with PBS, and coverslips were mounted with

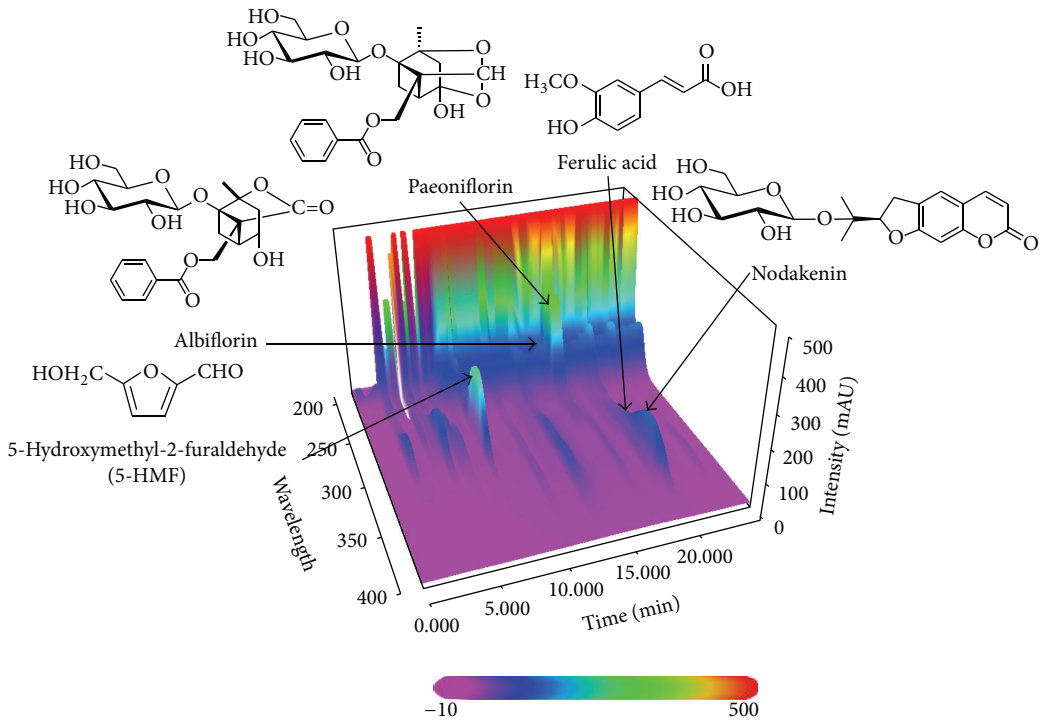

Figure 1: Three-dimensional chromatogram of Samul-Tang by HPLC-PDA.

mounting solution onto glass slides and examined under a fluorescence microscope (Eclipse Ti, Nikon).

2.14. Statistical Analysis. All the experiments were repeated at least three times. The results were expressed as a mean ± SE, and the data were analyzed using one-way ANOVA followed by Student's t-test to determine any significant differences. $p < 0.05$ was considered as statistically significant.

3. Results

3.1. HPLC Analysis of SMT. The developed HPLC-PDA method was subsequently applied for the quantitative analysis of the five marker compounds in SMT. Consequently, five compounds were eluted within 30 min and typical three-dimensional chromatogram using HPLC-PDA detector is shown in Figure 1. The retention times of the five marker components, 5-HMF, albiflorin, paeoniflorin, ferulic acid, and nodakenin, were 8.07, 16.05, 17.00, 19.65, and 20.15 min, respectively. The correlation coefficient (r^2) of the five compounds showed good linearity as ≥0.9999. Using optimized chromatography conditions, the amounts of the five compounds, 5-HMF, albiflorin, paeoniflorin, ferulic acid, and nodakenin, in SMT were 2.79 ± 0.04, 2.91 ± 0.06, 15.18 ± 0.12, 1.08 ± 0.02, and 5.99 ± 0.10 mg/g, respectively.

3.2. Effect of SMT on TNF-α Induced Expression of Cell Adhesion Molecules in HUVECs. MTT assay was performed to investigate cytotoxic potential of SMT on HUVECs. Cells were treated with different concentrations of SMT (10–200 μg/mL) for 24 h and performed as described in Section 2. Cell viability of HUVECs was not influenced by treatment of SMT alone in all concentrations ranging from 10 to 200 μg/mL concentration. On the basis of this result, concentration of SMT was less than 200 μg/mL in following experiments (data not shown). To investigate the effects of SMT on expression of cell adhesion molecules (CAMs) such as ICAM-1 (intracellular adhesion molecule-1), VCAM-1 (vascular cell adhesion molecule-1), and E-selectin (endothelial-selectin) induced by TNF-α in HUVECs, western blot was performed. As shown in Figure 2, 6 h of induction with TNF-α (50 ng/mL) significantly upregulated protein expression of VCAM-1, ICAM-1, and E-selectin compared to the control group ($^{*}p < 0.05$), whereas SMT pretreatment for 30 min inhibited VCAM, ICAM, and E-selectin expression against TNF-α induction over 30 μg/mL ($^{\#}p < 0.05$, $^{\#\#}p < 0.01$).

3.3. Effect of SMT on TNF-α Induced Monocyte Adhesion in HUVECs. Adhesion of BCECF-AM labeled HL-60 monocyte to HUVECs induced by TNF-α (50 ng/mL) was investigated. As shown in Figure 3, green fluorescent probes represent BCECF-AM labeled HL-60 cells. Monocyte adhesion was significantly increased by induction of TNF-α (50 ng/mL) for 6 h compared to the control group ($^{*}p < 0.05$), whereas SMT (50 μg/mL) pretreatment for 30 min significantly suppressed adhesion of HL-60 monocyte to HUVECs ($^{\#}p < 0.05$).

3.4. Effect of SMT on TNF-α Induced ROS Production in HUVECs. Intracellular production of ROS induced by TNF-α (50 ng/mL) was investigated. As shown in Figure 4, green fluorescent H_2DCFDA represents generated ROS. TNF-α

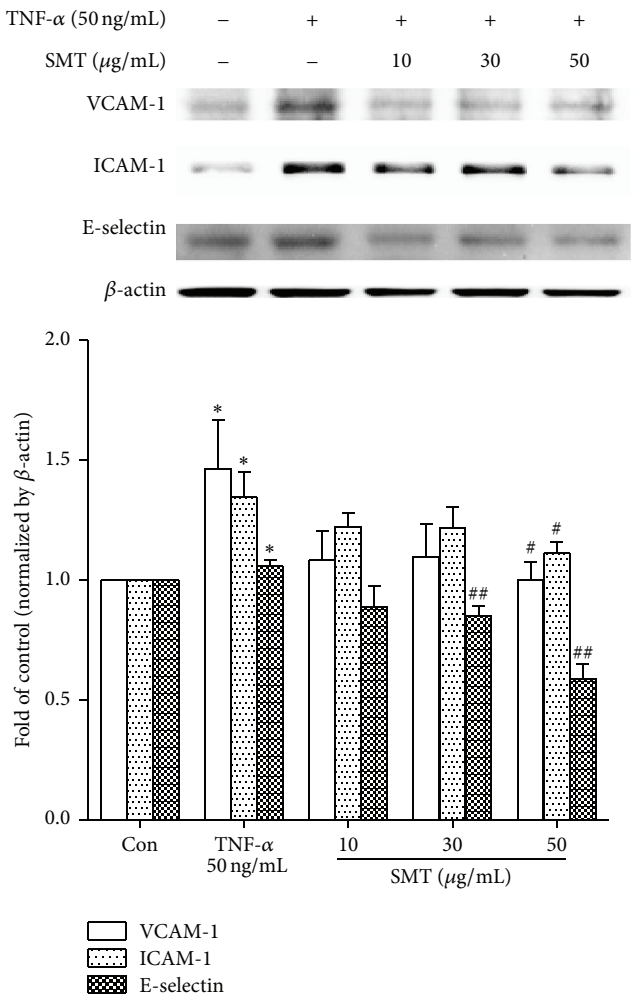

Figure 2: Effects of SMT on TNF-α induced cell adhesion molecules expression in HUVECs. Cells were treated with TNF-α (50 ng/mL) for 6 h in the absence or pretreatment of SMT (10, 30, and 50 μg/mL) for 30 min. Bar represents the mean ± SEM of 3 independent experiments. $^{*}p < 0.05$ versus con group. $^{\#}p < 0.05$ and $^{\#\#}p < 0.01$ versus TNF-α group.

(50 ng/mL) induced HUVECs produced ROS compared to the unstimulated control group ($^{*}p < 0.05$). However, SMT pretreatment inhibited ROS production against TNF-α induction and was significant in concentration of 50 μg/mL ($^{\#}p < 0.05$). Also, NAC (N-acetyl-L-cysteine), ROS scavenger, significantly blocked the production of ROS against TNF-α induction ($^{\#}p < 0.05$).

3.5. Effect of SMT on TNF-α Induced NF-κB Translocation in HUVECs. Nuclear and cytosol fraction extracts were isolated from HUVECs and western blot was performed to investigate effect of SMT on TNF-α induced phosphorylation of IκB-α and NF-κB translocation. As shown in Figure 5(a), phosphorylation of IκB-α was significantly upregulated by induction of TNF-α (50 ng/mL) for 1 h ($^{*}p < 0.05$); however, pretreatment of SMT for 30 min attenuated phosphorylation of IκB-α and was significant in 30 and 50 μg/mL ($^{\#}p < 0.05$).

As shown in Figure 5(b) nuclear extract (NE) protein level of NF-κB was significantly upregulated by TNF-α (50 ng/mL) induction compared to the control group ($^{**}p < 0.01$) and this means NF-κB translocated from the cytoplasm into the nucleus. Pretreatment of SMT for 30 min (10, 30, and 50 μg/mL) significantly inhibited translocation of NF-κB ($^{\#\#}p < 0.01$). To visualize nuclear localization of NF-κB, immunofluorescence was performed (Figure 5(c)). Green fluorescent NF-κB is translocated into the nucleus by induction of TNF-α (50 ng/mL) for 1 h compared to the control group. SMT pretreatment for 30 min inhibited translocation of NF-κB induced by TNF-α (50 ng/mL).

3.6. Effect of SMT on TNF-α Induced NF-κB Activation in HUVECs. Electrophoretic mobility shift assay (EMSA) and luciferase assay were performed to determine effect of SMT on TNF-α induced NF-κB activation for further confirmation. In EMSA, as shown in Figure 6(a), NF-κB-DNA binding complex shift is detected (Lanes 2–6) in nuclear protein added sample, but sample additionally added with a 20-fold excess of unlabeled oligonucleotide (Lane 7) did

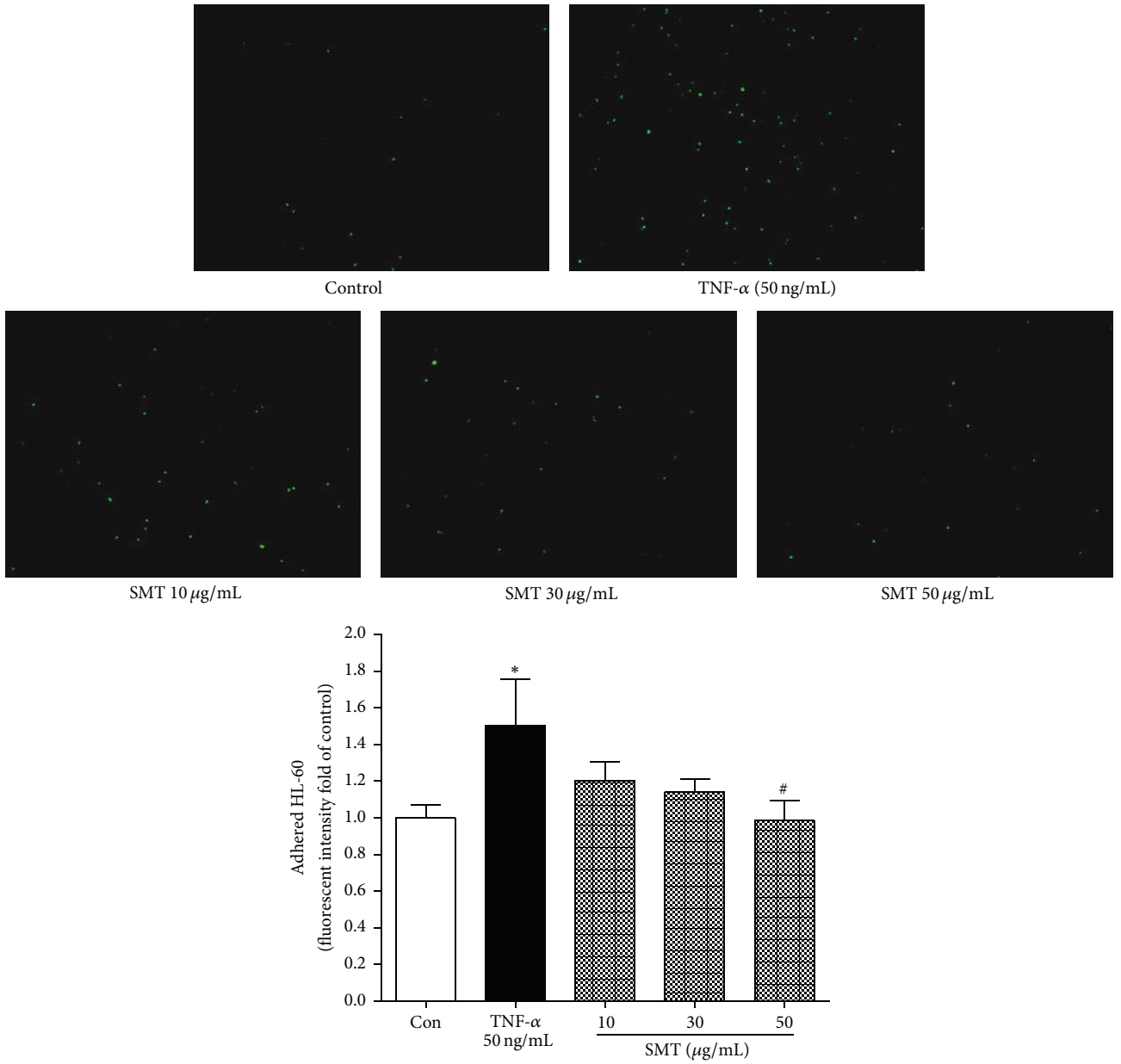

Figure 3: Effects of SMT on TNF-α induced cell adhesion of HL-60 in HUVECs. HUVECs were treated with TNF-α (50 ng/mL) for 6 h in the absence or pretreatment of SMT (10, 30, and 50 μg/mL) for 30 min and then incubated with BCECF-AM labeled HL-60 cells. Adhered monocytes were captured with fluorescent microscope. Bar represents the mean ± SEM of more than 3 independent experiments. $^{*}p < 0.05$ versus con group. $^{\#}p < 0.05$ versus TNF-α group.

not show NF-κB-DNA binding complex shift indicating that specific competitive reaction occurred and band was a NF-κB specific shift. TNF-α (50 ng/mL) induction for 1 h (Lane 3) upregulated NF-κB-DNA binding activity compared to the control group (Lane 2). SMT (10, 30, and 50 μg/mL) pretreatment for 30 min (Lanes 4–6) inhibited NF-κB-DNA binding activity against TNF-α induction in HUVECs.

As shown in Figure 6(b), luciferase promoter activity of TNF-α (50 ng/mL) treated cells was significantly increased compared to the control group ($^{**}p < 0.01$). However, cells pretreated with SMT for 30 min inhibited luciferase activity against TNF-α (50 ng/mL) induction and were significant in concentration of 30 and 50 μg/mL ($^{\#\#}p < 0.01$).

3.7. Effect of SMT on HO-1 Expression and ROS Production in HUVECs. To investigate whether SMT itself upregulates HO-1 protein expression in HUVECs, 50 μg/mL of SMT is treated for 1~12 h. As shown in Figure 7(a), 12 h of SMT (50 μg/mL) treatment significantly reached maximum HO-1 protein level ($^{**}p < 0.01$). To confirm effect of SMT on HO-1 protein expression, SnPP (tin protoporphyrin, HO-1 inhibitor) and CoPP (cobalt protoporphyrin, HO-1 inducer)

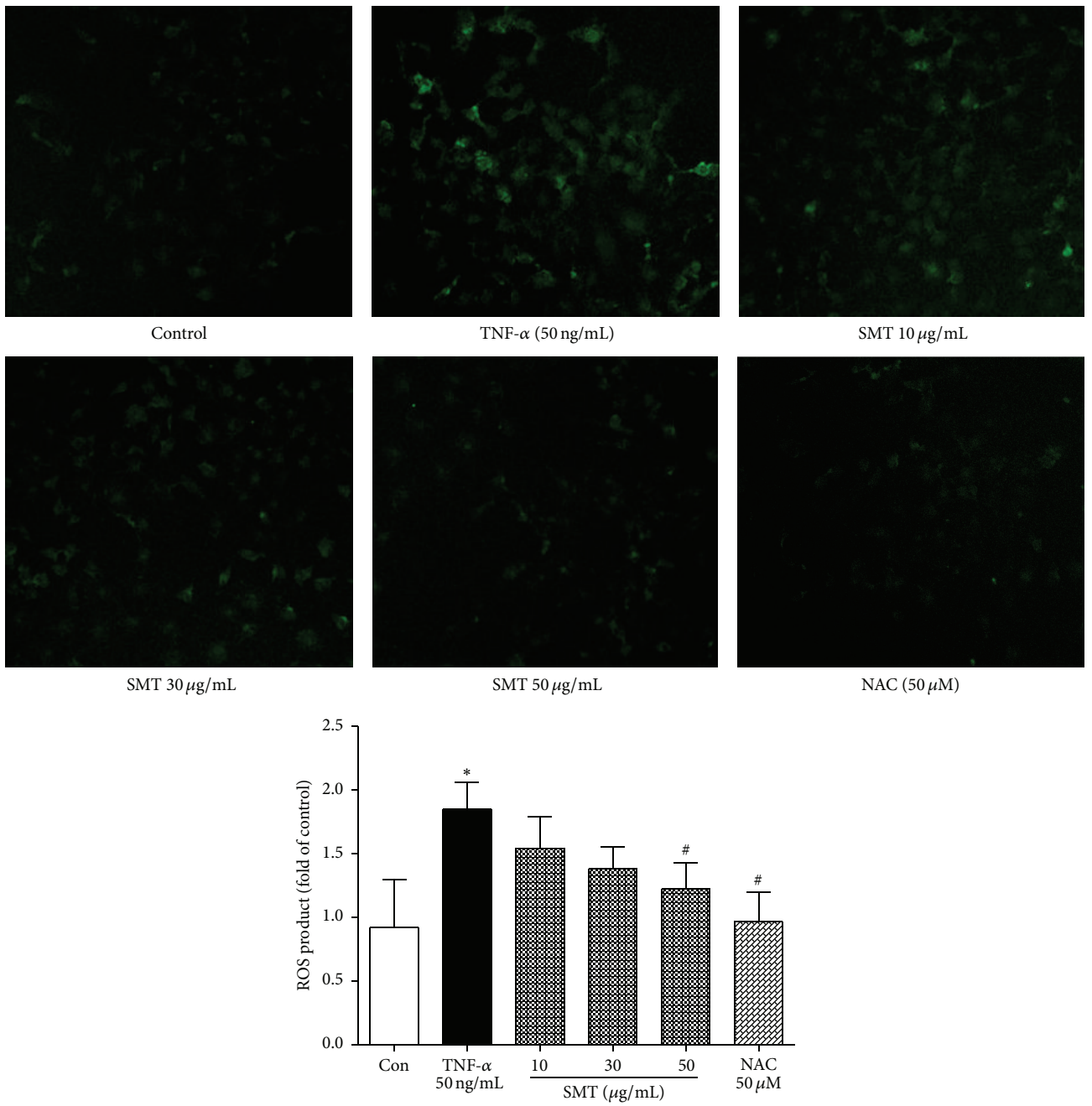

Figure 4: Effects of SMT on TNF-α induced intracellular ROS production in HUVECs. Cells were treated with TNF-α (50 ng/mL) for 6 hours in the absence or pretreatment of SMT (10, 30, and 50 μg/mL) for 30 min and then treated with H_2DCFDA. NAC (N-acetyl-L-cysteine) was used as ROS scavenger. Bar represents the mean ± SEM of more than 3 independent experiments. $^{*}p < 0.05$ versus con group. $^{\#}p < 0.05$ versus TNF-α group.

were used. As shown in Figure 7(b), 12 h of SMT treatment upregulated HO-1 expression and was significant in concentration of 30 and 50 μg/mL ($^{*}p < 0.05$); however, SnPP totally inhibited those effects ($^{\#}p < 0.05$). CoPP dramatically upregulates HO-1 protein level ($^{**}p < 0.01$). In addition, ROS was not produced by SMT treatment which means HO-1 was induced via ROS independent pathway (Figure 7(c)).

3.8. Effect of SMT on Nrf2 Translocation in HUVECs. To further investigate HO-1/Nrf2 pathway, nuclear and cytosol fraction was isolated and western blot performed. SMT (50 μg/mL) is treated for 0.5~6 h. As shown in Figure 8(a), 1 h of SMT (50 μg/mL) treatment significantly reached maximum nuclear Nrf2 protein level ($^{*}p < 0.05$). HO-1 induction by SMT treatment was significant in concentration of 30 and

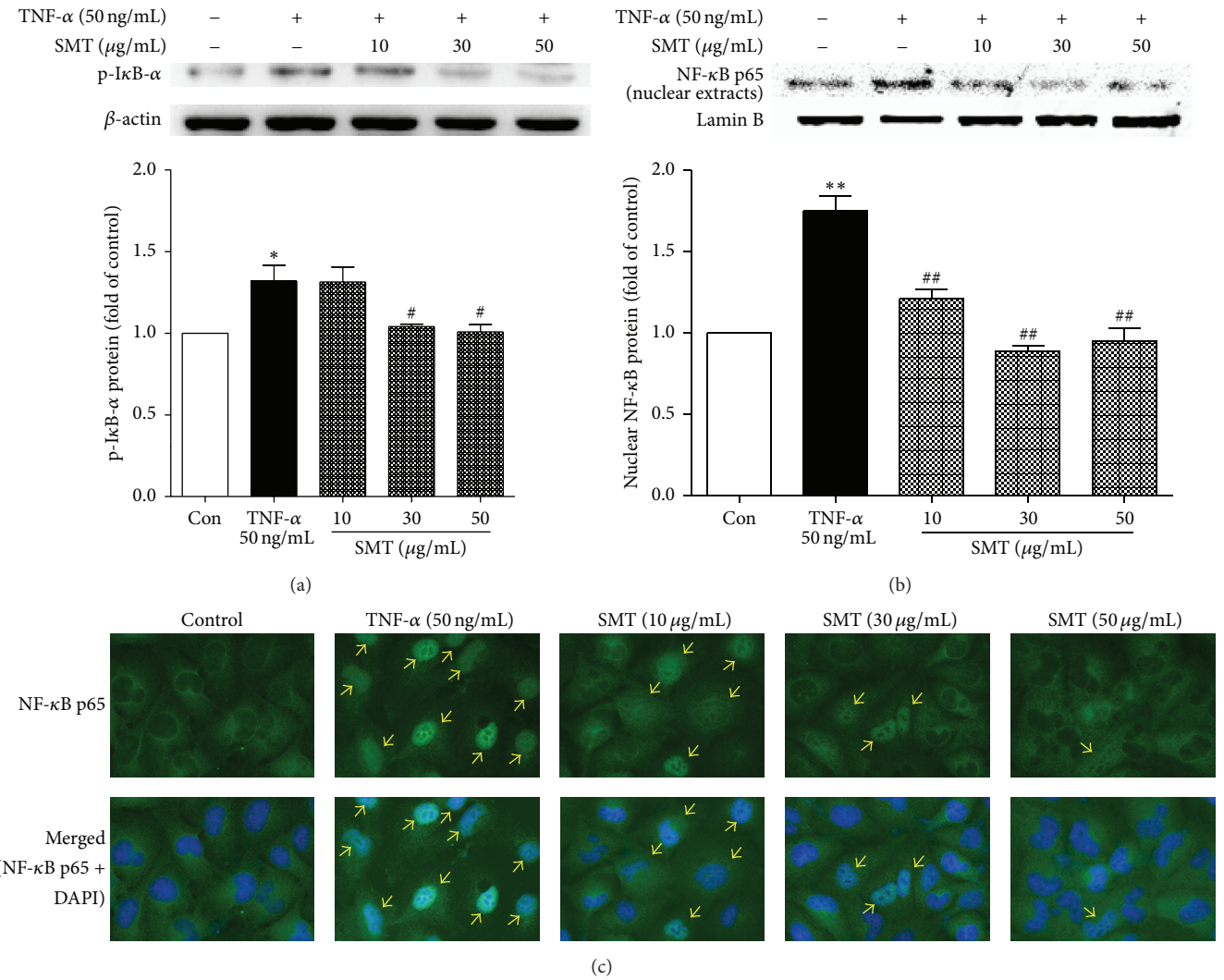

Figure 5: (a) Effects of SMT on TNF-α induced phosphorylation of IκB-α in HUVECs. (b, c) Effects of SMT on TNF-α induced NF-κB translocation in HUVECs. Cells were treated with TNF-α (50 ng/mL) for 1 hour in the absence or pretreatment of SMT (10, 30, and 50 μg/mL) for 30 min. NF-κB protein was detected by western blot and immunofluorescence. (Green: NF-κB, blue: nucleus; magnification: 400x.) Bar represents the mean ± SEM of 3 independent experiments. $^{*}p < 0.05$ and $^{**}p < 0.01$ versus con group. $^{\#}p < 0.05$ and $^{\#\#}p < 0.01$ versus TNF-α group.

50 μg/mL (Figure 8(b)). Immunofluorescence was performed to visualize Nrf2 localization (Figure 8(c)). Red fluorescent Nrf2 was translocated into the nucleus by SMT treatment.

3.9. Effect of SMT on NO Synthesis. We measured intracellular NO and supernatant nitrite level to investigate NO synthesis ability of SMT on HUVECs. As shown in Figure 9(a), acetylcholine treatment resulted in intracellular NO synthesis and reacted with DAF-FM to fluoresce green. SMT treated HUVECs also synthesized NO and were significant in concentration of 50 μg/mL ($^{**}p < 0.01$). Nitrite level accumulated in supernatant of cultured medium measured by Griess assay was also increased by 24 h treatment of SMT (Figure 9(b)). The result showed a dose-dependent manner and was significant in 30 ($^{*}p < 0.01$) and 50 ($^{**}p < 0.05$) μg/mL.

4. Discussion

This study showed that SMT suppressed expression of CAMs and monocyte adhesion via inhibition of ROS/NF-κB activation induced by TNF-α and upregulated HO-1 and NO production in HUVECs. The major cause of atherosclerosis and other vascular diseases is chronic vascular inflammation and is initiated by proinflammatory cytokines such as TNF-α. TNF-α is produced from endothelial tissue resident immune cells, to upregulate the expression of adhesion molecules on endothelial cells [22]. Expression of CAMs such as ICAM-1, VCAM-1, and E-selectin mediates proinflammatory state and leads to formation of atheroma resulting in atherosclerosis [23, 24]. Pretreatment with SMT suppressed expression of ICAM-1, VCAM-1, and E-selectin and consequently attenuated adhesion of HL-60 monocytes

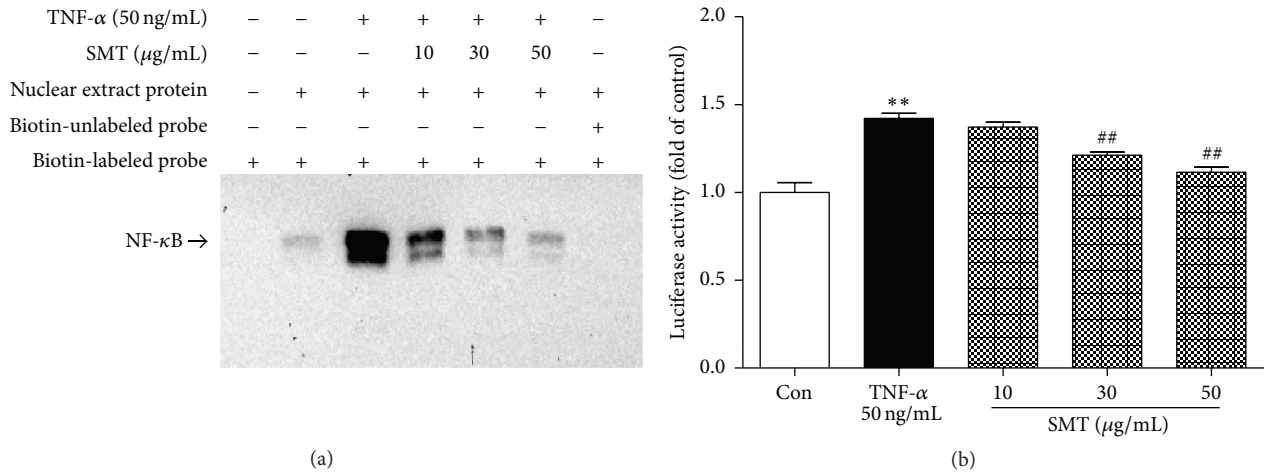

FIGURE 6: Effect of SMT on TNF-α induced NF-κB activation in HUVECs. Cells were treated with TNF-α (50 ng/mL) for 1 hour in the absence or pretreatment of SMT (10, 30, and 50 μg/mL) for 30 min and nuclear extracts were prepared to perform (a) electrophoretic mobility shift assay (EMSA) and (b) luciferase promoter assay. Bar represents the mean ± SEM of 3 independent experiments. $^{**}p < 0.01$ versus con group. $^{\#\#}p < 0.01$ versus TNF-α group.

induced by TNF-α in HUVECs. In expression of CAMs, NF-κB activation is prerequisite and ROS have been implicated in all stages of atherosclerosis [10, 11] acting as second messenger [25]. ROS production results in phosphorylation of I-κB-α and translocates NF-κB into the nucleus. Therefore we further investigated ROS production and NF-κB activation, upstream factor affecting expression of inflammatory genes including CAMs in HUVECs. IκB-α (inhibitory κB-α) is bound with NF-κB and inhibits translocation of NF-κB into the nucleus. Evaluating the concerned pathway, SMT pretreatment is found to suppress intracellular ROS production and phosphorylation of IκB-α. These phenomena led to suppression of nuclear localization of NF-κB and furthermore, results of EMSA and luciferase promoter assay showed NF-κB-DNA binding activity was also suppressed by SMT pretreatment. SMT attenuated vascular inflammation by suppressing expression of CAMs, primarily resulting from inhibiting NF-κB translocation and ROS production induced by TNF-α in HUVECs.

Recent studies suggest that HO-1 exerts vascular protective, antiatherogenic action and its expression in endothelial cells can attenuate atherosclerosis [26, 27]. *In vivo* studies have shown that HO-1 knockout mice were vulnerable to chronic vascular inflammation [28, 29]. Nrf2 (nuclear factor-erythroid 2-related factor 2) is a transcription factor regulating several antioxidant effective genes and HO-1 is one of Nrf2-target genes [10, 11]. In the present study, we determined Nrf2/HO-1 level by treatment by SMT alone without TNF-α. The reason is that TNF-α acts as a negative stimulus increasing ROS production. As a result, negative feedback system of HUVECs could be activated to protect from damage and it might lead to HO-1 upregulation [30, 31]. There is possibility that HO-1 level solely affected by SMT could not be measured if both SMT and TNF-α treated. SMT treatment alone upregulated HO-1 induction in a dose-dependent manner and it resulted from Nrf2 nuclear localization. Furthermore, our data demonstrates that HO-1 production induced by SMT treatment in HUVECs did not result from ROS generation, suggesting SMT induced HO-1 via ROS independent pathway.

NO (nitric oxide) is a well-known vasodilator synthesized by eNOS (endothelial NOS) from L-arginine and eNOS knockout mice are known to represent endothelial dysfunction [32]. NO exerts vascular protective effects by regulating blood pressure, inhibiting platelet aggregation and leukocyte adhesion [33]. To investigate effects of SMT on NO synthesis in HUVECs, intracellular NO and NO_2 (nitrite) secreted in medium are measured. DAF-FM, intracellular NO indicator, was preloaded with HUVECs in case of NO degradation. SMT treatment upregulated NO synthesis comparable to what acetylcholine did as a positive control and nitrite, an oxidative product of NO, was also found to increase in HUVECs treated with SMT for 24 h.

Relation between HO-1/Nrf2 and NO is controversial [34]. Heiss et al. reported that activation of Nrf2 led to increased intracellular NO level in primary human endothelial cells [35]. However, antioxidant effects of polyphenols result from NO mediated dissociation of Keap1-Nrf2 complex [36] and Pae et al. reported that NO can induce HO-1 particularly in endothelial cells [37] suggesting HO-1 as a biological target of NO. In the present study, whether Nrf2 translocation in HUVECs treated with SMT results from NO synthesis remains unclear. However, it is certain that, resultingly, numerous compounds in SMT led to induction of both intracellular NO and HO-1 in HUVECs and exhibited vascular protective effects.

Many researchers have studied with herbs and their compounds composing SMT are as follows: Angelica Gigantis Radix (*Angelica gigas* Nakai, root): its coumarin compounds such as decursin, decursinol angelate, and nodakenin upregulated HO-1 level in mouse vascular smooth muscle cells [38]; Cnidii Rhizoma (*Ligusticum officinale* Makino, rhizome): its

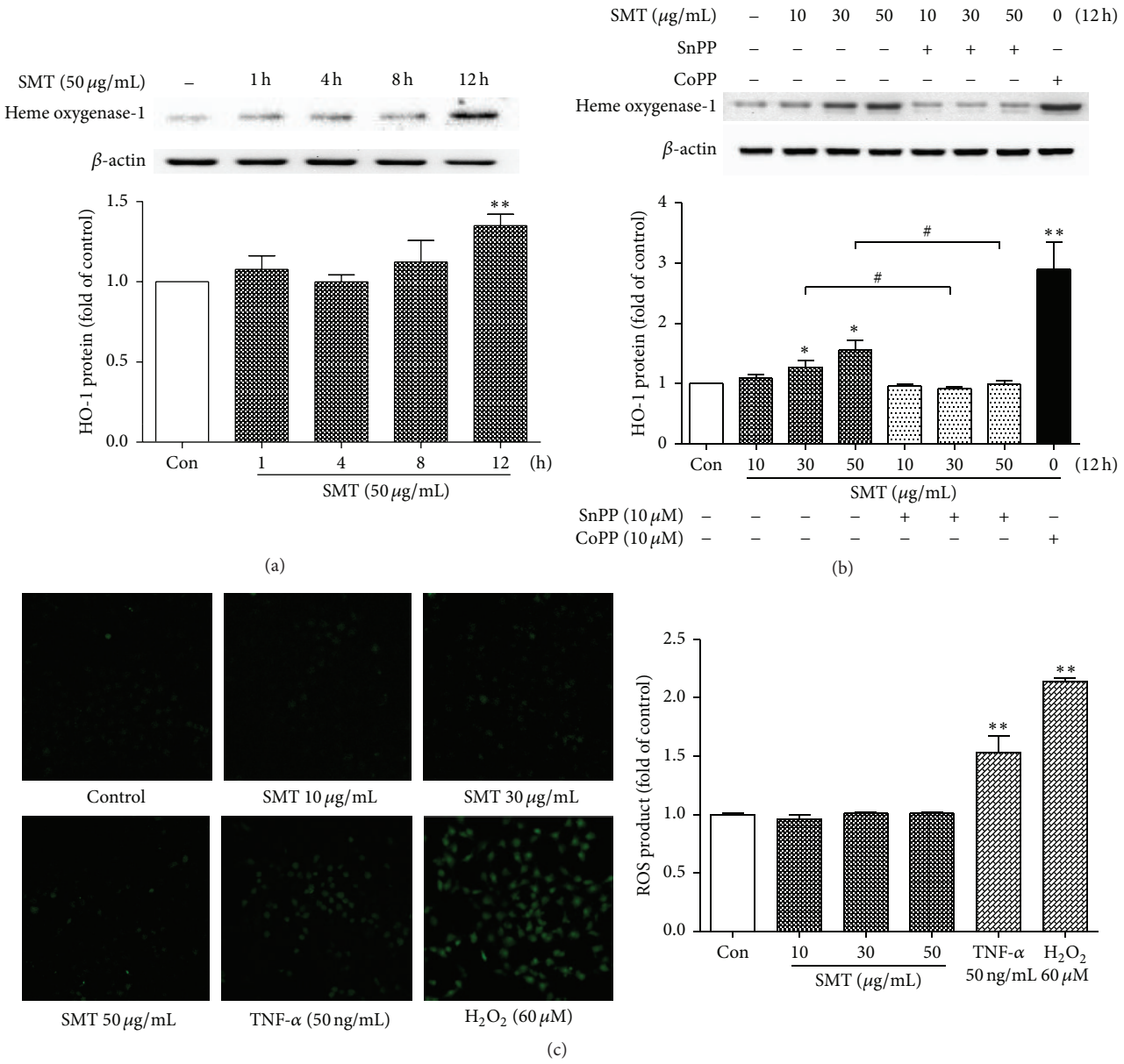

Figure 7: (a, b) Effects of SMT on heme oxygenase-1 induction in HUVECs. Cells were treated with SMT as indicated without TNF-α. (c) Effects of SMT on ROS production in HUVECs. Bar represents the mean ± SEM of 3 independent experiments. $^{*}p < 0.05$ and $^{**}p < 0.01$ versus con group. $^{\#}p < 0.05$ versus respectively indicated group.

phthalide derivatives such as ligustilide and senkyunolide were demonstrated to exert vasorelaxation action in rat isolated aorta [39]. So far which compound of SMT is responsible for vascular protective effect in HUVECs remains unclear and needs to be clarified in further study. Statins are a widely used drug for treating cardiovascular diseases inhibiting cholesterol synthesis [40]. Though statins can also pleiotropically attenuate inflammation or oxidative stress, adverse effects of statins are debatable [41] and some patients were reported to suffer from cognitive decline [42] and type 2 diabetes mellitus [43] due to statin medication. Therefore, investigating traditionally used herbal drugs such as SMT or "danshen dripping pill" [44] could be a complementary way to shed light on cardiovascular drug research.

5. Conclusion

SMT suppressed expression of CAMs via inhibition of ROS/NF-κB activation induced by TNF-α and upregulated HO-1 and NO production in HUVECs. We suggest that four medicinal herbs of SMT, a traditionally used herbal formula, mutually cooperated with each other acting as a multitarget drug and might act as a promising vascular protective drug.

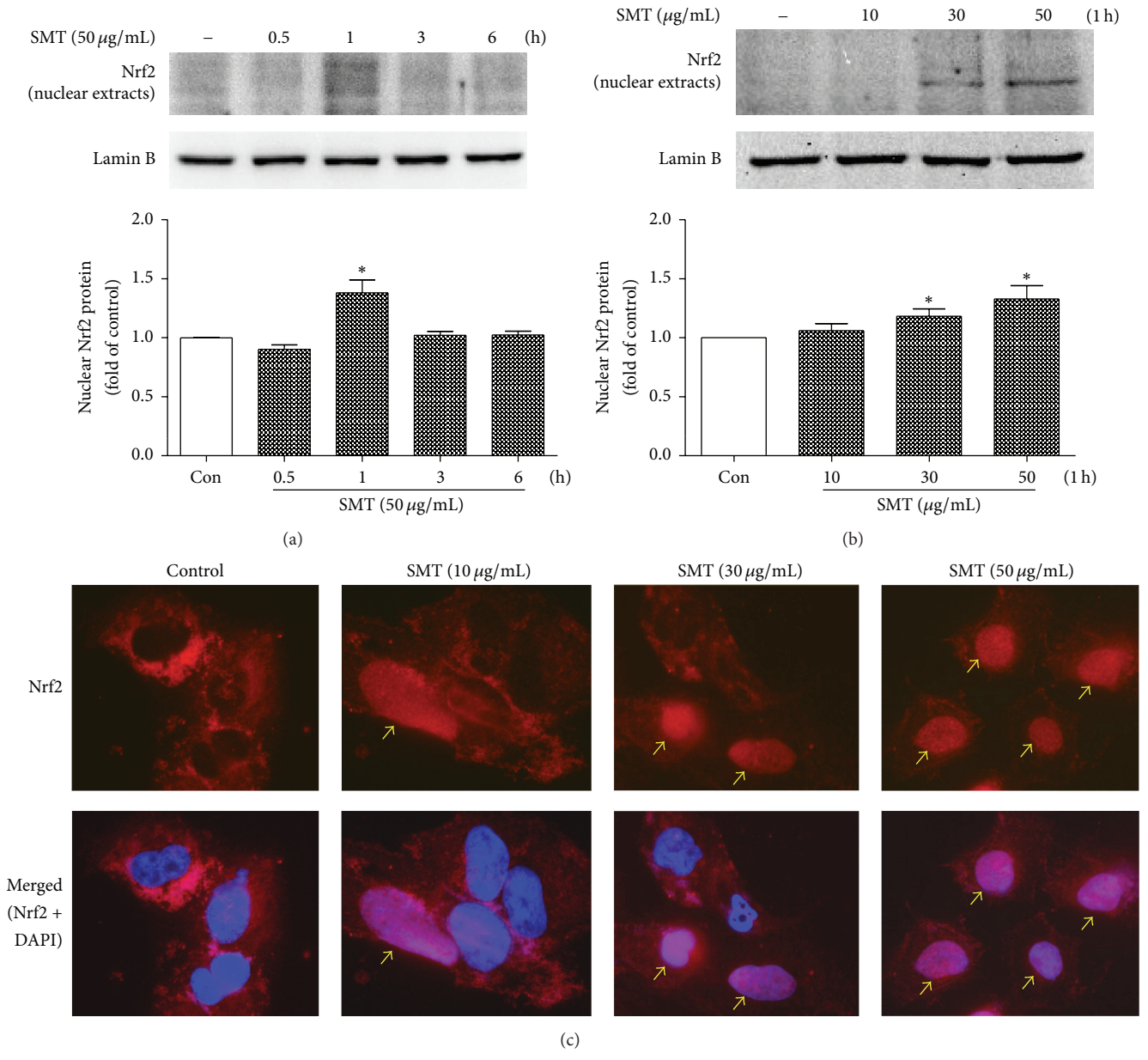

Figure 8: Effects of SMT on nuclear translocation of Nrf2 in HUVECs. Cells were incubated with SMT as indicated without TNF-α. Nrf2 was detected by (a, b) western blot and (c) immunofluorescence. (Red: Nrf2, blue: nucleus; magnification: 400x.) Bar represents the mean ± SEM of 3 independent experiments. $^{*}p < 0.05$ versus con group.

Abbreviations

SMT: Samul-Tang
HUVECs: Human umbilical vein endothelial cells
TNF-α: Tumor necrosis factor-alpha
ICAM-1: Intracellular adhesion molecule-1
VCAM-1: Vascular cell adhesion molecule-1
E-selectin: Endothelial-selectin
ROS: Reactive oxygen species
NO: Nitric oxide
NF-κB: Nuclear factor-kappa B
IκB: Inhibitory kappa B
Nrf2: NF-E2-related factor 2
HO-1: Heme oxygenase-1.

Competing Interests

The authors declare no competing interests.

Acknowledgments

The authors thank the Korea Institute of Oriental Medicine for supplying of Samul-Tang. This work was supported by the

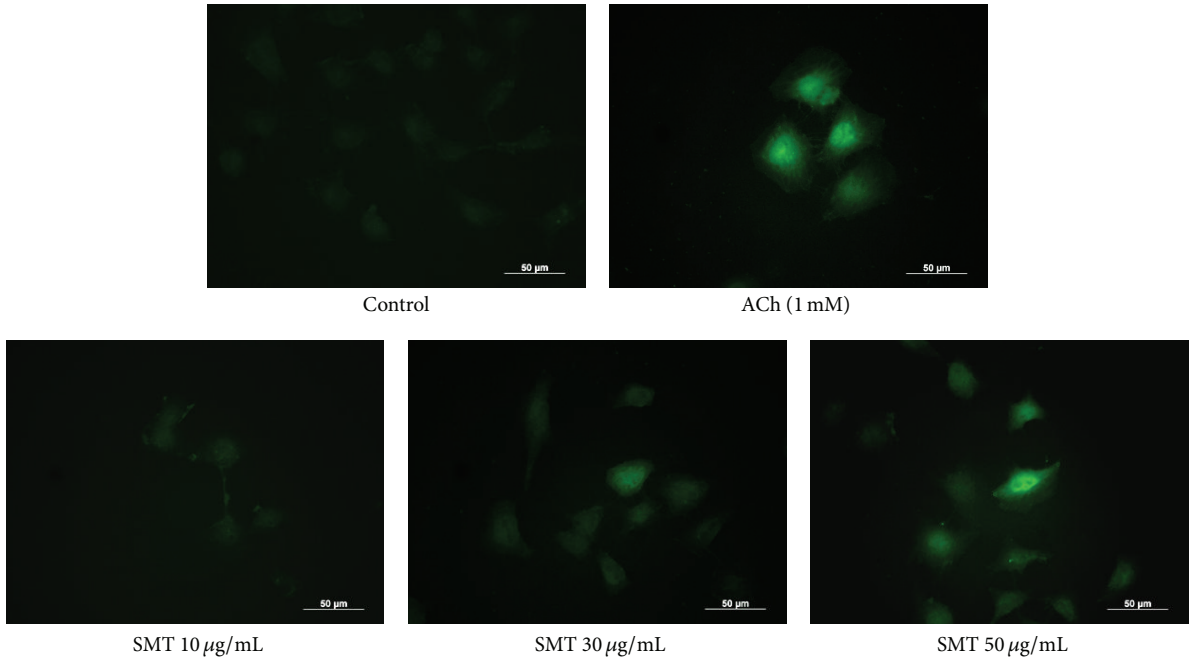

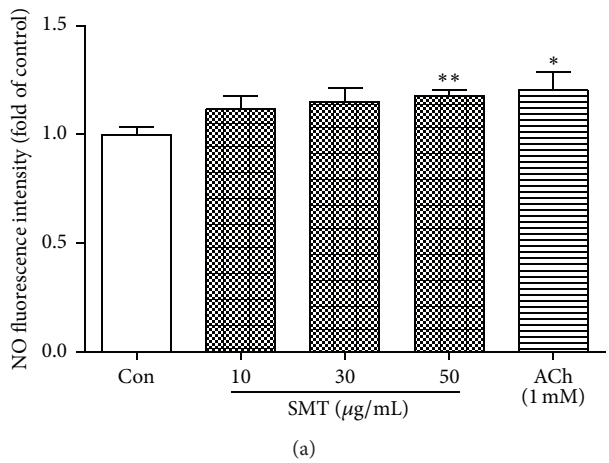

(a)

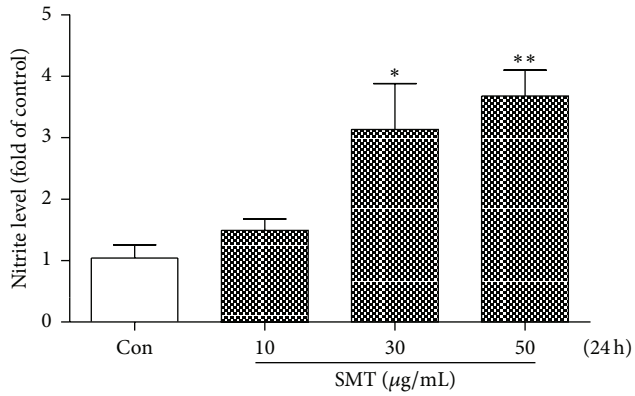

(b)

Figure 9: Effect of SMT on NO (nitric oxide) synthesis in HUVECs. (a) Cells were treated SMT or ACh for 30 minutes. DAF-FM diacetate was labeled as intracellular NO indicator. (400x magnification) ACh (acetylcholine) was used as positive control. (b) Supernatant of cell cultured medium was collected after 24 h of SMT treatment and performing Griess assay. $^{*}p < 0.05$ and $^{**}p < 0.01$ versus con group.

National Research Foundation of Korea (NRF) Grant funded by the Korean government (MSIP) (2008-0062484) (NRF-2015M3A9E3051054).

References

[1] J. M. Cook-Mills and T. L. Deem, "Active participation of endothelial cells in inflammation," *Journal of Leukocyte Biology*, vol. 77, no. 4, pp. 487–495, 2005.

[2] W. C. Aird, "Phenotypic heterogeneity of the endothelium: I. Structure, function, and mechanisms," *Circulation Research*, vol. 100, no. 2, pp. 158–173, 2007.

[3] A. Matsuda, K. Orihara, S. Fukuda, H. Fujinaga, K. Matsumoto, and H. Saito, "Corticosteroid enhances TNF-α-mediated leukocyte adhesion to pulmonary microvascular endothelial cells," *Allergy*, vol. 63, no. 12, pp. 1610–1616, 2008.

[4] S. Ghosh, M. J. May, and E. B. Kopp, "NF-κB and rel proteins: evolutionarily conserved mediators of immune responses," *Annual Review of Immunology*, vol. 16, pp. 225–260, 1998.

[5] S. Y. Foo and G. P. Nolan, "NF-κB to the rescue: RELs, apoptosis and cellular transformation," *Trends in Genetics*, vol. 15, no. 6, pp. 229–235, 1999.

[6] B. Lassègue, A. San Martín, and K. K. Griendling, "Biochemistry, physiology, and pathophysiology of NADPH oxidases in the cardiovascular system," *Circulation Research*, vol. 110, no. 10, pp. 1364–1390, 2012.

[7] Z. Ungvari, Z. Orosz, N. Labinskyy et al., "Increased mitochondrial H_2O_2 production promotes endothelial NF-κB activation in aged rat arteries," *American Journal of Physiology—Heart and Circulatory Physiology*, vol. 293, no. 1, pp. H37–H47, 2007.

[8] X. Mao, T. Wang, Y. Liu et al., "N-acetylcysteine and allopurinol confer synergy in attenuating myocardial ischemia injury via restoring HIF-1α/HO-1 signaling in diabetic rats," *PLoS ONE*, vol. 8, no. 7, Article ID e68949, 2013.

[9] M. D. Maines, G. M. Trakshel, and R. K. Kutty, "Characterization of two constitutive forms of rat liver microsomal heme oxygenase, only one molecular species of the enzyme is inducible," *Journal of Biological Chemistry*, vol. 261, no. 1, pp. 411–419, 1986.

[10] K. Ishikawa, D. Sugawara, J. Goto et al., "Heme oxygenase-1 inhibits atherogenesis in Watanabe heritable hyperlipidemic rabbits," *Circulation*, vol. 104, no. 15, pp. 1831–1836, 2001.

[11] K. Ishikawa, D. Sugawara, X.-P. Wang et al., "Heme oxygenase-1 inhibits atherosclerotic lesion formation in LDL-receptor knockout mice," *Circulation Research*, vol. 88, no. 5, pp. 506–512, 2001.

[12] J. A. Araujo, L. Meng, A. D. Tward et al., "Systemic rather than local heme oxygenase-1 overexpression improves cardiac allograft outcomes in a new transgenic mouse," *The Journal of Immunology*, vol. 171, no. 3, pp. 1572–1580, 2003.

[13] P. Kubes, M. Suzuki, and D. N. Granger, "Nitric oxide: an endogenous modulator of leukocyte adhesion," *Proceedings of the National Academy of Sciences of the United States of America*, vol. 88, no. 11, pp. 4651–4655, 1991.

[14] L. L. L. Yeh, J.-Y. Liu, Y.-S. Liu, K.-S. Lin, T.-F. Tsai, and L.-H. Wang, "Anemia-related hemogram, uterine artery pulsatility index, and blood pressure for the effects of four-agents-decoction (Si Wu Tang) in the treatment of primary dysmenorrhea," *Journal of Alternative and Complementary Medicine*, vol. 15, no. 5, pp. 531–538, 2009.

[15] L. L. L. Yeh, J.-Y. Liu, K.-S. Lin et al., "A randomised placebo-controlled trial of a traditional Chinese herbal formula in the treatment of primary dysmenorrhoea," *PLoS ONE*, vol. 2, no. 8, article e719, 2007.

[16] J.-F. Cheng, Z.-Y. J. Lu, Y.-C. Su, L.-C. Chiang, and R.-Y. Wang, "A traditional Chinese herbal medicine used to treat dysmenorrhoea among Taiwanese women," *Journal of Clinical Nursing*, vol. 17, no. 19, pp. 2588–2595, 2008.

[17] H.-W. Lee, H. Kim, J. A. Ryuk, K.-J. Kil, and B. S. Ko, "Hemopoietic effect of extracts from constituent herbal medicines of Samul-Tang on phenylhydrazine-induced hemolytic anemia in rats," *International Journal of Clinical and Experimental Pathology*, vol. 7, no. 9, pp. 6179–6185, 2014.

[18] W. Tan, C.-S. Song, H.-L. Tan et al., "Hematopoietic effect of Siwu decoction in the mice with blood deficiency induced by compound method of bleeding, starved feeding and exhausting," *Zhongguo Zhongyao Zazhi*, vol. 30, no. 12, pp. 926–929, 2005.

[19] Y. Dai, P. P.-H. But, Y.-P. Chan, H. Matsuda, and M. Kubo, "Antipruritic and antiinflammatory effects of aqueous extract from Si-Wu-Tang," *Biological and Pharmaceutical Bulletin*, vol. 25, no. 9, pp. 1175–1178, 2002.

[20] E. Tahara, T. Satoh, K. Toriizuka et al., "Effect of Shimotsu-to (a Kampo medicine, Si-Wu-Tang) and its constituents on triphasic skin reaction in passively sensitized mice," *Journal of Ethnopharmacology*, vol. 68, no. 1-3, pp. 219–228, 1999.

[21] Z. Fang, B. Lu, M. Liu et al., "Evaluating the pharmacological mechanism of Chinese Medicine Si-Wu-Tang through multi-level data integration," *PLoS ONE*, vol. 8, no. 11, Article ID e72334, 2013.

[22] J. S. Pober and W. C. Sessa, "Evolving functions of endothelial cells in inflammation," *Nature Reviews Immunology*, vol. 7, no. 10, pp. 803–815, 2007.

[23] T. Collins, "Endothelial nuclear factor-κB and the initiation the atherosclerotic lesion," *Laboratory Investigation*, vol. 68, no. 5, pp. 499–508, 1993.

[24] T. Collins, M. A. Read, A. S. Neish, M. Z. Whitley, D. Thanos, and T. Maniatis, "Transcriptional regulation of endothelial cell adhesion molecules: NF-κB and cytokine-inducible enhancers," *FASEB Journal*, vol. 9, no. 10, pp. 899–909, 1995.

[25] A. D. Ellington, "New ribozymes for old reactions," *Current Biology*, vol. 2, no. 8, pp. 437–439, 1992.

[26] A. J. Coito, R. Buelow, X.-D. Shen et al., "Heme oxygenase-1 gene transfer inhibits inducible nitric oxide synthase expression and protects genetically fat Zucker rat livers from ischemia-reperfusion injury," *Transplantation*, vol. 74, no. 1, pp. 96–102, 2002.

[27] H. Kato, F. Amersi, R. Buelow et al., "Heme oxygenase-1 overexpression protects rat livers from ischemia/reperfusion injury with extended cold preservation," *American Journal of Transplantation*, vol. 1, no. 2, pp. 121–128, 2001.

[28] K. D. Poss and S. Tonegawa, "Reduced stress defense in heme oxygenase 1-deficient cells," *Proceedings of the National Academy of Sciences of the United States of America*, vol. 94, no. 20, pp. 10925–10930, 1997.

[29] K. D. Poss and S. Tonegawa, "Heme oxygenase 1 is required for mammalian iron reutilization," *Proceedings of the National Academy of Sciences of the United States of America*, vol. 94, no. 20, pp. 10919–10924, 1997.

[30] D. Calay, A. Rousseau, L. Mattart et al., "Copper and myeloperoxidase-modified LDLs activate Nrf2 through different pathways of ros production in macrophages," *Antioxidants and Redox Signaling*, vol. 13, no. 10, pp. 1491–1502, 2010.

[31] S.-E. Cheng, I.-T. Lee, C.-C. Lin, Y. R. Kou, and C.-M. Yang, "Cigarette smoke particle-phase extract induces HO-1 expression in human tracheal smooth muscle cells: role of the c-Src/NADPH oxidase/MAPK/Nrf2 signaling pathway," *Free Radical Biology and Medicine*, vol. 48, no. 10, pp. 1410–1422, 2010.

[32] H. K. Shin, F. Oka, J. H. Kim, D. Atochin, P. L. Huang, and C. Ayata, "Endothelial dysfunction abrogates the efficacy of normobaric hyperoxia in stroke," *The Journal of Neuroscience*, vol. 34, no. 46, pp. 15200–15207, 2014.

[33] C. Napoli, F. de Nigris, S. Williams-Ignarro, O. Pignalosa, V. Sica, and L. J. Ignarro, "Nitric oxide and atherosclerosis: an update," *Nitric Oxide*, vol. 15, no. 4, pp. 265–279, 2006.

[34] S. M. Hwang, Y. J. Lee, J. J. Yoon et al., "Prunella vulgaris suppresses HG-induced vascular inflammation via Nrf2/HO-1/eNOS activation," *International Journal of Molecular Sciences*, vol. 13, no. 1, pp. 1258–1268, 2012.

[35] E. H. Heiss, D. Schachner, E. R. Werner, and V. M. Dirsch, "Active NF-E2-related factor (Nrf2) contributes to keep endothelial NO synthase (eNOS) in the coupled state: role of reactive oxygen species (ROS), eNOS, and heme oxygenase (HO-1) levels," *Journal of Biological Chemistry*, vol. 284, no. 46, pp. 31579–31586, 2009.

[36] G. E. Mann, D. J. Rowlands, F. Y. L. Li, P. de Winter, and R. C. M. Siow, "Activation of endothelial nitric oxide synthase by dietary isoflavones: role of NO in Nrf2-mediated antioxidant gene expression," *Cardiovascular Research*, vol. 75, no. 2, pp. 261–274, 2007.

[37] H.-O. Pae, G.-S. Oh, B.-M. Choi, Y.-M. Kim, and H.-T. Chung, "A molecular cascade showing nitric oxide-heme oxygenase-1-vascular endothelial growth factor-interleukin-8 sequence in human endothelial cells," *Endocrinology*, vol. 146, no. 5, pp. 2229–2238, 2005.

[38] J. H. Cho, J. E. Kwon, Y. Cho, I. Kim, and S. C. Kang, "Anti-inflammatory effect of Angelica gigas via heme oxygenase (HO)-1 expression," *Nutrients*, vol. 7, no. 6, pp. 4862–4874, 2015.

[39] S. S.-K. Chan, T.-Y. Cheng, and G. Lin, "Relaxation effects of ligustilide and senkyunolide A, two main constituents of *Ligusticum chuanxiong*, in rat isolated aorta," *Journal of Ethnopharmacology*, vol. 111, no. 3, pp. 677–680, 2007.

[40] F. Ali, M. Zakkar, K. Karu et al., "Induction of the cytoprotective enzyme heme oxygenase-1 by statins is enhanced in vascular endothelium exposed to laminar shear stress and impaired by disturbed flow," *Journal of Biological Chemistry*, vol. 284, no. 28, pp. 18882–18892, 2009.

[41] J. W. Jukema, C. P. Cannon, A. J. M. de Craen, R. G. J. Westendorp, and S. Trompet, "The controversies of statin therapy: weighing the evidence," *Journal of the American College of Cardiology*, vol. 60, no. 10, pp. 875–881, 2012.

[42] L. R. Wagstaff, M. W. Mitton, B. M. Arvik, and P. M. Doraiswamy, "Statin-associated memory loss: analysis of 60 case reports and review of the literature," *Pharmacotherapy*, vol. 23, no. 7, pp. 871–880, 2003.

[43] A. L. Culver, I. S. Ockene, R. Balasubramanian et al., "Statin use and risk of diabetes mellitus in postmenopausal women in the Women's Health Initiative," *Archives of Internal Medicine*, vol. 172, no. 2, pp. 144–152, 2012.

[44] G. Xu, W. Zhao, Z. Zhou, R. Zhang, W. Zhu, and X. Liu, "Danshen extracts decrease blood C reactive protein and prevent ischemic stroke recurrence: a controlled pilot study," *Phytotherapy Research*, vol. 23, no. 12, pp. 1721–1725, 2009.

Hindawi Publishing Corporation
Evidence-Based Complementary and Alternative Medicine
Volume 2016, Article ID 6836080, 11 pages
http://dx.doi.org/10.1155/2016/6836080

Research Article

Anti-Inflammatory Effects of Pomegranate Peel Extract in THP-1 Cells Exposed to Particulate Matter PM10

Soojin Park,[1] Jin Kyung Seok,[1] Jun Yup Kwak,[1] Hwa-Jin Suh,[2] Young Mi Kim,[3] and Yong Chool Boo[1,3]

[1]*Department of Molecular Medicine, Cell and Matrix Research Institute, BK21 Plus KNU Biomedical Convergence Program, School of Medicine, Kyungpook National University, 680 Gukchaebosang-ro, Jung-gu, Daegu 41944, Republic of Korea*
[2]*Gyeongbuk Natural Color Industry Institute, 181 Cheonmun-ro, Yeongcheon-si, Gyeongsangbuk-do 38896, Republic of Korea*
[3]*Ruby Crown Co., Ltd., 201 Kyungpook National University Business Incubation Center, 80 Daehak-ro, Buk-gu, Daegu 41566, Republic of Korea*

Correspondence should be addressed to Yong Chool Boo; ycboo@knu.ac.kr

Received 5 January 2016; Revised 14 April 2016; Accepted 18 April 2016

Academic Editor: Ying-Ju Lin

Epidemiological and experimental evidence support health risks associated with the exposure to airborne particulate matter with a diameter of <10 μM (PM10). PM10 stimulates the production of reactive oxygen species (ROS) and inflammatory mediators. Thus, we assumed that natural antioxidants might provide health benefits attenuating hazardous effects of PM10. In the present study, we examined the effects of pomegranate peel extract (PPE) on THP-1 monocytic cells exposed to PM10. PM10 induced cytotoxicity and the production of ROS. It also increased the expression and secretion of inflammatory cytokines, such as tumor necrosis factor-α (TNF-α), interleukin-1β (IL-1β), and monocyte chemoattractant protein-1 (MCP-1), and cell adhesion molecules, such as intercellular adhesion molecule-1 (ICAM-1) and vascular cell adhesion molecule-1 (VCAM-1). PPE at 10–100 μg mL^{-1} attenuated the production of ROS and the expression of TNF-α, IL-1β, MCP-1, and ICAM-1, but not VCAM-1, in THP-1 cells stimulated by PM10 (100 μg mL^{-1}). PPE also attenuated the adhesion of PM10-stimulated THP-1 cells to EA.hy926 endothelial cells. PPE constituents, punicalagin and ellagic acid, attenuated PM10-induced monocyte adhesion to endothelial cells, and punicalagin was less cytotoxic compared to ellagic acid. The present study suggests that PPE and punicalagin may be useful in alleviating inflammatory reactions due to particulate matter.

1. Introduction

Air pollution has become the world's largest single environmental health risk [1]. Major outdoor air pollutants include particulate matter, volatile organic compounds, and hazardous gases. Airborne particulate matter is a fine dust of natural and artificial origins suspended in the Earth's atmosphere. Natural particulates originate from volcanoes, dust storms, forest and land fires, and so on. Significant amounts of particulates are also generated from human activities, such as the burning of fossil fuels in vehicles, power plants, and various industrial processes. Many previous studies have demonstrated that a large number of deaths and other health problems were associated with particulate pollution [1–3].

Particulate matter is known to cause airway epithelium injury and endothelial dysfunction [4, 5]. Larger particles can be filtered in the nose and throat via cilia and mucus, but particulate matter smaller than 10 micrometers (PM10) can enter the deepest parts of the lungs, such as the bronchioles and alveoli [6]. PM10 may cause severe effects on human health due to the broad range of miscellaneous toxic compounds present in this particulate matter fraction, such as transition metals, endotoxins, and ultrafine components. The mechanism of action of PM10 may include the induction of oxidative stress and activation of nuclear factor kappa B (NF-κB) pathway, leading to inflammation [7]. PM10 increases the production of reactive oxygen species (ROS) and cytokines in human and rat alveolar macrophages [8]. In addition,

PM10-induced inflammation is attenuated by antioxidants from plant sources [9–11].

The pomegranate (*Punica granatum* L.) is a deciduous fruit tree belonging to the family Lythraceae. The rind of the fruit and the bark of the pomegranate tree have been used in traditional medicine for the treatment of diarrhea, dysentery, and intestinal parasites. Today, pomegranate juice is a popular drink worldwide. The major phytochemicals in pomegranate are ellagitannins, including punicalagin [12], which is a good antioxidant with potent free-radical scavenging properties [13]. Previous studies have examined the effects of pomegranate juice on various cardiovascular risk factors, including low density lipoprotein oxidation, macrophage oxidative status, foam cell formation, and high blood pressure [14–16]. However, no previous studies have examined the effects of pomegranate extracts on the cellular response to particulate matters.

In the present study, we hypothesized that pomegranate peel extract (PPE) may attenuate oxidative stress and inflammatory events induced by PM10. Therefore, we monitored the production of ROS and the expression of inflammatory cytokines and cell adhesion molecules in THP-1 monocytic cells exposed to PM10 in the absence and presence of PPE. Effects of PPE on the cell-cell adhesion between PM10-stimulated THP-1 cells and EA.hy926 endothelial cells were also examined.

2. Materials and Methods

2.1. Reagents. Punicalagin (purity > 98%, a mixture of 40% α and 60% β anomers) and ellagic acid (purity > 98%) were purchased from Sigma-Aldrich (St. Louis, MO, USA). Fine dust (PM10-like) (European reference material ERM-CZ120) was purchased from Sigma-Aldrich. PPE was obtained from Hwasoomok Co. (Youngchen, Korea). The extract was prepared by extracting dry raw materials with water at 55°C for 2 h, followed by concentration and spray drying.

2.2. High Performance Liquid Chromatography (HPLC) Analysis. HPLC analysis was performed using a Gilson HPLC system (Gilson, Inc., Middleton, WI, USA) equipped with an ultraviolet/visible (UV/VIS) 151 detector. The volume of sample injected was 20 μL, and separation was performed on a 5 μm Hector-M C18 column (4.6 mm × 250 mm) (RS Tech Co. Daejeon, Korea) using a mobile phase consisting of 1% formic acid in water (A) and 1% formic acid in acetonitrile (B). A linear gradient from 0% to 30% B for 40 min and 30% to 100% 40–45 min was applied. The flow rate of the mobile phase was 0.6 mL min^{-1}. The detector was set at 254 nm.

2.3. Cultivation of THP-1 Cells. THP-1 cells (human acute monocytic leukemia cell line) were obtained from the Korea Cell Line Bank (Seoul, Korea) and cultured in T-75 flasks (Nunc, Roskilde, Denmark) in an upright position. Culture medium was Roswell Park Memorial Institute (RPMI) 1640 medium (Gibco BRL, Grand Island, NY, USA) containing fetal bovine serum (10%), antibiotics (100 U mL^{-1} penicillin, 100 μg mL^{-1} streptomycin, and 0.25 μg mL^{-1} amphotericin B), and β-mercaptoethanol (0.05 mM). Cell viability was assessed using the trypan blue exclusion assay.

2.4. PM10 Treatments. THP-1 cells were seeded on 12-well plates at 4×10^5 cells cm^{-2} and treated with PM10 at 3–100 μg mL^{-1} for 24 h. In some experiments, cells were treated with PM10 (100 μg mL^{-1}) in the presence of test materials for the indicated time.

2.5. Assay for ROS Production. Cellular production of ROS was determined using dihydrorhodamine 123 (DHR123) (Sigma-Aldrich). THP-1 cells were treated with PM10 in the absence or presence of PPE for 24 h. Cells were labeled with 1.0 μM DHR123 for the last 6 h of PM10 treatment. The oxidized rhodamine 123 was extracted from cells using ice-cold 70% ethanol/0.1 N HCl, followed by centrifugation at 13,000 rpm for 15 min. The supernatants were neutralized with 1 M $NaHCO_3$ and spun down to obtain clear supernatants. Fluorescence intensity of the supernatants was measured at an excitation wavelength at 485 nm and an emission wavelength of 590 nm, using the Gemini EM fluorescence microplate reader (Molecular Devices, Sunnyvale, CA, USA).

2.6. Quantitative Reverse-Transcriptase Polymerase Chain Reaction (qRT-PCR) Analysis of Cytokine Expression. THP-1 cells were treated with PM10 in the absence or presence of PPE for 24 h. Cellular RNA was extracted from the treated cells with an RNeasy kit (Qiagen, Valencia, CA, USA). One microgram of cellular mRNA was reverse transcribed to prepare complementary DNA (cDNA), using a High Capacity cDNA Archive Kit (Applied Biosystems, Foster City, CA, USA). PCR was conducted with a StepOnePlus™ Real-Time PCR System (Applied Biosystems) in a reaction mixture (20 μL) containing SYBR® Green PCR Master Mix (Applied Biosystems), 60 ng of cDNA, and 2 pmol of gene-specific primer sets (Macrogen, Seoul, Korea). The primers used were as follows: tumor necrosis factor-α (TNF-α) (GenBank accession number, NM_000594.3) 5′-TGC TCC TCA CCC ACA CCA T-3′ (forward) and 5′-GAG ATA GTC GGG CCG ATT GA-3′ (reverse); interleukin-1β (IL-1β) (NM_000576.2) 5′-CCT GTC CTG CGT GTT GAA AGA-3′ (forward) and 5′-GGG AAC TGG GCA GAC TCA AA-3′ (reverse); monocyte chemoattractant protein-1 (MCP-1) (MCP-1) (NM_002982.3) 5′-GCA ATC AAT GCC CCA GTC A-3′ (forward) and 5′-TGC TTG TCC AGG TGG TCC AT3′ (reverse); intercellular adhesion molecule 1 (ICAM-1) (NM_000201.2) 5′-ATC TGT GTC CCC CTC AAA AGT C-3′ (forward) and 5′-TGG CTA TCT TCT TGC ACA TTG C-3′ (reverse); vascular cell adhesion molecule 1 (VCAM-1) (NM_001079.3) 5′-CTG ACC CTG AGC CCT GTG A-3′ (forward) and 5′-CTT ACA GTG ACA GAG CTC CCA TTC-3′ (reverse); glyceraldehyde-3-phosphate dehydrogenase (GAPDH) (NM_002046.3) 5′-ATG GGG AAG GTG AAG GTC G-3′ (forward) and 5′-GGG GTC ATT GAT GGC AAC AA-3′ (reverse). Reactions were performed using the following protocol: 50°C for 2 min, 95°C for 10 min, and 40 amplification cycles (95°C for 15 s and 60°C for 1 min), followed by a dissociation step. Melting curve analysis showed single peaks, supporting the homogeneity

of amplicons. The mRNA expression levels of TNF-α, IL-1β, MCP-1, ICAM-1, and VCAM-1 relative to that of the internal control GAPDH were calculated using the comparative threshold cycle method.

2.7. Enzyme-Linked Immunosorbent Assays (ELISA) for Cytokines. THP-1 cells were treated with PM10 in the absence and presence of test materials for 72 h in the serum-free culture medium. The conditioned medium was collected and the concentrations of TNF-α, IL-1β, MCP-1, and ICAM-1 were measured using Human Mini ELISA kits (Pepro-Tech, Rocky Hill, NJ, USA), according to the manufacturer's instructions. Briefly, samples (100 μL conditioned medium) or solutions of standard at varied concentrations were added to microplate wells which contained immobilized capture antibody. After 12 h incubation at 4°C, the wells were washed and solutions of biotinylated detection antibody were added and incubated for 2 h. After washing the wells, solutions of horseradish peroxidase conjugated to streptavidin or avidin were added and incubated for 30 min. The cells were washed, and 3,3′,5,5′-tetramethylbenzidine (TMB) or 2,2′-Azino-bis(3-ethylbenzothiazoline-6-sulphonic acid) (ABTS) substrate solution was added to the wells to initiate enzymatic color development. The TMB reaction was terminated using 1 M HCl and the absorbance of the reaction mixture was measured at 450 nm. The absorbance of the ABTS reaction mixture was measured at 405 nm.

2.8. Cultivation of Endothelial Cells. The human endothelial cell line EA.hy926 purchased from American Type Culture Collection (Manassas, VA, USA) was plated on 100 mm tissue culture dishes (BD Biosciences, San Jose, CA, USA) and cultured using Dulbecco's modified Eagle's medium (DMEM) (Gibco BRL) supplemented with 10% fetal bovine serum (Gibco BRL,) and antibiotics at 37°C and 5% CO_2.

2.9. Cell Adhesion Assay. Monocytic THP-1 cells were seeded in RPMI 1640 medium on 12-well tissue culture plates at 1×10^6 cells/well. Cells were treated with PPE for 60 min and then with PM10 (100 μg·mL^{-1}) for another 24 h. Cells were collected by centrifugation and fluorescence-labeled as follows: cells were washed with phosphate buffered saline (PBS) twice, suspended at 5×10^6 cells·mL^{-1} in PBS containing 5 μg·mL^{-1} 2′,7′-bis(carboxyethyl)-5(6)-carboxyfluorescein acetoxymethyl ester (BCECF-AM) (Molecular Probes, Carlsbad, CA, USA), and incubated at 37°C for 60 min. The cells were collected by centrifugation, washed with PBS twice, and suspended in RPMI 1640 medium prior to being added to endothelial cell culture. EA.hy926 endothelial cells were seeded in DMEM on 6-well tissue culture plates at 2×10^5 cells·cm^{-2} and cultured for 2 d. Then culture medium was replaced by RPMI 1640 medium. The fluorescence-labeled THP-1 cells were added to the EA.hy926 cell cultures at a 1 : 1 ratio. After coincubation of EA.hy926 cells and THP-1 cells in RPMI 1640 medium for 2 h, nonadherent THP-1 cells were washed twice with PBS, with caution taken not to disturb the endothelial cell monolayer. Fresh RPMI 1640 medium was supplied to the remaining cells on the culture plates. Florescence-labeled THP-1 cells adhering to the endothelial cell monolayer were observed with a Nikon eclipse TE2000-U microscope (Tokyo, Japan). For quantification, adherent cells were lysed in 200 μL of 0.1 M Tris-HCl containing 0.1% Triton X-100 and centrifuged at 13,000 rpm for 15 min. The fluorescence intensity of supernatants was determined at the excitation wavelength of 485 nm and emission wavelength of 535 nm, using an LS55 fluorescence spectrometer (Perkin Elmer instruments, Waltham, MA, USA), and normalized for a number of endothelial cells.

2.10. Statistical Analysis. Data are presented as the means ± standard error (SE) of three or more independent experiments. The differences between groups were statistically analyzed using Student's t-test, where a p value < 0.05 was considered statistically significant.

3. Results

Previous studies have shown that air-borne fine and coarse particles can cause cytotoxicity and induce proinflammatory cytokines from human monocytes [17]. In addition, it has been demonstrated that they increase the expression of cell adhesion molecules in endothelial cells [18]. Thus, we examined the cytotoxicity and proinflammatory effects of PM10 in our experimental conditions. Human monocytic THP-1 cells were treated with PM10 at various concentrations up to 100 μg mL^{-1} for 24 h, and trypan blue exclusion assay was performed to determine the number of alive and dead cells. As shown in Figure 1(a), PM10 significantly decreased cell viability. To analyze gene expression, total cellular mRNA was extracted from the treated THP-1 cells, and quantitative PCR analysis was performed. The expression levels of inflammatory cytokines and cell adhesion molecules were normalized to GAPDH, a control. As shown in Figures 1(b), 1(c), and 1(d), PM10 dose-dependently increased the expression of the inflammatory cytokines TNF-α, IL-1β, and MCP-1 at the mRNA level. It also increased the expression of the cell adhesion molecules ICAM-1 and VCAM-1, as shown in Figures 1(e) and 1(f). Taken together, these data support a role of air-borne particulate matter in the induction of inflammatory reactions.

Particulate matter induces inflammation *via* the generation of ROS and free radicals [19, 20]. Therefore, plant extracts with high contents of polyphenolic antioxidants may be protective effects against particulate matter-induced inflammation. This hypothesis was examined using PPE as a model plant extract. We determined the effects of PPE on cell viability and ROS production of THP-1 cells exposed to PM10. THP-1 cells were treated with PM10 at 100 μg mL^{-1} in the absence or presence of PPE at 10–100 μg mL^{-1} for 24 h. As shown in Figures 2(a) and 2(b), PM10 decreased cell viability and increased ROS production, indicating that PM10 caused oxidative stress in cells. The effect of PPE on the viability of PM10-treated cells was not significant, but it significantly and dose-dependently attenuated ROS production due to PM10 (Figures 2(a) and 2(b)). Thus, PPE can act as an antioxidant to inhibit ROS production and/or a scavenger of ROS inside cells.

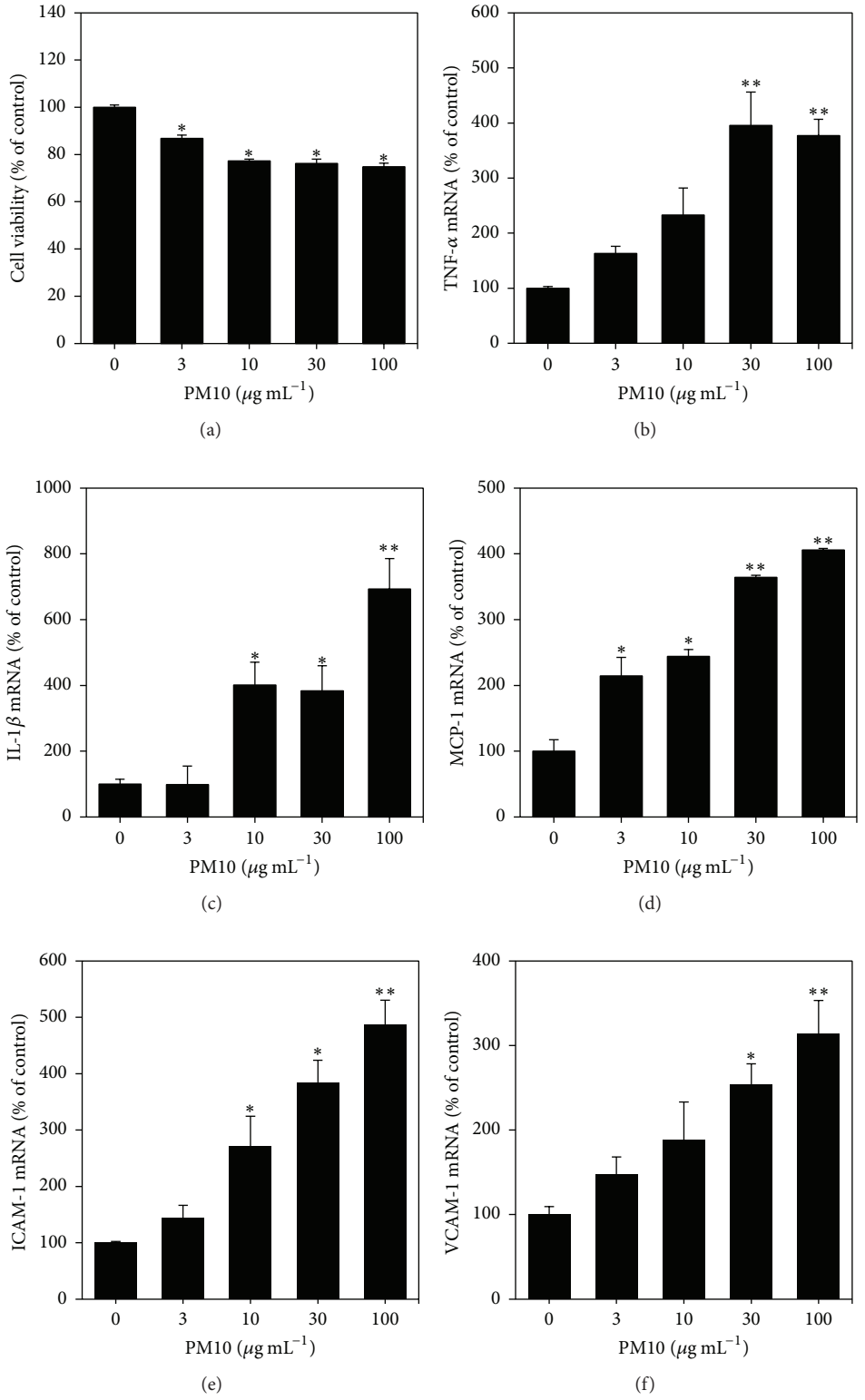

Figure 1: Effects of PM10 on cell viability and gene expression of inflammatory cytokines and cell adhesion molecules in THP-1 cells. Cells were treated with PM10 at the indicated concentrations for 24 h. (a) Cell viabilities are presented as percentages of viable cells per total cells. (b–f) Gene expression was analyzed by qRT-PCR and normalized to control GAPDH. Data are expressed as percentages. Data are means ± SEs ($n = 3$). $^{*}p < 0.05$ and $^{**}p < 0.01$ versus control.

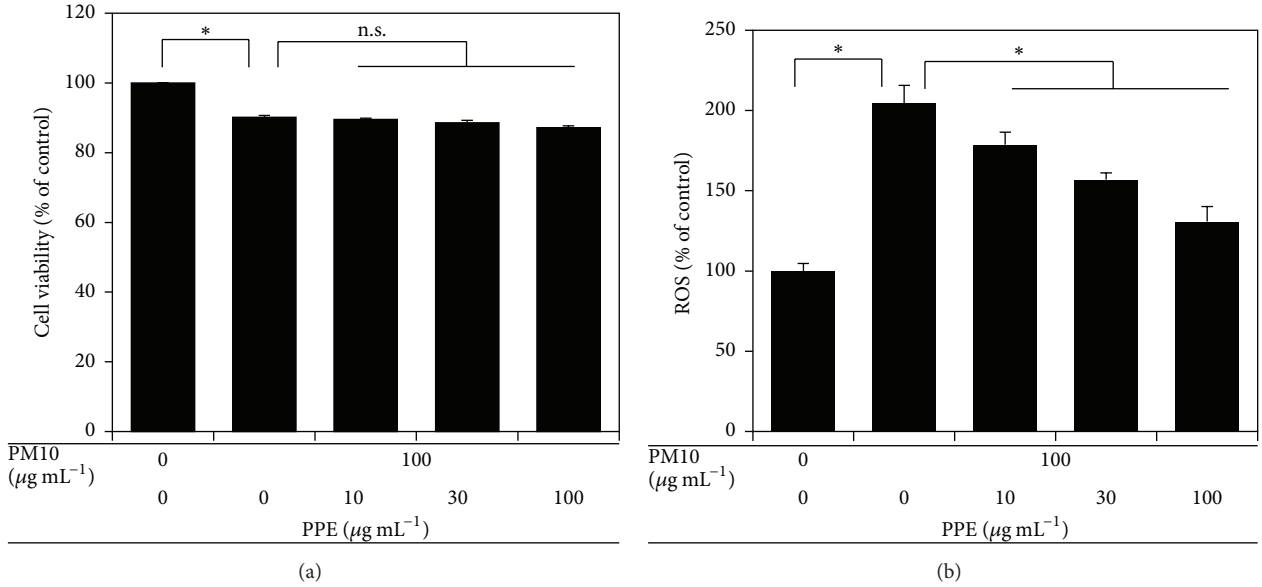

Figure 2: Effects of pomegranate peel extract (PPE) on cell viability and reactive oxygen species (ROS) production in THP-1 cells exposed to PM10. Cells were treated with PM10 in the absence or presence of PPE, followed by incubation for 24 h. (a) Cell viability is the percentage of viable cells out of total cells. (b) ROS production data are expressed as percentages of the control value. Data are means ± SEs ($n = 3$). $^{*}p < 0.05$; n.s., not significant.

The anti-inflammatory effects of PPE were examined by monitoring the expression levels of inflammatory cytokines and cell adhesion molecules in THP-1 cells exposed to PM10. As shown in Figures 3(a)–3(c), PPE dose-dependently attenuated the expression of TNF-α, IL-1β, and MCP-1 in THP-1 cells exposed to PM10. In addition, it decreased the expression of ICAM-1 but not VCAM-1 in THP-1 cells exposed to PM10 (Figures 3(d) and 3(e)).

The adhesion of activated monocytes to endothelial cells is a critical step of the inflammatory process, and particulate matter has been shown to increase cell adhesion [18, 21]. Thus, we examined whether PM10 activates THP-1 cells, rendering them more adhesive to endothelial cells, and whether the cell-cell interaction is attenuated by PPE. THP-1 monocytic cells were treated with PPE in the absence or presence of PPE before coincubation with EA.hy926 endothelial cells. The results showed that PM10 treatment increased adhesion of monocytes to endothelial cells, and this phenomenon was attenuated by PPE in a dose-dependent manner (Figures 4(a) and 4(b)).

Ellagitannins are the major polyphenolic compounds contained in pomegranate [12]. As shown in Figure 5, HPLC analysis of PPE indicated that punicalagin and ellagic acid are major constituents. Punicalagin appeared as two peaks, each corresponding to α and β anomers. Thus, we examined if punicalagin or ellagic acid is the active constituent of PPE responsible for the anti-inflammatory effect. In this experiment, commercial forms of punicalagin and ellagic acid were tested at 1–30 μg mL^{-1}. As shown in Figure 6(a), ellagic acid appeared to have significant cytotoxicity, whereas punicalagin showed no cytotoxicity at the tested concentrations. Punicalagin attenuated PM10-stimulated monocyte adhesion to endothelial cells at 3–30 μg mL^{-1} (Figures 6(b) and 6(c)). Ellagic acid attenuated PM10-stimulated monocyte adhesion to endothelial cells only at cytotoxic concentrations (Figure 6(b)). These data indicate that punicalagin has a better therapeutic window between efficacy concentration and toxicity concentration than ellagic acid.

Effects of PPE and punicalagin on the levels of TNF-α, IL-1β, MCP-1, and ICAM-1 proteins released from THP-1 cells exposed to PM10 were further examined. N-Acetyl cysteine was used as a reference antioxidant. As shown in Figure 7, PM10 elevated the secreted protein levels of TNF-α, IL-1β, MCP-1, and ICAM-1, and these changes were significantly attenuated by PPE and punicalagin as well as N-acetyl cysteine.

4. Discussion

The aims of this study were threefold. First aim was to examine whether PM10 stimulates inflammatory events at the cellular levels. Second aim was to examine whether such inflammatory events were attenuated by PPE. Third aim was to take insight into the active compounds of PPE.

PM10 exposure is associated with the incidence and development of cardiopulmonary disease [4, 5]. Although the precise molecular mechanisms are yet unclear, PM10 is known to stimulate alveolar macrophages and airway epithelial cells to produce inflammatory mediators such as TNF-α and IL-1β [22–24]. Particulate matter is also shown to activate endothelial cells involved in inflammation. PM10 has been shown to induce the expression of adhesion molecules and the adhesion of monocytes to human umbilical endothelial cells [18]. The mechanism of action of PM10 may include the

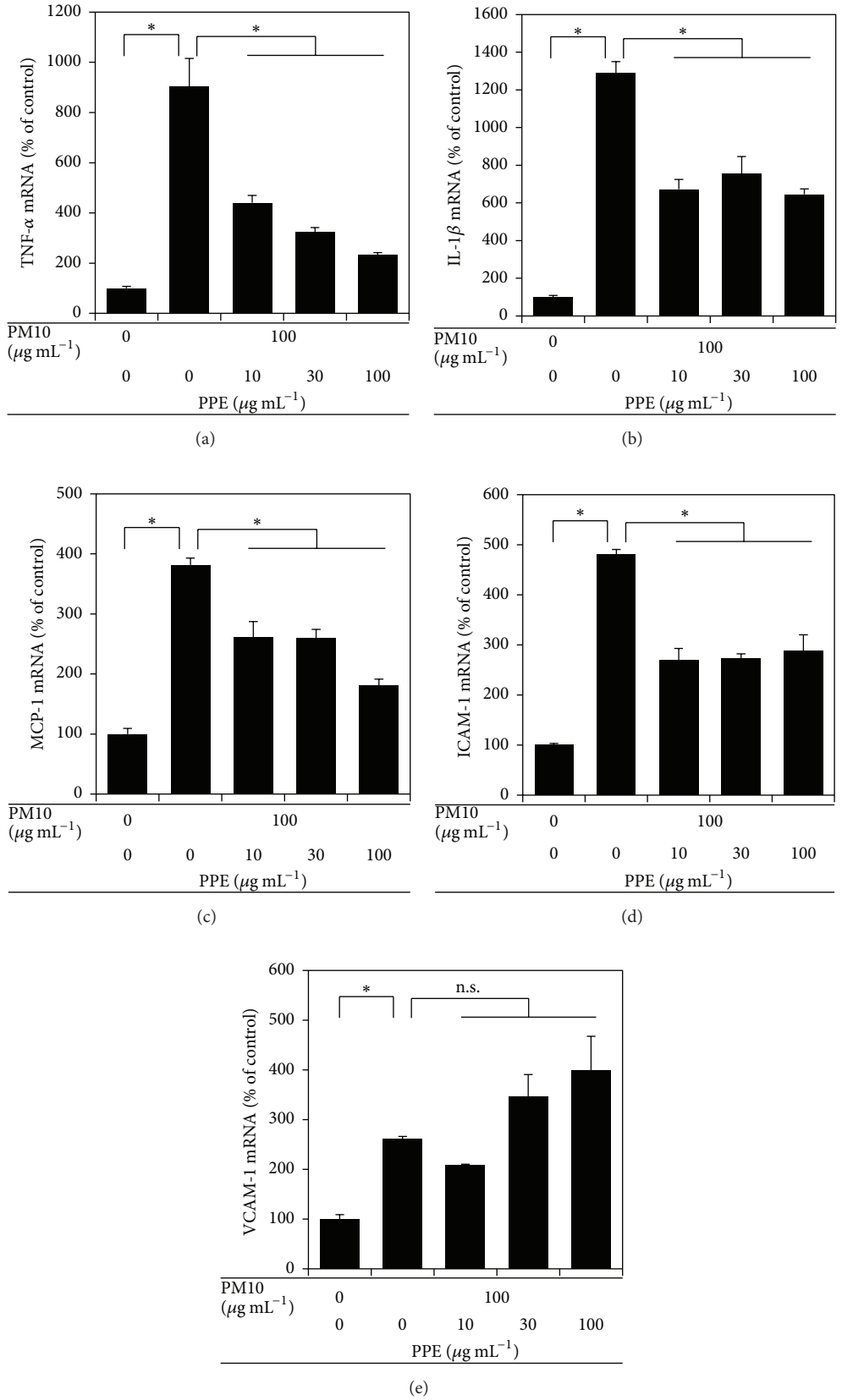

Figure 3: Effects of PPE on gene expression of inflammatory cytokines and cell adhesion molecules in THP-1 cells stimulated by PM10. Cells were treated with PM10 in the absence or presence of PPE, followed by incubation for 24 h. Gene expression was analyzed by qRT-PCR and normalized to control GAPDH. Data are expressed as percentages of the control value. Data are means ± SEs ($n = 3$). $^{*}p < 0.05$; n.s., not significant.

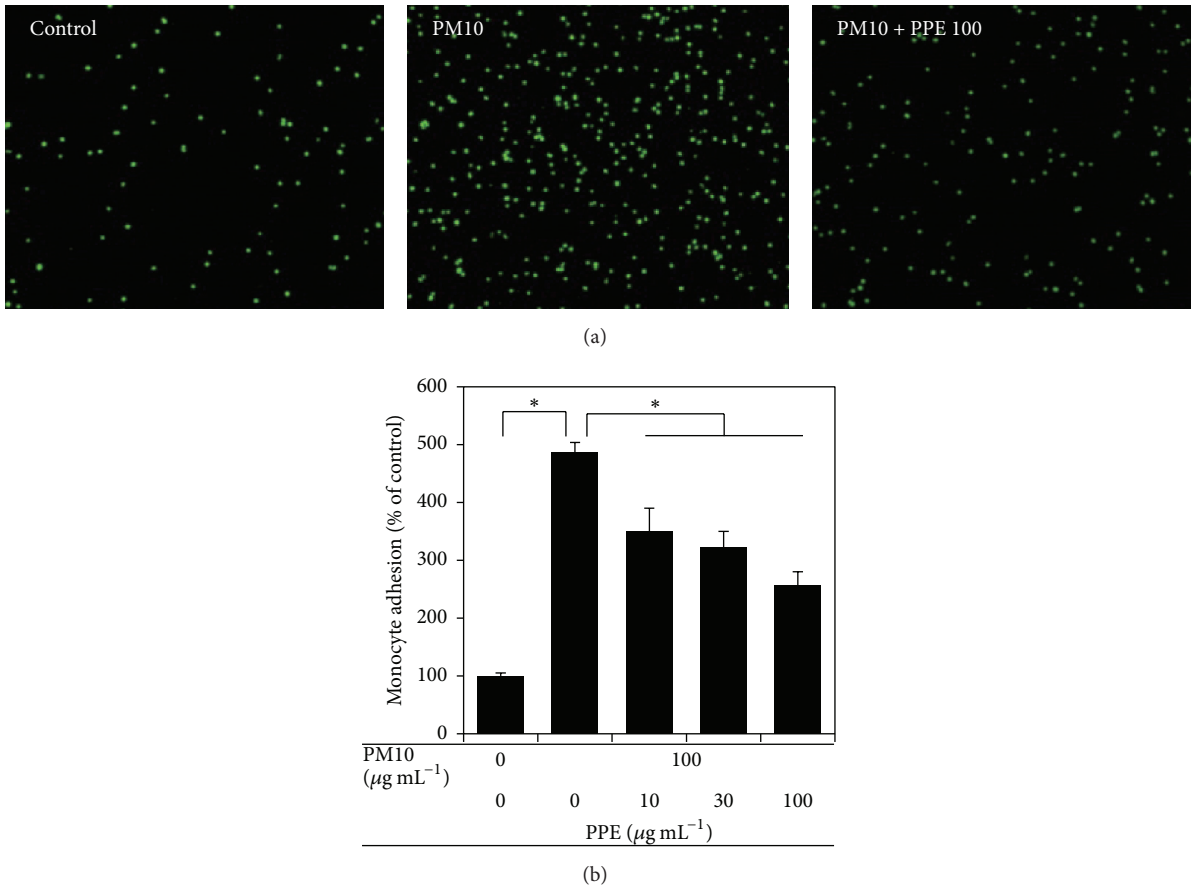

Figure 4: Effects of PPE on the adhesion of PM10-treated THP-1 monocytes to cells to EA.hy926 endothelial cells. THP-1 cells were treated with PM10 in the absence or presence of PPE, followed by incubation for 24 h. The treated monocytes were fluorescence-labeled and coincubated with EA.hy926 endothelial cells to monitor cell-cell adhesion. Fluorescing monocytes adhered on the endothelial cells were observed under a microscope (a) and quantified fluorometrically (b). Data are expressed as percentages of the control value. Data are means ± SEs ($n = 3$). $^{*}p < 0.05$.

production of ROS and activation of NF-κB pathway, leading to inflammation [7]. Thus, the inflammation due to PM10 is similar to sepsis in the clinical setting [25].

As expected, the data from the current study showed that PM10 induced cytotoxicity and increased the generation of ROS, the expression of inflammatory cytokines such as TNF-α, IL-1β, and MCP-1, and the expression of cell adhesion molecules such as ICAM-1 and VCAM-1 by monocytic THP-1 cells. In addition, PM10-exposed monocytic THP-1 cells showed stronger adherences to EA.hy926 endothelial cells, supporting proinflammatory properties of PM10.

PM10-induced inflammation may be reduced by minimizing outdoor activity while atmospheric levels of particulate matter are elevated high. Additionally, certain plant extracts enriched with antioxidants are expected to reduce oxidative stress and inflammatory injury due to particulate matter. In a previous study, exposure of mice to urban air pollution increased myocardial inflammatory genes such as TNF-α, IL-6, and cyclooxygenase-2 (COX-2) and chocolate administration resulted in a significant downregulation of TNF-α, IL-6, and IL-1β, implicating that regular consumption of dark chocolate may reduce cardiac inflammation in the setting of air pollution exposures [9]. Another study showed that the ethanolic extract of *Eucheuma cottonii* reduced the deposition of alveolar macrophages and serum levels of malondialdehyde (MDA) in PM10 coal dust-exposed rats, indicating that the extract attenuated inflammation and oxidative stress due to chronic exposure of coal dust [10].

PPE is a well-known source of polyphenolic antioxidants and its anti-inflammatory properties have been demonstrated in various experimental models [14–16]. However, its effects on PM10-induced inflammatory responses have not been reported until the current study. The results from this study showed that PPE attenuated the PM10-induced ROS generation, expression, and secretion of TNF-α, IL-1β, MCP-1, and ICAM-1. In addition, PPE was shown to attenuate the adhesion of PM10-stimulated THP-1 cells to endothelial cells. Thus, PPE is suggested to provide health benefits by mitigating inflammatory events stimulated by particulate matter.

Literature search and HPLC analysis of PPE indicated that punicalagin and ellagic acid are major polyphenolic compounds. Thus we compared the effects of these two compounds on cell viability and cell adherence of THP-1

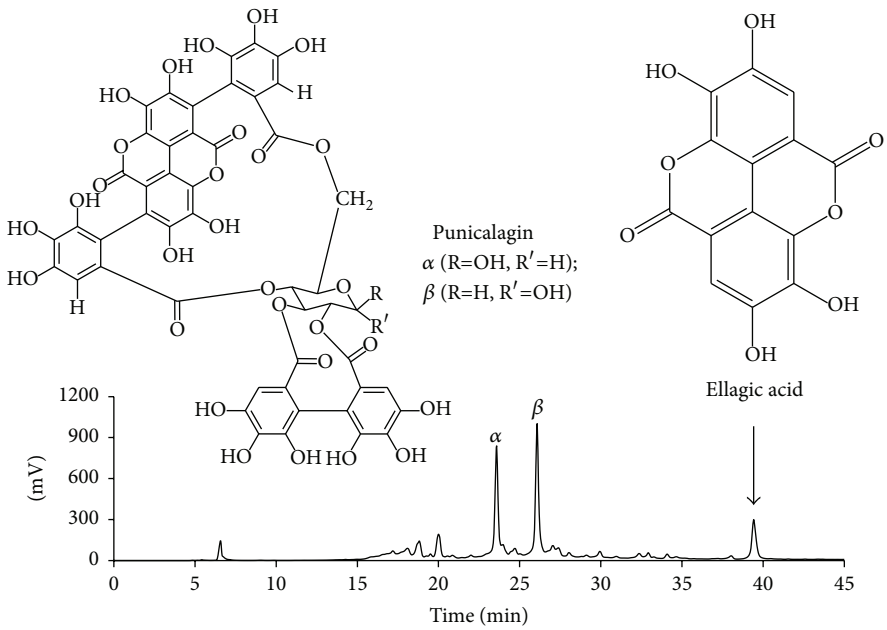

Figure 5: A typical high performance liquid chromatography (HPLC) chromatogram of PPE. The peaks for punicalagin and ellagic acid are indicated based on the retention times of authentic standards. Punicalagin appeared as two peaks, each corresponding to α and β anomers. Chemical structures of punicalagin α and β anomers and ellagic acid are shown.

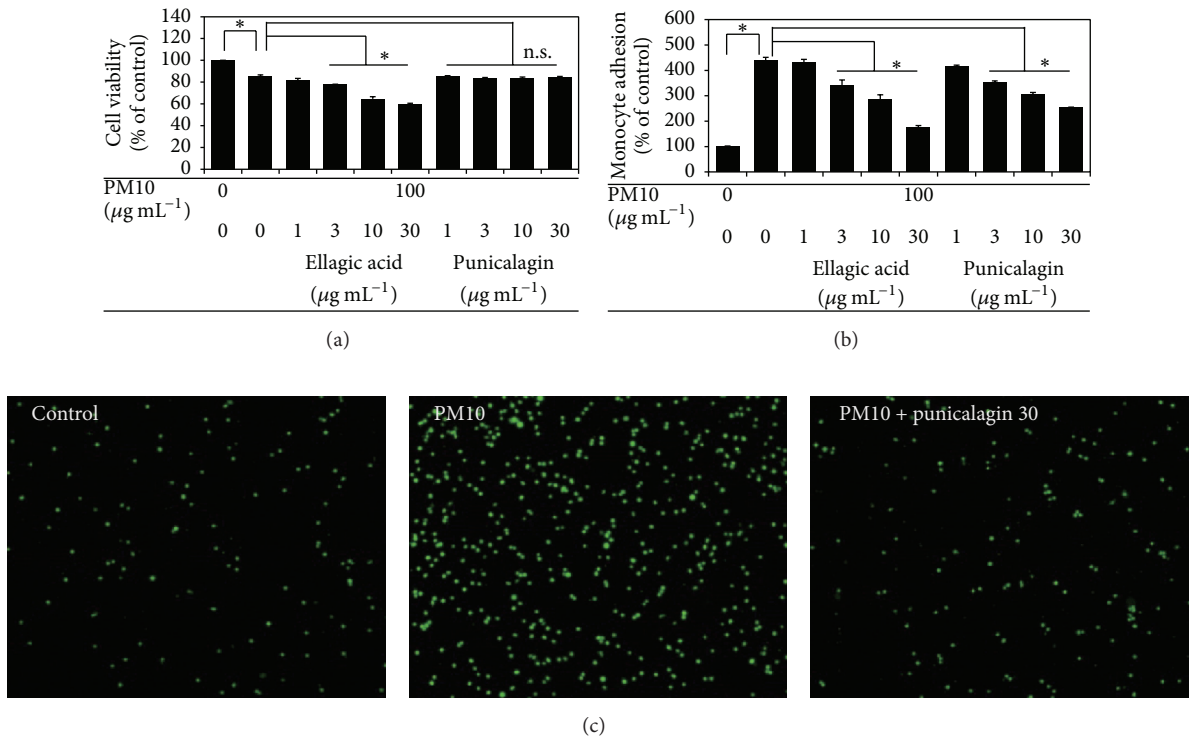

Figure 6: Effects of punicalagin and ellagic acid on cell viability and cell adhesiveness of THP-1 cells stimulated by PM10. THP-1 cells were treated with PM10 in the absence or presence of a test compound, followed by incubation for 24 h. Cell viabilities are presented as percentages of viable cells per total cells (a). The treated monocytes were fluorescence-labeled and coincubated with EA.hy926 endothelial cells to monitor cell-cell adhesion (b). Typical microscopic images of fluorescing monocytes adhered on the endothelial cells are shown (c). Data are expressed as percentages of the control value. Data are means ± SEs ($n = 3$). $^{*}p < 0.05$; n.s., not significant.

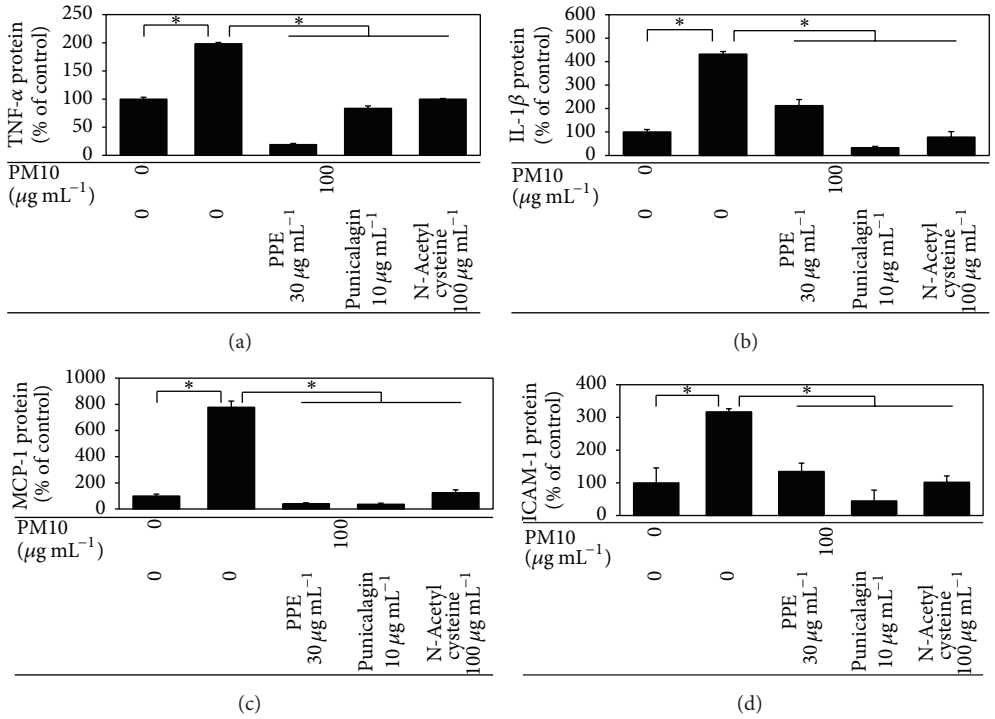

Figure 7: Effects of PPE, punicalagin, and N-acetyl cysteine on the levels of TNF-α, IL-1β, MCP-1, and ICAM-1 proteins released from THP-1 cells stimulated by PM10. THP-1 cells were treated with PM10 in the absence or presence of a test material for 72 h. The concentrations of TNF-α (a), IL-1β (b), MCP-1 (c), and ICAM-1 (d) proteins in the conditioned medium were measured by ELISA. Data are expressed as percentages of the control value. Data are means ± SEs ($n = 3$). $^*p < 0.05$.

cells. The results indicate that punicalagin would be more useful than ellagic acid as an anti-inflammatory agent against PM10, in terms of the efficacy to safety ratios. The present study is the first to demonstrate that punicalagin (a mixture of α and β anomers) attenuates the inflammatory cytokine secretion and cell adhesion of monocytic cells stimulated with airborne dust, although previous studies have reported that punicalagin can provide health benefits in various other experimental conditions [26–28]. Previous studies have shown that punicalagin is highly bioavailable and safe in animal models [29, 30]. Punicalagin is metabolized to punicalin, gallagic acid, and ellagic acid [31]. Therefore, not only does punicalagin offer antioxidant and anti-inflammatory effects on its own, but its metabolite can provide similar effects in the body.

Although the present study clearly demonstrated that PM10-induced inflammation can be attenuated by PPE at the cellular levels and identified punicalagin as an active constituent of PPE, the health benefits of PPE and punicalagin remain to be validated in additional *in vivo* studies.

In conclusion, we demonstrated that PPE prevented inflammatory events due to particulate matter. PPE attenuated ROS production, the expression of inflammatory cytokines, and cell adhesion molecules in THP-1 monocytic cells exposed to PM10. PPE also decreased the cell-cell adhesion between PM10-stimulated THP-1 cells and EA.hy926 endothelial cells. Punicalagin appeared to attenuate the cell-cell adhesion between PM10-stimulated THP-1 cells and EA.hy926 endothelial cells, without cytotoxicity. These results support the protective effects of PPE and punicalagin against oxidative stress and inflammatory responses induced by harmful airborne dust.

Competing Interests

The authors declare that there are no competing interests regarding the publication of this paper.

Authors' Contributions

Soojin Park and Jin Kyung Seok contributed equally to this work.

Acknowledgments

This study was supported by INNOPOLIS Foundation (Daegu) funded by the Ministry of Science, ICT and Future Planning, Republic of Korea (no. 2015-01-7005).

References

[1] J. O. Anderson, J. G. Thundiyil, and A. Stolbach, "Clearing the air: a review of the effects of particulate matter air pollution on human health," *Journal of Medical Toxicology*, vol. 8, no. 2, pp. 166–175, 2012.

[2] A. H. Mokdad, J. S. Marks, D. F. Stroup, and J. L. Gerberding, "Actual causes of death in the United States, 2000," *The Journal of the American Medical Association*, vol. 291, no. 10, pp. 1238–1245, 2004.

[3] J. D. Sacks, L. W. Stanek, T. J. Luben et al., "Particulate matter-induced health effects: who is susceptible?" *Environmental Health Perspectives*, vol. 119, no. 4, pp. 446–454, 2011.

[4] X. Y. Li, P. S. Gilmour, K. Donaldson, and W. MacNee, "Free radical activity and pro-inflammatory effects of particulate air pollution (PM10) in vivo and in vitro," *Thorax*, vol. 51, no. 12, pp. 1216–1222, 1996.

[5] L. Guo, N. Zhu, Z. Guo et al., "Particulate matter (PM_{10}) exposure induces endothelial dysfunction and inflammation in rat brain," *Journal of Hazardous Materials*, vol. 213-214, pp. 28–37, 2012.

[6] K. Donaldson, V. Stone, A. Clouter, L. Renwick, and W. MacNee, "Ultrafine particles," *Occupational and Environmental Medicine*, vol. 58, no. 3, pp. 211–216, 2001.

[7] K. Donaldson and V. Stone, "Current hypotheses on the mechanisms of toxicity of ultrafine particles," *Annali dell'Istituto Superiore di Sanita*, vol. 39, no. 3, pp. 405–410, 2003.

[8] R. Bengalli, E. Molteni, E. Longhin, M. Refsnes, M. Camatini, and M. Gualtieri, "Release of IL-1β triggered by milan summer PM_{10}: molecular pathways involved in the cytokine release," *BioMed Research International*, vol. 2013, Article ID 158093, 9 pages, 2013.

[9] R. Villarreal-Calderon, W. Reed, J. Palacios-Moreno et al., "Urban air pollution produces up-regulation of myocardial inflammatory genes and dark chocolate provides cardioprotection," *Experimental and Toxicologic Pathology*, vol. 64, no. 4, pp. 297–306, 2012.

[10] R. K. Saputri, B. Setiawan, D. Nugrahenny, N. Kania, E. Sri Wahyuni, and M. A. Widodo, "The effects of *Eucheuma cottonii* on alveolar macrophages and malondialdehyde levels in bronchoalveolar lavage fluid in chronically particulate matter 10 coal dust-exposed rats," *Iranian Journal of Basic Medical Sciences*, vol. 17, no. 7, pp. 541–545, 2014.

[11] X.-C. Liu, Y.-J. Li, Y.-J. Wang et al., "Protection of Shenlian extracts to PM2.5 infected RAW 264.7 cell damage," *Zhongguo Zhong Yao Za Zhi*, vol. 40, no. 10, pp. 1977–1983, 2015.

[12] R. P. Singh, K. N. Chidambara Murthy, and G. K. Jayaprakasha, "Studies on the antioxidant activity of pomegranate (*Punica granatum*) peel and seed extracts using in vitro models," *Journal of Agricultural and Food Chemistry*, vol. 50, no. 1, pp. 81–86, 2002.

[13] A. P. Kulkarni, H. S. Mahal, S. Kapoor, and S. M. Aradhya, "In vitro studies on the binding, antioxidant, and cytotoxic action of punicalagin," *Journal of Agricultural and Food Chemistry*, vol. 55, no. 4, pp. 1491–1500, 2007.

[14] M. Aviram, M. Rosenblat, D. Gaitini et al., "Pomegranate juice consumption for 3 years by patients with carotid artery stenosis reduces common carotid intima-media thickness, blood pressure and LDL oxidation," *Clinical Nutrition*, vol. 23, no. 3, pp. 423–433, 2004.

[15] A. Esmaillzadeh, F. Tahbaz, I. Gaieni, H. Alavi-Majd, and L. Azadbakht, "Concentrated pomegranate juice improves lipid profiles in diabetic patients with hyperlipidemia," *Journal of Medicinal Food*, vol. 7, no. 3, pp. 305–308, 2004.

[16] M. Aviram and L. Dornfeld, "Pomegranate juice consumption inhibits serum angiotensin converting enzyme activity and reduces systolic blood pressure," *Atherosclerosis*, vol. 158, no. 1, pp. 195–198, 2001.

[17] C. Monn and S. Becker, "Cytotoxicity and induction of proinflammatory cytokines from human monocytes exposed to fine (PM2.5) and coarse particles (PM10-2.5) in outdoor and indoor air," *Toxicology and Applied Pharmacology*, vol. 155, no. 3, pp. 245–252, 1999.

[18] A. Montiel-Dávalos, E. Alfaro-Moreno, and R. López-Marure, "$PM_{2.5}$ and PM_{10} induce the expression of adhesion molecules and the adhesion of monocytic cells to human umbilical vein endothelial cells," *Inhalation Toxicology*, vol. 19, supplement 1, pp. 91–98, 2007.

[19] D. H. Adams and G. B. Nash, "Disturbance of leucocyte circulation and adhesion to the endothelium as factors in circulatory pathology," *British Journal of Anaesthesia*, vol. 77, no. 1, pp. 17–31, 1996.

[20] J. O. Ogunbileje, R. S. Nawgiri, J. I. Anetor, O. M. Akinosun, E. O. Farombi, and A. O. Okorodudu, "Particles internalization, oxidative stress, apoptosis and pro-inflammatory cytokines in alveolar macrophages exposed to cement dust," *Environmental Toxicology and Pharmacology*, vol. 37, no. 3, pp. 1060–1070, 2014.

[21] R. González-Amaro, "Cell adhesion, inflammation and therapy: old ideas and a significant step forward," *Acta Pharmacologica Sinica*, vol. 32, no. 12, pp. 1431–1432, 2011.

[22] H. Ishii, T. Fujii, J. C. Hogg et al., "Contribution of IL-1β and TNF-α to the initiation of the peripheral lung response to atmospheric particulates (PM_{10})," *American Journal of Physiology—Lung Cellular and Molecular Physiology*, vol. 287, no. 1, pp. L176–L183, 2004.

[23] T. Fujii, S. Hayashi, J. C. Hogg et al., "Interaction of alveolar macrophages and airway epithelial cells following exposure to particulate matter produces mediators that stimulate the bone marrow," *American Journal of Respiratory Cell and Molecular Biology*, vol. 27, no. 1, pp. 34–41, 2002.

[24] T. Fujii, S. Hayashi, J. C. Hogg, R. Vincent, and S. F. Van Eeden, "Particulate matter induces cytokine expression in human bronchial epithelial cells," *American Journal of Respiratory Cell and Molecular Biology*, vol. 25, no. 3, pp. 265–271, 2001.

[25] K. V. Ramana, M. S. Willis, M. D. White et al., "Endotoxin-induced cardiomyopathy and systemic inflammation in mice is prevented by aldose reductase inhibition," *Circulation*, vol. 114, no. 17, pp. 1838–1846, 2006.

[26] D. Jean-Gilles, L. Li, V. G. Vaidyanathan et al., "Inhibitory effects of polyphenol punicalagin on type-II collagen degradation in vitro and inflammation in vivo," *Chemico-Biological Interactions*, vol. 205, no. 2, pp. 90–99, 2013.

[27] C.-C. Lin, Y.-F. Hsu, and T.-C. Lin, "Effects of punicalagin and punicalin on carrageenan-induced inflammation in rats," *The American Journal of Chinese Medicine*, vol. 27, no. 3-4, pp. 371–376, 1999.

[28] X. Xu, P. Yin, C. Wan et al., "Punicalagin inhibits inflammation in LPS-induced RAW264.7 macrophages via the suppression of TLR4-mediated MAPKs and NF-κB activation," *Inflammation*, vol. 37, no. 3, pp. 956–965, 2014.

[29] B. Cerdá, J. J. Cerón, F. A. Tomás-Barberán, and J. C. Espín, "Repeated oral administration of high doses of the pomegranate ellagitannin punicalagin to rats for 37 days is not toxic," *Journal of Agricultural and Food Chemistry*, vol. 51, no. 11, pp. 3493–3501, 2003.

[30] B. Cerdá, R. Llorach, J. J. Cerón, J. C. Espín, and F. A. Tomás-Barberán, "Evaluation of the bioavailability and metabolism

in the rat of punicalagin, an antioxidant polyphenol from pomegranate juice," *European Journal of Nutrition*, vol. 42, no. 1, pp. 18–28, 2003.

[31] F. J. Mininel, C. S. Leonardo Junior, L. G. Espanha et al., "Characterization and quantification of compounds in the hydroalcoholic extract of the leaves from *Terminalia catappa* Linn. (Combretaceae) and their mutagenic activity," *Evidence-Based Complementary and Alternative Medicine*, vol. 2014, Article ID 676902, 11 pages, 2014.

Hindawi Publishing Corporation
Evidence-Based Complementary and Alternative Medicine
Volume 2016, Article ID 1654056, 11 pages
http://dx.doi.org/10.1155/2016/1654056

Research Article

The *In Vitro* and *In Vivo* Wound Healing Properties of the Chinese Herbal Medicine "Jinchuang Ointment"

Tsung-Jung Ho,[1,2,3] Shinn-Jong Jiang,[4] Guang-Huey Lin,[5] Tzong Shiun Li,[6,7,8] Lih-Ming Yiin,[9] Jai-Sing Yang,[10] Ming-Chuan Hsieh,[5] Chun-Chang Wu,[1] Jaung-Geng Lin,[11] and Hao-Ping Chen[4]

[1] *Division of Chinese Medicine, China Medical University Beigang Hospital, Yulin 65152, Taiwan*
[2] *Division of Chinese Medicine, An Nan Hospital, China Medical University, Tainan 70965, Taiwan*
[3] *College of Chinese Medicine, China Medical University, Taichung 40421, Taiwan*
[4] *Department of Biochemistry, School of Medicine, Tzu Chi University, Hualien 97004, Taiwan*
[5] *Department of Microbiology, School of Medicine, Tzu Chi University, Hualien 97004, Taiwan*
[6] *Department of Plastic Surgery, China Medical University Beigang Hospital, Yulin 65152, Taiwan*
[7] *School of Medicine, China Medical University, Taichung 40421, Taiwan*
[8] *Department of Plastic Surgery, China Medical University Hospital, Taichung 40447, Taiwan*
[9] *Department of Public Health, School of Medicine, Tzu Chi University, Hualien 97004, Taiwan*
[10] *Department of Medical Research, China Medical University Hospital, China Medical University, Taichung 40447, Taiwan*
[11] *Graduate Institute of Chinese Medicine, China Medical University, Taichung 40421, Taiwan*

Correspondence should be addressed to Shinn-Jong Jiang; sjjiang@mail.tcu.edu.tw and Hao-Ping Chen; hpchen@mail.tcu.edu.tw

Received 18 January 2016; Accepted 10 March 2016

Academic Editor: Yoshiji Ohta

"Jinchuang ointment" is a traditional Chinese herbal medicine complex for treatment of incised wounds. For more than ten years, it has been used at China Medical University Hospital (Taichung, Taiwan) for the treatment of diabetic foot infections and decubitus ulcers. Three different cases are presented in this study. "Jinchuang" ointment is a mixture of natural product complexes from nine different components, making it difficult to analyze its exact chemical compositions. To further characterize the herbal ingredients used in this study, the contents of reference standards present in a subset of the ointment ingredients (dragon's blood, catechu, frankincense, and myrrh) were determined by HPLC. Two *in vitro* cell based assay platforms, wound healing and tube formation, were used to examine the biological activity of this medicine. Our results show that this herbal medicine possesses strong activities including stimulation of angiogenesis, cell proliferation, and cell migration, which provide the scientific basis for its clinically observed curative effects on nonhealing diabetic wounds.

1. Introduction

It is well-known that diabetic foot ulcers are extremely difficult to be treated and are the dominant complication leading to amputations [1]. "Jinchuang ointment" is a traditional Chinese herbal medicine complex for treatment of incised wounds. Its recipe was first described in one ancient Chinese book of medicine, *Medicine Comprehended*, published in 1732. Clinical applications of this herbal medicine for diabetic foot infections and decubitus ulcers have been a successful course of treatment in the Division of Chinese Medicine, China Medical University Hospital, Taichung, Taiwan, for more than ten years. Despite its track record of curative effects, there is no literature published in the English language describing the clinical efficacy of "Jinchuang ointment" [2]. Moreover, neither a biological mechanism nor the compositions of effective components have yet to be systematically investigated. Like many Chinese herbal medicines, "Jinchuang ointment" is also a mixture of natural product complexes. The combination of compounds results

in complications when it determines the chemical composition and bioactivity of each component [3].

"Jinchuang ointment" is composed of lard, wax, starch, synthetic borneol, camphor, frankincense, dragon's blood, myrrh, and catechu. To further characterize the chemical content of each component in this complex, the ratio of stereoisomers in chemically synthesized borneol used in this study was analyzed by chiral gas chromatography (GC). Meanwhile, the content of reference standards in the herbal components, like frankincense, myrrh, dragon's blood, and catechin, was determined by high performance liquid chromatography (HPLC). Lard is the major component in this complex, and its weight percentage is as high as 67%. It is of great interest to determine the role of lard in this complex. Lard was therefore substituted for synthetic triacylglycerol, coconut oil, Vaseline®, and sesame oil. The activity of these reconstituted complexes was examined in this study.

"Jinchuang ointment" is directly applied to the wound surface during treatment. The components in this complex are neither digested nor absorbed in the gastrointestinal tract. It is therefore reasonable to evaluate its bioactivity by direct addition of this complex into media containing cultured human skin or endothelial cells. Wound healing is a very complicated process. In this study, an *in vitro* tube formation assay, a wound healing assay, and a cell proliferation test were carried out to examine the activity of "Jinchuang ointment." Here, we report the outcomes of treating patients with "Jinchuang ointment," the results of cell based activity assays, and characterization of herbal components by HPLC.

2. Materials and Methods

2.1. Materials. The reference standards of dracorhodin perchlorate, acetyl-11-keto-β-boswellic acid, catechin, and epicatechin were purchased from the National Institute for the Control of Pharmaceutical and Biological Products (Beijing, China). (E)-Guggulsterone and (+)-borneol were obtained from Sigma-Aldrich (St. Louis, MO, USA). (−)-Borneol and (±)-isoborneol were purchased from Alfa Assar (Lancashire, UK). DMEM high glucose with sodium pyruvate media, Catalog number: I-26F55-I, was bought from Amimed® BioConcept (Allschwil, Switzerland). Chemically synthesized borneol and camphor were bought from Cheng Yi Chemical Co., Ltd. (Taipei, Taiwan). Herbal medicine, dragon's blood, catechu, frankincense, and myrrh were bought from Healthy Beautiful Biotech. Co. Ltd. (Taichung, Taiwan). Vascular endothelial growth factor (VEGF) was bought from B&D Systems (Minneapolis, MN, USA). Antibodies for western blot analysis were bought from Santa Cruz Biotechnology, Inc. (Dallas, Texas, USA). Food-grade lard was obtained from I-Mei Food Company (Taipei, Taiwan). Synthetic triacylglycerol (glyceryl tricaprylate-caprate, $C_8 : C_{10}$, 60 : 40) was obtained from InterMed Manufacturing Sdn. Bhd. (Kuala Lumpur, Malaysia). Food-grade sesame oil was from Fwusow Industry Co. Ltd. (Taichung, Taiwan). Coconut oil was bought from First Chemical Co., Ltd. (Taipei, Taiwan). Vaseline was bought from Unilever (Trumbull, Connecticut, USA).

The composition of "Jinchuang ointment" (100 g) is as follows: lard 67.3 g, dragon's blood 2.1 g, catechu 2.1 g, frankincense 2.1 g, myrrh 2.1 g, camphor 6.3 g, borneol 0.1 g, corn starch 8.4 g, and wax 9.5 g. For wound healing and tube formation assays, the DMSO stock solution of "Jinchuang ointment" is prepared as follows: two grams of "Jinchuang ointment" is dissolved in 10 mL DMSO and homogenized by ultrasonication just before use.

2.2. Determination of Reference Standard Content in Dragon's Blood, Catechu, Frankincense, and Myrrh by HPLC. All experiments were carried out on a Hitachi L-7000 HPLC system, equipped with L-7100 quaternary gradient pump and a L-7450 photo diode array detector. Hitachi HSM software was used for machine controlling, data collecting, and processing. A Mightysil, RP-18, 5 μm, 250 × 4.6 mm, analytic column (Kanto Chemical Co., Inc., Tokyo, Japan) was used for analysis.

For samples of dragon's blood, catechu, and frankincense, 0.1 g grounded solids were weighed and dissolved in 10 mL of methanol. After ultrasonicating for 30 minutes at room temperature, methanol extracts were transferred to a new glass vial by using disposable glass Pasteur pipettes. 4 mL of methanol was then added and ultrasonicated for another 30 minutes at room temperature. The final volume of the extract was adjusted to 25 mL by adding methanol. Undissolved particles were removed by centrifugation at 2500 ×g for 10 minutes at room temperature and filtrated through a 0.22 μm syringe filter. For myrrh, 95% ethanol was used for extraction rather than methanol. Other preparation steps were identical to those of dragon's blood, catechu, frankincense, and myrrh.

The methanol extract of dragon's blood was separated using a gradient elution of solvent A (10% CH_3CN containing 0.1% formic acid) and solvent B (90% CH_3CN containing 0.1% formic acid) with a flow rate of 1 mL/min [4]. The elution program is given in Table 1. The UV detection wavelength was 254 nm.

The catechu methanol extract was separated using a gradient elution of A (H_2O containing 0.1% formic acid), B (10% CH_3CN containing 0.1% formic acid), and C (90% CH_3CN containing 0.1% formic acid) with a flow rate of 1 mL/min [5]. The elution program is given in Table 1. The UV detection wavelength was 270 nm.

The frankincense methanol extract was separated using a gradient elution of solvent A (9.5% methanol containing 0.5% H_3PO_4, 85%) and solvent B (45% methanol, 55% CH_3CN containing 0.5% H_3PO_4, 85%) with a flow rate of 1 mL/min [6]. The elution program is given in Table 1. The UV detection wavelength was 250 nm.

To determine the content of (E)-guggulsterones in myrrh, an ethanol extract was separated using an isocratic elution of 0.1% $H_3PO_4 : CH_3CN$ (45 : 55, v/v) with a flow rate of 1 mL/min for 25 minutes [7]. The UV detection wavelength was 240 nm.

2.3. Determination of the Ratio of Stereoisomers in Synthetic Borneol. Chiral GC was used to determine the ratio of stereoisomers in synthetic borneol. Analysis was performed

Table 1: HPLC elution program for dragon's blood, catechu, and frankincense.

Dragon's blood		Catechu		Frankincense	
Time (min)	Eluent (B%)	Time (min)	Eluent (B, C%)	Time (min)	Eluent (B%)
0–2	19	0–5	0,0	0–5	90
2–20	19–100	5–7	0,0–100,0	5–11	90–100
20-21	100	7–12	100,0–20,80	11–23	100
		12–26	20,80–0,100		

using an Agilent GC system model HP 6890N (Santa Clara, CA, USA) equipped with a split/splitless injector, liner of silanized quartz with a 4 mm i.d. (effective volume 0.49 mL), and an Agilent 6890 autosampler for 100 vials. A Cydex-B chiral GC column (25 m × 0.22 mm ID; 0.25 μm) was obtained from SGE Analytical Science (Austin, TX, USA). Chromatographic conditions were as follows: helium used as a gas carrier; a constant flow of 1.0 mL/min; 2 μL injection volume (splitless model), and a 280°C injector temperature. The GC temperature program was as follows: 90°C (1 min), 90°C to 130°C (41 min), 130°C (10 min), and 200°C (3 min). An Agilent 5973N quadrupole mass spectrometer was operated in selective ion monitoring (SIM) mode, with ionization source by electron impact at 70 eV, transfer line at 280°C, ion source at 280°C, and quadrupole at 150°C.

2.4. In Vitro Wound Healing Assay. Confluent HaCaT cells in 12-well plates were starved overnight in DMEM medium. The surface of the plate was scraped with a 200 μL pipette tip to generate a cell-free zone. Free cells were then removed by two HBSS washes, and cells were incubated in DMEM medium containing 200 μg/mL, 20 μg/mL, or 2 μg/mL "Jinchuang ointment." After 24 hours of incubation, cells were imaged using microscopy. The area of wound closure was quantitatively determined using Image J software (National Institutes of Health, Bethesda, MD).

Stimulation effects on *in vitro* wound healing assay by "Jinchuang ointment" were also examined using human microvascular endothelial cells (HMEC-1). Ibidi Culture-Inserts (Ibidi Gmbh, Martinsried, Germany) were placed on the chamber of 24-well cell culture plates. About 70 μL of HMEC-1 (5×10^5 cells/mL) was seeded per well and plates were incubated at 37°C and 5% CO_2. After 24-hour incubation, Ibidi Culture-Inserts were removed, and 1 mL of MCDB131 media containing 1 μL DMSO solution of "Jinchuang ointment" was then added into individual wells. The migration of cells was observed by microscopy over a period of 6–24 hours. The gap size was measured by using software Image J.

2.5. Cell Proliferation Assay. HaCaT cells (5×10^4/well) were seeded in 96-well plates. The medium containing "Jinchuang ointment" at various concentrations was then added after cell adhesion. Cells were incubated in DMEM medium for the indicated time. The proliferation of HaCaT cells was subsequently determined by using Cell Proliferation Reagent WST-1 (Roche, Indianapolis, IN, USA). The statistical method used is Student's *t*-test.

2.6. Western Blotting. Confluent monolayers of HaCaT cells were treated with various concentrations of Jinchuang ointment for the indicated time. Equal quantities of cell lysate proteins were separated by 10% SDS-PAGE and electroblotted onto PVDF membranes (Millipore, Billerica, MA). Membranes were blocked for 1 h with 5% low-fat milk powder solubilized in phosphate-buffered saline (PBS) containing 0.05% Tween 20. Levels of Cdc25b, Cdc25c, CDK2, CDC D2, Cyclin B, Cyclin D3, and α-tubulin were determined by western blotting using specific antibodies and enhanced chemiluminescence detection methods. The intensity of the resulting bands was measured by densitometric analysis using Image J software and presented as the ratio relative to the internal control.

2.7. In Vitro Tube Formation Assay. Human umbilical vein endothelial cells (HUVEC) were bought from Bioresource Collection and Research Center (Hsinchu, Taiwan). 1 mL of HUVEC (1×10^5 cells/well) was placed into the wells of a 24-well flat bottomed plates precoated with 200 μL Matrigel (BD Biosciences, Bedford, MA, USA). Cells were then mixed with 1 mL medium containing "Jinchuang ointment" (final concentration of 200 μg/mL). Cells were incubated at 37°C for a 24 h exposure [8]. After incubation, cell tube or network formation was observed using a phase-contrast microscope.

2.8. Statistical Analysis. Results are expressed as the means ± SD from at least three independent experiments. Differences between groups were assessed by one-way analysis of variance (ANOVA). A P value less than 0.05 was considered statistically significant.

3. Results and Discussion

3.1. Clinical Treatment Observations on a Nonhealing Diabetic Wound by Treating with "Jinchuang Ointment". To the best of our knowledge, there are no English language case reports describing "Jinchuang ointment" treatment for nonhealing diabetic wounds. Three different cases are presented in this study. The first subject, Mrs. Wu, is a 75-year-old female patient with type II insulin-dependent diabetes accompanied by peripheral arterial occlusion disease (PAOD) which led to left lateral leg and ankle necrotizing fasciitis. She was treated with percutaneous transluminal angiography (PTA) to improve lower limb circulation on Feb 6, 2013. As a result of reperfusion injury, the ulcer had enlarged with erythema. After examination, a below-knee amputation was immediately scheduled two weeks later at the Surgery Division,

Figure 1: The wound area of the patient Mrs. Wu during "Jinchuang ointment" treatment. Wound dimensions measured on the date specified are as follows: May 25, 2013, 26 × 9 cm; Jun 5, 2013, 26 × 9 cm; Sep 4, 2013, 8 × 4 cm; Aug 27, 2014, 2.5 × 3 cm.

the China Medical University Beigang Hospital. As suggested by a doctor from the Division of Chinese Medicine, she decided to use traditional Chinese medicine to treat her wound. She was referred to the Division of Chinese Medicine for wound management. Normal saline was first used to clean the wound. About 2-3 g "Jinchuang ointment" was applied directly to the wound once daily. Pictures depicting wound healing under treatment with "Jinchuang ointment" are shown in Figure 1.

Mr. Tsai, a 71-year-old male, with past history of type II diabetes was diagnosed on September 8, 2013. He had a 3 × 0.8 cm and a 4 × 1.5 cm grade 3 pressure sore in the sacral region. 1 g of "Jinchuang ointment" was applied topically to the wound area once per day. Pictures documenting wound healing under treatment of "Jinchuang ointment" are shown in Figure 2. It is well-known that all treatments for bedsores are to prevent wounds from worsening. Complete wound closure was observed on October 27, 2013.

Mr. Wang, a 64-year-old male with a past history of hypertension, had a chronic wound measuring 6.2 × 5.3 cm which had not healed for more than six months. He received the topical application of "Jinchuang ointment" once per day beginning November 26, 2014. A great improvement was observed after two months of treatment as shown in Figure 3.

3.2. Content of Reference Standards Present in Dragon's Blood, Catechu, Frankincense, and Myrrh. One of the main problems associated with herbal medicine is the high level of batch to batch variation in the amounts of active components. The content of pure chemical reference standards in herbal products is therefore used as an indicator for the purposes of quality control and standardization. Accordingly, the content of reference standards in dragon's blood, catechu, frankincense, and myrrh used was measured by HPLC in this study. All the calibration curves of reference compounds were linear over the concentration range studied (Table 2). A linear interpolation method was used to calculate the percentage by mass of each reference standard in the herbal extract that we examined.

Dracorhodin is a red anthocyanin pigment that is a major component in "dragon's blood" resin of the plant *Daemonorops draco*. It possesses antimicrobial, anticancer, and cytotoxic activity [9, 10]. Figure 4(a) shows the separation of dracorhodin in dragon's blood. The mass percentage of dracorhodin in the "dragon's blood" used in this study is 0.15%.

Both catechin and epicatechin are phenol-type antioxidants in catechu, an extract of acacia trees. Catechu is a common component of herbal medicine. In addition to their ability to scavenge free radicals in plasma, the health benefits of catechin and epicatechin also include stimulation of fat oxidation, expansion of the brachial artery, and resistance of LDLs to oxidation [11]. At the cellular and molecular level, catechin can enhance the expression of human PTGS2 (a dioxygenase gene), 1L1B (cyclooxygenase-2 gene), SOD (superoxide dismutase gene), MAPK1 (Mitogen-activated protein kinase 1), and MAPK3 [12–14]. Figure 4(b) shows the separation of catechin and epicatechin in catechu. The mass percentage of catechin and epicatechin in the catechu used in this study is 24.2% and 1.7%, respectively.

Frankincense is a resin from plants in the genus *Boswellia*. In Africa and Asia, it is widely used in incense, perfume, and traditional medicine. Boswellic acids, a series of pentacyclic triterpene molecules, are one of the major components of frankincense. Theiranti-inflammatory properties and ability to induce cancer cell apoptosis have been reported *in vitro* [15–17]. The expression of TOP1 (DNA topoisomerase I) and TOP2A (DNA topoisomerase II) genes can be altered in the presence of 11-keto-β-boswellic acid derivatives and

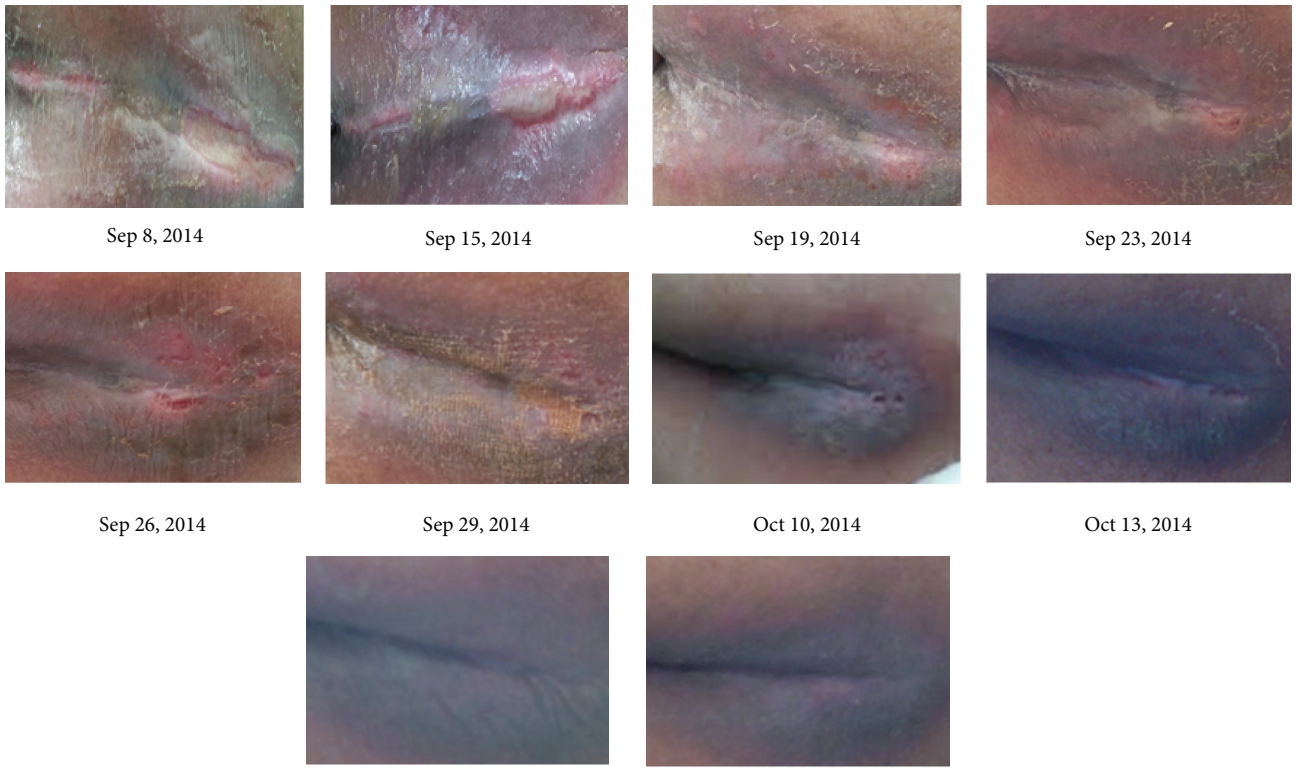

Figure 2: The pressure sore of the patient Mr. Tsai during "Jinchuang ointment" treatment. This wound was located at the sacral region and was completely closed after a 50-day treatment.

Figure 3: The previously nonhealing wound of patient Mr. Wang during "Jinchuang ointment" treatment. Wound dimensions were measured on the following dates: Nov 26, 2014, 6.2 × 5.3 × 0.3 cm; Dec 27, 2014, 4.5 × 4 × 0.1 cm; Jan 21, 2015, 2.5 × 1.5 × 0.1 cm; Feb 21, 2015, wound complete closure.

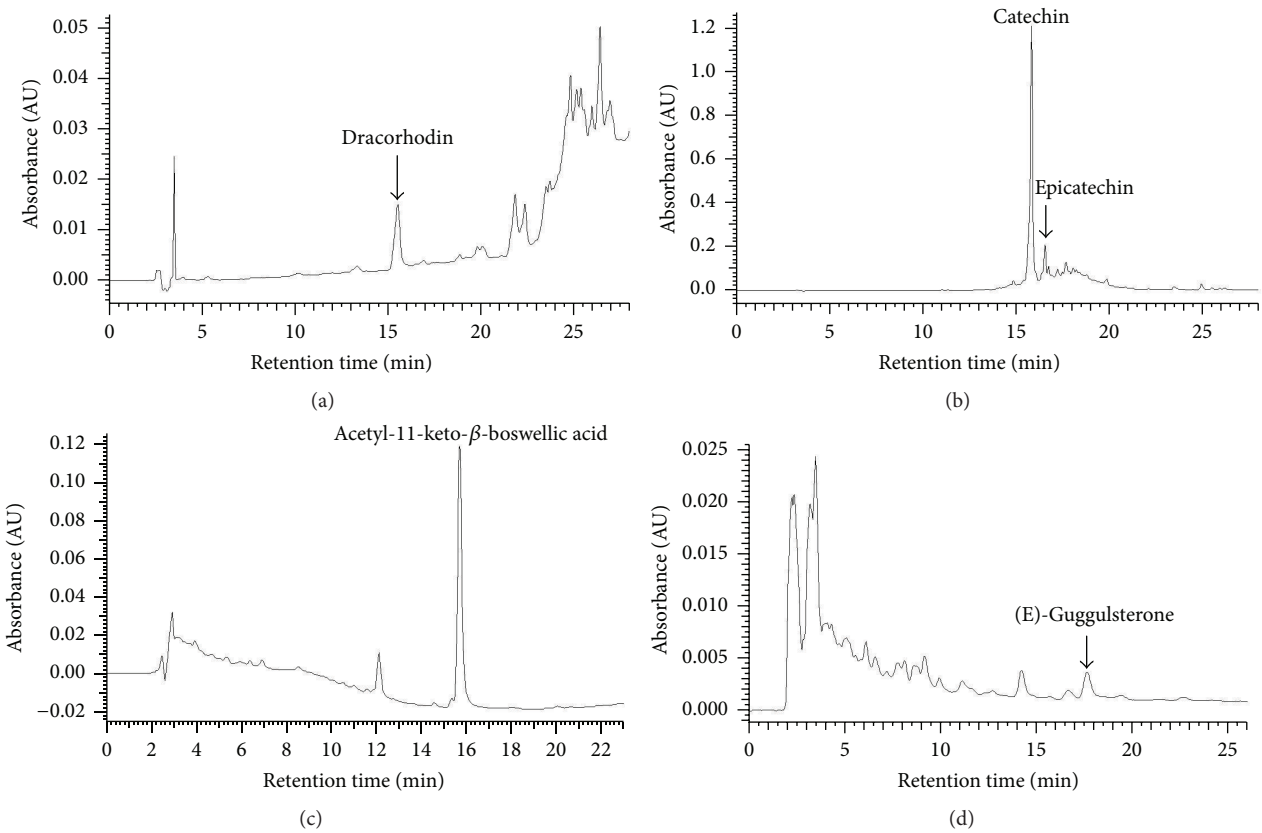

Figure 4: HPLC separation of reference compounds present in extracts of herbal components. HPLC traces of (a) dracorhodin in "dragon's blood," (b) catechin and epicatechin in catechu, (c) acetyl-11-keto-β-boswellic acid in frankincense, and (d) (E)-guggulsterone in myrrh.

acetyl-boswellic acid [16, 18]. Figure 4(c) shows the separation of acetyl-11-keto-β-boswellic acid in frankincense. The mass percentage of acetyl-11-keto-β-boswellic acid in the frankincense used in this study is 1.62%.

Myrrh is also a resin from plants in the genus *Commiphora*. The usage of myrrh is similar to that of frankincense. In fact, both myrrh and frankincense are frequently used in concert in many traditional Chinese medicine recipes. In western medicine, myrrh is also used in liniment and healing salves for minor skin ailments. The chemical composition of myrrh is rather complicated [19]. Notably, both (Z)- and (E)-isomers of guggulsterone possess high affinity toward a variety of steroid receptors [20]. Both isomers seem equipotent as inhibitors of HUVEC tube formation [21]. The mass percentage of (E)-guggulsterone in the myrrh used in this study is 0.02%. Figure 4(d) shows the separation of (E)-guggulsterone in myrrh.

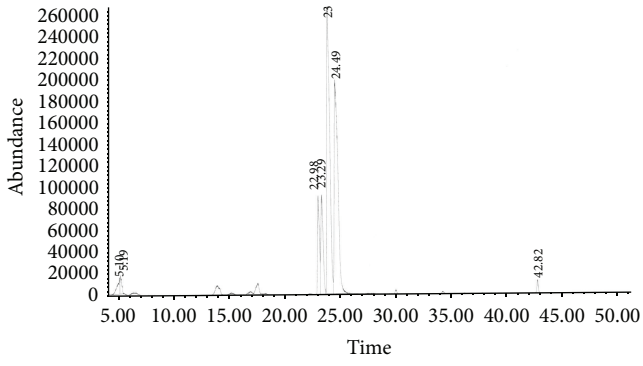

Figure 5: Chiral GC separations of synthetic borneol. The four major peaks from 22.0 to 26.0 min are (+)-isoborneol, (−)-isoborneol, (−)-borneol, and (+)-borneol, respectively.

3.3. The Ratio of Stereoisomers in Chemically Synthesized Borneol. Borneol is a bicyclic monoterpene plant secondary metabolite. (+)-Borneol, mainly isolated from the plant family of Dipterocarpaceae, is the major form used for analgesia and anesthesia in traditional Chinese medicine. More recently, chemically synthesized borneol and (−)-borneol isolated from the plant species *Blumea balsamifera* have enjoyed more widespread use. The price of synthetic borneol is the lowest among the sources discussed above. Previous results show that borneol stereoisomers can interact with GABA receptors [22, 23] and possess antimicrobial activity [24]. Chiral GC was used to analyze the composition of borneol stereoisomers in synthetic borneol used in this study. Our results show that (+)-isoborneol : (−)-isoborneol : (−)-borneol : (+)-borneol is in the ratio of 8.9 : 10.9 : 41.6 : 38.6 (Figure 5).

Table 2: HPLC calibration curves of reference compounds including regression equations, the coefficients of determination (R^2), and calibration ranges.

Reference compound	Regression equation	R^2	Calibration range	Mass percentage
Dracorhodin perchlorate	$y = 2000000x - 19368$	0.999	0.0125–0.2 μg	0.15%
Catechin	$y = 26508x - 35003$	0.997	0.25–4 μg	24.2%
Epicatechin	$y = 33500x - 65614$	0.999	0.5–4 μg	1.7%
Acetyl-11-keto-β-boswellic acid	$y = 79427x - 54832$	0.999	0.125–2 μg	1.62%
(E)-Guggulsterone	$y = 2466634x + 12554$	0.999	0.0625–1 μg	0.02%

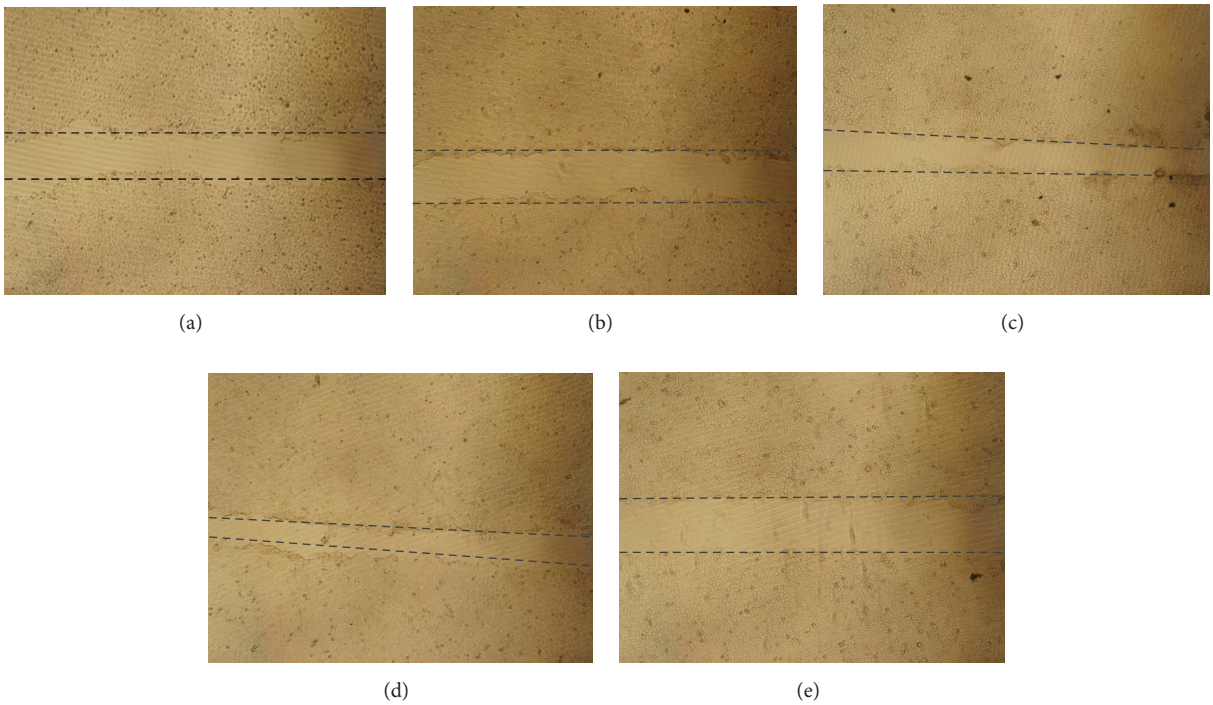

Figure 6: Wound healing assay with HaCaT cells displaying the increased cell migration induced by "Jinchuang ointment." Cells were treated with (a) DMSO alone (control), (b) 100 ng/mL EGF (positive control), (c) 200 μg/mL "Jinchuang ointment," (d) 20 μg/mL "Jinchuang ointment," and (e) 2 μg/mL "Jinchuang ointment." Cell migration was documented by phase contrast microscopy over a 24-hour time course where time 0 is the time of wound scratching.

3.4. In Vitro Wound Healing Assay. Confluent HaCaT cells were scratched and treated with "Jinchuang ointment." The wound area was measured after 24 hours of treatment. All experiments were performed in triplicate. The percentage of wound closure was calculated as follows: (initial wound area − 24 h posttreatment wound area)/initial wound area × 100%. The wound closure percentage with 200 μg/mL, 20 μg/mL, and 2 μg/mL "Jinchuang ointment" treatment was 78.2±5.3%, 78.2 ± 4.3%, and 63.8 ± 1.7%, respectively. In contrast, the negative control HaCaT cells without "Jinchuang ointment" treatment only showed 64.4 ± 4.0% wound closure. The positive control treated with 100 ng/mL EGF treatment showed 71.8 ± 1.0% wound closure. It is obvious that application of 200 μg/mL or 20 μg/mL "Jinchuang ointment" is more potent than 100 ng/mL EGF in promoting *in vitro* wound closure, showing statistically significant differences when compared to both positive and negative controls (Figure 6).

The wound-healing assay was also used to assess the stimulatory effect of "Jinchuang ointment" on the migration of HMEC-1 cells. The wound closure percentage with 200 μg/mL "Jinchuang ointment" 24 hours after treatment was 85.0 ± 12.3%, whereas the wound closure percentage observed with the DMSO control was only 43.3 ± 8.2% (Figures 7(a) and 7(b)). The weight percentage of lard is as high as 67% in "Jinchuang ointment," and sesame oil is used to prepare another famous traditional Chinese herbal ointment, Shiunko. The contribution of lard to the total cell migratory activity was therefore evaluated by reconstituting "Jinchuang ointment" with various fats. It is apparent that the significant cell migration into the wound region is seen with Jinchuang ointment-treated cells when compared to the control group (Figure 8). When sesame oil, synthetic triacylglycerol, coconut oil, and Vaseline were used as lard substituents, 85%, 91%, 74%, and 105% migration activity

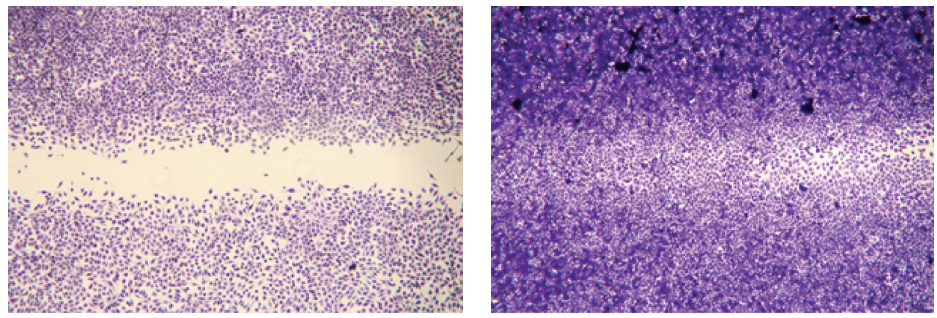

(a) (b)

Figure 7: Wound healing assay with HMEC-1 cells displaying the increased cell migration induced by "Jinchuang ointment." Cells were treated with (a) DMSO alone (control) or (b) 200 μg/mL "Jinchuang ointment." Cell migration was recorded and cells were stained by microscopy over a 24-hour time course.

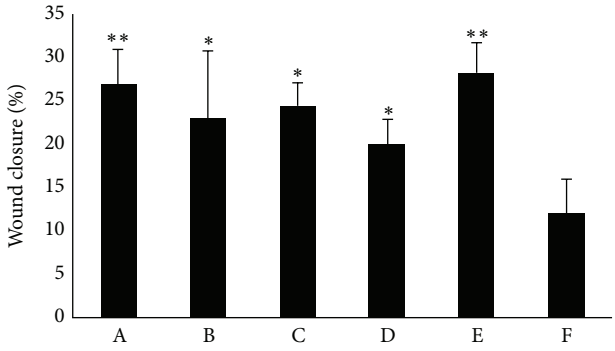

Figure 8: The percentage of wound closure with HMEC-1 cells after six hours of treatment in response to reconstituted variants "Jinchuang ointments." Lard is replaced by sesame oil (group B), synthetic triacylglycerol (group C), coconut oil (group D), and Vaseline (group E). Group A is the original recipe of Jinchuang ointment, and group F is DMSO only (control). Values are the mean ± SD. $^{*}P < 0.05$ and $^{**}P < 0.01$ compared with control.

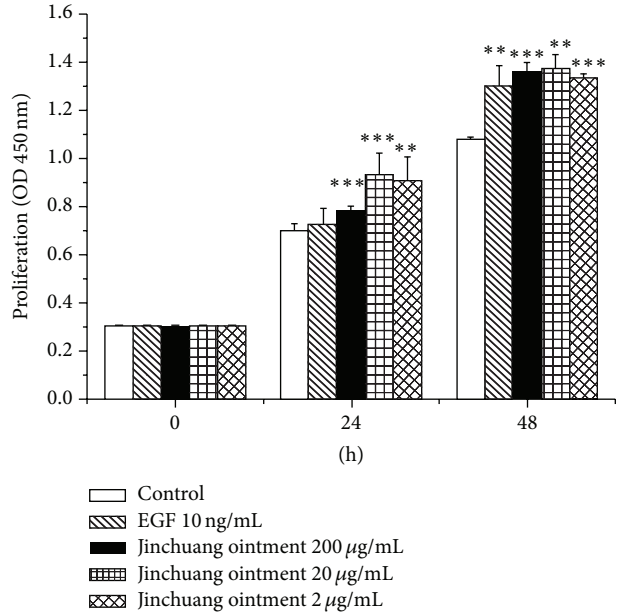

Figure 9: Proliferation of HaCaT cells measured by a WST-1 assay. Increased cell proliferation of HaCaT cells was observed in the presence of 200 μg/mL, 20 μg/mL, and 2 μg/mL "Jinchuang ointment." Negative and positive controls are in the presence of DMSO and 10 ng/mL EGF, respectively. Values are the mean ± SD. $^{**}P < 0.01$ and $^{***}P < 0.001$ compared with control.

can be observed (Figure 8). Unlike natural fat, Vaseline is mainly made from petroleum jelly, a semisolid mixture of hydrocarbons with carbon numbers greater than 25. The chain length of carbon atoms in the synthetic triacylglycerols used in this study is C_8 and C_{10} . These results suggest that the carbon chain length of the fat used in the ointment plays a minor role in stimulating cell migration.

3.5. The Effect of "Jinchuang Ointment" on HaCaT Cell Proliferation. The stimulatory effect of "Jinchuang ointment" on HaCaT cell proliferation was evaluated in the presence of 10% fetal bovine serum (FBS) by WST-1 assay. The increased percentages of cell proliferation by 200 μg/mL, 20 μg/mL, and 2 μg/mL "Jinchuang ointment" at 24 and 48 hours were 117 ± 2.66%, 133 ± 12.7%, and 129.7 ± 14.1% and 126.4 ± 3.5%, 127.3 ± 5.8%, and 124.1 ± 1.3%, respectively (Figure 9). These results indicate that treatment with "Jinchuang ointment" leads to an increase in HaCaT cell growth.

3.6. The Effect of "Jinchuang Ointment" on the Expression of G1/S Transition-Related Regulators. To further investigate the underlying mechanisms involved in "Jinchuang ointment"-induced effects on cell proliferation in HaCaT cells, the expression of several key cellular proteins involved in cell cycle progression was investigated by western blot analysis. As shown in Figure 10, a six-hour treatment with "Jinchuang ointment" leads to a dose-dependent increase in Cdc25b, Cdc25c, and Cyclin D3 levels. After treatment for 12 hours, significant changes in the expression pattern of those proteins between experiment and control groups were observed,

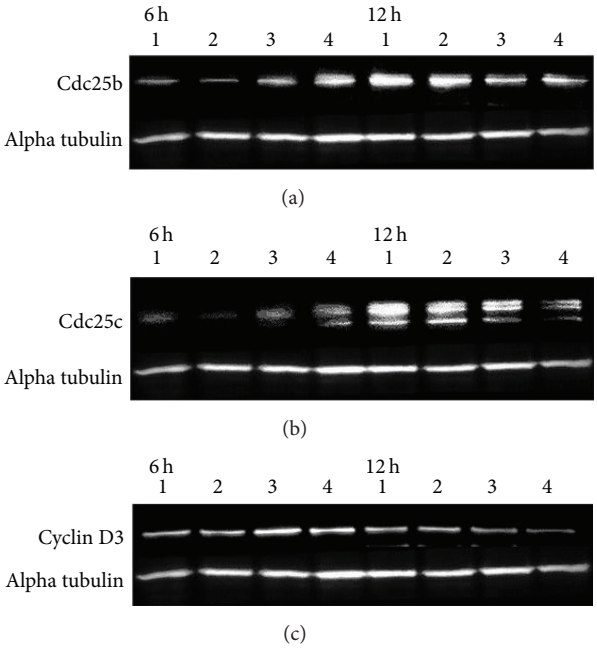

Figure 10: Treatment of HaCaT cells with "Jinchuang ointment" leads to altered expression of cell cycle-related proteins.Western blot analysis of (a) Cdc25b, (b) Cdc25c, and (c) cyclic D3 protein expression in HaCaT cell extracts after six and 12 hours of treatment. Lanes one to four are as follows: control, 100 ng/mL EGF, 200 μg/mL "Jinchuang ointment," and 20 μg/mL "Jinchuang ointment," respectively.

suggesting that "Jinchuang ointment" alters HaCaT cell cycle progression.

3.7. Tube Formation Assay. The process of wound healing has been divided into three different stages, inflammatory, proliferative, and remodeling phases [25]. Angiogenesis is responsible for new blood vessel formation and oxygen and nutrient supply and plays an important role in the proliferative phase of wound healing [26]. The tube formation assay was used to evaluate the *in vitro* angiogenic effect of "Jinchuang ointment" on HUVEC cells. As shown in Figure 11, treatment of HUVEC cell with 200 μg/mL "Jinchuang ointment" for 24 hours can efficiently induce endothelial cell capillary tubes and network formation.

3.8. Conclusions. "Jinchuang ointment" is a Chinese herbal medicine complex. It has been clinically used in the treatment of diabetic foot infection and decubitus ulcers in China Medical University Hospital for more than ten years. Because of its complicated composition, its biological activities have never been investigated. To further characterize its herb ingredients, the content of reference standards present in dragon's blood, catechu, frankincense, and myrrh was determined by HPLC. Two cell based assay platforms, *in vitro* wound healing and tube formation, were used to examine activity. Our results show that this herbal medicine possesses potent activities stimulating cell proliferation, migration, and

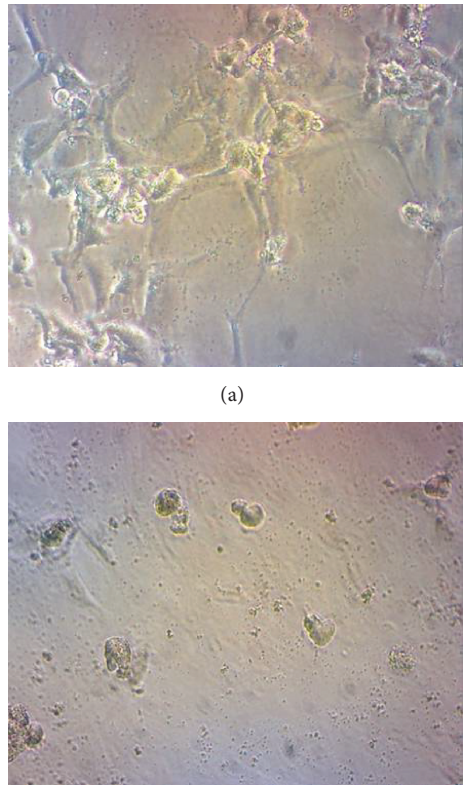

Figure 11: *In vitro* tube formation assay displaying the stimulation of angiogenesis by "Jinchuang ointment" in HUVEC cells. Cells were treated with (a) 200 μg/mL "Jinchuang ointment" and (b) DMSO only (negative control).

angiogenesis. This provides a scientific rationale to account for the observed clinical curative effects on wound healing by "Jinchuang ointment."

According to current pharmaceutical regulations in Taiwan, only traditional Chinese herbal medicine manufactured from cGMP pharmaceutical factories can be sold in drug stores or by hospital marketing channels. However, for homemade traditional Chinese herbal medicine, they can only be administered to patients by the doctors who made the respective medicine. For this reason, "Jinchuang ointment" cannot be widely used in the Taiwan area since many clinicians are not able or unwilling to prepare this remedy. To facilitate the manufacturing process of "Jinchuang ointment" by cGMP factories, it will be very important to find out the activity indicator markers for components, such as dragon's blood, catechu, frankincense, and myrrh.

Competing Interests

The authors declare no conflict of interests.

Authors' Contributions

Tsung-Jung Ho, Tzong Shiun Li, Chun-Chang Wu, and Jaung-Geng Lin are responsible for "Jinchuang ointment"

preparations, clinical treatment, and observations; Shinn-Jong Jiang helped in western blot analysis, cell proliferation, and wound healing assay of HaCaT cells; Guang-Huey Lin and Ming-Chuan Hsieh helped in wound healing assay of HMEC-1 cells; Jai-Sing Yang helped in tube formation assay; Lih-Ming Yiin helped in GC analysis; Hao-Ping Chen helped in HPLC analysis, experiment design, "Jinchuang ointment" preparation, and paper preparation.

Acknowledgments

This work was supported by Grant CMUBH R104-007 from China Medical University Beigang Hospital, Grant TCMRC-P-101014 from Tzu Chi University, and, in part, Grant MOST 104-2320-B-039-023 from the Ministry of Science and Technology, Taiwan.

References

[1] L. R. Braun, W. A. Fisk, H. Lev-Tov, R. S. Kirsner, and R. R. Isseroff, "Diabetic foot ulcer: an evidence-based treatment update," *American Journal of Clinical Dermatology*, vol. 15, no. 3, pp. 267–281, 2014.

[2] C. Y. Tu, H. C. Hsu, and J. J. Lu, "To examine the quality, safety, and efficacy of Jin Chuang Gao without moshus," *The Journal of Taiwan Pharmacy*, vol. 27, 2011.

[3] M. Yang, J. Sun, Z. Lu et al., "Phytochemical analysis of traditional Chinese medicine using liquid chromatography coupled with mass spectrometry," *Journal of Chromatography A*, vol. 1216, no. 11, pp. 2045–2062, 2009.

[4] T. Yi, Y. Tang, J. Zhang, Z. Zhao, Z. Yang, and H. Chen, "Characterization and determination of six flavonoids in the ethnomedicine 'Dragon's Blood' by UPLC-PAD-MS," *Chemistry Central Journal*, vol. 6, article 116, 2012.

[5] D. Shen, Q. Wu, M. Wang, Y. Yang, E. J. Lavoie, and J. E. Simon, "Determination of the predominant catechins in *Acacia catechu* by liquid chromatography/electrospray ionization-mass spectrometry," *Journal of Agricultural and Food Chemistry*, vol. 54, no. 9, pp. 3219–3224, 2006.

[6] M. A. Tawab, A. Kaunzinger, U. Bahr, M. Karas, M. Wurglics, and M. Schubert-Zsilavecz, "Development of a high-performance liquid chromatographic method for the determination of 11-keto-β-boswellic acid in human plasma," *Journal of Chromatography B: Biomedical Sciences and Applications*, vol. 761, no. 2, pp. 221–227, 2001.

[7] A. L. Gottumukkala, T. Ramakrishna, S. K. Babu, and G. V. Subbaraju, "Determination of (E) & (Z)-Guggulsterones in Guggul formulations by high performance liquid chromatography," *Asian Journal of Chemistry*, vol. 17, no. 3, pp. 1789–1793, 2005.

[8] J.-H. Chiang, J.-S. Yang, C.-C. Lu et al., "Newly synthesized quinazolinone HMJ-38 suppresses angiogenetic responses and triggers human umbilical vein endothelial cell apoptosis through p53-modulated Fas/death receptor signaling," *Toxicology and Applied Pharmacology*, vol. 269, no. 2, pp. 150–162, 2013.

[9] M. Xia, D. Wang, M. Wang et al., "Dracorhodin perchlorate induces apoptosis via activation of caspases and generation of reactive oxygen species," *Journal of Pharmacological Sciences*, vol. 95, no. 2, pp. 273–283, 2004.

[10] J. Shi, R. Hu, Y. Lu, C. Sun, and T. Wu, "Single-step purification of dracorhodin from dragon's blood resin of Daemonorops draco using high-speed counter-current chromatography combined with pH modulation," *Journal of Separation Science*, vol. 32, no. 23-24, pp. 4040–4047, 2009.

[11] G. Williamson and C. Manach, "Bioavailability and bioefficacy of polyphenols in humans. II. Review of 93 intervention studies," *The American Journal of Clinical Nutrition*, vol. 81, no. 1, pp. 243S–255S, 2005.

[12] C.-H. Wu, C.-F. Wu, H.-W. Huang, Y.-C. Jao, and G.-C. Yen, "Naturally occurring flavonoids attenuate high glucose-induced expression of proinflammatory cytokines in human monocytic THP-1 cells," *Molecular Nutrition and Food Research*, vol. 53, no. 8, pp. 984–995, 2009.

[13] S. Y. H. Lee, B. Munerol, S. Pollard et al., "The reaction of flavanols with nitrous acid protects against N-nitrosamine formation and leads to the formation of nitroso derivatives which inhibit cancer cell growth," *Free Radical Biology and Medicine*, vol. 40, no. 2, pp. 323–334, 2006.

[14] Y. M. Li, H. Y. E. Chan, Y. Huang, and Z. Y. Chen, "Green tea catechins upregulate superoxide dismutase and catalase in fruit flies," *Molecular Nutrition and Food Research*, vol. 51, no. 5, pp. 546–554, 2007.

[15] H. P. T. Ammon, N. Safayhi, T. Mack, and J. Sabieraj, "Mechanism of antiinflammatory actions of curcumine and boswellic acids," *Journal of Ethnopharmacology*, vol. 38, no. 2-3, pp. 113–119, 1993.

[16] G. Chashoo, S. K. Singh, P. R. Sharma et al., "A propionyloxy derivative of 11-keto-β-boswellic acid induces apoptosis in HL-60 cells mediated through topoisomerase I & II inhibition," *Chemico-Biological Interactions*, vol. 189, no. 1-2, pp. 60–71, 2011.

[17] J.-J. Liu, Å. Nilsson, S. Oredsson, V. Badmaev, W.-Z. Zhao, and R.-D. Duan, "Boswellic acids trigger apoptosis via a pathway dependent on caspase-8 activation but independent on Fas/Fas ligand interaction in colon cancer HT-29 cells," *Carcinogenesis*, vol. 23, no. 12, pp. 2087–2093, 2002.

[18] T. Syrovets, B. Büchele, E. Gedig, J. R. Slupsky, and T. Simmet, "Acetyl-boswellic acids are novel catalytic inhibitors of human topoisomerases I and IIα," *Molecular Pharmacology*, vol. 58, no. 1, pp. 71–81, 2000.

[19] Y. Chen, C. Zhou, Z. Ge et al., "Composition and potential anticancer activities of essential oils obtained from myrrh and frankincense," *Oncology Letters*, vol. 6, no. 4, pp. 1140–1146, 2013.

[20] T. P. Burris, C. Montrose, K. A. Houck et al., "The hypolipidemic natural product guggulsterone is a promiscuous steroid receptor ligand," *Molecular Pharmacology*, vol. 67, no. 3, pp. 948–954, 2005.

[21] D. Xiao and S. V. Singh, "z-Guggulsterone, a constituent of Ayurvedic medicinal plant *Commiphora mukul*, inhibits angiogenesis *in vitro* and *in vivo*," *Molecular Cancer Therapeutics*, vol. 7, no. 1, pp. 171–180, 2008.

[22] R. E. Granger, E. L. Campbell, and G. A. R. Johnston, "(+)- And (−)-borneol: efficacious positive modulators of GABA action at human recombinant $\alpha1\beta2\gamma2$L GABAA receptors," *Biochemical Pharmacology*, vol. 69, no. 7, pp. 1101–1111, 2005.

[23] A. C. Hall, C. M. Turcotte, B. A. Betts, W.-Y. Yeung, A. S. Agyeman, and L. A. Burk, "Modulation of human GABAA and glycine receptor currents by menthol and related monoterpenoids," *European Journal of Pharmacology*, vol. 506, no. 1, pp. 9–16, 2004.

[24] K. A. Al-Farhan, I. Warad, S. I. Al-Resayes, M. M. Fouda, and M. Ghazzali, "Synthesis, structural chemistry and antimicrobial activity of −(−) borneol derivative," *Central European Journal of Chemistry*, vol. 8, no. 5, pp. 1127–1133, 2010.

[25] R. J. Mendonça and J. Coutinho-Netto, "Cellular aspects of wound healing," *Anais Brasileiros de Dermatologia*, vol. 84, no. 3, pp. 257–262, 2009.

[26] M. Schäfer and S. Werner, "Cancer as an overhealing wound: an old hypothesis revisited," *Nature Reviews Molecular Cell Biology*, vol. 9, no. 8, pp. 628–638, 2008.

Hindawi Publishing Corporation
Evidence-Based Complementary and Alternative Medicine
Volume 2016, Article ID 6916353, 7 pages
http://dx.doi.org/10.1155/2016/6916353

Research Article

Yupingfeng Pulvis Regulates the Balance of T Cell Subsets in Asthma Mice

Zhigang Wang,[1,2] Xueting Cai,[1,2] Zhonghua Pang,[1,2] Dawei Wang,[1,2] Juan Ye,[1,2] Kelei Su,[1,2] Xiaoyan Sun,[1,2] Jing Li,[1,2] Peng Cao,[1,2] and Chunping Hu[1,2]

[1] *Affiliated Hospital of Integrated Traditional Chinese and Western Medicine, Nanjing University of Chinese Medicine, Nanjing, Jiangsu 210028, China*
[2] *Laboratory of Cellular and Molecular Biology, Jiangsu Province Academy of Traditional Chinese Medicine, Nanjing, Jiangsu 210028, China*

Correspondence should be addressed to Chunping Hu; njhcp66@126.com

Received 10 January 2016; Accepted 22 March 2016

Academic Editor: Vincenzo De Feo

Background. Yupingfeng Pulvis (HFBP) had played an active role in many diseases, especially respiratory tract infections. Exploring the possible prevention mechanism of HFBP may provide new ideas in clinical applications for this well-known herbal formula. *Purpose*. To study the possible mechanisms of therapy effect of HFBP on asthma mice via regulating the balance of Tregs and Th17 cells. *Method*. The female BALB/c mice were divided into five groups: control group, model group, prednisone (5.5 mg/kg) group, and 22 g/kg HFBP and 44 g/kg HFBP groups. Ovalbumin was used to make the asthma model of mice; the drug was ig administered daily after atomization for consecutive 15 d. The mice were killed after the last administration. The paraffin-embedded tissue sections of the lungs were stained by H&E. Tregs and Th17 cells in bronchoalveolar lavage fluid were detected by flow cytometry. IL-4, TGF-β, and TNF-α in the serum were detected by ELISA assay. *Results*. HFBP could alleviate the inflammation in the lung tissue of mice, decrease the proportion of Th17 cells, and increase the proportion of Treg cells in bronchoalveolar lavage fluid. HFBP could decrease IL-4 and TNF-α level and increase TGF-β level in blood. *Conclusion*. HFBP could treat the asthma through impacting the balance of Th17 cells and Treg cells as well as the levels of related inflammatory cytokines in asthma mice.

1. Introduction

Asthma is a common chronic inflammatory disease of the airways characterized by variable and recurring symptoms, reversible airflow obstruction, and bronchospasm. Common symptoms include wheezing, coughing, chest tightness, and shortness of breath. Over the past few decades the world asthma prevalence and mortality have been a rising trend year by year, having impact on social economy and health. The disease is affecting more than 300 million persons all over the world, with approximately 250,000 annual deaths [1], and it is expected that the number of the patients will increase by more than 100 million by 2025 [2].

The pathogenesis of asthma is not yet clear and may be related to genetic, immune, environment, spirit, sex, and other related factors, in which the immunological pathogenesis of asthma has become a current research hot spot. Asthma is classically recognized as the typical Th2 disease, with increased IgE levels and eosinophilic inflammation in the airway. Emerging Th2 cytokines modulate the airway inflammation, which induces airway remodeling [3]. Biological agents, which have specific molecular targets for these Th2 cytokines, are available and clinical trials for asthma are ongoing. However, the relatively simple paradigm has been doubted because of the realization that strategies designed to suppress Th2 function are not effective enough for all patients in the clinical trials. In the future, it is required to understand more details for phenotypes of asthma.

Nowadays, it is known that Th17 cells and Treg cells also modulate asthma. Th17 cells produce IL-17A, IL-17F, and IL-22. These cytokines induce airway inflammation and IL-17A enhances smooth muscle contractility. IL-17 can promote fibroblast cells, epithelial cells, endothelial cells, macrophages, and smooth muscle cells activation, make

Table 1: The composition of HFBP.

Species	Chinese name	Plant part	Origin	Grams, g	%
Saposhnikovia divaricata (Trucz.) Schischk.	Fangfeng	Root	Hebei, China	30	25.0
Astragalus membranaceus (Fisch.) Bunge.	Huangqi	Root	Shanxi, China	30	25.0
Atractylodes macrocephala Koidz.	Baizhu	Rhizoma	Jiangsu, China	60	50.0
Total amount				120	100.0

these cells highly express a variety of proinflammatory factor, such as IL-6 and IL-8, and release granulocyte colony stimulating factor. IL-17 also recruits dendritic cells, T cells, and neutrophils to inflammation section, increasing airway inflammation [4, 5]. $CD4^+CD25^+Foxp3^+$ regulatory T cells (regulatory T cells, Tregs) are a group which has the function of immune suppression of T cell subgroup. Treg cells produce inhibitory cytokines (TGF-β and IL-10) and express membrane molecules (CTLA-4, GITR, etc.) and Foxp3. Studies have found that, in patients with asthma, the specific transcription factor Foxp3 expression reduced, and the inhibition function and the proportion of $CD25^{hi}$ regulatory T cells also reduced [6, 7]. Therefore, studying the differentiation and regulation mechanism of Th17 cell will help us to deepen understanding of the relationship between Th17 cells and the pathogenesis of asthma, as well as the development of new immunosuppressive drugs.

Yupingfeng Pulvis (HFBP) is recorded in Effective Prescriptions Handed Down for Generations written by Yi-lin Wei in Yuan Dynasty. It consists of three commonly used herbs including *Saposhnikovia divaricata* (*Trucz.*) *Schischk.*, *Astragalus membranaceus* (*Fisch.*) *Bunge.*, and *Atractylodes macrocephala Koidz*. Currently, clinical reports about HFBP are increasing. It had played an active role in many diseases, especially treatment of respiratory tract infections. To study the possible mechanisms of therapy effect of HFBP on asthma, asthma model mice were established and the balance of Tregs and Th17 cells was evaluated. Exploring the possible prevention mechanism of HFBP may provide new ideas in clinical applications for this well-known herbal formula.

2. Materials and Methods

2.1. Animals. Female BALB/c mice were purchased from Shanghai SLRC Laboratory Animal Co., Ltd. (Shanghai, China). Mice were housed under specific pathogen-free conditions and provided with a standard rodent laboratory diet from Shanghai SLRC Laboratory Animal Co., Ltd.

2.2. HFBP Preparation. HFBP is composed of three medicinal components: *Saposhnikovia divaricata* (*Trucz.*) *Schischk.*, *Astragalus membranaceus* (*Fisch.*) *Bunge.*, and *Atractylodes macrocephala Koidz* (Table 1). All medicinal plants used to prepare formulas were provided by Jiangsu Province Hospital on Integration of Chinese and Western Medicine (Nanjing, Jiangsu, China). The plant name and part used were shown in Table 1 (the plant name has been checked with http://www.theplantlist.org). All the herbal drugs were authenticated by Professor Song-Lin Li (Jiangsu Province Academy of Traditional Chinese Medicine, Nanjing, China) according to the monographs documented in the Chinese Pharmacopeia (Part I, 2010 Version). Voucher specimens of crude drugs were deposited at the Laboratory of Cellular and Molecular Biology at Jiangsu Province Academy of Traditional Chinese Medicine (Nanjing, China). HFBP extract was prepared according to the following procedure: single crude herb was homogenized with a Waring blender. The powders of three medicinal herbs were mixed in proportion (Table 1) and refluxed with ten volumes of water for 2 h after maceration for 24 h. The filtrates obtained from 2 cycles of the extraction procedure were combined and dried by a vacuum-drier at 60°C and ground. The yield of dried extracts for HFBP was 22% (w/w) of the weight of original herbs.

2.3. HPLC Analysis of HFBP. After the centrifugation at 3000 rpm for 5 min, the HFBP supernatant was filtered by membrane filter (0.45 μm) and subjected for HPLC analysis. The experiment was conducted by an Agilent 1200 HPLC instrument (Agilent, USA) equipped with a XTerra@ MS C18 (250 mm × 4.6 mm, 5 μm) column. The mobile phase consisted of 0.1% (v/v) formic acid (A) and acetonitrile (B) at a flow rate of 1.0 mL/min. A gradient program was used as follows: 0 min, 5% B; 10 min, 15% B; 20 min, 20% B; 30 min, 28% B; 40 min, 40% B; 45–50 min, 60% B; 60 min, 70% B; 65–70 min, 95% B. The diode array detector scanned from 200 nm to 400 nm, and the monitor wavelength was set at 250 nm.

2.4. The Establishment of Mouse Models of Asthma. We used a protocol slightly modified from that described by McMillan and Lloyd [8]. Briefly, female BALB/c mice were sensitized intraperitoneally with 20 μg ovalbumin (OVA) and 2 mg $Al(OH)_3$ on days 1 and 14 (OVA groups, $n = 40$). The blank control group ($n = 10$) was injected with saline at the respective time points. On day 28, OVA groups' mice were random divided into four groups (model group, 22 g/kg HFBP group, 44 g/kg HFBP group, and 5.5 mg/kg prednisone group) ($n = 10$) and inhaled aerosol 1% OVA solution for 30 min for five days. The blank control group was given the respective vehicle aerosol inhalation. HFBP groups with different doses were administrated intragastrically with HFBP every day. 5.5 mg/kg prednisone was administrated intragastrically every day to the positive control group. The blank control group and model group were administrated with equal volume of saline since aerosol inhalation. All groups were administrated for 15 days. Blood was drawn at 24 h after the last intragastric administration to detect cytokines IL-4, TGF-β, and TNF-α. Bronchoalveolar lavage

fluid (BALF) was collected to count the number of Th17 cells and Treg cells. Left upper lung lobes were collected for pathologic histology.

2.5. ELISA. The concentrations of cytokines IL-4, TGF-β, and TNF-α in the blood from all groups were measured using a commercially available ELISA kit (Nanjing Jiancheng Bioengineering Institute, China). ELISA assay was performed according to the manufacturer's instructions of the ELISA kits.

2.6. Flow Cytometric Analysis. For detecting the percentage of Th17 cells, cells in BALF were collected and stimulated with 10 ng/mL phorbol 12-myristate 13-acetate (PMA) (Sigma-Aldrich, USA) and 10 ng/mL brefeldin A (BFA) (Sigma-Aldrich, USA) in RPMI-1640 medium (Invitrogen, USA) in 96-well plates. After being stimulated for 5 h (37°C, 5% CO_2), the cells were collected and washed once with PBS. The cells were then incubated with CD4-FITC antibody at 4°C for 30 minutes. Next, the cells were fixed and permeabilized and stained with anti-human IL-17-PE antibody at 37°C for 30 minutes. For detecting the percentage of Treg cells, the cells were washed in PBS. Then, the cells were stained with CD4-FITC and CD25-APC antibodies at 4°C for 30 minutes. Then, the cells were incubated with Foxp3-PE antibody after fixation and permeabilization according to the manufacturer's instruction. All stained cells were analyzed by flow cytometer (Guava 6HT, Merck-Millipore, USA). The data were analyzed using the software Guava 2.5.

2.7. Immunohistochemistry Assay. Lung tissue samples of each group were cut into sections of approximately 0.5 cm^2 sizes and fixed in 10% formalin for at least 48 hours. The fixed samples were placed in plastic cassettes and dehydrated using an automated tissue processor. The processed tissues were embedded in paraffin wax (Leica, Germany) and the blocks trimmed and sectioned to about $5 \times 5 \times 4\,\mu$m size using a microtome. The tissue sections were mounted on glass slides using a hot plate and subsequently treated in order with 100, 90, and 70% ethanol for two minutes each. Finally, the sections were rinsed with tap water and stained with Harris's haematoxylin and eosin for light microscopy.

2.8. Statistical Evaluation. All results shown represent the Mean ± SD from triplicate experiments performed in a parallel manner unless otherwise indicated. Statistical analyses were performed using an unpaired, two-tailed Student's t-test.

3. Results

3.1. HPLC Fingerprint of HFBP Extracts. HPLC analysis was conducted to confirm the biological composition of HFBP extract, resulting in the identification of 9 chemical components with reference standards (Figure 1). Since HFBP is a polyherbal formulation with complicated composition, two batches of HFBP extracts were thus prepared under the same condition and analyzed by HPLC. The results showed that all the main chromatographic peaks detected in batch I coincided with batch II, demonstrating a good reproducibility of HFBP chemical composition. Figure 1 shows the HPLC fingerprint of two batches of HFBP extracts and 3D-HPLC chromatogram of batch I HFBP extracts. In order to evaluate the quality of HFBP extracts, an external standard method was applied to quantitatively analyze five major compounds (prim-O-glucosylcimifugin, calycosin-7-O-β-D-glucoside, macrotin, 5-O-methylvisammioside, and ononin) in the HFBP samples. The external standard method was validated in terms of linearity, precision, accuracy, and stability. The quantitative results are presented in Table 2.

3.2. HFBP Impact on Serum Inflammatory Factors in Asthma Mice. Experiments were made to determine the serum inflammatory cytokines IL-4, TGF-β, and TNF-α; as shown in Figure 2, IL-4 and TNF-α increased in model group; two HFBP groups could significantly reduce serum IL-4 and TNF-α levels, so did prednisone group. TGF-β as a suppression of inflammation factor reduced in the model group; prednisone can raise TGF-β level; by contrast, HFBP groups could increase the level of the serum content of TGF-β more than prednisone group.

3.3. The Percentages of Th17 and Treg Cells in BALF in Five Groups. Flow cytometry results showed that the percentage of Th17 cells in model group significantly enhanced compared with blank control group, and the proportion of Treg cells decreased obviously. Positive medicine prednisone could reduce Th17 cells and increase Treg cells. Both HFBP groups could reduce the percentage of Th17 cells and increase the proportion of Treg cells, and the effect of HFBP was better than prednisone (Figures 3(a) and 3(b)).

3.4. Effect of HFBP on Lung Tissue Pathology in Asthma Mice. H&E staining of lung tissue showed that there were no obvious pathological changes of lung tissue observed in the blank control group mice. In the model group mice, a large number of inflammatory cells infiltrated bronchial wall of lung tissue. The prednisone group could improve the lung tissue of the inflammatory cells invasion; both high and low dose HFBP groups could improve the bronchial inflammation situation; lung damage had a greater degree of recovery after HFBP treatment, showing that HFBP had a good treatment effect, as shown in Figure 4.

4. Discussion

Asthma treatment goal is to reduce attack frequency, improve respiratory function and life quality, control acute onset, prevent deterioration, and avoid death. At present the treatment of asthma is mainly western medicine; traditional Chinese medicine (TCM) is used as complementary therapies. Western medicine treatment of asthma is mainly with anti-inflammatory drugs, complementary with spasmolytic agents and apophlegmatisant. Western medicine has achieved very good curative effect in the control of asthma symptoms but still cannot reduce the recurrence rate of asthma and has the side effects due to long-term use of these drugs. Traditional Chinese medicine has a long history in treating

Table 2: The contents of five major compounds in HFBP by HPLC analysis.

Peak number	t_R (min)	Compound name	Linearity Equation	R^2	Sensitivity (μg/mL) LOD	LOQ	Precision (RSD%, $n = 6$) Intra-day	Inter-day	Stability (RSD%, $n = 3$)	Content (%)
1	16.37	Prim-O-glucosylcimifugin	$y = 40565x + 149.55$	0.9998	0.03	0.05	0.24	1.38	0.40	0.202
2	19.23	Calycosin-7-O-β-D-glucoside	$y = 73499x + 64.019$	0.9997	0.027	0.055	0.26	1.58	0.51	0.043
3	21.33	Macrotin	$y = 60171x + 50.145$	0.9997	0.047	0.023	0.16	1.59	0.56	0.035
4	24.03	4′-O-β-D-Glucosyl-5-O-methylvisamminol	$y = 45658x + 179.85$	0.9996	0.031	0.051	0.17	1.33	0.18	0.221
5	29.69	Ononin	$y = 76593x + 60.616$	0.9997			0.20	1.40	0.48	0.021

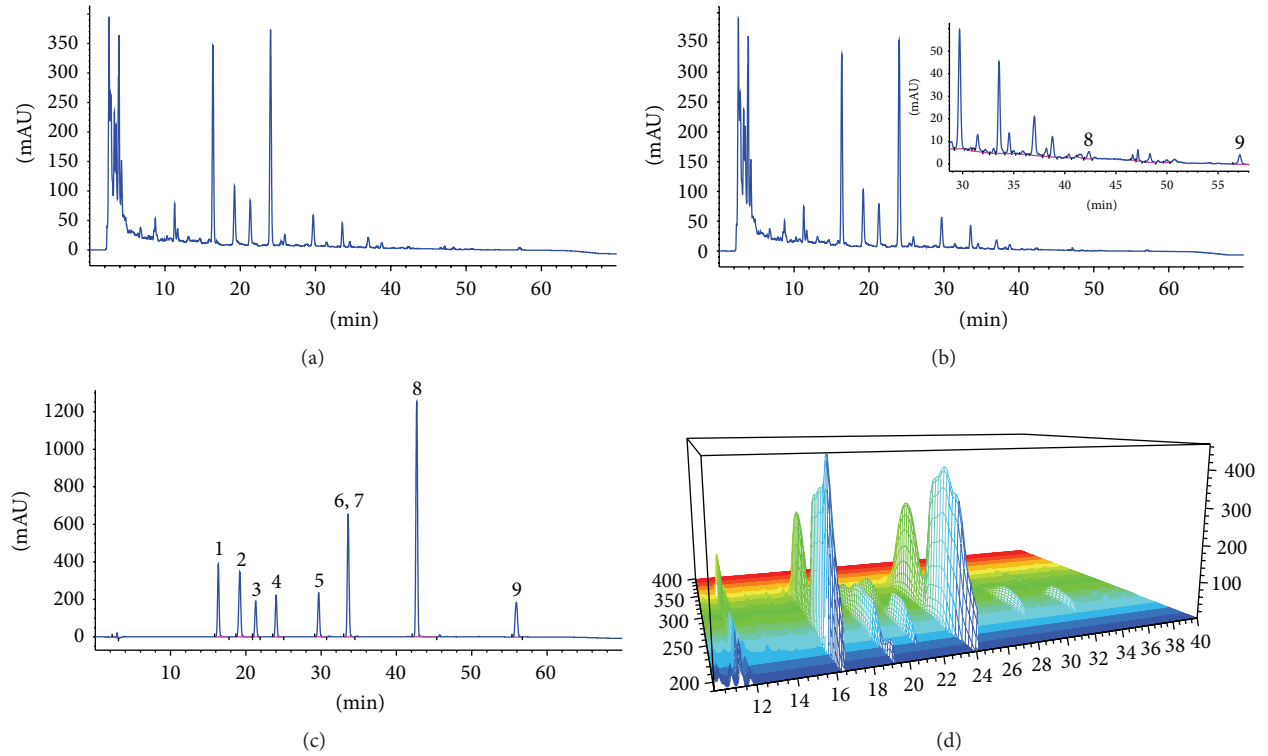

Figure 1: HPLC fingerprint of HFBP extracts and reference compounds. (a) HFB extract (batch I), (b) HFB extract (batch II), (c) reference compounds, (d) 3D-HPLC fingerprint of HFBP extract (batch I). 1, prim-O-glucosylcimifugin; 2, calycosin-7-O-β-D-glucoside; 3, macrotin; 4, 5-O-methylvisammioside; 5, ononin; 6, calycosin; 7, sec-O-glucosylhamaudol; 8, formononetin; 9, atractylenolide I.

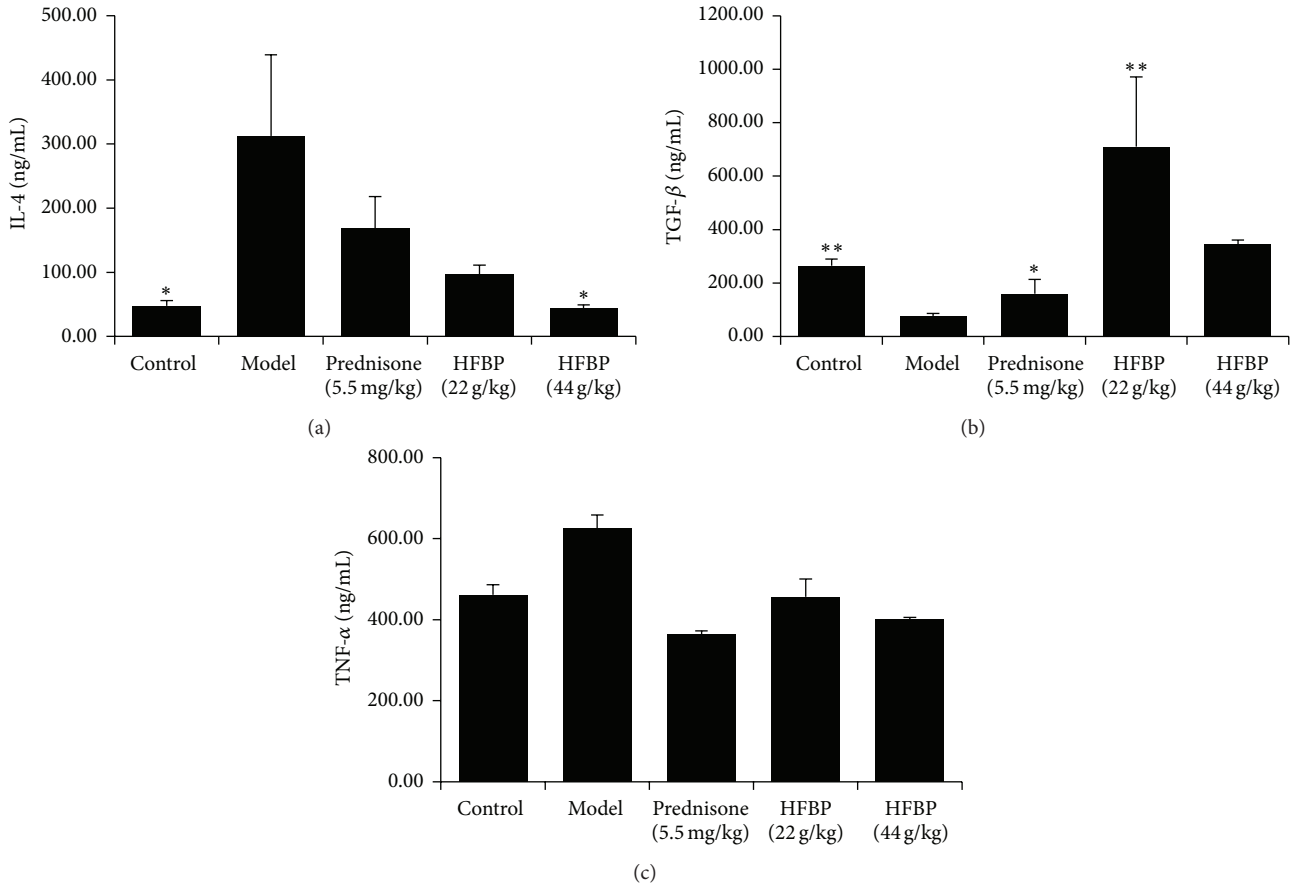

Figure 2: Detection of levels of IL-4 (a), TGF-β (b), and TNF-α (c) in serum of mice by ELISA (Mean ± SD, $n = 10$). $^{*}P < 0.05$ and $^{**}P < 0.01$ versus model group.

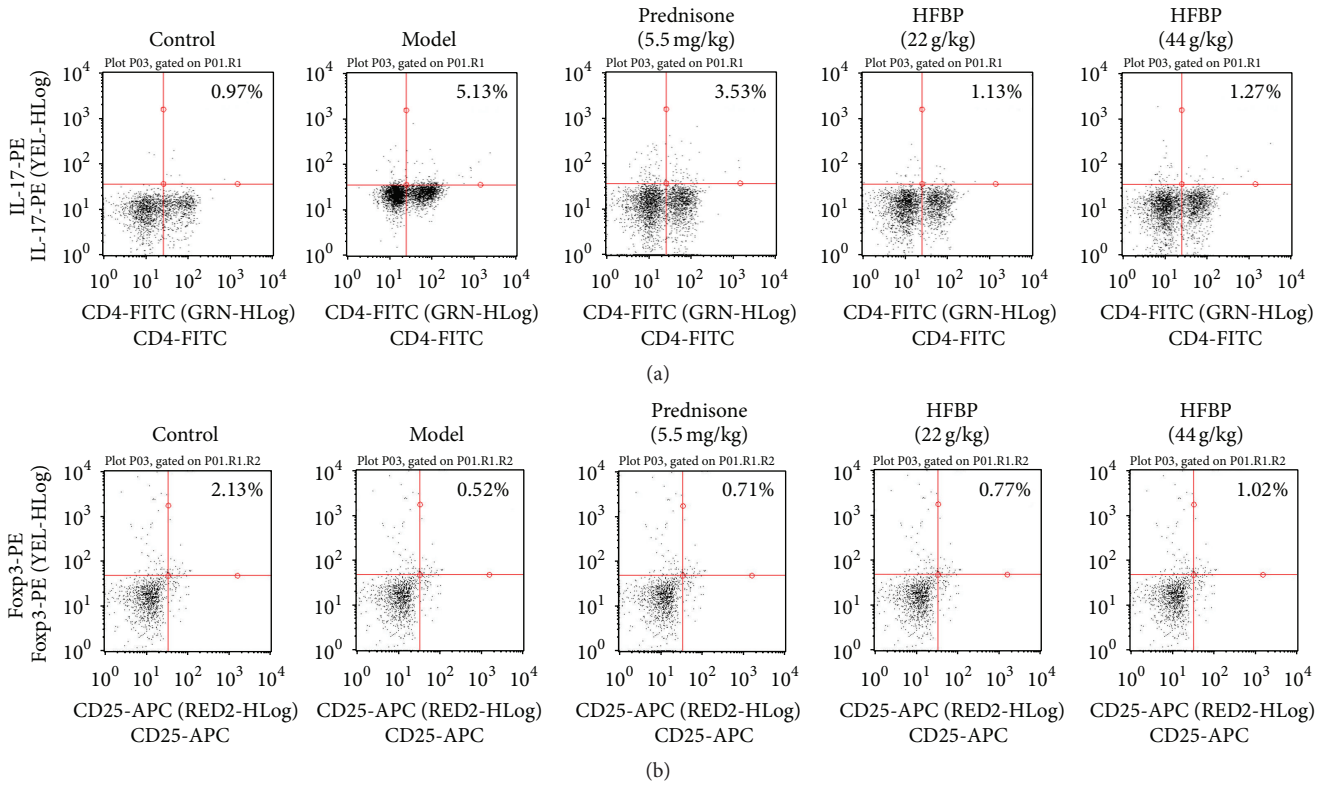

Figure 3: Detection for proportion of Th17 cells (a) and Treg cells (b) in mice by flow cytometry (Mean ± SD, $n = 10$). $^{*}P < 0.05$ and $^{**}P < 0.01$ versus model group.

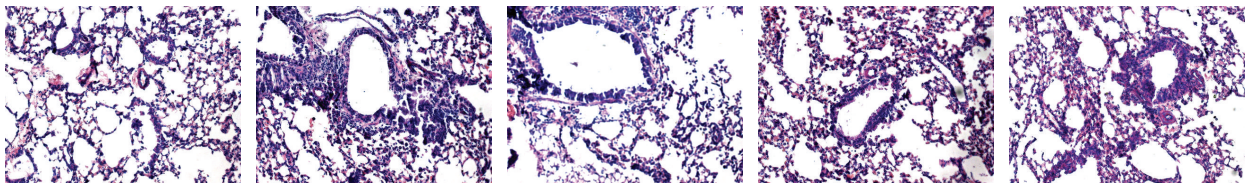

Figure 4: H&E staining of lung of asthma mice of each group (optical microscopy, ×200).

asthma, and has rich pharmaceutical with low cost and small side effects. Traditional Chinese medicine blocked a chain reaction of inflammation, in particular, to improve the microenvironment to eliminate airway chronic inflammation in the airway, prevent the occurrence of airway remodeling, and regulate the immune system by changing the immune gene expression, reduce airway hyperresponsiveness, stabilize environment within the body, and enhance the adaptive adjustment ability. TCM gives full play to the advantages of the overall treatment.

The ingredients of HFBP are fewer but better, only three components, *radix astragali*, *radix saposhnikoviae,* and *rhizoma atractylodis macrocephalae*. *Radix astragali* is especially suitable for the treatment of deficiency and night sweat people, which is the main drug of the formulas. *Rhizoma atractylodis macrocephalae* is the adjuvant drug of the formulas. *Radix saposhnikoviae*, called "Pinfeng," can release exterior and dispel wind. In recent years, more and more pharmacological effects of HFBP have been revealed for its "replenishing qi and consolidating exterior" pharmacodynamics basis. Previous studies have shown that HFBP has good immunity effect on allergic diseases such as asthma, allergic rhinitis, and allergic conjunctivitis [9–11]. Its pharmacological mechanism may be through promoting Th1 cells and the expression of IFN-γ, inhibition of Th2 cells, and the secretion of cytokines, thus improving the Th1/Th2 ratio and the state of inflammation of the respiratory tract [9]. Th17 cells and Treg cells have obvious change in bronchial asthma patients. Higher levels of Th17 cells raise the inflammation of lung tissue; lower level of Treg cells reduces the inhibition effect of inflammatory cells and inflammatory factor, which can promote the occurrence of asthma disease [12, 13]. HFBP has a good immunity effect on allergic diseases, yet there is no evidence about its relationship with the balance of Th17 cells and Treg cells.

Therefore, we designed the experiment to investigate the relationship between Th17 cells differentiation mechanism and the onset of asthma and at the same time observe Th17 related cytokines expression with HFBP treatment in acute asthma mice. The results showed that HFBP could reduce asthma mice lung tissue bronchioles and perivascular inflammatory cell infiltration, improve the state of airway inflammation, and reduce mucus secretion. ELISA assay was used to detect IL-4, TGF-β, and TNF-α level in the blood of mice. According to the results, IL-4 and TNF-α of asthma mice were increased, compared with the blank control group ($P < 0.05$), suggesting that IL-4 and TNF-α participate in the onset of asthma. After treating with prednisone or HFBP, IL-4 and TNF-α level significantly reduced ($P < 0.05$), suggesting that HFBP could inhibit IL-4 and TNF-α expression in the blood of asthma mice. TGF-β as a suppression of inflammation factor reduced in the model group; after treatment with prednisone or HFBP, TGF-β level increased obviously. Flow cytometry analysis showed that HFBP could decrease the proportion of Th17 cells and increase the proportion of Treg cells in bronchoalveolar lavage fluid, which indicated that HFBP could treat the asthma through impacting the balance of Th17 cells and Treg cells as well as the levels of related inflammatory cytokines in mice.

Differentiation of naïve T cells into effector cells is required for optimal protection against different classes of microbial pathogen and for the development of immune memory. Recent findings have revealed important roles for the Notch signaling pathway in T cell differentiation into all known effector subsets, including Th1, Th2, and Tregs [14]. Inhibiting Notch signaling has been shown to block Th2 polarization by preventing Notch mediated upregulation of GATA-3. Zhou found that Astragalus injection exerted protective effects on bleomycin-induced pulmonary fibrosis via downregulating Jagged1/Notch1 in lung [15]. Atractylenolide I, one of the main naturally occurring compounds of *Atractylodes macrocephala Koidz.*, had the effect of reduction of expressions of Notch1, Jagged1, and downstream protein Hes1, Hey1 of Notch pathway [16]. Above all, we doubted that HFBP may impact the balance of Th17 cells and Treg cells through Notch signaling pathway. Of course, further experiments needed to be done.

Abbreviations

HFBP: Yupingfeng Pulvis
TCM: Traditional Chinese medicine
Tregs: Regulatory T cells
OVA: Ovalbumin
BALF: Bronchoalveolar lavage fluid.

Competing Interests

The authors declare that they have no competing interests.

Acknowledgments

This work was supported by the National Natural Science Foundation of China (nos. 81503573, 81202967, and 81470179) and Jiangsu Province's Outstanding Leader Program of Traditional Chinese Medicine.

References

[1] J. Bousquet, T. J. H. Clark, S. Hurd et al., "GINA guidelines on asthma and beyond," *Allergy*, vol. 62, no. 2, pp. 102–112, 2007.

[2] M. Masoli, D. Fabian, S. Holt, R. Beasley, and Global Initiative for Asthma (GINA) Program, "The global burden of asthma: executive summary of the GINA Dissemination Committee report," *Allergy*, vol. 59, no. 5, pp. 469–478, 2004.

[3] M. Kudo, Y. Ishigatsubo, and I. Aoki, "Pathology of asthma," *Frontiers in Microbiology*, vol. 4, article 263, 2013.

[4] Y. Zhao, J. Yang, Y.-D. Gao, and W. Guo, "Th17 immunity in patients with allergic asthma," *International Archives of Allergy and Immunology*, vol. 151, no. 4, pp. 297–307, 2010.

[5] L. Cosmi, F. Liotta, E. Maggi, S. Romagnani, and F. Annunziato, "Th17 cells: new players in asthma pathogenesis," *Allergy*, vol. 66, no. 8, pp. 989–998, 2011.

[6] A. Ray, A. Khare, N. Krishnamoorthy, Z. Qi, and P. Ray, "Regulatory T cells in many flavors control asthma," *Mucosal Immunology*, vol. 3, no. 3, pp. 216–229, 2010.

[7] N. Ohkura, Y. Kitagawa, and S. Sakaguchi, "Development and maintenance of regulatory T cells," *Immunity*, vol. 38, no. 3, pp. 414–423, 2013.

[8] S. J. McMillan and C. M. Lloyd, "Prolonged allergen challenge in mice leads to persistent airway remodelling," *Clinical and Experimental Allergy*, vol. 34, no. 3, pp. 497–507, 2004.

[9] H.-Z. Wang, M. Hong, L.-L. Gui, Y.-Q. Hua, and H.-Q. Xu, "Effect of Yupingfeng San against OVA-induced allergic asthma in mice," *hongguo Zhong Yao Za Zhi*, vol. 38, no. 7, pp. 1052–1055, 2013.

[10] H.-Y. Shi, Y. Zhuang, and X.-Y. Wang, "Effect of yupingfeng droppill in treatment of allergic rhinitis," *Zhongguo Zhong Yao Za Zhi*, vol. 39, no. 12, pp. 2364–2366, 2014.

[11] Y. Chen, "Efficacy of sodium cromoglicate eye drops combined with yupingfeng granules in the treatment of allergic conjunctivitis," *Eye science*, vol. 28, no. 4, pp. 201–203, 2013.

[12] S. Langier, K. Sade, and S. Kivity, "Regulatory T cells in allergic asthma," *Israel Medical Association Journal*, vol. 14, no. 3, pp. 180–183, 2012.

[13] H. Y. Kim, R. H. Dekruyff, and D. T. Umetsu, "The many paths to asthma: phenotype shaped by innate and adaptive immunity," *Nature Immunology*, vol. 11, no. 7, pp. 577–584, 2010.

[14] D. Amsen, C. Helbig, and R. A. Backer, "Notch in T cell differentiation: all things considered," *Trends in Immunology*, vol. 36, no. 12, pp. 802–814, 2015.

[15] Y. Zhou, S. Liao, Z. Zhang, B. Wang, and L. Wan, "Astragalus injection attenuates bleomycin-induced pulmonary fibrosis via down-regulating Jagged1/Notch1 in lungs," *Journal of Pharmacy and Pharmacology*, 2016.

[16] L. Ma, R. Mao, K. Shen et al., "Atractylenolide I-mediated Notch pathway inhibition attenuates gastric cancer stem cell traits," *Biochemical and Biophysical Research Communications*, vol. 450, no. 1, pp. 353–359, 2014.

Hindawi Publishing Corporation
Evidence-Based Complementary and Alternative Medicine
Volume 2016, Article ID 5381290, 9 pages
http://dx.doi.org/10.1155/2016/5381290

Research Article

Cardioprotective Effects of Genistin in Rat Myocardial Ischemia-Reperfusion Injury Studies by Regulation of P2X7/NF-κB Pathway

Meng Gu,[1] Ai-bin Zheng,[1] Jing Jin,[1] Yue Cui,[1] Ning Zhang,[1] Zhi-ping Che,[1] Yan Wang,[1] Jie Zhan,[1] and Wen-juan Tu[2]

[1]*Department of Clinical Laboratory, Changzhou Children's Hospital, Changzhou, Jiangsu 213001, China*
[2]*Department of Neonatal, Changzhou Children's Hospital, Changzhou, Jiangsu 213001, China*

Correspondence should be addressed to Wen-juan Tu; tuwenjuan2015@126.com

Received 23 December 2015; Accepted 2 March 2016

Academic Editor: Ying-Ju Lin

The present study aimed to assess the effects and mechanisms of genistin in the rat model of myocardial ischemia reperfusion injury. The rat hearts were exposed to the left anterior descending coronary artery (LAD) ligation for 30 min followed by 1 h of reperfusion. In the rat of myocardial ischemia/reperfusion (MI/R), it was found that genistin pretreatment reduced myocardial infarct size, improved the heart rate, and decreased creatine kinase (CK) and lactate dehydrogenase (LDH) levels in coronary flow. This pretreatment also increased catalase (CAT), superoxide dismutase (SOD) activities but decreased glutathione (GSH), malondialdehyde (MDA) levels. Furthermore, we determined that genistin can ameliorate the impaired mitochondrial morphology and oxidation system; interleukin-6 (IL-6), interleukin-8 (IL-8), interleukin-10 (IL-10), and tumor necrosis factor-α (TNF-α) levels were also recovered. Besides, related-proteins of nuclear factor kappa-B (NF-κB) signal pathway activated by P2X7 were investigated to determine the molecular mechanism of genistin and their expressions were measured by western blot. These results presented here demonstrated that genistin enhanced the protective effect on the rats with myocardial ischemia reperfusion injury. Therefore, the cardioprotective effects of genistin may rely on its antioxidant and anti-inflammatory activities via suppression of P2X7/NF-κB pathways.

1. Introduction

The myocardial injury in ischemic heart diseases is mainly associated with ischemia/reperfusion (I/R) injury. It is a principal cause of death and disability all over the world [1]. Previous studies showed that promptly resuming the blood supply in the ischemic tissue is the most effective way of treating acute myocardial infarction and reperfusion induced oxidative stress plays a critical role in this pathology [2]. Thus, many studies exerted considerable efforts to elucidate the mechanism of cardioprotection. However, reperfusion itself after even brief duration of ischemia causes other irreversible myocardial damages, which is called myocardial ischemia reperfusion (IR) injuries. It is often associated with microvascular dysfunction including impaired endothelial-dependent dilation in arterioles, excess fluid filtration, and leukocyte plugging of capillaries [3]. As a complicated pathological process, the mechanism of MI/R is still largely unclear.

Recently, P2X7, an ion channel protein, has been reported to play a key role in the immune system and oxidative stress. The P2X7 receptor is expressed in very different tissues, and its activation can trigger multiple cellular responses. It has been reported that reactive oxygen species (ROS) overproduction is responsible for P2X7 receptor activation [4]. In addition, P2X7 has been shown to increase NADPH oxidase activity. It was developed as a potential new target for the treatment of inflammatory diseases of which the specific P2X7 receptor antagonist and P2X7 receptor knockout animal model has been used extensively in some studies [5]. The activation of P2X7/NF-κB signal pathway stimulated the expression of upstream gene IKK, as well as the p65 subunit of NF-κB, both of which intervened in inflammatory responses

and oxidative stress. Taking together, these evidences indicate that P2X7/NF-κB signal may play a significant role in lung regulatory pathways.

Flavonoids, which are a group of naturally occurring secondary metabolites that are widely distributed in the plant kingdom, possess unique antioxidant activities and other pharmacological effects that may be relevant in protecting the heart from I/R injury [6]. These flavonoids prevent oxidant production through xanthine oxidase inhibition and transition metal chelation, which could reduce oxidative stress from attacking cellular targets, block oxidative reactions, and enhance cellular antioxidant capacity by minimizing the effects of oxidants [7]. Flavonoids have also demonstrated that they could play the effects of anti-inflammatory and antiplatelet aggregation by controlling correlative enzymes and signal pathways. So they could ultimately reduce oxidant production and enhance the reestablishment of blood flow in the ischemic site. In addition, the recently research has focused on the mitochondrial pathway, through which certain flavonoids can play a target of the cardioprotection [8]. Finally, flavonoids also exhibit vasodilator effects via various mechanisms, one of which may be interacted with ion channels [9]. These diverse effects of flavonoids raise their utility as potential therapeutic intervention tools to protect I/R injury.

Genistin, a flavonoid which is abundant in the annual plant of Fabaceae family especially *Glycine max* (L.) MERR, has been reported to possess various therapeutic effects, including anti-inflammatory and anticancer activities [10, 11]. It can prevent oxidant damage and cell apoptosis by several mechanisms [12]. Furthermore, genistin has been shown to be a strong antioxidative agent [13]. Meanwhile, genistin, the aglycone of genistin, could also inhibit lipid peroxidation and reduce infarct size and apoptosis of myocytes, suggesting the effect on myocardial ischemia/reperfusion injury [14, 15]. Here, we explored the antioxidative and cardioprotective effects of pretreatment with genistin against IR injuries. The study presented here was undertaken to evaluate the protective effects of genistin on the I/R rats and to illustrate whether its cardioprotective effects associated with P2X7/NF-κB pathway.

2. Materials and Methods

2.1. Materials. Genistin (pure: 95%) was provided by the National Institutes for the Control of Pharmaceutical and Biological Products (Beijing, China), and its purity was identified by high performance liquid chromatography (HPLC). Superoxide dismutase (SOD), malondialdehyde (MDA), and lactate dehydrogenase (LDH) kits were purchased from Nanjing Jiancheng Bioengineering Research Institute (Nanjing, China). Interleukin-6 (IL-6), interleukin-8 (IL-8), interleukin-10 (IL-10), and tumor necrosis factor-α (TNF-α) Elisa kits were obtained from R&D Systems Inc. (Minneapolis, MN, USA).

2.2. Animals. Sprague-Dawley rats (male, 250–300 g) were purchased from Shanghai Slac Laboratory Animal Ltd. (Shanghai, China). All animals were housed with free access to water and food with a 12 h light/dark cycle at the constant temperature (22 ± 2°C). Rats were acclimated for 7 days before any experimental procedures. The experiments were conducted in adherence with the National Institutes of Health Guidelines for the Use of Laboratory Animals.

2.3. Experimental Design. The I/R injury animal model was established by the left anterior descending (LAD) coronary artery ligation for 30 min followed by 1 h reperfusion. Briefly, after being anesthetized with a 30 mg/kg pentobarbital sodium intraperitoneally, rats were ventilated with a positive pressure respirator at a stroke volume of 12 mL/kg and a rate of 60 strokes per minute with 95% O_2 and 5% CO_2 throughout the experiment. The rat heart was exposed through a left thoracotomy. Then, the LAD was ligated 2-3 mm from its origin and loosened to simulate I/R rat model (ischemia for 30 min and reperfusion for 1 h). Rats were randomly apportioned in equal animals ($n = 10$) to five experimental groups: (1) sham group: rats were subjected to the entire surgical procedure but without the induction of I/R; (2) model group: I/R injury animal model was constructed by LAD ligation for 30 min, and then the LAD was allowed 1 h reperfusion; and (3) three genistin-treated groups: different doses (20, 40, and 60 mg/kg body weight, resp.) of genistin dissolved in 0.5% sodium carboxyl methyl cellulose (CMC-Na) solution were given intragastrically for 5 days before operation.

2.4. Evaluation of Myocardial Infarct Area. To further evaluate the myocardial infarct sizes, tetrazolium chloride (TTC) staining was adopted. After reperfusion, the isolated rat hearts were immediately washed in phosphate-buffered saline, frozen, stored at −20°C for 30 min, and then sectioned into 5 mm transverse slices. After incubation in 1% (0.01 g/mL) TTC at 37°C in PBS for 15 min, the heart slices were photographed with a digital camera to distinguish the red-stained viable tissues and the white-unstained necrotic tissues. Areas of infarct size were measured digitally using Image Pro Plus software.

2.5. Histopathologic Examination of Hearts. To investigate the effects of genistin on the protecting from the myocardial ischemia-reperfusion injury (MIRI) rats, hematoxylin-eosin staining (HE) was performed for hearts. A small piece of subendocardial myocardium from the root of the left ventricular papillary muscle was excised, rinsed with saline solution, fixed overnight in 4% fresh paraformaldehyde, and embedded in paraffin. Of 5 μm sections were obtained, stained with HE, and performed of the section for observation of pathological changes in the heart tissues under a light microscopy and photomicrographs were taken.

2.6. Determination of Creatine Kinase (CK) and Lactate Dehydrogenase (LDH) in Serum. At the end of reperfusion, 2 mL of femoral vein blood was collected and centrifuged at 3,000 rpm for 20 min. Serum CK and LDH levels were analyzed by colorimetry according to the manufacturer's

instructions. The activities of these enzymes were expressed in U/L.

2.7. Assay of Oxidative Stress. After perfusions, hearts were harvested and maintained at −70°C for later analysis. The frozen ventricles were crushed to a powder by liquid nitrogen-chilled tissue pulverizer. For tissue analysis, weighed amounts of the frozen tissues were homogenized in appropriate buffer using a microcentrifuge tube homogenizer.

SOD activity, MDA level, CAT activity, and GSH level were spectrophotometrically analyzed according to the instruction of assay kits.

2.8. Assay of Inflammation. TNF-α, IL-6, IL-8, and IL-10 were spectrophotometrically analyzed using ELISA following the manufacturer's instructions.

2.9. Western Blot of P2X7/NF-κB Pathways. The myocardial tissues were removed and washed with PBS. Then the samples were cut into pieces and homogenized. Proteins were extracted with lysis buffer (RIPA with protease and phosphatase inhibitor) for 20 min on ice. The samples were loaded to 12% sodium dodecyl sulphate polyacrylamide gel electrophoresis (SDS-PAGE) gels and transferred to polyvinylidene fluoride (PVDF) membranes. The membrane was blocked with blocking reagent (20 mM Tris (pH 7.4), 125 mM NaCl, and 0.2% (vol/vol) Tween 20, 4% (wt/vol) nonfat dry milk, and 0.1% (wt/vol) sodium azide) for 2 h at room temperature and then incubated with primary antibodies diluted 1 : 1000 overnight at 4°C. After incubation with the corresponding horseradish peroxidase-conjugated secondary antibodies for 2 h, the bounds were detected using the SuperSignal West Pico Chemiluminescent Substrate and quantified using the Quantity One System (Bio-Rad, Hercules, CA, USA).

2.10. Statistical Analysis. The results were expressed as mean ± SEM. All data were processed with SPSS 11.0 statistical package for Windows version. The comparison of data from multigroup was analyzed using one-way ANOVA, followed by Student-Newman-Keuls's post hoc test. P values < 0.05 or < 0.01 were considered significant or highly significant, respectively.

3. Results

3.1. Effect of Genistin on the Myocardial Infarction Size of Hearts. To evaluate the direct effect of genistin on myocardial I/R injury, TTC staining was used to analyze the infarct area (Figure 1). Myocardial infarct was significantly increased in IR group compared with the sham group. In contrast, this effect was markedly diminished by pretreatment with genistin, particularly at the high dose.

3.2. Genistin Impaired Myocardial Structure Turbulence Induced by I/R Injury. The changes in the morphological

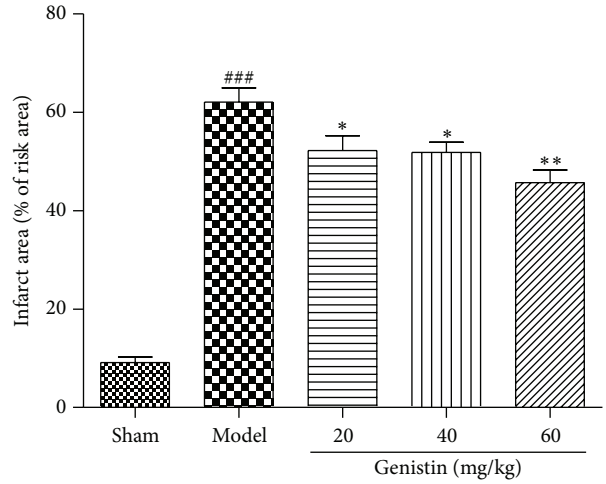

Figure 1: Effect of genistin on myocardial damage in rats subjected to MI/R. TTC staining to assess the extent of myocardial necrosis. Bars represent the percent of ischemic area at risk in hearts. Values are means ± SEM, $n = 6$ per group. $^{###}P < 0.001$ compared with the sham group; $^{*}P < 0.05$, $^{**}P < 0.01$ compared with the model group.

structures of myocardial tissues were evaluated by HE coloration. Optical micrographs of rat myocardial structures are shown in Figure 2. The myocardial membrane damage and infiltration of inflammatory cells were observed in the myocardial structures of I/R group as compared to those of sham control group. Moreover, compared with the I/R group, the group pretreated with genistin showed marked improvement evidenced by reduced degree of myonecrosis, edema, infiltration of inflammatory cells, and lesser vacuolar changes compared to the I/R group.

3.3. Genistin Reduces LDH, CK Release after I/R Injury in Rats. As shown in Figure 3, levels of serum CK and LDH were remarkably increased in rats of I/R group compared with control group. After 1 h of reperfusion, preconditioning with genistin at dosages of 20–60 mg/kg significantly attenuated the release of LDH, CK in a dose-dependent manner compared with the I/R group.

3.4. Genistin Ameliorated Oxidative Stress of Myocardial Tissues Induced by I/R Injury. SOD activity, CAT activity, MDA level, and GSH are indicators of oxidative stress. These indicators were determined in myocardial tissues to identify the possible mechanisms underlying the cardioprotective effects of genistin. As illustrated in Figure 3, the result showed that the level of MDA was decreased and the activities of SOD and CAT were increased as well as an increased GSH level in a dose-dependent manner by genistin treatment in I/R.

3.5. The Expression of IL-6, IL-8, IL-10, and TNF-α. Figure 4 showed the change of serum IL-6, IL-8, IL-10, and TNF-α concentration of all the tested rats. In this study, we found that the plasma levels of IL-6, IL-8, IL-10, and TNF-α were significantly elevated following I/R injury compared with sham group. Furthermore, our results determined that

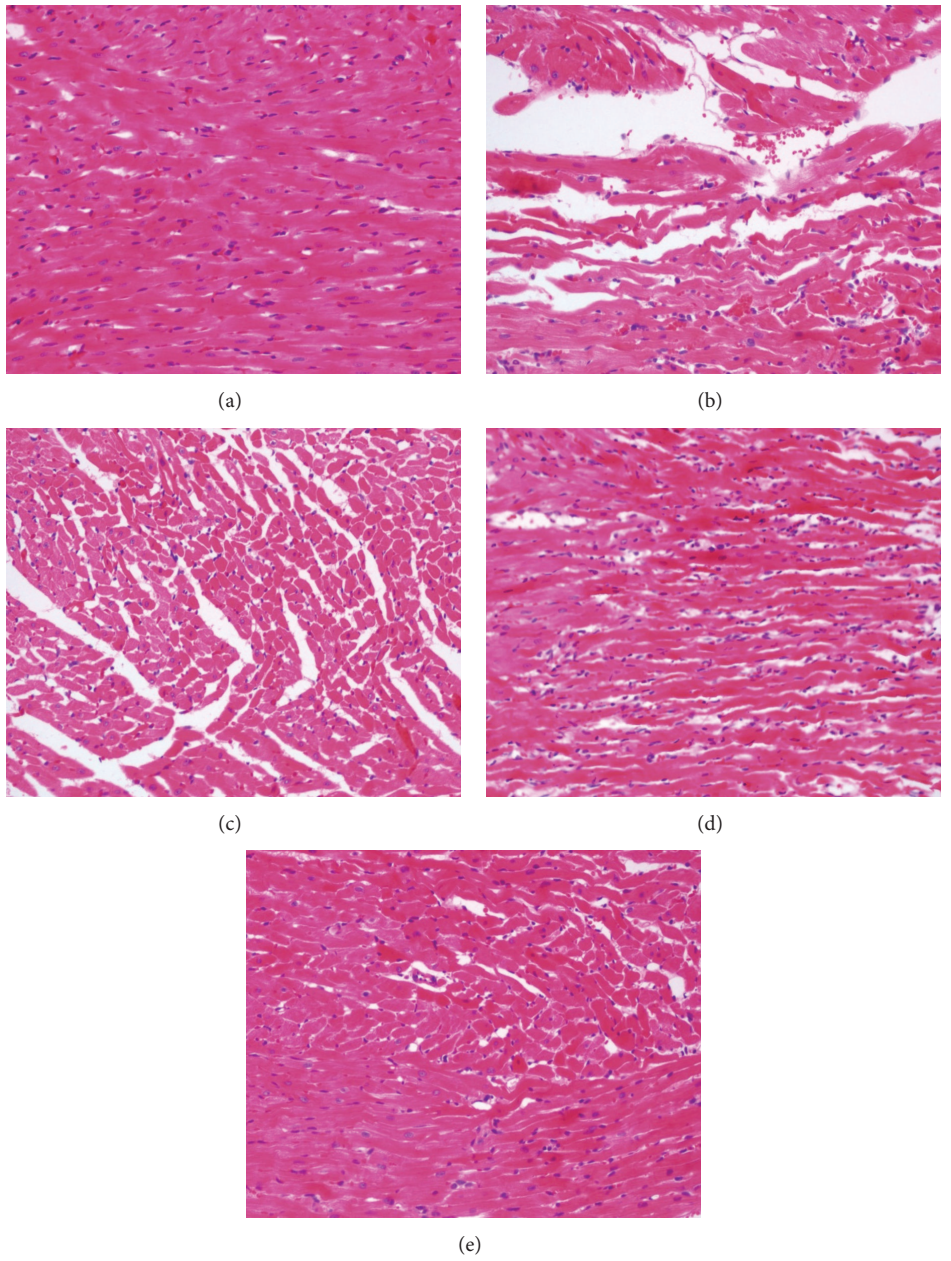

Figure 2: Histopathological changes in the myocardium following reperfusion (magnification, ×100). Sham-operated group (a); model group (b); genistin (20, 40, and 60 mg/kg) group (c, d, and e).

pretreatment with genistin significantly attenuated the cytokines release. As expected, the treatment of genistin dose-dependently protected the rats of I/R injury. In the high dosage group, the levels of inflammatory cytokines were mostly close to the sham rats. Serum IL-6, IL-8, IL-10, and TNF-α concentrations decreased 21.3%, 36.9%, 28.1%, and 44.4%, respectively.

3.6. Effect of Genistin on P2X7/NF-κB Pathway and Related Proteins. To further determine the underlying damage mechanism, the western blot was performed to investigate the activation of IκBα, NF-κBp65, and their corresponding phosphorylated forms, as well as P2X7. As shown in Figure 5, it could be observed that the expression of p-IκBα, p-NF-κBP65, and P2X7 protein levels was significantly increased in model group compared with the sham group. Moreover, pretreatment with genistin (20, 40 and 60 mg/kg) prevented the expression of P2X7, p-IκBα, and p-NF-κB p65 compared with the model group.

4. Discussion

In the present study, we investigated for the first time the protective effects of genistin on myocardial ischemia-reperfusion

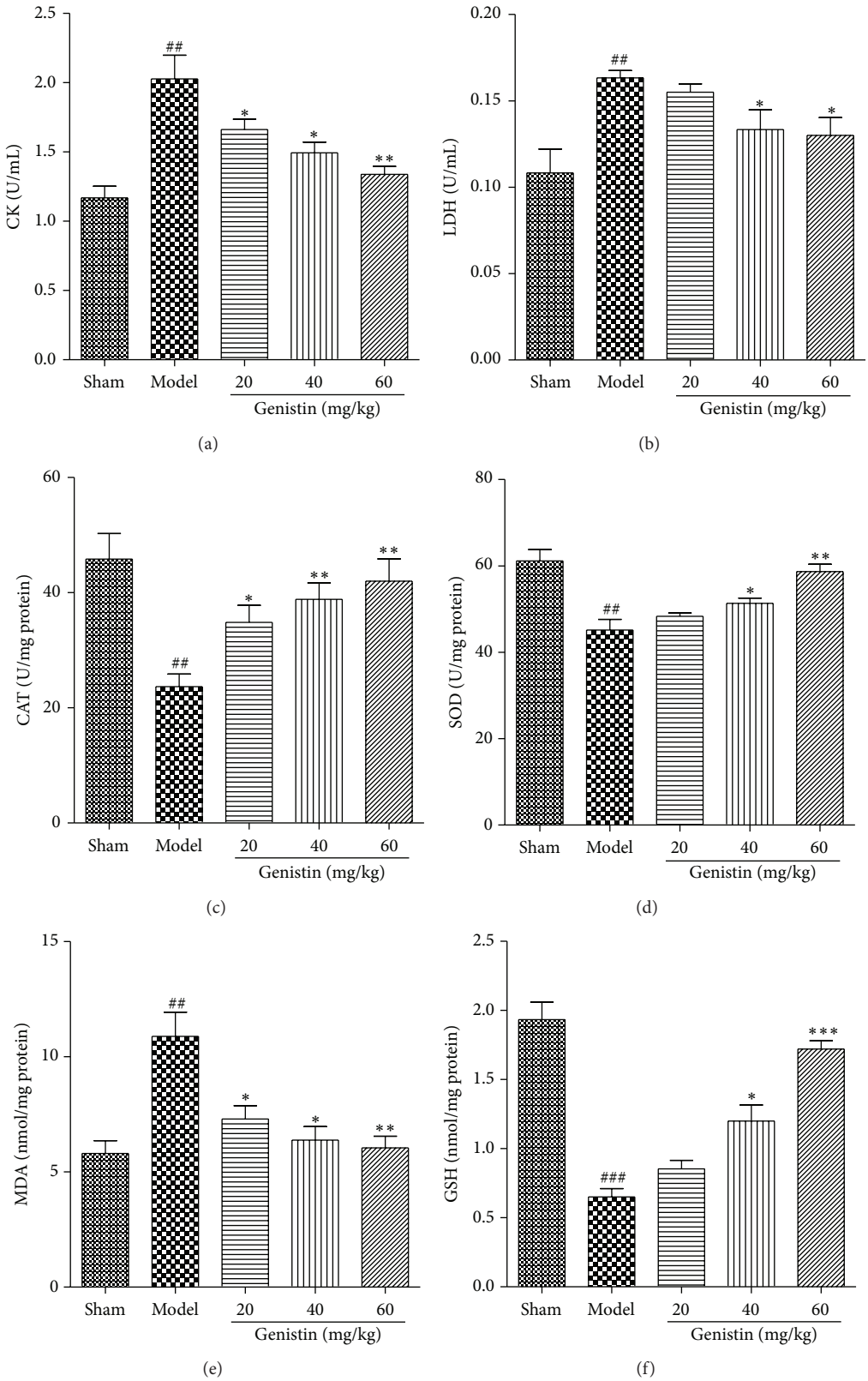

Figure 3: Effect of genistin treatment on serum CK (a) and LDH (b) levels in rats subjected to myocardial ischemia-reperfusion. And effect of genistin treatment on CAT activity (c), SOD activity (d), MDA level (e), and GSH level (f). Data represent the means ± SEM in each group ($n = 6$); $^{\#\#}P < 0.01$, $^{\#\#\#}P < 0.001$ compared with the sham group; $^{*}P < 0.05$, $^{**}P < 0.01$, and $^{***}P < 0.001$ compared with the model group.

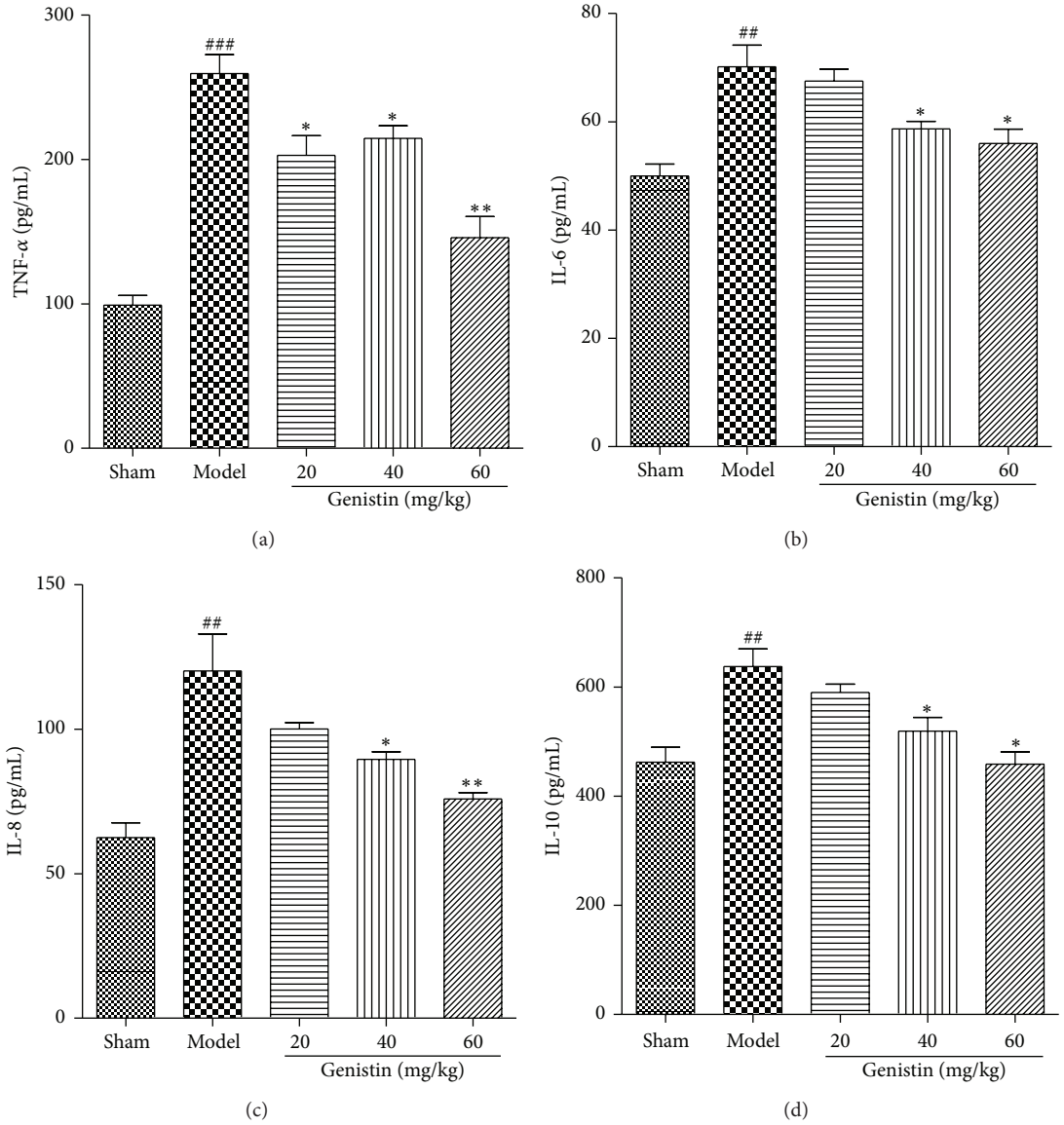

Figure 4: Effect of genistin on inflammatory cytokine production in the serum. The levels of TNF-α, IL-6, IL-8, and IL-10 were measured by ELISA kits. Data represent the means ± SEM in each group ($n = 6$); $^{\#\#}P < 0.01$, $^{\#\#\#}P < 0.001$ compared with the sham group; $^{*}P < 0.05$, $^{**}P < 0.01$ compared with the model group.

injury. The results demonstrated that preconditioning with genistin remarkably improved the I/R-induced cardiac injury through inhibition inflammation and relieved the oxidative stress, whereas genistin affected the pathway of P2X7/NF-κB. Moreover, the treatment of genistin, which reduced the myocardial infarct size, may work as a cardioprotective agent.

Nowadays, a number of epidemiological studies have reported that inflammatory lesions play a core role in the MI/R process. Cytokines, a heterogeneous group of proteins, have been associated with the inflammatory response in the progress of ischemia/reperfusion injury [16]. It has been shown that ischemia/reperfusion (I/R) increases the relative levels of various cytokines, such as TNF-α, IL-6, IL-8, and IL-10, in the myocardium. TNF-α, as a critical early mediator, plays a very crucial role in the genesis of a systemic inflammatory response [17]. In addition, it could stimulate the secretion of secondary cytokines, including the proinflammatory IL-6 and the anti-inflammatory IL-10 [18]. Here, we determined the serum levels of IL-6, IL-8, IL-10, and TNF-α. The levels of these cytokines in the I/R rats are in accordance with those presented in other investigations which showed that myocardium synthesizes and releases TNF-α, IL-6, IL-8, and IL-10 in response to I/R. Moreover, the genistin, the aglycone of genistin, mainly derived from soybean, has been demonstrated to be able to play many protective effects on the cardiovascular system. These beneficial actions of genistin showed the protected against myocardial I/R injury [14]. However, genistin preconditioning significantly reversed

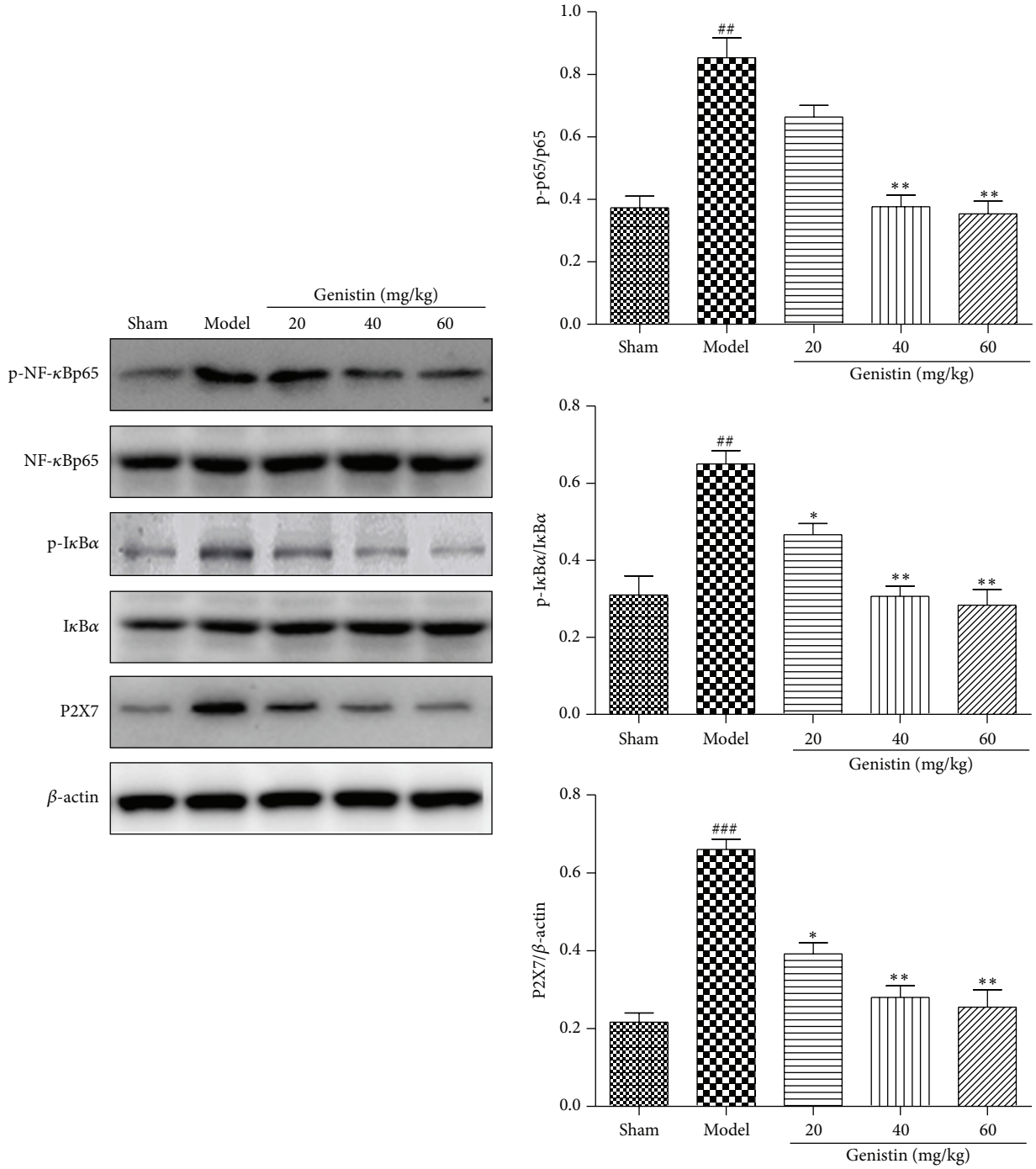

Figure 5: The protein levels of p-IκBα, IκBα, NF-κB, p-NF-κB, and P2X7 in rat myocardial tissue were detected by western blot. Data represent the means ± SEM in each group ($n = 3$); $^{\#\#}P < 0.01$, $^{\#\#\#}P < 0.001$ compared with the sham group; $^{*}P < 0.05$, $^{**}P < 0.01$ compared with the model group.

the response, suggesting the anti-inflammation properties of genistin were involved in its cardioprotective effect in the I/R rats.

To further clearly determine the relationship between inoxidizability and the cardioprotection of genistin, an experiment was carried out to examine whether genistin affected the changes in MDA and GSH levels, SOD and CAT activities induced by I/R. From the results, we found the I/R rats showed an increase in MDA production as well as a decrease in SOD level and GSH. MDA is considered to affect the generation and production of the ROS, which is caused by peroxidation of cell membrane lipids [19]. SOD, as one

of the most significant intracellular antioxidant enzymes, could function as a ROS scavenger. GSH, a tripeptide composed of glutamate, exerts a critical role as antioxidant and neuromodulator in the central nervous system [20]. The imbalance between oxidation and antioxidation leads to the oxidation injury. In our study, genistin dose-dependently reduced the increased levels of MDA, LDH, and CK, especially at 60 mg/kg dose. Moreover, genistin increased the activity of the antioxidase SOD, compared with the I/R group. Taken these results together with the experiment data, it was suggested that the protective ability of genistin against ischemia/reperfusion injury in vivo was exerted by means of mediating reactive oxygen species. To further characterize the cardioprotective mechanism of genistin on MIRI rat, we evaluated the effects of genistin on the activation of the P2X7/NF-κB signaling pathways. P2X7 can selectively target NFκB-p65 and activation of P2X7 is required for the production and release of many inflammatory factors like IL-1β, IL-18, IL-6, and TNF-α [21]. Moreover, P2X7 participate in the regulation of oxidative stress [22]. In this study, we observed that the level of P2X7 was basically recovered to the normal level after genistin treatment at the 60-dose group. The levels of phosphorylation of NF-κB P65 and IκBα were markedly increased in the I/R group, and administration of genistin impairs phosphorylation of these molecules in a dose-dependent manner. The present results clearly demonstrate that genistin obviously regulated P2X7/NF-κB pathway.

In conclusion, on the basis of present study findings from the hemodynamic, biochemical, and histopathological results, we confirmed that genistin, as an antioxidant and anti-inflammation agent, could attenuate the myocardial ischemia-reperfusion injury. The present results also clearly demonstrated the mechanism of genistin by regulating the P2X7/NF-κB pathway to protect the MIRI rats. Our findings may advance the possible utility of genistin as an ideal agent for patients with I/R injury.

Competing Interests

The authors declare that they have no competing interests.

References

[1] G. M. Fröhlich, P. Meier, S. K. White, D. M. Yellon, and D. J. Hausenloy, "Myocardial reperfusion injury: looking beyond primary PCI," *European Heart Journal*, vol. 34, no. 23, pp. 1714–1722, 2013.

[2] C. Li, J. He, Y. Gao, Y. Xing, J. Hou, and J. Tian, "Preventive effect of total flavones of *Choerospondias axillaries* on ischemia/reperfusion-induced myocardial infarction-related MAPK signaling pathway," *Cardiovascular Toxicology*, vol. 14, no. 2, pp. 145–152, 2014.

[3] D. L. Carden and D. N. Granger, "Pathophysiology of ischaemia-reperfusion injury," *Journal of Pathology*, vol. 190, no. 3, pp. 255–266, 2000.

[4] D. Mélody, L. Hong, P. Thierry et al., "Effects of toxic cellular stresses and divalent cations on the human P2X7 cell death receptor," *Molecular Vision*, vol. 14, pp. 889–897, 2008.

[5] D. L. Donnelly-Roberts, M. T. Namovic, P. Han, and M. F. Jarvis, "Mammalian P2X7 receptor pharmacology: comparison of recombinant mouse, rat and human P2X7 receptors," *British Journal of Pharmacology*, vol. 157, no. 7, pp. 1203–1214, 2009.

[6] X. Hou, J. Han, C. Yuan et al., "Cardioprotective effects of total flavonoids extracted from xinjiang sprig rosa rugosa against acute ischemia/reperfusion-induced myocardial injury in isolated rat heart," *Cardiovascular Toxicology*, vol. 16, no. 1, pp. 1–13, 2015.

[7] J. Mierziak, W. Wojtasik, K. Kostyn, T. Czuj, J. Szopa, and A. Kulma, "Crossbreeding of transgenic flax plants overproducing flavonoids and glucosyltransferase results in progeny with improved antifungal and antioxidative properties," *Molecular Breeding*, vol. 34, no. 4, pp. 1917–1932, 2014.

[8] L. Testai, "Flavonoids and mitochondrial pharmacology: a new paradigm for cardioprotection," *Life Sciences*, vol. 135, pp. 68–76, 2015.

[9] V. Calderone, S. Chericoni, C. Martinelli et al., "Vasorelaxing effects of flavonoids: Investigation on the possible involvement of potassium channels," *Naunyn-Schmiedeberg's Archives of Pharmacology*, vol. 370, no. 4, pp. 290–298, 2004.

[10] J.-H. Zhao, Y. Arao, S.-J. Sun, A. Kikuchi, and F. Kayama, "Oral administration of soy-derived genistin suppresses lipopolysaccharide-induced acute liver inflammation but does not induce thymic atrophy in the rat," *Life Sciences*, vol. 78, no. 8, pp. 812–819, 2006.

[11] C. Spagnuolo, G. L. Russo, I. E. Orhan et al., "Genistein and cancer: current status, challenges, and future directions," *Advances in Nutrition*, vol. 6, no. 4, pp. 408–419, 2015.

[12] S. H. Kwon, M. J. Kang, J. S. Huh et al., "Comparison of oral bioavailability of genistein and genistin in rats," *International Journal of Pharmaceutics*, vol. 337, no. 1-2, pp. 148–154, 2007.

[13] A. Russo, V. Cardile, L. Lombardo, L. Vanella, and R. Acquaviva, "Genistin inhibits UV light-induced plasmid DNA damage and cell growth in human melanoma cells," *Journal of Nutritional Biochemistry*, vol. 17, no. 2, pp. 103–108, 2006.

[14] E.-S. Ji, H. Yue, Y.-M. Wu, and R.-R. He, "Effects of phytoestrogen genistein on myocardial ischemia/reperfusion injury and apoptosis in rabbits," *Acta Pharmacologica Sinica*, vol. 25, no. 3, pp. 306–312, 2004.

[15] E. Sbarouni, E. K. Iliodromitis, A. Zoga, G. Vlachou, I. Andreadou, and D. T. Kremastinos, "The effect of the phytoestrogen genistein on myocardial protection, preconditioning and oxidative stress," *Cardiovascular Drugs and Therapy*, vol. 20, no. 4, pp. 253–258, 2006.

[16] H. K. Saini, Y.-J. Xu, M. Zhang, P. P. Liu, L. A. Kirshenbaum, and N. S. Dhalla, "Role of tumour necrosis factor-alpha and other cytokines in ischemia-reperfusion-induced injury in the heart," *Experimental and Clinical Cardiology*, vol. 10, no. 4, pp. 213–222, 2005.

[17] I. Garcia, M. L. Olleros, V. F. J. Quesniaux et al., "Roles of soluble and membrane TNF and related ligands in mycobacterial infections: effects of selective and non-selective TNF inhibitors during infection," *Advances in Experimental Medicine and Biology*, vol. 691, pp. 187–201, 2011.

[18] R. Hussain, H. Shiratsuchi, M. Phillips, J. Ellner, and R. S. Wallis, "Opsonizing antibodies (IgG1) up-regulate monocyte proinflammatory cytokines tumour necrosis factor-α (TNF-α) and IL-6 but not anti-inflammatory cytokine IL-10 in mycobacterial antigen-stimulated monocytes-implications for pathogenesis," *Clinical & Experimental Immunology*, vol. 123, no. 2, pp. 210–218, 2001.

[19] H. Chen, X. Yan, P. Zhu, and J. Lin, "Antioxidant activity and hepatoprotective potential of agaro-oligosaccharides *in vitro* and *in vivo*," *Nutrition Journal*, vol. 5, no. 1, article 31, 2006.

[20] F. E. Emiliani, T. W. Sedlak, and A. Sawa, "Oxidative stress and schizophrenia: recent breakthroughs from an old story," *Current Opinion in Psychiatry*, vol. 27, no. 3, pp. 185–190, 2014.

[21] M. L. Gavala, Y.-P. Liu, L. Y. Lenertz et al., "Nucleotide receptor P2RX7 stimulation enhances LPS-induced interferon-β production in murine macrophages," *Journal of Leukocyte Biology*, vol. 94, no. 4, pp. 759–768, 2013.

[22] Y. Deng, X.-L. Guo, X. Yuan, J. Shang, D. Zhu, and H.-G. Liu, "P2X7 receptor antagonism attenuates the intermittent hypoxia-induced spatial deficits in a murine model of sleep apnea via inhibiting neuroinflammation and oxidative stress," *Chinese Medical Journal*, vol. 128, no. 16, pp. 2168–2175, 2015.

Hindawi Publishing Corporation
Evidence-Based Complementary and Alternative Medicine
Volume 2016, Article ID 5936354, 9 pages
http://dx.doi.org/10.1155/2016/5936354

Research Article

Effect of *Dangguibohyul-Tang*, a Mixed Extract of *Astragalus membranaceus* and *Angelica sinensis*, on Allergic and Inflammatory Skin Reaction Compared with Single Extracts of *Astragalus membranaceus* or *Angelica sinensis*

You Yeon Choi,[1] Mi Hye Kim,[1] Jongki Hong,[2] Kyuseok Kim,[3] and Woong Mo Yang[1]

[1]*Department of Convergence Korean Medical Science, College of Korean Medicine, Kyung Hee University, Seoul 02447, Republic of Korea*
[2]*College of Pharmacy, Kyung Hee University, Seoul 02447, Republic of Korea*
[3]*Department of Ophthalmology, Otorhinolaryngology and Dermatology of Korean Medicine, College of Korean Medicine, Kyung Hee University, Seoul 02447, Republic of Korea*

Correspondence should be addressed to Kyuseok Kim; kmdkskim@khu.ac.kr and Woong Mo Yang; wmyang@khu.ac.kr

Received 11 December 2015; Revised 30 January 2016; Accepted 17 February 2016

Academic Editor: Ying-Ju Lin

Dangguibohyul-tang (DBT), herbal formula composed of *Astragalus membranaceus* (AM) and *Angelica sinensis* (AS) at a ratio of 5 : 1, has been used for the treatment of various skin diseases in traditional medicine. We investigated the effect of DBT on allergic and inflammatory skin reaction in atopic dermatitis-like model compared to the single extract of AM or AS. DBT treatment showed the remission of clinical symptoms, including decreased skin thickness and scratching behavior, the total serum IgE level, and the number of mast cells compared to DNCB group as well as the single extract of AM- or AS-treated group. Levels of cytokines (IL-4, IL-6, IFN-γ, TNF-α, and IL-1β) and inflammatory mediators (NF-κB, phospho-IκBα, and phospho-MAPKs) were significantly decreased in AM, AS, and DBT groups. These results demonstrated that AM, AS, and DBT may have the therapeutic property on atopic dermatitis by inhibition of allergic and inflammatory mediators and DBT formula; a mixed extract of AM and AS based on the herb pairs theory especially might be more effective on antiallergic reaction as compared with the single extract of AM or AS.

1. Introduction

Atopic dermatitis (AD) is one of the most common chronic and recurrent inflammatory skin diseases which affect environmental, genetic, immunologic, and biochemical factors [1]. The pathogenesis of AD has been known to be caused by T helper (Th) 1/2 dysregulation and skin barrier disorder [2, 3]. In addition, mast cells (MCs) in allergic diseases including AD have shown playing a crucial role in the secretion of histamine, leukotrienes, prostaglandin D2, proteolytic enzymes, and several cytokines including interleukin- (IL-) 1β, IL-4, IL-6, tumor necrosis factor- (TNF-) α, and interferon- (IFN-) γ [4].

In conventional medicine, most clinicians mainly focus on the regulation of T cell inflammation with corticosteroids, antihistamines, or immunosuppressive agents [5]. However, long-term uses of these agents can induce serious side effects such as facial edema, skin atrophy, striae distensae, and perioral dermatitis [6]. Therefore, a wide variety of plant-derived medicines with fewer side effects have been investigated as potential alternatives for allergic skin diseases instead of conventional therapy [7, 8].

Many studies have reported that natural products and their compounds inhibit the development of allergic skin diseases. *Dangguibohyul-tang* (DBT; herbal decoction), which combines simply with two herbs, *Astragalus membranaceus* (AM) and *Angelica sinensis* (AS), is widely used herbal formulas for the treatment of hematopoietic function, menopausal symptoms, and immune responses [9–11]. A recent pharmacological study indicated that DBT reduces inflammatory

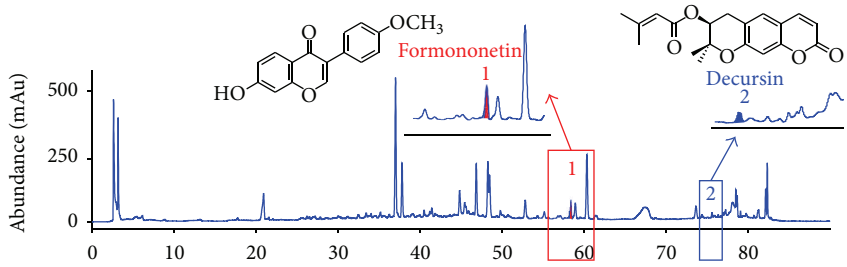

Figure 1: HPLC chromatogram of the DBT by HPLC analysis. The amounts of formononetin and decursin in the DBT extracts were determined as marker chemicals.

symptoms in AD-like mice [12]. Also, Dang-Gui-Yin-Zi, a similar herbal formula containing AM and AS, is commonly used for treating atopic dermatitis in clinical practice [13]. Additionally, the weight ratio of 5 : 1 for AM to AS in accord with the ancient preparation showed the best properties of DBT to achieve the maximum activity [14–16]. However, until now, there was no study to assess the antiallergic and anti-inflammatory effect of multiformulas DBT prepared from AM and AS compared with the single extract of AM or AS from the perspective of herb pairs [17].

Based on these backgrounds, we investigated the efficacy and the mechanism of DBT (the weight ratio of 5 : 1 for AM to AS) on allergic and inflammatory skin reaction compared to the single extract of AM or AS via AD-like mouse model.

2. Materials and Methods

2.1. Preparation of Sample. AM and AS were prepared same as previous reports [18, 19]. Briefly, each of the AM and AS crude materials was extracted with 300 mL of 70% ethanol for 24 h. The extracts were filtered, concentrated, lyophilized, and stored at −80°C. The yield of AM dried extract was approximately 25.0% (w/w, dry weight 7.5 g) and the extract of AS yielded 37.3% (w/w) for dry weight 11.2 g. Each voucher specimen (# AM001 and # AS070) was deposited in the herbarium of the college of pharmacy's laboratory. DBT mixture amounts of AM and AS were weighed according to a ratio of 5 to 1 and then mixed well in a vortex. A voucher specimen of DBT (# DBD E70) was deposited at our laboratory.

2.2. Standardization of DBT. DBT was identified by formononetin and decursin using reverse-phase high-performance liquid chromatography (HPLC). 50 mg DBT was mixed with 1 mL methanol, sonicated for 30 min, and filtered through a 0.2 μm filter membrane. HPLC was performed by an Agilent 1100 series instrument and chromatographic separation was achieved on a SHISEIDO CAPCELL PAK C18 column (250 mm × 4.6 mm, 5 μm). Gradient elution was carried out with A : B (water : acetonitrile) as follows: 0 min, 99 : 1; 10 min, 99 : 1; 70 min, 50 : 50; 80 min, 0 : 100; 90 min, 0 : 100. The flow rate was 1.0 mL/min and the detection wavelength was 230 nm. The column temperature was maintained at 40°C. AM and AS were, respectively, characterized based on the content of formononetin and decursin (Figure 1).

2.3. Animal Treatment. Six-week-old female BALB/c mice were supplied by Raon Bio (Yongin, Republic of Korea). The mice were maintained in climate-controlled quarters with a 12 h light/12 h dark cycle (at 22–24°C, 55–60% humidity) and provided with access to a standard laboratory diet and water *ad libitum*. After 1 week of adaptation, the mice were randomly divided into six groups of 5 animals each: (1) vehicle: vehicle application, (2) DNCB: 2,4-dinitrochlorobenzene application with vehicle application as a negative control group, (3) DEX: dexamethasone (10 μM/100 μL/day, Sigma Aldrich, MO, USA) treatment with DNCB application as a positive control group, (4) AM: AM (100 mg/mL, 100 μL/day) treatment with DNCB application, (5) AS: AS (20 mg/mL, 100 μL/day) treatment with DNCB application, and (6) DBT: DBT (120 mg/mL, 100 μL/day) treatment with DNCB application.

In brief, the dorsal hair of mice was removed by an electronic hair clipper for sensitive skin. After 24 h, 100 μL of 1% DNCB solution (acetone : olive oil = 4 : 1, v/v solution) was applied on the back skin once a day for 3 d. After 4 days of sensitization, 100 μL of 0.5% DNCB solution was treated on the back during 10 days. 4 h before DNCB application, DEX, AM, AS, and DBT dissolved in phosphate-buffered saline (PBS) were topically applied to the dorsal skin. Before sample treatment, 100 μL of 4% sodium dodecyl sulfate (SDS) was applied to the lesions in order to remove cuticle and to help the absorption of sample [20]. At the end of experiment, serum was obtained by cardiac puncture and the dorsal skin was collected for molecular indicators. All procedures were performed in accordance with the guidelines of the Committee on Care and Use of Laboratory Animals of Kyung Hee University (KHUASP (SE)-14-030).

2.4. Histological Observation. To investigate the effects of DBT on DNCB-induced AD-like symptoms in mice, we evaluated the skin thickness. To evaluate skin thickening and mast cell infiltration, the dorsal skin samples (1 × 0.4 cm^2) were obtained at the end of the experiment (on day 19). The sample was fixed in 10% buffered formalin (Sigma Aldrich, MO, USA) for at least 24 h, progressively dehydrated in solution containing an increasing percentage of ethanol (70%, 80%, 95%, and 100%, v/v), embedded in paraffin under vacuum, and sectioned at 4 μm thickness. Deparaffinized skin sections were stained with hematoxylin and eosin (H&E) for skin thickening and toluidine blue for mast cell infiltration. Histopathological changes were examined using the Leica

Application Suite (LAS; Leica Microsystems, Buffalo Grove, IL). The magnification was ×100. The epidermal thickness was measured from the top layer (stratum corneum) to the bottom layer (stratum basale). The dermis thickness was measured in vertical distance between stratum basale layer and the subcutaneous tissues. Thickness was measured 3 times at regular intervals in one slide and obtained 15 results per group [21]. The number of mast cells was measured in the entire area of slides for each sample ($n = 5$).

2.5. Measurement of Scratching Behavior. The mice were monitored for 20 min using a digital-camera (model NEX-C3, Sony, Japan), 1 h after last DNCB sensitization. Scratching movement was determined by replaying the recorded video. One incident of scratching was defined as raising to lowering of a leg including a series of scratches at one time.

2.6. Measurement of Total Serum Immunoglobulin E (IgE) Levels and Cytokines. The collected blood was centrifuged for 30 min at 16,000 ×g, and serum sample was stored in −80°C until analysis. Serum concentrations of IgE were measured using mouse IgE ELISA kit (BD Pharmingen, CA, USA) according to the manufacturers' instructions. To measure cytokine on dorsal skin changes according to the topical application, the dorsal skin was removed from each mouse (100 mg, $n = 5$ per group) and homogenized. The dorsal skin was lysed using tissue protein extraction reagent (T-PER; Pierce, Rockford, IL, USA) containing a protease inhibitor cocktail (Roche, Indianapolis, IN, USA). The resulting lysate was centrifuged at 16,000 ×g for 30 min at 4°C and stored at −80°C until analysis. Protein concentrations were requantified under identical conditions using a protein assay reagent (Bio-Rad, Hercules, CA, USA).

2.7. Preparation of Protein Extraction in Dorsal Skin. Extraction of cytoplasmic and nuclear proteins was performed with standard protocols and our previous paper [22]. In brief, the cytoplasmic buffer (10 mM HEPES, pH 7.9, 10 mM KCl, 0.1 mM EDTA, 0.1 mM EGTA, 1 mM DTT, 0.15% Nonidet P-40, 50 mM β-glycerophosphate, 10 mM NaF, and 5 mM Na_3VO_4, containing the protease inhibitor cocktail) was used to analyze the phosphorylated IκBα in the cytoplasm and nuclear buffer (20 mM HEPES, pH 7.9, 400 mM NaCl, 1 mM EDTA, 1 mM EGTA, 1 mM DTT, 0.50% Nonidet P-40, 50 mM β-glycerophosphate, 10 mM NaF, and 5 mM Na_3VO_4, containing the protease inhibitor cocktail) was used to analyze the NF-κB protein levels in the nucleus. MAPKs (extracellular signal-regulated kinases; ERK1/2, p38 kinases, the c-Jun N-terminal kinases; JNK) were confirmed by total protein extracts using RIPA assay buffer containing protease inhibitor cocktail.

2.8. Detection of Inflammatory Protein Expression. Each denatured protein (30 μg; nuclear, cytoplasmic, and whole fraction) was loaded onto 15% polyacrylamide gels for electrophoresis. Then, the proteins were transferred to polyvinylidene fluoride (PVDF) membranes and incubated at room temperature for 1 h with 5% BSA (diluted in TBS-T; TBS buffer containing 0.1% Tween) to block nonspecific binding. Primary antibodies reactive to mouse β-actin (Santa Cruz, USA), phosphorylated NF-κB (Santa Cruz, USA), phosphorylated IκBα (Santa Cruz, USA), ERK1/2 (Cell Signaling, USA), phosphorylated ERK1/2 (Cell Signaling, USA), p38 MAPK (Cell Signaling, USA), phosphorylated p38 MAPK (Cell Signaling, USA), JNK (Cell Signaling, USA), and phosphorylated JNK (Cell Signaling, USA) were used overnight (1 : 1,000 dilution; in TBS-T). The membrane was washed three times in TBS-T for 30 min, incubated with horseradish peroxidase-conjugated secondary antibodies (1 : 2,000 dilution; in TBS-T) for 2 h at room temperature (RT), washed three times in TBS-T for 30 min, and revealed with enhanced chemiluminescence (ECL). Immunoreactive bands were detected using an LAS-4000 mini system (Fujifilm Corporation, Tokyo, Kumamoto, Japan).

2.9. Statistical Analysis. All data are expressed as the mean ± standard deviation (SD). Significance was determined using one-way ANOVA with Duncan's multiple range test. In all analyses, $P < 0.05$ indicated statistical significance. GraphPad Prism 5 software (San Diego, CA, USA) was used for the statistical analysis.

3. Results

3.1. Amelioration of Hyperkeratosis and Hyperplasia. AD symptoms including dryness, erythema, and swelling were evidently seen in DNCB group. On the other hand, DBT-treated group significantly reduced AD symptoms (Figure 2(a)). As shown in microscopic analysis (Figure 2(b)), the dorsal skin of DNCB-treated mice (epidermis: 111.6 ± 15.5 μm, dermis: 505.3 ± 31.0 μm) was swollen and significantly thicker than those of the vehicle group (32.3 ± 6.3 μm, dermis: 178.3 ± 31.2 μm). Treatment with AM (epidermis: 43 ± 9.1 μm, dermis: 312.2 ± 51.0 μm), AS (epidermis: 65.8 ± 13.5 μm, dermis: 354.9 ± 49.3 μm), and DBT (epidermis: 39.1 ± 6.9 μm, dermis: 327.8 ± 38.2 μm) markedly attenuated DNCB-induced hyperkeratosis and hyperplasia. Particularly, the epidermis and dermis thickness of DBT-treated group were lower than those in AS-treated group.

3.2. Attenuation of Scratching Behavior. Intensive pruritus leads to extensive scratching as a hallmark of AD [23]. The distribution of the assessed level of scratching behavior was illustrated as the dot plot (Figure 3). The scratching behavior was markedly increased in DNCB-treated mice (179 ± 50) compared with the vehicle group (27 ± 5). This increased scratching behavior was significantly reduced by AM (50 ± 16), AS (63 ± 35), and DBT (40 ± 19) treatment. Consistently with histologic analysis, the reduction of pruritus by DBT treatment was greater than AS single treatment.

3.3. Inhibition of the Number of Mast Cells. The number of toluidine blue-stained mast cells of DNCB-treated mice (151 ± 15) was significantly increased compared with that of the vehicle group (44 ± 6). AM (56 ± 9), AS (70 ± 12), and DBT (45 ± 6) markedly lowered the number of mast cells in the skin of DNCB-treated mice (Figures 4(a) and 4(b)).

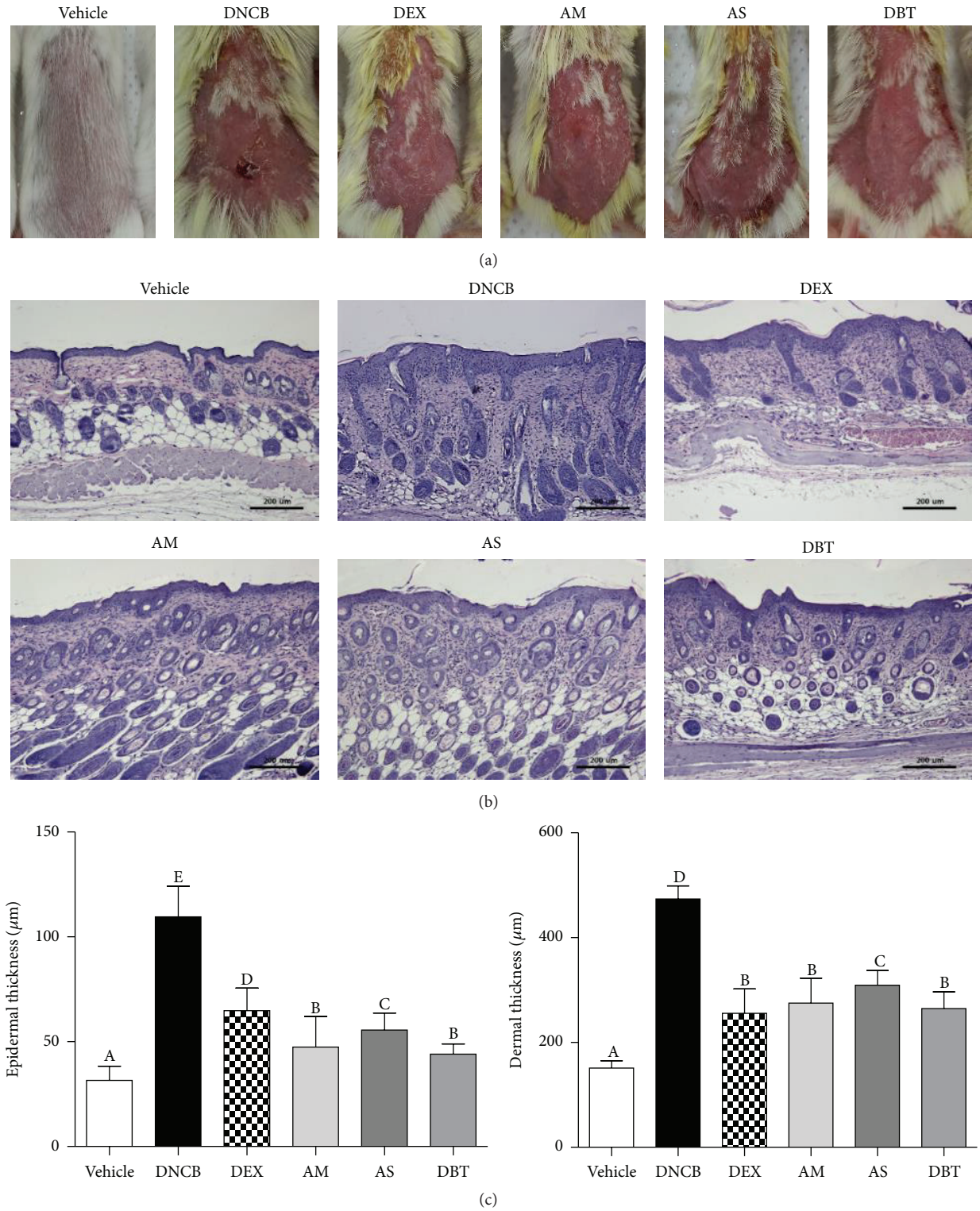

Figure 2: Effects of DBT on histological features of dorsal skin in DNCB-induced AD mice. (a) Representative mice of each treatment group on day 19. (b) Histological observation of the dorsal skin of each group by H&E staining. (c) The thickness of epidermis and dermis. Results are expressed as mean ± SD ($n = 5$). Magnifications are ×100 (scale bar: 200 μm).

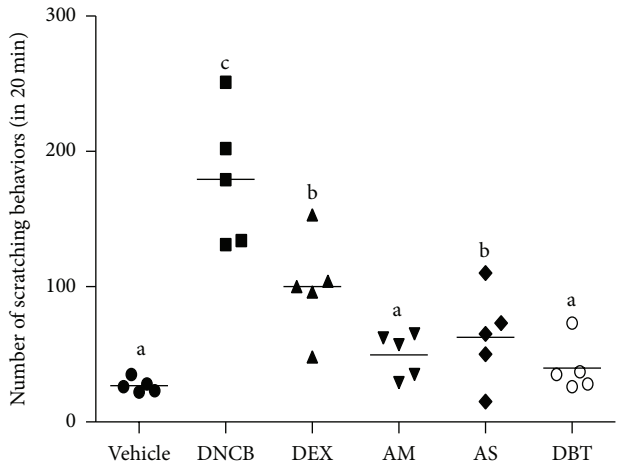

Figure 3: Effects of DBT on scratching behavior. The numbers of scratching behaviors are expressed as mean ± SD ($n = 5$).

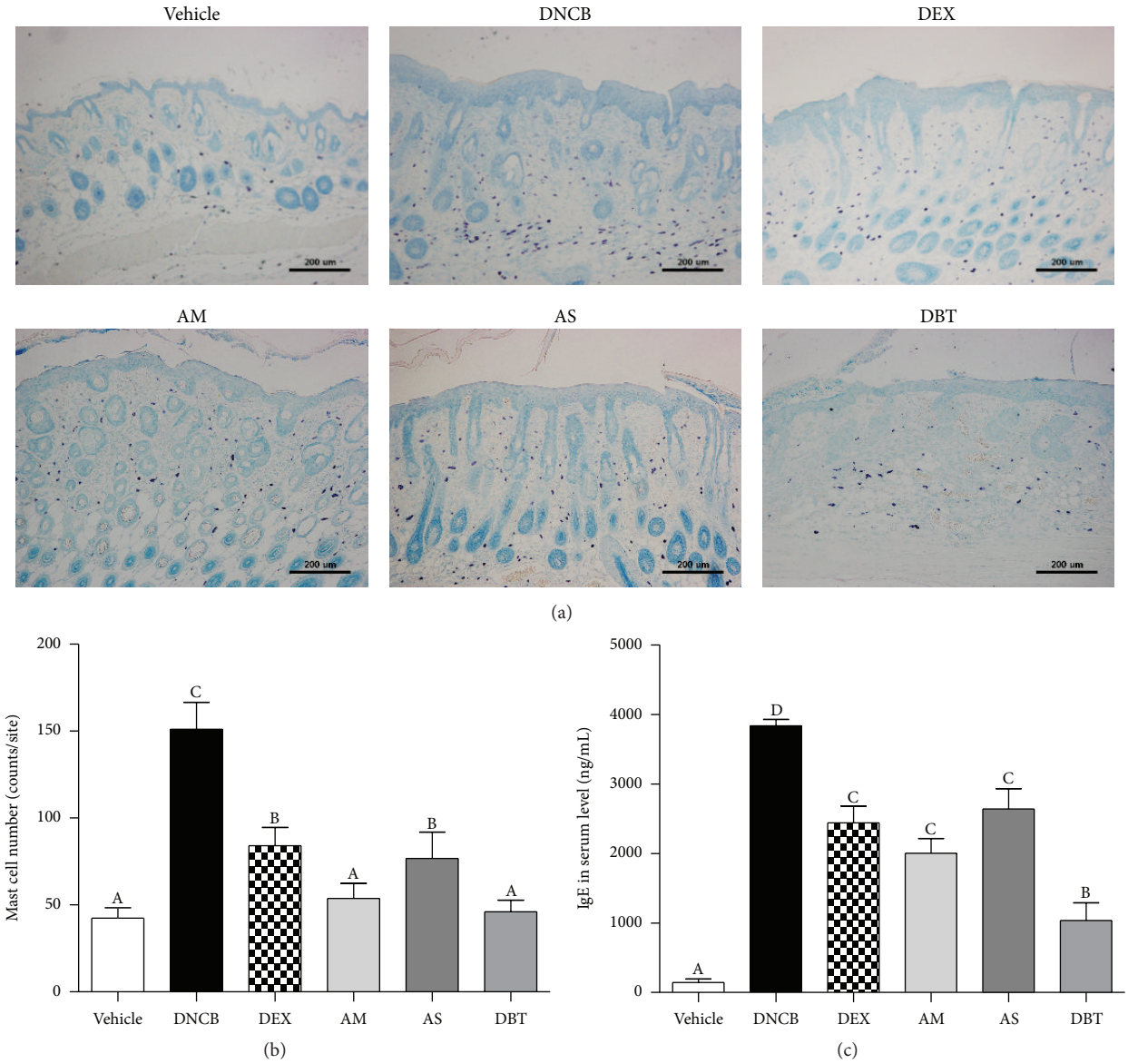

Figure 4: The number of mast cells and the level of IgE in DNCB-induced AD mice. (a, b) The number of mast cells observed by toluidine blue staining. Magnifications are ×100 (scale bar: 200 μm). (c) The level of IgE in serum. Results are expressed as mean ± SD ($n = 5$).

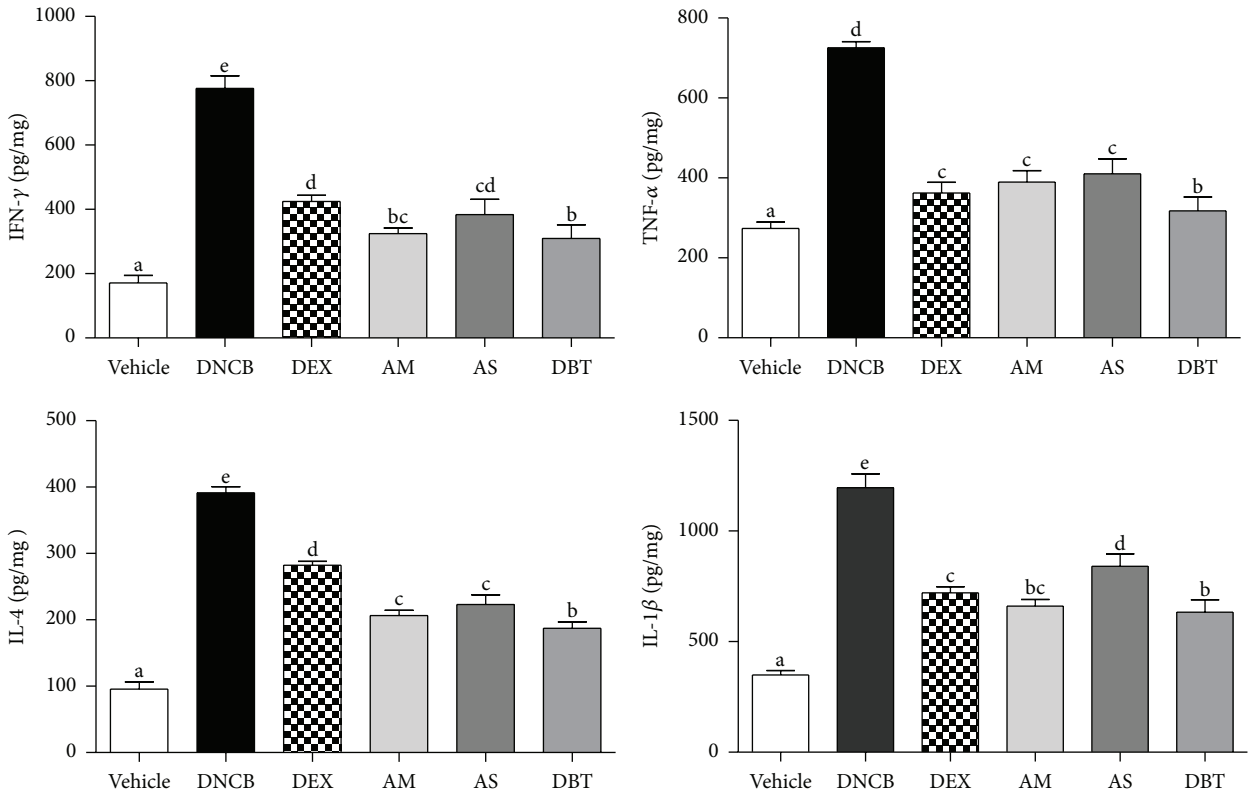

Figure 5: Effects of DBT on levels of Th2- and Th1-type cytokines. Values of cytokines are means ± standard error of the mean.

Compared with AS, DBT significantly decreased the number of mast cells.

3.4. Reduction of Serum IgE Level. We investigated whether DBT alters the serum level of IgE in DNCB-induced AD-like mice. We found that the level of IgE was markedly increased by DNCB application, compared to vehicle group. Treatment with AM, AS, DBT, and DEX group significantly reduced the IgE level of DNCB group (Figure 4(c)). DBT treatment showed more effective reduction in IgE level than the single extract of AM or AS.

3.5. Downregulation of Cytokines. Lesional skin of AD patients exhibits increased expression of Th2, Th1 cytokines and proinflammatory cytokines [24]. The cytokine levels in dorsal skin were significantly increased in DNCB (IL-4: 454.9%, IL-6: 1339.7%, IFN-γ: 524.6%, TNF-α: 247.8%, and IL-1β: 342.0%) compared to vehicle. Topical treatment of DEX, AM, AS, and DBT showed significantly lower levels of various cytokines compared with DNCB group (Figure 5). Particularly, the levels of IL-4 and TNF-α in DBT are significantly lower than in the single extract of AM or AS.

3.6. Inhibition of Inflammatory Mediators. Western blot analysis showed that DNCB challenge markedly upregulated the NF-κB (about 1.7-fold) and phosphorylation of IκBα (about 2.6-fold) compared to the vehicle group, whereas simultaneous treatment with DEX, AM, AS, and DBT attenuated the DNCB-induced NF-κB activation and phosphorylation of IκBα (Figure 6(a)). Moreover, DBT significantly reduced NF-κB and phosphor-IκBα expressions as compared with the AM and AS groups. MAPKs phosphorylation was significantly upregulated by DNCB, including phosphorylation ERK, p38, and JNK pathways (Figure 6(b)). AM, AS, and DBT treatment inhibited the increased level of phosphorylation of ERK, p38, and JNK. The regulation of phospho-ERK and phospho-p38 levels in DBT was more effective than AS, whereas phospho-JNK level was even higher than that of AS.

4. Discussion

Hyperplasia is one of the main symptoms in AD [24]. In histological analysis, we confirmed that the dermis and epidermis were thickened in the DNCB-induced group compared to vehicle group. Our findings showed that thickening of the epidermis and dermis was significantly reduced in DBT, AS, and AM groups. These findings are in agreement with those of a previous study presenting that DBT significantly inhibited ear swelling compared with DNCB-sensitized mice [12]. Particularly, topical application of DBT markedly suppressed a skin thickening and hyperkeratosis of the epidermis as compared with the AS groups. Scratching behavior in DNCB-induced model could be a major feature in skin lesions as results of various immunological responses such as the elevation of serum IgE concentration and number of mast cells [1, 22]. Therefore, it is important to decrease the scratching behavior in controlling the skin lesions and

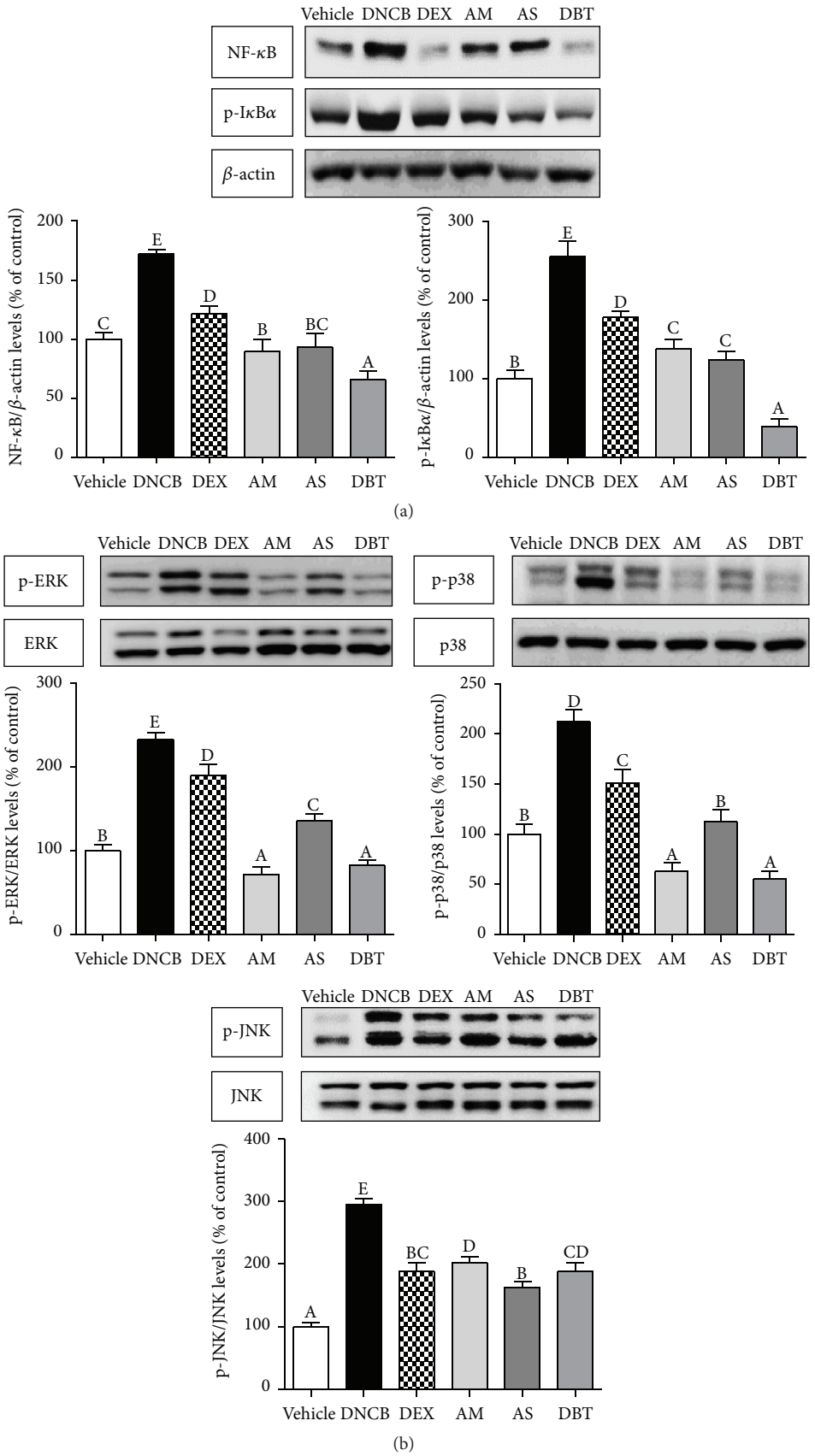

Figure 6: Effects of DBT on inflammatory mediators in DNCB-induced AD mice. (a) NF-κB and phosphor-IκBα levels (b) phosphor-MAPKs (ERK1/2, p38, and JNK) levels. Results are expressed as mean ± SD ($n = 5$).

various immunological reactions. DBT significantly inhibited the itching sign and decreased the elevation of serum IgE levels and degranulation of mast cells (MCs) compared to DNCB-induced group. These results are in close agreement with the findings of a similar previous study [12]. Particularly, DBT was more significantly effective on the inhibition of serum IgE levels compared to the single extract of AM or AS. These improvements could be partially attributed the antiallergic properties of DBT compared to the single extract of AM or AS in AD.

AD is involved in the dysregulation of Th type 1 and 2 cell-mediated immune responses [2]. Th2 cytokines, such as IL-4 and IL-6, promote B cell proliferation and cause IgE class switching in both acute and chronic AD [25]. On the other hand, Th1 cytokines, such as IFN-γ and IL-1β, are upregulated mainly in chronic stage [26]. Specifically, TNF-α regulates dermal-epidermal interactions in keratinocyte during inflammation, wound healing, and epidermal growth. Also, TNF-α stimulates IL-6 with enhancing the IL-4-induced IgE production [18, 22]. In close accordance with a previous study [12], topical application of DBT significantly inhibited the expression of AD-related pathogenic cytokines such as IL-4, IL-6, IFN-γ, TNF-α, and IL-1β regardless of Th1 and Th2 cytokines similarly to DEX group. Furthermore, DBT significantly suppressed DNCB-induced elevation of IL-4 and TNF-α compared to the single extract of AM or AS. Our comprehensive findings indicate that DBT may be more effective on suppressing an immune response by inhibiting both Th1- and Th2-type cytokine production as compared with the single extract of AM or AS in AD.

NF-κB signaling pathway, which is mediated by TNF-α, plays a critical role in the cellular immune and inflammatory response in epidermal keratinocytes [27]. In this study, we confirmed that activation of NF-κB results in skin thickening and that DBT reduced hyperplasia of epidermis in mice by suppressing expression of NF-κB. In addition, we have observed that the translocation of NF-κB to nucleus by DBT was inhibited as shown by a marked decrease of NF-κB in the nucleus and a decrease of phosphorylated IκBα in the cytoplasm.

Mitogen-activated protein kinase (MAPK) signaling is important in inflammatory skin diseases by controlling the activation, proliferation, degranulation, and migration of various immune cells. MAPK is divided into three groups: ERK controlling cell cycle progression, JNK regulating the cell proliferation and survival, and p38 MAPK relating to cell growth and differentiation, cell death, and inflammation [28]. Several studies have suggested that the development of MAPK inhibitors could be a therapeutic target for allergic diseases [29]. In the present study, DNCB challenge induced the increased activities of MAPK in consistency with the results of previous studies. Topical application of DBT inhibited the phosphorylation of ERK and p38 more than AS groups. These data suggest that inhibition of MAPK by DBT may contribute to its antiallergic and anti-inflammatory activities.

In conclusion, DBT with the weight ratio of 5 : 1 for AM to AS in accord with the ancient preparation not only prevented the degranulation of MCs and regulated the NF-κB signaling pathway, but also suppressed the phosphorylation of MAPK signaling molecules. Particularly, DBT formula could be more effective than AM or AS single treated groups on the antiallergic reactions by suppressing NF-κB signaling pathway and Th2-type cytokines mediating by TNF-α. These consecutive antiallergic and anti-inflammatory effects of DBT are believed to inhibit epidermal and dermal thickness and scratching behavior and to contribute significantly to the clinical efficacy in the management of AD.

Competing Interests

The authors have declared that there are no competing interests.

Authors' Contributions

You Yeon Choi participated in the data analysis and drafted this paper. Mi Hye Kim and Jongki Hong carried out the immunoassays and data analysis. Kyuseok Kim and Woong Mo Yang were the general supervisors for this research and participated in both the study design and critical revision of the paper and all agreed to accept equal responsibility for the accuracy of the content of the paper.

Acknowledgments

This work was supported by the National Research Foundation of Korea Grant funded by the Korean Government (NRF-2014R1A1A1005859).

References

[1] G. Yang, K. Lee, M.-H. Lee, S.-H. Kim, I.-H. Ham, and H.-Y. Choi, "Inhibitory effects of *Chelidonium majus* extract on atopic dermatitis-like skin lesions in NC/Nga mice," *Journal of Ethnopharmacology*, vol. 138, no. 2, pp. 398–403, 2011.

[2] D. Navi, J. Saegusa, and F. T. Liu, "Mast cells and immunological skin diseases," *Clinical Reviews in Allergy & Immunology*, vol. 33, no. 1-2, pp. 144–155, 2007.

[3] Y. Tomimori, Y. Tanaka, M. Goto, and Y. Fukuda, "Repeated topical challenge with chemical antigen elicits sustained dermatitis in NC/Nga mice in specific-pathogen-free condition," *Journal of Investigative Dermatology*, vol. 124, no. 1, pp. 119–124, 2005.

[4] B. S. Kim, J. K. Choi, H. J. Jung et al., "Effects of topical application of a recombinant staphylococcal enterotoxin A on DNCB and dust mite extract-induced atopic dermatitis-like lesions in a murine model," *European Journal of Dermatology*, vol. 24, no. 2, pp. 186–193, 2014.

[5] J. Del Rosso and S. F. Friedlander, "Corticosteroids: options in the era of steroid-sparing therapy," *Journal of the American Academy of Dermatology*, vol. 53, supplement 1, pp. S50–S58, 2005.

[6] M. Kawai, T. Hirano, S. Higa et al., "Flavonoids and related compounds as anti-allergic substances," *Allergology International*, vol. 56, no. 2, pp. 113–123, 2007.

[7] H. Kim, M. Kim, H. Kim, G. San Lee, W. G. An, and S. I. Cho, "Anti-inflammatory activities of *Dictamnus dasycarpus* Turcz., root bark on allergic contact dermatitis induced by dinitrofluorobenzene in mice," *Journal of Ethnopharmacology*, vol. 149, no. 2, pp. 471–477, 2013.

[8] K. Yamaura, M. Shimada, and K. Ueno, "Anthocyanins from bilberry (*Vaccinium myrtillus* L.) alleviate pruritus in a mouse model of chronic allergic contact dermatitis," *Pharmacognosy Research*, vol. 3, no. 3, pp. 173–177, 2011.

[9] K. Y. Z. Zheng, R. C. Y. Choi, H. Q. H. Xie et al., "The expression of erythropoietin triggered by danggui buxue tang, a Chinese herbal decoction prepared from radix Astragali and radix Angelicae Sinensis, is mediated by the hypoxia-inducible factor in cultured HEK293T cells," *Journal of Ethnopharmacology*, vol. 132, no. 1, pp. 259–267, 2010.

[10] M. Yang, G. C. F. Chan, R. Deng et al., "An herbal decoction of *Radix astragali* and *Radix angelicae* sinensis promotes hematopoiesis and thrombopoiesis," *Journal of Ethnopharmacology*, vol. 124, no. 1, pp. 87–97, 2009.

[11] Q. T. Gao, J. K. H. Cheung, J. Li et al., "A Chinese herbal decoction, Danggui Buxue Tang, activates extracellular signal-regulated kinase in cultured T-lymphocytes," *FEBS Letters*, vol. 581, no. 26, pp. 5087–5093, 2007.

[12] L.-W. Fang, C.-C. Cheng, T.-S. Hwang et al., "Danggui buxue tang inhibits 2,4-dinitrochlorobenzene: induced atopic dermatitis in mice," *Evidence-Based Complementary and Alternative Medicine*, vol. 2015, Article ID 672891, 10 pages, 2015.

[13] J. F. Lin, P. H. Liu, T. P. Huang et al., "Characteristics and prescription patterns of traditional Chinese medicine in atopic dermatitis patients: ten-year experiences at a Medical Center in Taiwan," *Complementary Therapies in Medicine*, vol. 22, no. 1, pp. 141–147, 2014.

[14] T. T. X. Dong, K. J. Zhao, Q. T. Gao et al., "Chemical and biological assessment of a Chinese herbal decoction containing *Radix astragali* and *Radix angelicae* sinensis: determination of drug ratio in having optimized properties," *Journal of Agricultural and Food Chemistry*, vol. 54, no. 7, pp. 2767–2774, 2006.

[15] Q. Gao, J. Li, J. K. H. Cheung et al., "Verification of the formulation and efficacy of Danggui Buxue Tang (a decoction of Radix Astragali and Radix Angelicae Sinensis): an exemplifying systematic approach to revealing the complexity of Chinese herbal medicine formulae," *Chinese Medicine*, vol. 2, article 12, 2007.

[16] Q. T. Gao, R. C. Y. Choi, A. W. H. Cheung et al., "Danggui buxue tang—a Chinese herbal decoction activates the phosphorylations of extracellular signal-regulated kinase and estrogen receptor α in cultured MCF-7 cells," *FEBS Letters*, vol. 581, no. 2, pp. 233–240, 2007.

[17] S. Wang, Y. Hu, W. Tan et al., "Compatibility art of traditional Chinese medicine: from the perspective of herb pairs," *Journal of Ethnopharmacology*, vol. 143, no. 2, pp. 412–423, 2012.

[18] J. H. Kim, M. H. Kim, G. Yang, Y. Huh, S. H. Kim, and W. M. Yang, "Effects of topical application of *Astragalus membranaceus* on allergic dermatitis," *Immunopharmacology and Immunotoxicology*, vol. 35, no. 1, pp. 151–156, 2012.

[19] M. H. Kim, Y. Y. Choi, I. H. Cho, J. Hong, S. H. Kim, and W. M. Yang, "*Angelica sinensis* induces hair regrowth via the inhibition of apoptosis signaling," *The American Journal of Chinese Medicine*, vol. 42, no. 4, pp. 1021–1034, 2014.

[20] Y.-Y. Sung, T. Yoon, J. Y. Jang, S.-J. Park, G.-H. Jeong, and H. K. Kim, "Inhibitory effects of Cinnamomum cassia extract on atopic dermatitis-like skin lesions induced by mite antigen in NC/Nga mice," *Journal of Ethnopharmacology*, vol. 133, no. 2, pp. 621–628, 2011.

[21] S. M. A. Hassan, A. J. Hussein, and A. K. Saeed, "Role of green tea in reducing epidermal thickness upon ultraviolet light-B injury in BALB/c mice," *Advances in Biology*, vol. 2015, Article ID 890632, 6 pages, 2015.

[22] Y. Y. Choi, M. H. Kim, J. Y. Lee, J. Hong, S.-H. Kim, and W. M. Yang, "Topical application of Kochia scoparia inhibits the development of contact dermatitis in mice," *Journal of Ethnopharmacology*, vol. 154, no. 2, pp. 380–385, 2014.

[23] K. Abe, K. Kobayashi, S. Yoshino, K. Taguchi, and H. Nojima, "Withdrawal of repeated morphine enhances histamine-induced scratching responses in mice," *Drug and Chemical Toxicology*, vol. 38, no. 2, pp. 167–173, 2014.

[24] L. S. Fonacier, S. C. Dreskin, and D. Y. Leung, "Allergic skin diseases," *Journal of Allergy and Clinical Immunology*, vol. 125, no. 2, supplement 2, pp. S138–S149, 2010.

[25] S.-L. Zhou, G.-H. Tan, F.-Y. Huang, H. Wang, Y.-Y. Lin, and S.-L. Chen, "Sanpao herbs inhibit development of atopic dermatitis in Balb/c mice," *Asian Pacific Journal of Allergy and Immunology*, vol. 32, no. 2, pp. 140–144, 2014.

[26] M. H. Kim, Y. Y. Choi, G. Yang, I.-H. Cho, D. Nam, and W. M. Yang, "Indirubin, a purple 3,2- bisindole, inhibited allergic contact dermatitis via regulating T helper (Th)-mediated immune system in DNCB-induced model," *Journal of Ethnopharmacology*, vol. 145, no. 1, pp. 214–219, 2013.

[27] J. Lee, YY. Choi, MH. Kim, JM. Han, JE. Lee, and EH. Kim, *Topical Application of Angelica sinensis Improves Pruritus and Skin Inflammation in Mice with Atopic Dermatitis-Like Symptoms. J Med Food*, doi, 10.1089/jmf.2015.3489, 2015.

[28] B. Kaminska, "MAPK signalling pathways as molecular targets for anti-inflammatory therapy—from molecular mechanisms to therapeutic benefits," *Biochimica et Biophysica Acta—Proteins and Proteomics*, vol. 1754, no. 1-2, pp. 253–262, 2005.

[29] S. R. Kim, K. S. Lee, S. J. Park, M. S. Jeon, and Y. C. Lee, "Inhibition of p38 MAPK reduces expression of vascular endothelial growth factor in allergic airway disease," *Journal of Clinical Immunology*, vol. 32, no. 3, pp. 574–586, 2012.